UNIVERSIDAD AUTÓNOMA DE MADRID
FACULTAD DE CIENCIAS

Departamento de Química-Física Aplicada
Sección Departamental de Ciencias de la Alimentación

SCALING-UP SUPERCRITICAL BATCH EXTRACTION OF VEGETAL MATERIALS

ESCALADO DE PROCESOS DE EXTRACCIÓN SUPERCRÍTICA EN *BATCH* DE MATERIALES VEGETALES

ALEXIS LÓPEZ PADILLA

Tesis Doctoral

Madrid, Junio 2017

Instituto de Investigación en Ciencias de la Alimentación (CIAL, UAM-CSIC)

Departamento de Producción y Caracterización de Nuevos Alimentos

UNIVERSIDAD AUTÓNOMA DE MADRID
FACULTAD DE CIENCIAS

Departamento de Química-Física Aplicada

Sección Departamental de Ciencias de la Alimentación

SCALING-UP BATCH SUPERCRITICAL FLUID EXTRACTION OF VEGETAL MATERIALS

ESCALADO DE PROCESOS DE EXTRACCIÓN SUPERCRÍTICA EN *BATCH* DE MATERIALES VEGETALES

Memoria presentada por:

Alexis López Padilla

Para optar al grado de

Doctor en Ciencias de la Alimentación

Trabajo realizado bajo la dirección de:

Dra. Tiziana Fornari Reale

Dra. Alejandro Ruiz Rodríguez

Instituto de Investigación en Ciencias de la Alimentación (CIAL, UAM-CSIC)

Departamento de Producción y Caracterización de Nuevos Alimentos

Dª. TIZIANA FORNARI REALE, DRA EN INGENIERÍA QUÍMICA Y PROFESORA TITULAR DE LA UNIVERSIDAD AUTÓNOMA DE MADRID Y D. ALEJANDRO RUIZ RODRÍGUEZ, DR. EN CIENCIAS Y PROFESOR CONTRATADO DOCTOR DE LA UNIVERSIDAD AUTÓNOMA DE MADRID.

INFORMAN,

Que el presente trabajo titulado: **"Escalado de Procesos de Extracción Supercrítica en *Batch* de Materiales Vegetales / *Scaling-Up Batch Supercritical Fluid Extraction of Vegetal Materials"*** y que constituye la memoria que presenta D. Alexis López Padilla para optar al grado de Doctor en Ciencias de la Alimentación, ha sido realizado en el Instituto de Investigación en Ciencias de la Alimentación CIAL (UAM-CSIC) bajo su dirección.

Y para que así conste firman el presente informe en Madrid a 23 de junio de 2017.

Fdo: Tiziana Fornari Reale

Fdo: Alejandro Ruiz Rodríguez

A mis padres y a mi hermano porque siempre estuvieron, están y estarán conmigo.

“Sometimes perfect is the enemy of good”.

Christophe Bliard

Agradecimientos

A Tiziana y Alejandro, mis tutores, por la gran oportunidad que me brindaron al formar parte de este gran grupo de trabajo, por su paciencia, su apoyo incondicional durante el desarrollo de mi trabajo y por todo lo que han aportado a mi formación personal y profesional.

A Colciencias por la beca de formación doctoral otorgada a través de la convocatoria 568/2012.

A Guillermo Reglero por su apoyo y colaboración durante la realización de mi tesis.

Al personal docente, investigador y administrativo con quienes compartí estos cuatro años: Mónica Rodríguez, Diana, Laura Jaime, Susana Santoyo, Cristina Soler, Elena Ibañez, José Mendiola, Montse, José, Macarena.

A mis amigos del Cial con quienes compartí esta gran experiencia durante estos cuatro años: Gonzalo, Juanan, Lydia Montero, Bienve, Marta, Tanize, Giuseppe 'Peppe', Inés, Engin Koçak, Lamia, Francesco, Ana Rita, Marisol, Alba, Gloria, Silvia, Fouad, Lilia, Flora, Somaris, Honoria, Diego Morales, Nieves, Aelson, Giusy y Oumayma.

A mis amigos colombianos en España con quienes compartí muchas historias: Daniel Bahamón, Ana María Jiménez, Diego Tirado, Diana Mantilla, Mariana Isaza, Luna Caicedo y Andrea Sánchez.

A todos mis compañeros y amigos del Club de Rugby Subacuático Osos Rugby Sub de Madrid, especialmente a Claudia Holgueras y Ana Ramírez por los grandes e inolvidables momentos compartidos. A Félix Muñoz, Jesús Plaza Benito, Nacho Martorell, Mark Wellings, Edu Villoria, Cristian Castrillón, Dacho Covaleda, Maxi Díaz, Markus Vetter, Carlos, Esther, Taty Arias, Patrix, Irene, Isabel, Víctor Alegría, Víctor Donoso, Tero Suomalainen, Edu Arraz, Alex Forero, Pedro Villena, Bora, Diego, Jorge, Tonino, porque con ustedes he aprendido que las pequeñas cosas son las que más importan y que hay que vivir a tope porque cada día es irrepetible. Los echaré de menos hasta que nos volvamos a ver bajo el agua.

A mis amigos en Colombia, Juan Andrés, Hernán Restrepo, Shirley Echeverri, Lenna Tule, Carlos Alejandro Correa, Nathaly Rubio, Nafer Mejía, Karina Correa, Paula Padilla, Abel Tejada, Edwin Muñoz, Edgar Alonso, Angélica, Isabel, Liseth, Cristina, Gildarly, Rafa, porque siempre hemos mantenido el contacto sin importar la distancia ni la diferencia horaria y por recordarme que siempre estarán allí aguardando para un reencuentro más.

A mis compañeros de Piso: Nico, Tamarán y Lupe a los cuales estoy muy agradecido y a Víctor Carretero, el propietario del piso por su gran disposición y amabilidad y porque en estos 4 años siempre estuvo atento a que nada me hiciera falta.

Al Doctor y DJ, Sorel Jatunov, por todo lo que aprendimos viajando, por tus sabios consejos y porque además de ser un gran amigo eres mi hermano.

A María Mielgo Ibañez, por tu amistad, compañía y por los grandes momentos en los que departimos sobre historia, globalización, política y la vida.

A mis amigos de la Universidad de Aveiro: Ana Lu Magalhaes, José Pedro, Marcelo, Simão, Aleine, Ivo, Joana, Paulo Roberto, Elaine, Bruno y al profesor Carlos M. Silva, por la gran oportunidad aprender, compartir y formar parte de ese gran equipo.

A mis amigos de Oporto: Catarina, Gonçalo, Ana, Miguel, Salomé, Diogo, Mariana, Roby, Teresa y un agradecimiento muy especial a mi familia portuguesa que me acogió como un hijo más: Manuel, Alda, Ana Lilia, Miguel, Inés, Ricardo, Amy, Alfonso.

A Maria João, Biju, porque conocerte y compartir tantos momentos ha sido una de las mejores cosas que me han pasado en la vida, gracias por sacar siempre lo mejor de mí.

To Rommy, because the time with you transforms easily into a big smile, thank you very much for those nice, crazy and amazing moments, it was in a short time but they will remain in my memory forever.

A David Villanueva, a quien considero un hermano y al que siempre recordaré y echaré de menos. Siempre te estaré muy agradecido por todas las conversaciones de tan diversa índole y sobre todo por hacer muy amena mi estancia en Madrid. Hasta la próxima Sporco.

A mis padres, Félix y Yolanda por todo el amor que me han dado, por creer siempre en mí, por empujarme en la búsqueda y realización de mis sueños sin importar donde estuvieran y por su apoyo incondicional en mi formación como persona y profesional. A mi hermano Daiver, porque siempre has estado ahí cuando más te he necesitado y a mi abuelo, José Ángel Padilla (Q.E.P.D.), porque entre tantas cosas me enseñaste que el objetivo más importante en esta vida es Ser Feliz.

¡Gracias totales!

Alexis

Madrid, Junio de 2017

Esta Tesis Doctoral se ha realizado gracias a la financiación de la beca pre-doctoral del programa “Doctorados en el exterior 568/2012” concedida por el Departamento Administrativo de Ciencia Tecnología e Innovación de Colombia (COLCIENCIAS).

ÍNDICE

ABREVIATURAS

a_0: área superficial específica (m^{-1})

A: Área transversal de la celda de extracción (m^2)

CER: *Constant Extraction Rate period* (periodo con tasa de extracción constante)

CO_2: Dióxido de carbono

d_p: Diámetro de partícula medio (μm)

D: Diámetro de la celda de extracción (m)

D_{12}: Coeficiente de difusión ($cm^2 \cdot s^{-1}$)

DC: *Diffusion Controlled rate period* (período de difusión controlada)

F: Masa de material vegetal (kg)

FER: *Falling Extraction Rate period* (periodo con tasa decreciente de extracción)

L: Altura de la celda de extracción (m)

k_f: Coeficiente de transferencia de masa en fase fluida ($m \cdot s^{-1}$)

k_s: Coeficiente de transferencia de masa en fase sólida ($m \cdot s^{-1}$)

k_{YA}: Coeficiente volumétrico de transferencia de masa en la fase fluida del modelo BIC ($k_f \times a_0$, s^{-1})

k_{XA}: Coeficiente volumétrico de transferencia de masa en la fase sólida del modelo BIC ($k_s \times a_{0,}$ s^{-1})

M_{CER}: tasa de transferencia de masa en la etapa CER

OEC: *Overall Extraction Curve* (curva global de extracción)

P: Presión (MPa)

Q_{CO2}: Caudal de CO_2 ($k \cdot s^{-1}$)

Re: Número Reynolds, $(\rho u d_p/\mu)$

Sc: Número Schmidt, $(\mu/\rho D_{12})$

Sh: Número Sherwood, $(k d_p/D_{12})$

SFE: *Supercritical Fluid Extraction* (Extracción con Fluidos Supercríticos)

T: Temperatura

t: Tiempo de extracción

t_{CER}: Tiempo de extracción en la etapa CER

t_{FER}: Tiempo de extracción en la etapa FER

t_{RES}: Tiempo de residencia del disolvente en la celda de extracción

u: Velocidad lineal del fluido supercrítico ($m \cdot s^{-1}$)

X_k: Relación másica de soluto de difícil acceso ($kg \cdot kg^{-1}$)

X_o: Rendimiento global de extracción ($kg \cdot kg^{-1}$)

Xp: Relación másico de soluto fácilmente accesible ($kg \cdot kg^{-1}$)

Y: Rendimiento de extracción ($kg \cdot kg^{-1}$)

Y*: Solubilidad ($kg \cdot kg^{-1}$)

Y_∞: Rendimiento de extracción a tiempo infinito.

Símbolos griegos

μ: Viscosidad del fluido supercrítico ($Pa \cdot s$)

ρ: Densidad del fluido supercrítico ($kg \cdot m^{-3}$)

ρ_s: Densidad del material vegetal sólido ($kg \cdot m^{-3}$)

ε: Porosidad del lecho

RESUMEN / SUMMARY

RESUMEN

Los fluidos supercríticos han abierto un amplio campo de posibilidades y nuevas alternativas en la tecnología de los alimentos. La razón principal es el hecho del empleo del CO_2 como disolvente, una sustancia permitida en alimentos. Ciertamente, la extracción con fluidos supercríticos (SFE) de materiales vegetales sólidos es actualmente la aplicación más explotada.

Bajo el concepto de química verde, La SFE es una de las más eficientes y prometedoras alternativas para la producción de extractos vegetales de alta calidad. La tecnología SFE puede considerarse como una técnica óptima de extracción de biomoléculas, debido a la completa ausencia de disolventes orgánicos durante el proceso y en el producto final, su adecuación para extraer especies termosensibles, la ausencia de daño oxidativo y la posibilidad de poder ser aplicada tanto a escala analítica como a escala industrial.

El comportamiento cinético de la SFE de materiales vegetales en lecho fijo se suele representar mediante un gráfico de la masa extraída en función del tiempo, o en función de masa de disolvente consumido, comúnmente conocido como curva de extracción (OEC, *Overall Extraction Curve*). No solo el rendimiento másico varía durante el tiempo de extracción, sino también la composicióny las propiedades fisicoquímicas y biológicas del extracto. El escalado en un proceso de SFE busca reproducir la misma OEC en diferentes celdas de extracción con diferente capacidad y/o forma. Existe un gran número de modelos cinéticos en la literatura, los cuales han sido desarrollados y/o adaptados para representar la OEC de un proceso SFE. Estos modelos incluyen desde correlaciones simples basadas en cinéticas de primer orden, tales como el modelo de Barton, hasta modelos fenomenológicos integrales basados en la transferencia de masa diferencial en el interior de la celda de extracción. Sin embargo, los estudios o enfoques sobre el escalado SFE son escasos en la bibliografía y están basados en la aplicación de algunas reglas de pulgar o enfoques semi-empíricos tradicionales de la ingeniería química.

En esta tesis doctoral se estudió el comportamiento cinético de dos materiales vegetales: mortiño (*Vaccinium meridionals* Swartz) y caléndula (*Calendula officinalis*). Las OECs se obtuvieron a diferentes presiones y temperaturas de extracción, así como utilizando diferentes caudales de CO_2 y distintas celdas de extracción (de 0.3, 1.35 y 5.2 L de capacidad) disponibles en la Plataforma Novalindus (CIAL UAM+CSIC). Todas las OECs

fueron representadas siguiendo el modelo *Broken and Intact Cells* (BIC), el cual fue posteriormente empleado para evaluar la aplicación de dos criterios de escalado muy utilizados en la bibliografía, a saber, a) mantener constante la velocidad lineal del CO_2 o b) mantener constante el tiempo de residencia del CO_2 a través del lecho empacado. De acuerdo con las predicciones del modelo BIC, este último criterio debería proporcionar una buena estimación del caudal másico de CO_2 para factores de escalado de 5 y 19. Sin embargo, los resultados experimentales no concuerdan con las predicciones teóricas (*Materials*, 2016, 9(519) DOI: 10.3390/ma9070519; *The Journal of Supercritical Fluids*, 2017, DOI: 10.1016/j.supflu.2017.03.033). Esta conclusión coincide con lo señalado por otros estudios previos de escalado de la bibliografía, corroborando la evidencia general de que no hay un criterio único y efectivo para el escalado de la SFE de materiales vegetales.

No obstante, utilizando las OECs generadas en esta Tesis Doctoral se consiguió desarrollar una correlación general que sirviera como herramienta para el cálculo del caudal másico de CO_2 en el salto de escala SFE de las unidades que dispone la Plataforma Novalindus. Los coeficientes de transferencia de masa en la fase supercrítica fueron estimados mediante dos modelos diferentes (modelo de Barton y modelo BIC) para todas las OECs obtenidas para mortiño y caléndula en celdas de extracción de diferente tamaño, y se correlacionaron satisfactoriamente ($R^2 > 0.96$) en función de los parámetros geométricos de la celda de extracción (diámetro y longitud), el número adimensional de Schmidt, y el tamaño de partícula y la porosidad del lecho empacado (*Journal of Food Engineering*, enviado en junio de 2017). Además, para calcular el coeficiente de difusión de un extracto natural, el cual forma parte del número de Schmidt, se desarrolló en esta Tesis Doctoral un método propio (*The Journal of Supercritical Fluids*, 109 (2016) 148-156).

Finalmente, se extendió la correlación desarrollada entre el caudal de CO_2 y el coeficiente de transferencia de masa a un conjunto más amplio de datos, incluyendo 19 OECs obtenidas en la Plataforma Novalindus y 34 OECs recopiladas de la bibliografía. Este conjunto de datos comprende 10 materiales vegetales diferentes, temperaturas entre 298 y 333 K, presiones en el rango de 10 a 30 MPa, diámetros de partículas entre 250 y 1400 µm, volúmenes de celdas de extracción desde 50 a 5200 cm^3, así como porosidades de lecho en el rango de 0.59 a 0.97. La correlación resultante presentó un coeficiente de regresión mayor a 0.86, indicando la validez de la tendencia general observada y estableciendo su potencial como una herramienta para estimar el caudal de CO_2 requerido en el escalado SFE de materiales vegetales (*Journal of Food Engineering*, enviado en junio de 2017).

SUMMARY

Supercritical fluids have opened a wide range of new alternatives for the expansion of food technology. Certainly, the most remarkable reason is the use of a substance permitted in foods, namely carbon dioxide (CO_2), as solvent. The supercritical fluid extraction (SFE) of solid vegetable materials is currently one of the most exploited applications.

Under the concept of green processing, SFE is one of the most efficient and promising alternatives to produce high-quality vegetal extracts. SFE technology can be awarded as a superior extraction technique for biomolecules because it is organic solvent free, adequate for thermo-sensitive species, avoid oxidation damage, and can be applied from analytical scale to large industrial scale.

The kinetic behavior of SFE of vegetal packed beds is usually represented by the plot of the mass extracted as a function of time or as a function of the mass of spent solvent, commonly denoted Overall Extraction Curve (OEC). Not only mass yield varies along extraction time, but also composition, physicochemical and biological properties of the extract. SFE scaling aims to reproduce the same OEC in extraction vessels with different shape and/or capacity.

A large number of kinetic models can be found in the literature, which were developed and/or adapted to represent the OEC of SFE processes, including simple correlations based on first order kinetics, such as the Barton model, to comprehensive phenomenological models based on mass transfer differential occurred in the cell extraction. Yet, more limited approaches and studies are available in the literature regarding SFE scaling, and are based on some thumb rules or semi-empirical approaches of traditional chemical engineering.

In this PhD Thesis the kinetic behavior of two vegetal materials, namely *Vaccinium meridionale Swartz* (mortiño) and *Calendula officinalis* (calendula), was study. The OECs were obtained at different extraction pressures and temperatures, as well as at different CO_2 mass flow rates and using extraction cells of different size (0.5 and 2 L vol.) available in Novalindus Platform (CIAL UAM+CSIC). All OECs were adequately represented by the Broken and Intact Cells (BIC) model, and the model was then used to assess the accuracy of two different scaling up criteria: maintaining throughout the packed bed the CO_2 linear velocity constant, or maintaining the CO_2 residence time constant. According to BIC model

predictions, this last criterion should provide good estimation of the CO_2 mass flow rate for scaling factors of 5 and 19. Nevertheless, experimental results do not agree with the theoretical prediction (Materials, 2016, 9(519) DOI: 10.3390/ma9070519; The Journal of Supercritical Fluids, 2017, DOI: 10.1016/j.supflu.2017.03.033). This conclusion agrees with other scaling-up studies reported in the literature, supporting the general evidence that there is not a single criterion effective for SFE scaling up of vegetal materials.

Then, using all OECs generated in this Doctoral Thesis a general correlation was developed with the aim to generate a tool to estimate the CO_2 mass flow rate in scaling up within Novalindus facilities. The mass transfer coefficients in the supercritical fluid phase were estimated by two different models (Barton kinetic model and BIC model) of the OECs obtained for mortiño and calendula in the different size extraction cells were satisfactorily correlated ($R^2 > 0.96$) in terms of the cell geometric parameters, diameter and length, the dimensionless Schmidt number, the material particle size and the bed porosity (Journal of Food Engineering, submitted in June 2017). Yet, to calculate the diffusion coefficient of a natural extract, which is part of Schmidt number, an own method, developed in this Thesis was used (The Journal of Supercritical Fluids, 109 (2016) 148-156).

The resulted relation between the CO_2 flow rate and the mass transfer coefficient was also studied enlarging the OEC data set, including 19 OECs obtained in Novalindus Platform and 34 OECs from the literature. This set of data comprise 10 different plant materials, temperatures in the range of 298 to 333 K, pressures in the range of 10 to 30 MPa, particle diameter varied from 250 to 1400 μm, extractor volumes from 50 to 5200 cm^3 and bed porosities in the range of 0.59 to 0.97. The correlation presented a regression coefficient higher than 0.86, indicating the validity of the general trend observed and setting its potential to be used for estimating the CO_2 flow rate required in SFE scale up of plant materials (Journal of Food Engineering, submitted in June 2017).

ESTRUCTURA DE LA MEMORIA

La presente memoria se encuentra estructurada en siete secciones, las que se detallan a continuación:

Introducción, presentación de los fundamentos y antecedentes correspondientes a los trabajos realizados en esta Tesis, donde se incluye también una descripción detallada de las plantas de extracción supercrítica de la Plataforma Novalindus utilizados para desarrollar el plan de trabajo.

Objetivos y Plan de Trabajo, planteamiento de los objetivos generales y parciales, y descripción de la metodología y los procedimientos aplicados, los materiales utilizados, y las tareas realizadas para alcanzar los objetivos planteados.

Resultados, presentación de los resultados obtenidos según cuatro artículos publicados, y encabezados por un prefacio donde se explica sus contenidos en forma general y resumida.

Discusión, se presenta una explicación general del trabajo de Tesis que integra todos los trabajos publicados.

Conclusiones, incluye las conclusiones más relevantes, parciales y generales, obtenidas en esta Tesis Doctoral.

Bibliografía, utilizada en esta memoria y en las publicaciones que ha dado lugar la Tesis Doctoral.

Anexos, se incluye la lista de otras publicaciones vinculadas a esta Tesis, así como publicaciones desarrolladas para la formación del doctorando, pero no vinculadas directamente con esta memoria.

1

CAPÍTULO 1.

INTRODUCCIÓN

1. INTRODUCCIÓN

1.1 La Extracción con Fluidos Supercríticos y la Industria Alimentaria

La extracción con fluidos supercríticos (SFE: *Supercritical Fluid Extraction*) ha demostrado ser una de las tecnologías verdes con grandes ventajas y posibilidades de aplicación en diversos campos, entre las cuales se destacan la industria alimentaria, cosmética, farmacéutica, materiales, química, energética y tratamiento de residuos. Entre ellas, la industria alimentaria se ha beneficiado de forma sustancial, debido al uso como fluido supercrítico de una sustancia permitida en alimentos: el dióxido de carbono (CO_2). Siendo un disolvente ideal para la extracción de compuestos de afinidad lipídica, el CO_2 ofrece grandes ventajas frente a los métodos tradicionales de extracción [1].

Por otro lado, la SFE es un proceso alternativo que se adapta al cumplimiento de algunas de las restricciones impuestas por algunos organismos en materia de salud, seguridad, reducción de residuos tóxicos y minimización del impacto sobre el medioambiente.

En la región supercrítica, las propiedades fisicoquímicas de una sustancia pura asumen valores intermedios entre los estados líquido y gaseoso. En la figura 1.1., se representa el diagrama de fases presión vs temperatura, donde la figura (i) muestra la separación de fases entre gas y líquido para el CO_2, al mantener la presión constante y a medida que la temperatura se incrementa el menisco que las separa comienza a reducirse (ii), a mayores incrementos de temperatura el menisco se hace casi imperceptible (iii) hasta que la presión y la temperatura crítica son alcanzadas y superadas, observándose cómo las fases líquido y vapor forman una sola fase fluida en la región supercrítica (iv) [1,2]. Al encontrarse en dicha región, las propiedades relacionadas con la capacidad de disolución, como es la densidad del fluido supercrítico, se aproximan a valores cercanos a las de un líquido. En lo referente a propiedades relacionadas con el transporte de materia, como la difusividad y la viscosidad, se alcanzan valores próximos a las de un gas. Como es sabido, los líquidos actúan como excelentes disolventes, pero se caracterizan por poseer una difusión lenta y una alta viscosidad. Los gases, a su vez, no son buenos disolventes, pero tienen un alto coeficiente de difusión, así como una baja viscosidad. Así, la combinación de densidades tipo líquido y propiedades de transporte similares a los gases convierten a los fluidos

supercríticos en una clase de disolvente con propiedades óptimas para los procesos de extracción y fraccionamiento [3,4].

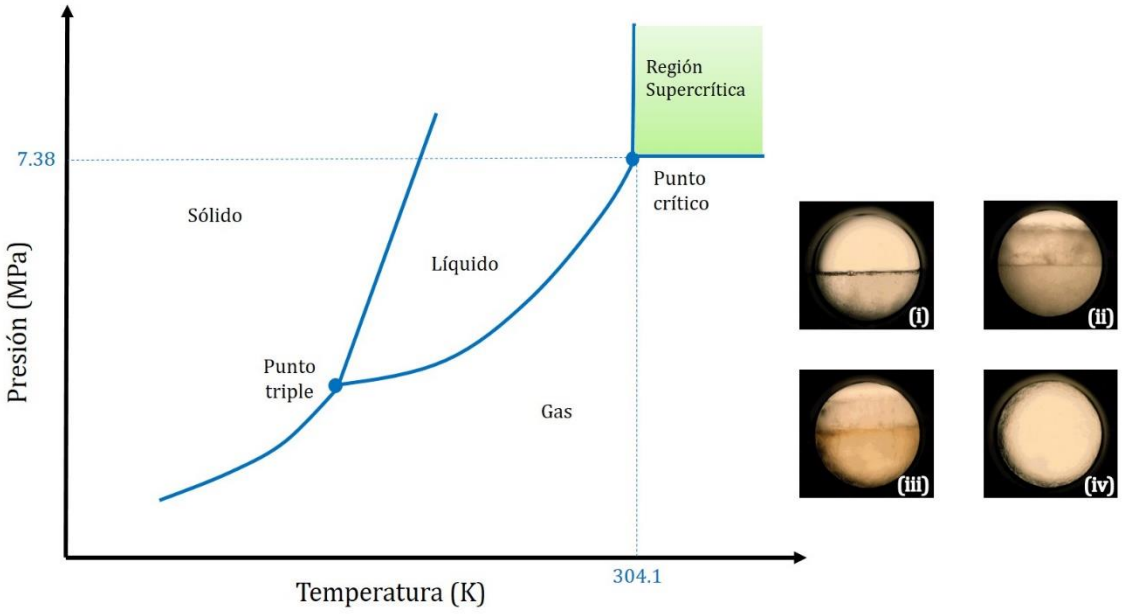

Figura 1.1 Diagrama de fases de una sustancia pura (Adaptado de Palmer y Ting, 1995 [1] y Barry y col. (2006) [2])

En la tabla 1.1 se muestran algunos disolventes y sus respectivos valores de temperatura, presión y densidad en el punto crítico. De los valores se puede apreciar las ventajas operativas que posee el dióxido de carbono para alcanzar las condiciones críticas (Presión: 7.38 MPa; Temperatura: 304.1 K) frente a otros disolventes convencionales.

Tabla 1.1 Propiedades críticas de algunas sustancias puras

Disolvente	**T_c (K)** [5,6]	**P_c (MPa)** [5]	**ρ_c (kg·m^3)** [7]
Dióxido de Carbono (CO_2)	304,15	7,38	468
Agua (H_2O)	647,3	22,12	322
Etanol (CH_3CH_2OH)	513,9	6,14	276
Metanol (CH_3OH)	512,6	8,09	272
Amonio (NH_3)	455,55	11,35	253
Isopropanol ($CH_3CHOHCH_3$)	508,3	4,76	273

T_c: Temperatura crítica; P_c: Presión crítica; ρ_c: densidad crítica

El CO_2 supercrítico (SC-CO_2) se comporta como un disolvente lipofílico, aunque comparado con otros disolventes líquidos, como pentano o hexano, posee la ventaja de ser selectivo, es decir, su poder de solvatación puede ser ajustado variando la presión y la temperatura de operación [8]. Según Brunner (2005), el poder de solvatación del SC-CO_2 puede resumirse de acuerdo con las siguientes reglas [4]:

i. Buena disolución de compuestos apolares o ligeramente polares.

ii. La solvatación de compuestos de baja masa molar es alta y disminuye con el aumento de la misma.

iii. El SC-CO_2 posee alta afinidad con compuestos orgánicos oxigenados o de masa molar media.

iv. Ácidos grasos libres y sus glicéridos exhiben bajas solubilidades.

v. Los pigmentos son moderadamente solubles.

vi. El agua tiene una baja solubilidad (< 0.5 % m/m) a temperaturas inferiores a 100°C.

vii. Proteínas, polisacáridos, azúcares y sales minerales son insolubles.

viii. A medida que aumenta la presión del CO_2 es capaz de separar compuestos que son menos volátiles, tienen masa molar más alta y/o son más polares.

La aplicación de la tecnología de extracción supercrítica en el procesamiento de alimentos se inició en la década de 1970. En el año 2003, Tzia y Liadakis (2003) publicaron un listado con más de 20 industrias de procesamiento de alimentos y productos naturales que han incorporado en sus procesos la SFE a nivel global [9]. Sin embargo, algunas de las aplicaciones más reconocidas y a menudo muy citadas en la industria alimentaria y de bebidas incluyen la extracción de sabores amargos a partir del lúpulo y la descafeinización de los granos de café [4], la extracción de tricloroanisol, responsable del llamado "sabor a corcho" en el corcho empleado para el embotellado del vino [10], entre otras.

Shütz (2007) realizó una búsqueda de solicitudes de patentes basadas en fluidos supercríticos encontrando que de las 8600 solicitudes presentadas entre 1992 y 2006, 4960 correspondían a 4 países: Japón, Estados Unidos, Alemania y China; de ellas, un 37.5 %, de las solicitudes presentadas en estos países correspondían a aplicaciones en la industria alimentaria y farmacéutica, indicando un fuerte y constante interés a nivel mundial de estos sectores industriales por la aplicación de los fluidos supercríticos [11].

Moraes y col. (2014) realizaron un análisis de las publicaciones sobre SFE entre 2004 – 2014 reportando un total de 10.164 artículos disponibles en la base Web of Science y 12.668 en Scopus. En un análisis más detallado por países, describieron que el 20 % de las publicaciones fueron aportadas por los Estados Unidos, alrededor de un 15 % provenían de China, un 10 % de Japón y aproximadamente un 6.5 % de España, observando además un crecimiento del 2.5 % (observado antes de 2010) al 4.8 % en la contribución de Latinoamérica a las publicaciones a nivel mundial sobre SFE para el periodo analizado entre 2010 a 2013 [12].

La aplicación de la tecnología SFE en la industria de alimentos y afines continúa creciendo y este hecho puede constatarse al revisar las numerosas publicaciones sobre aplicaciones de la SFE con alta viabilidad técnico-económica basadas en la extracción de compuestos de alto valor a partir de hierbas [13], especias [14–16], material vegetal [17,18], tejidos animales [19], microalgas, frutas [20–22], hojas [23], lípidos [24], semillas [25], arroz [26], entre otros.

Según King (2014) y del Valle (2014), en la actualidad existen más de 150 plantas de extracción con fluidos supercríticos en el mundo, las cuales cuentan con celdas de extracción cuya capacidad supera los 0.5 m^3 de volumen [27,28].

1.2 Fundamentos de la Extracción con Fluidos Supercríticos en *Batch*

La extracción de matrices sólidas con SC-CO_2 en *batch* es un proceso discontinuo en el cual se utiliza un extractor de lecho fijo (ver figura 1.2), donde el lecho se encuentra formado por el propio material vegetal. Durante el proceso de extracción el disolvente es bombeado hacia la celda de extracción donde se encuentra depositado el material desde un tanque de almacenamiento (C), mediante una bomba de CO_2 (D). El disolvente pasa a través de un intercambiador de calor (F) donde se garantiza que alcance la temperatura de operación requerida. El caudal de CO_2 es controlado mediante un medidor de flujo (D), y se distribuye uniformemente en el interior del lecho de partículas sólidas (A ó B). Dentro de la celda de extracción, el CO_2 se desplaza a través del material vegetal solubilizando los componentes presentes en él. Conforme el disolvente fluye a través del material vegetal ocurre la transferencia de masa del soluto desde la fase sólida a la fase fluida, y en cualquier punto de la celda de extracción la concentración del extracto en la fase sólida y fluida varía de forma continua, pudiendo alcanzar la condición de equilibrio. Debido a que el lecho permanece fijo, la concentración del extracto en la fase fluida varía con el tiempo y la posición, de esta forma el proceso ocurre en régimen transitorio. Una vez que la mezcla formada por el soluto y el disolvente abandona el extractor pasa a través de una válvula de regulación de presión o BPR (G) y luego a un separador (H) donde la presión se reduce, el extracto precipita y el CO_2, en fase gas en estas condiciones, pasa a un sistema de recirculación que contiene filtros y demisters (J) para su purificación, así como un sistema de enfriamiento (K) para su condensación.

La extracción en *batch*, cuya descripción gráfica puede verse en la figura 1.3 [28], fue descrita por Brunner (1994) en las siguientes etapas:

i. La matriz solida depositada en la celda de extracción absorbe el disolvente supercrítico, dilatando la estructura de las células y los canales intercelulares, haciendo que la resistencia a la transferencia de masa disminuya.
ii. Al mismo tiempo ocurre la disolución de los compuestos que son solubles en el disolvente supercrítico.
iii. Los compuestos solubilizados son transferidos desde la parte interna del solido hasta la superficie.
iv. Los compuestos solubilizados alcanzan la superficie externa.

v. Ocurre la transferencia de las sustancias extraídas desde las superficies hacia el seno del disolvente supercrítico.

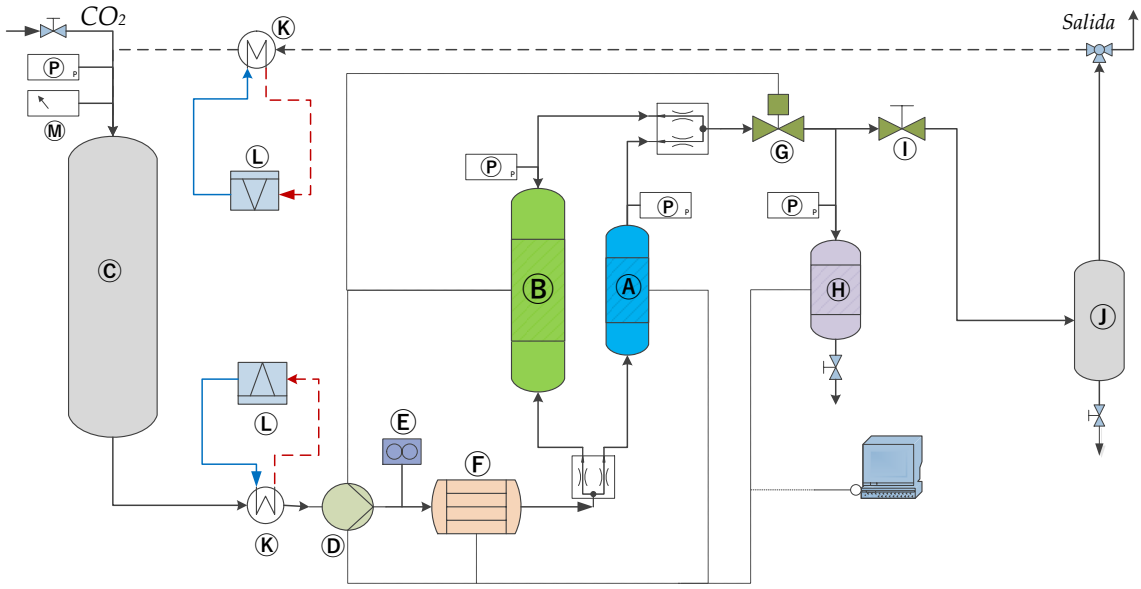

A = Celda de Extracción escala laboratorio
B = Celda de Extracción escala piloto
C = Tanque de Almacenamiento de CO_2
D = Bomba de CO_2
E = Caudalímetro
F = Intercambiador de Calor
G = Válvula BPR automática
H = Separador Ciclónico
I = Válvula BPR manual
J = Demister
K = Condensadores
L = Sistema de enfriamiento
M = Indicador de Volumen de CO_2
P = Manómetros
(·····) = Sistema de control PLC
(---) Recirculación

Figura 1.2 Diagrama esquemático de una planta de SFE (Thar SF2000) y su configuración para escalas de laboratorio y piloto.

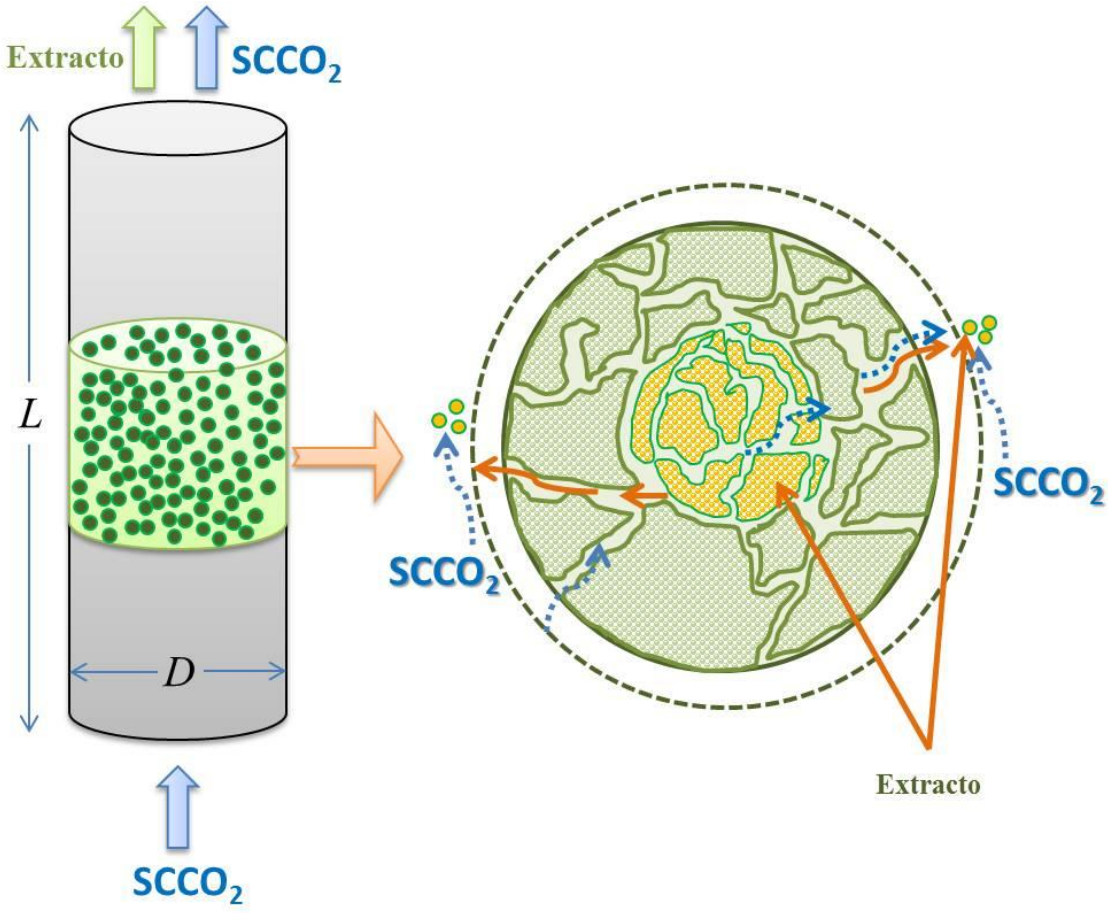

Figura 1.3 Esquema de una partícula de material vegetal durante la extracción SFE.

1.2.1 Cinética de Extracción

La extracción supercrítica en *batch* es un proceso discontinuo, es decir, que cambia en función del tiempo. La velocidad de extracción puede representarse gráficamente mediante una curva en la cual se relaciona la masa de extracto o soluto obtenido, a veces en relación a la masa de muestra inicial, en función del tiempo o la cantidad de disolvente consumido. Esta curva se denomina Curva Global de Extracción (OEC = *Overall Extraction Curve*).

Según Brunner (1994) a través del análisis de una OEC se puede extraer información clave sobre el comportamiento de un determinado extracto durante una extracción SFE, lo que permitirá la selección de variables que ayuden a garantizar una mayor viabilidad al proceso, entre las cuales se destaca el tiempo de extracción [29].

Sovová (1994) dividió la OEC en tres etapas: etapa de extracción constante CER (*Constant Extraction Rate period*), etapa con tasa de extracción decreciente FER (*Falling*

Extraction Rate period) y la etapa controlada por la difusión DC (*Diffusion Controlled Rate period*) [30]. De acuerdo con Brunner (2005) la primera parte de la curva sería muy aproximada a una línea recta, y correspondería a la etapa CER; en la segunda etapa FER la extracción disminuye hasta alcanzar valores muy cercanos al límite del rendimiento de extracción [4].

Una curva OEC típica puede describirse de la siguiente manera [31]:

1) Etapa CER: periodo en el que la retirada del extracto de la superficie externa de la partícula ocurre a una velocidad aproximadamente constante, predominando el fenómeno de convección. En la etapa CER, ocurre la extracción del soluto fácilmente accesible, es decir aquel contenido en las células rotas del material vegetal (el que ha sido previamente sometido a un proceso de molienda). La etapa CER se caracteriza por los parámetros cinéticos: tasa de transferencia de masa (M_{CER}), duración del periodo CER (t_{CER}), rendimiento durante el periodo CER (R_{CER}) y la concentración de soluto en la fase fluida a la salida del extractor (Y_{CER}).

2) Etapa FER: periodo en el que comienza a ser importante la resistencia a la transferencia de masa en la interfase sólido-fluido, siendo importante el efecto tanto de la transferencia de masa por convección como por la difusión del soluto dentro del material sólido. Parte del soluto se encuentra menos accesible, porque está contenido en células intactas y/o lejos de la superficie del material vegetal.

3) Etapa DC: periodo controlado por el mecanismo de difusión del soluto en la fase sólida, por haberse agotado el soluto fácilmente accesible contenido en la superficie de las partículas sólidas.

En la figura 1.5 se observa una OEC obtenida experimentalmente en la extracción con CO_2 supercrítico de flores de *Calendula officinalis*, en la cual se señalan los tres segmentos que corresponden a las etapas previamente descritas (CER, FER y DC).

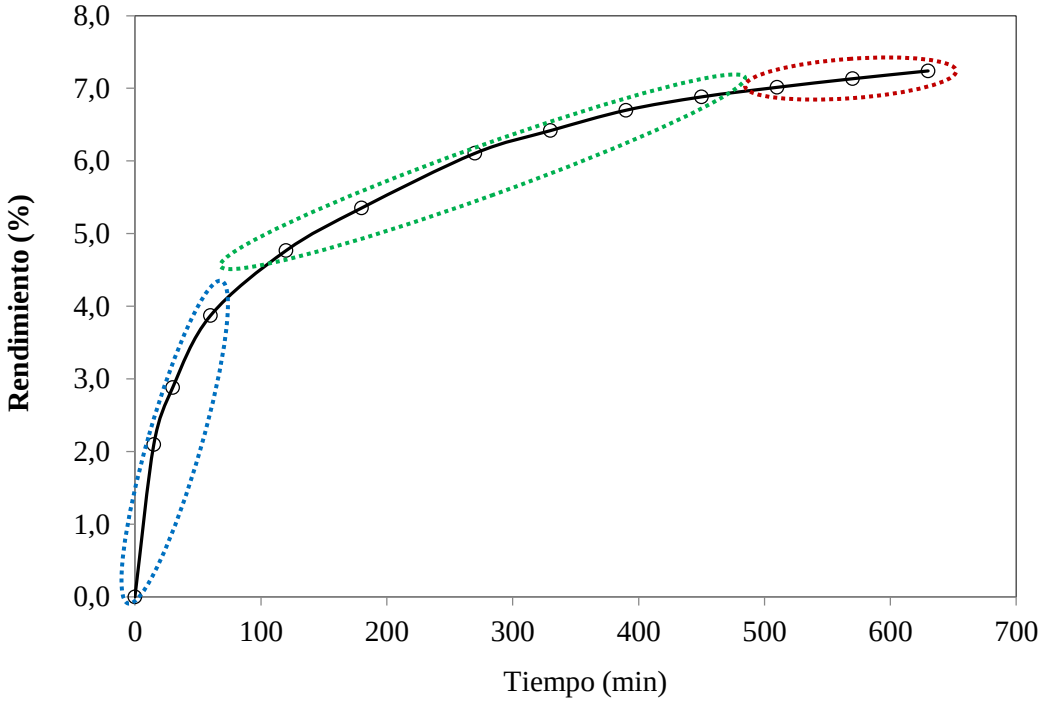

Figura 1.5 Cinética de extracción descrita mediante una OEC. (----) etapa CER, (----) Etapa FER y (----) Etapa DC.

1.2.1.1 Factores que afectan la cinética de extracción

Algunos de los factores que mayor efecto tienen sobre la cinética de extracción son parámetros de proceso como la temperatura, la presión, el caudal y de las características del material vegetal empleado, así como los parámetros geométricos de la celda de extracción. Debido a que éstas generalmente son diseñadas de forma cilíndrica, los factores geométricos que más efecto tienen sobre la cinética de extracción son el diámetro (D), la altura (L) y/o la relación entre ambos (L/D). Con respecto a la materia prima, se puede destacar el origen, las condiciones de cultivo y las operaciones de pretratamiento del material, como el secado y la molienda, además de las características estructurales de la materia prima. La porosidad del lecho (ε), también juega un papel importante en el proceso SFE, ésta se encuentra relacionada con la densidad real de la muestra y la densidad aparente (ver ecuaciones 1.1 y 1.2).

$$\varepsilon = 1 - \frac{\rho_s}{\rho_{ap}} \qquad \text{(Ecuación 1.1)}$$

Donde ε es la porosidad del lecho, $\rho_s\ (kg \cdot m^{-3})$ es la densidad real del sólido y $\rho_{ap}\ (kg \cdot m^{-3})$ es la densidad aparente.

$$\rho_{ap} = \frac{F}{V_{celda}} \qquad \text{(Ecuación 1.2)}$$

El tamaño de partícula tiene un gran efecto sobre el rendimiento de extracción, cuanto menor sea éste, mayor es la relación entre el área superficial y el volumen de la partícula, con lo que se consigue exponer una mayor proporción del soluto o extracto al contacto directo con el disolvente supercrítico, así como aumentar la facilidad para que el disolvente pueda difundir hacia el interior de la partícula. Del Valle y col. (2000) demuestran que es posible obtener mayores rendimientos de extracción a menores tamaños de partícula en la extracción de aceites esenciales [32]. Sin embargo, Reverchon y Marrone (2001) demostraron que al emplear muestras con tamaños de partícula demasiado pequeños existe una gran posibilidad que el disolvente forme caminos o rutas preferenciales, evitando con ello entrar en contacto con el soluto o extracto, y obteniéndose como resultado menores rendimientos de extracción [33]. Así, es fundamental que el lecho de extracción sea homogéneo evitando con ello la formación de bloques o agregados de partículas que afecten a la densidad del lecho.

1.3 Fundamentos del Escalado de Procesos de Extracción con Fluidos Supercríticos en *Batch*

Según Martínez (2005), uno de los mayores obstáculos en la implementación de la tecnología SFE es la alta inversión que se requiere para la instalación de una planta de extracción. Las condiciones de operación, especialmente la presión de extracción, y las dimensiones del equipo afectan significativamente esta inversión. Conocidas las condiciones de temperatura y presión, las que están fuertemente determinadas por la solubilidad de los solutos en el fluido supercrítico, el modelado matemático del proceso y el análisis de la cinética de extracción permiten definir tanto el volumen de la celda de extracción como el caudal requerido de disolvente para conseguir la tasa de extracción deseada en la escala de producción que se pretende desarrollar. Es por ello que una de las herramientas claves para estudiar el cambio de escala en un proceso SFE resulta de la aplicación de modelos matemáticos, los que al ajustar parámetros al fenómeno que se estudia a escala de laboratorio permitirán predecir el comportamiento a una escala mayor [34].

Para que un proceso alcance una escala de producción adecuada, se espera que haya sido previamente evaluado mediante la optimización de las condiciones de operación, incluido el tiempo de extracción, a partir de las cinéticas de extracción y el modelado de las mismas para revelar los mecanismos de transferencia de materia, que caracterizan la tasa a la cual los solutos son retirados del material vegetal [35,36]. Por otro lado, la eficiencia de la extracción y su selectividad están condicionadas a las condiciones de proceso, las propiedades del extracto o soluto y las características geométricas del equipo de extracción [37]. El análisis que se haga sobre esas condiciones de proceso permitirá maximizar la velocidad de extracción y el rendimiento de extracción.

En general, la ingeniería básica que suele aplicarse en el diseño de procesos SFE se encuentra disponible en estudios llevados a cabo a escala de laboratorio [38,39]. Debido a ello, las relaciones que existen entre los datos experimentales y los obtenidos a escalas piloto e industrial no deben asumirse o emplearse sin un análisis más profundo de los mismos. Las variaciones que presentan los equipos utilizados aportan diferencias que pueden ser significativas en cuanto a su capacidad operativa, y deben ser analizadas cuidadosamente para evitar errores en el momento de trasladar los datos en un proceso de escalado [40,41]. En la literatura se encuentran muy pocos datos disponibles referidos a cálculos de escalado de unidades en procesos de SFE para materiales sólidos [42,43].

Por otro lado, la biomasa utilizada en la SFE de materiales sólidos suele ser de alta complejidad debido a su origen vegetal, por lo que las características del sistema no pueden ser descritas mediante un único modelo [31]. Por todo ello, es de gran importancia establecer una metodología que permita la predicción del comportamiento de un proceso SFE a escala industrial a partir de los datos obtenidos en el laboratorio [38].

El uso del SC-CO_2, por ser un disolvente que no deja trazas en sus productos, posee una ventaja en términos de aplicación industrial en el contexto de las regulaciones sobre el uso de disolventes orgánicos que, además de un detrimento ambiental, aumentan los posibles riesgos para la salud de los consumidores. Sin embargo, una de las desventajas que limitan la aplicación de la tecnología SFE en la industria son los costos elevados de la instalación, así como el peligro inherente al empleo de altas presiones de trabajo [44].

Perrut (2000) demostró que los costos de puesta marcha de una planta o instalación para la extracción supercrítica suelen ser altos si se comparan con procesos que se realizan a bajas presiones o a presión atmosférica; también calculó el incremento al efectuar un cambio de

escala en un proceso SFE como la raíz cuarta de su capacidad $(V_T \times Q)^{0.24}$, donde V_T es el volumen total y Q el caudal de CO_2, partiendo de datos obtenidos en equipos de 0.5 l hasta 500 l de capacidad. Además, mediante la correlación obtenida a partir del índice de precios vs la capacidad de operación de diferentes plantas de SFE, demostró que la amortización del capital disminuye drásticamente cuando la capacidad aumenta [45].

Al estudiar la bibliografía existente referida al escalado de la SFE se observa que existen resultados divergentes en cuanto a los datos que se obtienen a escala de laboratorio, piloto e industrial. Algunos investigadores y académicos afirman que los resultados en torno a los rendimientos de extracción tienden a disminuir al aumentar la escala. Sin embargo, algunos fabricantes afirman que el rendimiento de extracción tiende a aumentar al incrementar la escala [41].

Por ejemplo, del Valle y col. (2005), observaron que los parámetros de transferencia de masa cambian cuando se pasa de la escala analítica a la escala industrial, y que además el rendimiento industrial no es correlativo al conseguido a escala de laboratorio, aun habiéndose utilizado los parámetros de mejor ajuste para la escala analítica [46]. Kotnik y col. (2007) encontraron una disminución del rendimiento de extracción al realizar un estudio de escalado de extracto de canela (*Matricaria chamomilla*) y pasar de escala laboratorio (celda de extracción con volumen de 6×10^{-5} m^3 con un rendimiento de 3.81 %) a piloto (celda de extracción con volumen de 4×10^{-3} m^3 con un rendimiento de 2.09 %) [47]. Prado y col. (2012) observaron un rendimiento global y un comportamiento cinético similar para la extracción supercrítica de semillas de uva (*Vitis vinífera* L.) a escala laboratorio y piloto, para un aumento de escala de 17 (celdas de extracción de 2.9×10^{-4} m^3 y 5.15×10^{-3} m^3). Sin embargo, Fernández-Ponce y col. (2016) hallaron un rendimiento global similar en la extracción de hojas de mango (*Mangifera indica* L.) al incrementar el volumen de la celda de extracción de 1×10^{-4} m^3, utilizado en escala de laboratorio, a una celda con un volumen de 5×0^{-3} m^3 empleado en la escala piloto, mientras que el rendimiento de los compuestos de interés aumentó de forma considerable en la escala piloto [23].

Teniendo en cuenta estas dificultades y divergencias, el aumento de escala se convierte en una cuestión fundamental para el estudio de un proceso de SFE. A partir de datos obtenidos en el laboratorio o planta piloto, se hace necesario desarrollar métodos para predecir el desempeño de procesos a escala industrial, para entonces evaluar la viabilidad técnica y económica del proceso. En este sentido, se debe destacar que mientras algunas

variables el proceso deben mantenerse constantes (por ejemplo, temperatura y presión de extracción) otras variables deben modificarse (por ejemplo, cantidad de material a extraer y caudal de fluido supercrítico) para reproducir a una mayor escala las curvas de extracción SFE (rendimiento en función del tiempo) obtenidas a escala analítica y/o laboratorio [48]. En este sentido, dentro de la SFE se han empleado diversos criterios de escalado, entre los cuales cabe destacar: a) la aplicación de las tradicionales reglas de pulgar de la ingeniería, b) el uso de modelos matemáticos simples y/o semi-empíricos, y c) los modelos basados en el balance de masa diferencial en el interior de la celda de extracción, entre otros.

1.3.1 Reglas de Pulgar de la Ingeniería

Las reglas de pulgar de la ingeniería son valores numéricos y sugerencias razonables de asumir que se han determinado a partir de la experiencia. Se basan en la aplicación de los fundamentos y la experiencia práctica. El objetivo de las reglas de pulgar no es el de sustituir los fundamentos teóricos, sino el de enriquecer el uso correcto de los mismos para resolver problemas [49].

El concepto de reglas de pulgar según Woods (2017) fue descrito por primera vez en el Diccionario de Frases y Fábulas de E. Cobhan Brewer en 1894, viniendo a ser: "*Una medida aproximada, práctica o de experiencia, distinta de la teoría, que hace alusión al uso del pulgar para mediciones groseras. La primera articulación del pulgar adulto mide aproximadamente 1 pulgada (2.5 cm)*" [49].

En la actualidad existen muchos trabajos publicados en los que se aplican las reglas de pulgar en diferentes campos de la ciencia, que van desde el diseño de equipos y procesos [49,50], la programación [51], simulación [52], modelado [53], producción de fármacos [54], energía [55], economía [56,57], etc.

Hall (2012) publicó un compendio de aplicaciones de las reglas de pulgar en el diseño de equipos y procesos en ingeniería química, en donde hace referencia al uso de relaciones de aspecto entre la altura vertical y el diámetro de recipientes (L/D) en rangos de 4:1 para el diseño de tanques que requieren maximizar la transferencia de calor a través de una camisa, y maximizar el tiempo de contacto de un gas, entre otras [50].

Algunos autores han propuesto varias reglas de pulgar para el escalado en la SFE de productos naturales, algunas de ellas se basan en las leyes de afinidad establecidas para estudio de la dinámica de fluidos y la operación de bombas [50].

Perrut (2000) sugiere que al elegir los posibles criterios o reglas para el escalado de un proceso SFE, se debería tener en cuenta las relaciones geométricas, físicas y químicas, las cuales deben permanecer sin cambios intencionales en función de los mecanismos que conducen el proceso. Tal cuidado asegura una mayor precisión al comparar los resultados obtenidos a escalas diferentes, y asegura que estos resultados sean fenomenológicamente consistentes. Teniendo en cuenta esto, se han propuesto varias relaciones o criterios para el escalado SFE, los cuáles pueden definirse de forma general como la aplicación de las reglas de pulgar de la ingeniería en un proceso SFE [45]:

i. Cuando la solubilidad limita el proceso, la masa de disolvente supercrítico consumido (S) por unidad de masa de materia prima (F), es decir la relación (S/F), debe permanecer constante;

ii. Cuando la difusión es el mecanismo limitante, la relación del caudal de disolvente supercrítico (Q) por unidad de masa de materia prima F, es decir la relación (Q/F), debe mantenerse constante;

iii. Cuando ambas limitaciones son relevantes, las relaciones (S/F) y (Q/F) deben mantenerse constantes;

iv. Una alternativa aproximada es fijar tanto la relación (S/F), como (Q/F) y fijar también el número adimensional de Reynolds (Re); esto puede implicar efectos relacionados con el tamaño de partícula de la materia prima, siempre que variables como la presión y la temperatura se mantengan constantes [58];

Existen además criterios que buscan establecer las similitudes geométricas de las celdas de extracción. En general, las celdas de extracción son cilíndricas, por lo que estos criterios aportan detalles sobre la relación entre la longitud o altura y el diámetro del lecho empacado (L/D). En este sentido, al revisar la literatura es posible encontrar diversas aplicaciones en el escalado de procesos SFE [35,59–61].

Rosa y Meireles (2005), al realizar un estudio sobre la estimación de los costos de manufactura de un proceso SFE, describieron de forma general, que al aplicar la regla de pulgar que consiste en mantener la relación (S/F) constante en un aumento de escala es

posible obtener una buena repetitividad de los datos obtenidos a escala de laboratorio. En este estudio indicaron además que en un proceso en el cual se pretende alcanzar un nivel adecuado de escalado, se espera que previamente se haya valorado la optimización de las condiciones de operación, selección del tiempo de extracción a partir de curvas de rendimiento vs tiempo, y la modelización de dichas curvas con el objeto de revelar los mecanismos que caracterizan las tasas a las que los solutos son removidos desde la materia prima [62].

Moura y col. (2005) y Carvalho y col. (2005) desarrollaron experimentos para procesos de escalado supercrítico de hinojo (*Foeniculum vulgare)* y Romero (*Rosmarinus officinalis*), respectivamente. Las extracciones se llevaron a cabo en dos equipos de extracción con diferentes relaciones de altura y diámetro de celda de extracción (L/D); los resultados les llevaron a la formulación de dos ecuaciones semi-empíricas de escalado, a partir de las variables de proceso (masa de muestras, F, caudal de SC-CO_2, Q y geometría de la celda de extracción; altura, L y diámetro, D) [15,63].

La ecuación 1.3 corresponde a un sistema en el cual se busca mantener constante la relación entre el rendimiento global de extracción y la relación (S/F). Esto resulta útil para efectuar el cálculo del caudal a partir de la masa de la muestra y la geometría de la celda de extracción, permitiendo con ello obtener rendimientos globales similares en experimentos con diferentes unidades de extracción a una determinada cantidad de disolvente [64].

$$\frac{Q_2}{Q_1} = \left(\frac{F_2}{F_1}\right)^2 \left(\frac{L_1}{L_2}\right)\left(\frac{D_1}{D_2}\right) \qquad \text{(Ecuación 1.3)}$$

Donde los números 1 y 2 se refieren a las respectivas unidades o equipos de extracción de distinto tamaño y/o forma.

La ecuación 1.4, por su parte, corresponde a un sistema en el cual se mantiene constante la relación entre la tasa de extracción y el tiempo de extracción, buscando con ello obtener cinéticas similares en dos unidades de extracción supercrítica con diferente geometría de la celda de extracción.

$$\frac{Q_2}{Q_1} = \left(\frac{F_2}{F_1}\right)^2 \left(\frac{L_1}{L_2}\right)\left(\frac{D_1}{D_2}\right)^3 \qquad \text{(Ecuación 1.4.)}$$

Martínez y col. (2007) propusieron dos reglas de pulgar adicionales como criterios de escalado para la extracción supercrítica de aceite esencial de brotes de clavo (*Eugenia*

caryophillus) y raíces de vetiveria (*Vetiveria zizanioides* L.), empleando una celda de extracción de 5×10^{-6} m^3 para los experimentos a menor escala y una de 3×10^{-4} m^3 en escala mayor. Durante las extracciones se mantuvo constante la velocidad lineal del disolvente (ecuación 1.5) y el tiempo de residencia del disolvente (ecuación 1.6) [65].

$$u = \frac{Q}{A} \qquad \text{(Ecuación 1.5)}$$

La Ecuación 1.6, surge de la condición de mantener constante el tiempo de residencia del disolvente a través del lecho fijo, definida por:

$$t_{res} = \frac{\pi D^2 L \varepsilon \rho_{CO_2}}{4Q} \qquad \text{(Ecuación 1.6)}$$

Donde, t_{res} es el tiempo de residencia del SC-CO_2, ε es la porosidad del lecho, ρ_{CO_2} es la densidad del CO_2, u es su velocidad lineal y A es el área de la sección transversal de la celda de extracción.

Quispe-Condori y col. (2008) desarrollaron un estudio sobre el efecto de cambio de altura de la celda de extracción sobre los parámetros cinéticos en la SFE de β-cariofileno a partir de María Milagrosa o "Erba-Baleeira" (*Cordia verbenácea* DC) a 30 MPa, 323 K, y 20 MPa y 314 K, respectivamente. Al mantener la regla de pulgar S/F, obtuvieron curvas OEC con rendimientos de extracción y comportamiento similar [66].

Yesil-Celiktas y col. (2009) obtuvieron extractos SFE a partir de corteza de *Pinus brutia* en las condiciones de 20 MPa, 333 K, y empleando un 3 % de etanol como cosolvente, manteniendo una relación $(S/F) = 30$ constante como criterio de escalado. Los autores encontraron que al adoptar esta regla de pulgar el escalado resultó adecuado al efectuar un cambio de escala desde una celda de 3×10^{-4} a una de 6.5×10^{-3} m^3 [67].

Prado (2010) desarrolló un estudio sobre el cambio de escala aplicando la regla de pulgar (S/F) y manteniendo constante el tiempo de residencia del CO_2 en la SFE de clavo (*Syzygium aromaticum*), jengibre (*Zingiber officinale)*, residuo de caña de azúcar (*Saccharum officinarum*), cidrón (*Lippia alba)* y semillas de uva (*Vitis vinífera*). Sus resultados demostraron que la regla de pulgar adoptada resultó eficiente al reproducir de forma similar las cinéticas que fueron obtenidas tanto a escala de laboratorio como piloto [64].

Albuquerque y Meireles (2012) efectuaron un estudio de escalado para la producción de bixina a partir de semillas de achiote o urucum (*Bixa Orellana* L.) a 333K y 40 MPa, empleando celdas de extracción de 7×10^{-6} y 2.9×10^{-4} m^3 y manteniendo constante $(S/F) = 35$, obteniendo rendimientos y cinéticas similares en ambas escalas [68]. Para este caso las cinéticas fueron modeladas según un método simple propuesto por Meireles (2008), en el cual las curvas OEC fueron descritas mediante un *spline* lineal donde la masa de extracto fue obtenida a partir de la división en diferentes rectas [31].

Por otra parte, Prado y col. (2012) desarrollaron un proceso de escalado en la extracción de semillas de uva *Vitis vinífera* de volúmenes de 3×10^{-4} hasta 5.15×10^{-3} m^3, empleando entre sus criterios el mantener constante las reglas de pulgar (S/F) y (Q/F), siendo la relación (S/F) la que resultó ser más consistente y adecuada al obtener curvas OEC con similar comportamiento en ambas escalas [41].

Zabot y col. (2014) estudiaron el efecto de la geometría sobre los parámetros cinéticos en la extracción SFE de brotes de clavo (*Eugenia caryophyllus*), a las condiciones operacionales de 15 MPa y 314 K con tres relaciones para la regla de pulgar (S/F) de 2.6, 4.6 y 6.6. Los resultados mostraron que al mantener la regla de pulgar (S/F) se obtuvieron cinéticas similares al efectuar un cambio de geometría (relación L/D) en las celdas de extracción, demostrando ser un criterio adecuado para el escalado de aceite de *E. caryophyllus* [60].

Fernández-Ponce y col. (2016), realizaron un escalado para la obtención de extractos de hojas de mango (*Mangifera indica* L.) de 1×10^{-4} a 5×10^{-3} m^3 utilizando la regla de pulgar $Q \times (D/F)$, con la que obtuvieron buenos resultados en los resultados experimentales al efectuar el aumento de escala [23].

De Melo y col. (2014) desarrollaron una operación de escalado en la extracción SFE de ácidos triterpénicos a partir de corteza de Eucalipto (*Eucalyptus globulus)* desde escala laboratorio (5×10^{-4} m^3), a escala piloto (5×10^{-3} m^3) e industrial (8×10^{-2} m^3), a 20 MPa y 313 K como condiciones de operación, y con uso de etanol (2.5 y 5 %) como cosolvente. Para el escalado aplicaron la regla de pulgar de mantener S/F constante $(S/F) = 10$ y el ajuste de las curvas OEC fue realizado utilizando diferentes modelos matemáticos. Los resultados indicaron que la regla de pulgar (S/F) permitió obtener resultados válidos e independientes de la geometría de la celda de extracción [18].

Mezzomo y col. (2009) llevaron a cabo diversos experimentos de escalado SFE de melocotón (*Prunus pérsica*) para dos escalas 1×10^{-5} y 8.8×10^{-5} m^3, empleando diferentes reglas de pulgar como criterios de escalado: (S/F), (Q/F), $[Q/F + (S/F)]$, $[Re + (S/F) + Q]$. Las curvas OEC fueron ajustadas siguiendo varios modelos matemáticos, indicando que la regla de pulgar que mejor describía los resultados al efectuar el cambio de escala fue la de mantener constante la relación Q/F [58].

Haan y col. (2009) realizaron experimentos de escalado de aceite de semillas cártamo (*Carthamus tinctorious*) desde una escala de laboratorio (5×10^{-4} m^3) a una escala semi-industrial de 0.26 m^3, empleando la regla de pulgar Q/F, obtenido rendimientos de extracción similares entre la escala de laboratorio y la semi-industrial [69].

Hatami y col. (2010) realizaron experimentos de escalado de SFE de aceite de clavo (*Eugenia caryophillus*) utilizando dos escalas (6×10^{-6} m^3 y 2.8×10^{-6} m^3), empleando como criterios de escalado las reglas de pulgar de mantener constante el tiempo de residencia y la velocidad lineal del SC-CO_2; los resultados indicaron que ambas reglas de pulgar predijeron de forma adecuada el comportamiento cinético de extracción durante el escalado [70].

Vale la pena señalar que, además de la elección de los criterios adecuados de escalado, los resultados pueden no ser confirmados a escalas mayores debido a la presencia de fenómenos irrelevantes a menor escala que llegan a ser no despreciables a grandes escalas [42,71]. La agregación de biomasa y la canalización son dos ejemplos ilustrativos que deben ser citados al respecto [72].

1.3.2 Modelos Matemáticos

Desde el punto de vista de la ingeniería, el escalado en proceso de extracción SFE requiere tanto del conocimiento de las condiciones óptimas de operación como de los parámetros de proceso, tales como la cinética de la transferencia de masa y las condiciones de equilibrio. Frecuentemente estos parámetros se determinan mediante la implementación de modelos matemáticos que describen el proceso de extracción a partir de datos experimentales previamente obtenidos a escala analítica o laboratorio.

Según Oliveira y col. (2011), el modelado matemático de la SFE de productos con alto valor añadido a partir de matrices vegetales suele presentar dificultades para su aplicación

debido a la existencia de diferentes estructuras en el interior de cada material. Para reducir la complejidad del modelo es necesario asumir determinadas consideraciones, como son las relacionadas con la forma en la cual el extracto o soluto se encuentra distribuido en el interior de las partículas, la forma en que se halla en contacto el disolvente con la red de poros del material vegetal, su distribución en el interior de las partículas y, además de ello, considerar la resistencia interna y externa a la transferencia de masa [73].

Debido a esto, previo a la SFE, el material vegetal deshidratado se suele someter a una molienda con el objetivo de incrementar el área superficial que estará en contacto con el disolvente supercrítico, provocando la rotura de las paredes celulares, especialmente en la superficie de las partículas, incrementando las posibilidades de que el disolvente pueda acceder al interior de las células y/o paredes vegetales y entrar en contacto con el soluto, favoreciendo así el aumento de la tasa de extracción. Usualmente este efecto puede notarse observando las cinéticas de extracción. La reducción del tamaño de partícula genera estructuras con diferentes formas geométricas, las cuales pueden ser esféricas, cilíndricas o en forma de rodajas. Estas formas dependen a su vez de las características intrínsecas del material vegetal.

Los modelos matemáticos son una herramienta poderosa y útil que permiten describir los resultados experimentales, describiendo los principales fenómenos del proceso de extracción a través de una ecuación o un sistema de ecuaciones, las que posteriormente podrán ser aplicadas a condiciones de trabajo diferentes de aquellas inicialmente investigadas, permitiendo obtener la información necesaria para el diseño y escalado del proceso.

Muchos de estos modelos matemáticos se han descrito en la literatura enfocándose en el ajuste de la curva OEC o cinética de extracción, siendo la mayoría desarrollados a partir de ecuaciones semi-empíricas o del balance diferencial de masa aplicado en el lecho empacado. De manera general estos modelos consideran que, en la extracción de un soluto a partir de la matriz sólida, el extracto está compuesto principalmente de una única sustancia, independientemente de su composición química. Algunos modelos consideran la resistencia a la transferencia de masa en la fase fluida o en la fase sólida como controlador de proceso, mientras que otros consideran las dos resistencias de manera combinada controlan el proceso de extracción [74].

Según Silvestre y col. (2011), los modelos empleados en la extracción supercrítica a partir de materiales vegetales aplican, básicamente, las siguientes consideraciones: es una operación isotérmica, con caída de presión despreciable a lo largo de la celda de extracción, con una porosidad y densidad sólida del lecho empacado constante durante la extracción. Además de esto, se asume que la carga de soluto en el fluido supercrítico es suficientemente pequeña como para despreciar la dispersión axial, y asumir que la densidad y la velocidad del fluido supercríticos permanecen aproximadamente constantes. La asunción de estos factores permite reducir el número de ecuaciones necesarias para describir balance de masas del proceso de extracción supercrítica, así como las relaciones de equilibrio y las leyes cinéticas [73].

Los modelos matemáticos para la SFE se desarrollaron a partir de múltiples experimentos llevados a cabo a escala laboratorio. Según Sovová (2017), los primeros modelos publicados aparecieron en la década de los ochenta con los trabajos de Brunner (1984), con un estudio de dos modelos para la SFE, y más tarde con Reverchón (1997), quien realizó una análisis de los modelos aplicados a la SFE clasificándolos en tres categorías [75]:

- Modelos teóricos que utilizan funciones matemáticas simples para describir el rendimiento de extracción en función del tiempo, y cuyo comportamiento generalmente obedece aproximadamente a una cinética de reacción de primer orden.
- Modelos que consideran una analogía entre la transferencia de calor y de masa.
- Modelos basados en el balance de masa diferencial a lo largo de la celda de extracción. Estos modelos consideran el efecto del equilibrio de fases, las resistencias interna y externa a la transferencia de masa y patrones de flujo, para describir la velocidad de extracción.

1.3.2.1 Modelos teóricos

Uno de los primeros modelos teóricos desarrollados se basa en el uso de una ecuación cinética (ecuación 1.7) y fue publicado en 1989 por Naik y Lenz, quienes propusieron un modelo empírico para describir el rendimiento de extracción como una función del tiempo, utilizando CO_2 líquido y diferentes materias primas de origen vegetal [76]:

$$Y = Y_{\infty}\left(\frac{t}{b+t}\right) \qquad \text{(Ecuación 1.7)}$$

Donde ***Y*** es la relación entre la masa de extracto obtenido en el tiempo t y la masa inicial de muestra (kg/kg), e Y_∞ es el valor de rendimiento para un tiempo de extracción infinito.

El cambio del rendimiento con respecto al tiempo de extracción predicho mediante este tipo de modelos se describe de forma similar a una isoterma de Langmuir y, según Esquivel y col. (1999) Y_∞ depende sólo del material que está siendo utilizado. En términos del modelo (Y_∞/b) es la pendiente inicial que resulta de graficar Y vs t. Ahora bien, desde la definición de Y, la pendiente inicial debería ser a su vez una función creciente de la carga inicial del soluto en la fase extraíble y el caudal másico del disolvente por unidad de masa del material vegetal. Por lo tanto, b puede considerarse una función del caudal másico, la temperatura y la presión [77].

El modelo de Barton (1992), es otro modelo empírico citado por Reverchon (1997), entre otros, que sigue el comportamiento de una cinética de primer orden. Este modelo, que ha sido aplicado satisfactoriamente por ejemplo en la SFE de la oleorresina de vainilla, en lugar de emplear relaciones de transferencia de masa y de equilibrio, utiliza una constante cinética asumiendo que la tasa de extracción es proporcional a la concentración de soluto que queda en la partícula del material vegetal. El modelo matemático se describe mediante la ecuación 1.8 [3,78]:

$$Y = Y_\infty(1 - exp\{-kt\}) \qquad \text{(Ecuación 1.8)}$$

Donde ***Y*** es el rendimiento de extracción (kg/kg), t es el tiempo (s), Y_∞ es el valor de rendimiento para un tiempo de extracción infinito ($t \to \infty$) y k es la constante cinética de Barton. Utilizando la ecuación 1.8 en términos de $ln(1 - Y/Y_\infty)$ vs t, es posible llevar a cabo una regresión lineal de los datos cinéticos experimentales y obtener los parámetros del modelo (k e Y_∞) minimizando el correspondiente coeficiente de regresión (R^2).

La constante cinética de Barton (k) puede asociarse al coeficiente de transferencia de masa en la fase fluida (k_f) a través del área interfacial específica (a_0) según la siguiente ecuación:

$$k_f = k/a_0 \qquad \text{(Ecuación 1.9)}$$

Dónde:

$$a_0 = 6\,(1 - \varepsilon)/d_p \qquad \text{(Ecuación 1.10)}$$

Siendo ε la porosidad del lecho empacado y d_p rel diámetro medio de la partícula sólida.

Cháfer y Berna (2014), aplicaron los modelos empíricos propuestos por Naik y Barton y encontraron buen ajuste con los datos experimentales para describir el proceso SFE de D-pinitol [79].

No obstante, este tipo de modelos empíricos no tienen en cuenta las interacciones entre el soluto y la matriz sólida. Sin embargo, resultan útiles cuando no existe suficiente información sobre el equilibrio de fases del sistema y/o los mecanismos de transferencia de masa, siendo la ventaja su gran simplicidad a la hora de ser aplicados [80–82].

1.3.2.2 Modelos Basados en la Analogía a la Transferencia de Calor

Reverchón (1997) propuso tratar el proceso SFE como un fenómeno de transferencia de calor en el cual cada partícula de biomasa se considera como una esfera caliente que se enfría en un medio uniforme. También asumió que los solutos siguen la segunda ley de difusión de Fick al considerar que se encuentran distribuidos uniformemente en el interior de la partícula. La ecuación 1.11 representa el modelo análogo a la transferencia de calor [3].

$$\frac{q}{q_0} = \left(\frac{6}{\pi^2}\right)\sum_{n=1}^{\infty}\frac{1}{n^2}\,exp\left(-\frac{n^2\pi^2 D_{12}t}{r^2}\right) \qquad \text{(Ecuación 1.11)}$$

Donde *n* es un integrador, *r* es el radio de la esfera (m), D_{12} es el coeficiente de difusión en la esfera ($m^2 \cdot s^{-1}$), *t* es el tiempo de extracción (s), q es la concentración del soluto que permanece en la esfera ($kg \cdot m^3$), y q_0 es la concentración inicial del material extraíble.

1.3.2.3 Modelos Basados en la Transferencia de Masa

El balance de masa de la fase sólida en el interior de la celda de extracción se encuentra condicionado por las simplificaciones y las condiciones asumidas por cada investigador con respecto a la composición de la matriz sólida y a las cinéticas de extracción que se han obtenido [73].

En la realización del balance de masa convencional sobre un proceso de SFE de sólidos, inicialmente se debe considerar el sistema como un sistema cilíndrico el cual se encuentra formado por las partículas de la materia prima o biomasa y cuya disposición en el interior

de dicho cilindro es homogénea. El disolvente se desplaza a través del lecho de extracción de forma axial, retirando el extracto o soluto de la materia prima. En la figura 1.6 se observa el esquema simple de un proceso de SFE donde L_B es la altura del lecho de extracción y l es la coordenada axial.

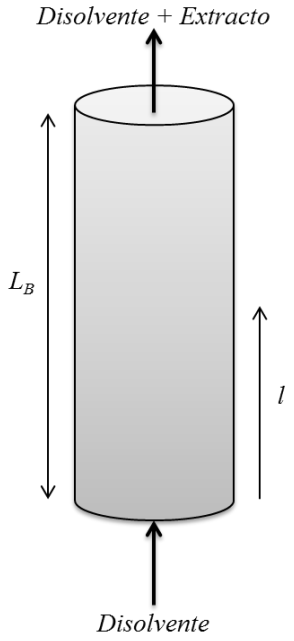

Figura 1.6 Esquema de un proceso de SFE (Adaptado de Martínez, 2005) [34]

Brunner (1994) describió el sistema de extracción supercrítica para sólidos tomando las siguientes consideraciones: existe una fase sólida, la cual se encuentra formada por la biomasa o materia prima que se someterá a extracción y una fase fluida, la cual estará formada por el disolvente con el extracto o una parte de éste disuelto en el disolvente. El contacto entre la biomasa y el disolvente creará un movimiento o transferencia de compuestos entre ambas fases, y en dicho movimiento se encuentran presentes diversos fenómenos de transporte como la convección (fase fluida), dispersión (soluto en el disolvente o fase fluida), difusión (mezcla entre el soluto y disolvente en la fase fluida), y transferencia de masa en la interfaz sólido-fluido [29]. Debido a esto el proceso de extracción es representado a través de ecuaciones de balances de masa para el soluto tanto en su fase sólida como en su fase fluida, donde las diferencias residen en la caracterización de su fase de equilibrio, los patrones de flujo del disolvente y la difusión del soluto en la fase sólida.

Según Sovová (2005), la fase de equilibrio depende de la temperatura del sistema y de la composición del disolvente, el soluto y la biomasa o matriz sólida, habiendo que tener en

cuenta dos consideraciones: en la primera de ellas, el proceso se encuentra gobernado por la transferencia de masa y la interacción entre el soluto y la matriz. En esta fase, la solubilidad del soluto en el disolvente alcanza el valor de la fase de equilibrio, lo cual ocurre en la primera etapa de la extracción, cuando el soluto se encuentra aún en el interior de las partículas a una alta concentración, y a medida que la extracción se va llevando a cabo su concentración disminuye hasta el punto en que la fase de equilibrio pasa a ser menor que la solubilidad. La segunda consideración se basa en la gran importancia que representa la forma, el tamaño y el área superficial de las partículas, así como la estructura interna de la muestra y la interacción que puede haber entre el soluto o extracto y la misma muestra que se somete a un proceso SFE, puesto que pueden afectar la segunda etapa de extracción al estar involucradas en la difusión del soluto en la fase sólida, lo cual suele estar caracterizada por una baja concentración y porque en esta etapa la resistencia a la transferencia de masa interna la variable que gobierna el proceso [83].

El patrón de flujo del disolvente suele reflejarse en la primera etapa de la extracción supercrítica y una de las consideraciones ideales es asumir que el patrón de comportamiento del fluido ocurre de forma “plug-flow”; de este modo, el disolvente se desplazará con velocidad radial homogénea asegurando con ello una buena distribución y mayor efecto sobre el rendimiento de extracción. Al asumir este comportamiento del fluido se desprecia la dispersión axial, es decir, la probabilidad de que se dé lugar a una convección natural y a la formación de canales por el disolvente durante la extracción. La dispersión axial suele ocurrir a menudo cuando la relación entre la altura y el diámetro de la celda de extracción es muy baja, esto aumenta el riesgo de formación de canales y la convección natural es una consecuencia de posibles gradientes de densidad a causa de diferencias en la concentración o temperatura de extracción.

Además, tomando en cuenta lo anteriormente expuesto y partiendo de que en un lecho cilíndrico con velocidad en dirección axial y cuya longitud es superior a la del diámetro, se puede despreciar cualquier forma de transferencia de masa que pueda ocurrir en las direcciones radiales o tangenciales, debido a que éstas se vuelven insignificantes durante la transferencia de masa axial. Es por ello que generalmente, en la aplicación de los modelos matemáticos más utilizados en la extracción supercrítica, la dispersión axial suele despreciarse siguiendo la regla de pulgar siguiente: $\left({}^{L}/_{d_p} > 50\right)$, donde d_p es el diámetro medio de las partículas de la biomasa. Además, se suele asumir que el comportamiento del

fluido del disolvente es ideal, siguiendo dos tipos de comportamientos: "plug-flow" en celdas de extracción grandes y mezcla ideal en celdas pequeñas [35].

En este orden de ideas, los modelos basados en la transferencia de masa pueden dividirse en modelos de un solo estado y modelos basados en la estructura compleja del material sólido. Los primeros consideran que el proceso SFE se encuentra caracterizado por un solo estado, mientras que la segunda categoría de modelos se enfoca en la descripción de la estructura del material, y dividen la extracción en diferentes periodos o etapas, cada una de las cuales se encuentra gobernada por diferentes parámetros [84]. Algunos de los modelos de un solo estado más relevantes y que se han descrito en la literatura son:

Modelo de difusión: propuesto por Crank (1975), considera que el material es un sólido homogéneo no poroso y el proceso se caracteriza por poseer una difusión interna en la partícula, equilibrio de fases en la superficie externa y transferencia externa de masa desde la superficie hacia el fluido [85].

Modelo de desorción: propuesto por Tan y Liou (1989), este modelo a diferencia del modelo de difusión propuesto por Crank (1975) considera que el material es poroso y que el soluto se desplaza desde las paredes de los poros mediante desorción, seguido por una difusión interna, equilibrio de fase en la superficie de la partícula y transferencia de masa externa [86].

Modelo de encogimiento o "Shrinking Core" (SC): este modelo fue propuesto por Goto y col. (1996) y en él se describe la desorción irreversible seguida por una difusión en partículas porosas a través de sus poros [87]. En términos generales, el modelo SC, considera que la partícula se encuentra caracterizada por un núcleo o *core*, lleno de soluto y durante la extracción supercrítica, el núcleo disminuye sus dimensiones, es decir, se encoge debido a que el soluto se desplaza hacia su frontera, disolviéndose en el disolvente y difundiéndose a través de la corteza de la partícula [88].

Este modelo ha sido aplicado por algunos autores en diferentes materiales. Por ejemplo, Ahmed y col. (2012) aplicaron el modelo SC en el modelado de la extracción supercrítica de hojas de romero proveniente de Algeria, a 22 MPa y 313 K, con unos resultados experimentales que presentaron buen ajuste según el modelo [89]. Por otro lado, Kitzberg y col. (2009) aplicaron diferentes modelos matemáticos en la obtención de extractos supercríticos de Shiitake *Lentinula edodes* bajo unas condiciones de extracción de 303 a 323

K y 15 a 35 MPa; los resultados indicaron que el modelo SC fue uno de los que mejores ajustes presentó con sus datos experimentales [90].

Modelo matemático microestructurado: existen otros modelos basados en la estructura compleja de las partículas, los cuales incluyen y se ha enfocado en la microestructura de las plantas aplicando conocimientos provenientes de la fisiología de las mismas. Estos modelos describen la estructura, forma y ubicación de las estructuras secretoras y profundizan en el comportamiento que tiene lugar durante la extracción. Mediante el análisis de imágenes obtenidas a través de micrografías electrónicas de barrido (SEM) antes y después del proceso SFE es posible determinar las estructuras secretoras en donde se hallaba el extracto y su morfología consiguiendo así identificar tres tipos de estados de extracción: desde las estructuras secretoras que se han quebrado o deformado durante el pretatamiento, las estructuras rotas después de cierto tiempo de extracción y las que han sufrido menos el proceso SFE y permanecen intactas [91,92].

1.3.2.3.1 Modelo BIC (*Broken and Intact Cells*)

El modelo BIC publicado en 1994 y generalmente denominado como *Modelo de Sovová* está basado en una extensión del modelo fenomenológico propuesto inicialmente por Edward Lack en su tesis doctoral en 1985, donde la ecuación que propuso fue adoptada a partir de un modelo de secado desarrollado por Krisher en 1978 y que ha sido descrito en algunas publicaciones como el modelo “plug-flow” de Lack [75,77].

El modelo de BIC planteó en su concepción la existencia de células intactas y células quebradas (*Broken and Intact Cells*, BIC) considerando que la fase solida se encuentra dividida entre células intactas y células quebradas. Es decir, en las plantas, debido a su naturaleza, el soluto, el cual puede entenderse como un aceite volátil, se encuentra contenido en el interior de las células vegetales protegido por la pared celular, por lo que una forma de pretratamiento de este tipo de materiales debe involucrar procesos como la molienda o trituración con el objeto de aumentar la superficie de contacto entre la partícula sólida y el disolvente. Esto va a dar lugar a una rotura de una fracción de las paredes celulares provocando de esta forma que el soluto se encuentre libre y pueda entrar en contacto con el disolvente. Sin embargo, el tratamiento de molienda o reducción de tamaño de partícula al que se somete la muestra no logra romper la totalidad de las paredes celulares de tal manera que una parte del soluto permanece protegido o aislado, siendo de difícil acceso para el

disolvente. A partir de estas consideraciones, se puede dividir la cantidad total de soluto disponible en dos fracciones; una de fácil acceso y otra de difícil acceso [84,93].

Según Sovová (1994) el modelo BIC describe el fenómeno ocurrido en un lecho cilíndrico a través del cual un disolvente se desplaza en dirección axial, con velocidad U. El disolvente entra puro en el extractor con presión y temperatura constantes durante el proceso de extracción. Además, se considera que el lecho de extracción es homogéneo con respecto al tamaño de partículas sólidas que componen la biomasa o muestra y a la distribución inicial del soluto [30].

El modelo BIC desprecia en sus ecuaciones de balance de masa los términos referentes a la dispersión en la fase fluida y la difusión en la fase sólida, además de la variación de Y en función del tiempo, al considerar que este tipo de fenómenos tienen un efecto no significativo sobre el proceso si se comparan con la convección en la fase fluida causada por el desplazamiento del disolvente a una determinada velocidad [75,93].

Una descripción detallada del balance de masa diferencial aplicado en el modelo BIC fue publicada por Huang (2014) [94] y Sovová (2017) [75]:

Para el balance de masa diferencial en la fase sólida, donde la concentración en la superficie de la partícula depende del contenido de extracto en la fase sólida, es decir, x, se tiene la siguiente ecuación:

$$\rho_s(1-\varepsilon)\frac{\partial x}{\partial t} = -J(x,y) \qquad \text{(Ecuación 1.12)}$$

Donde ρ_s es la densidad real del sólido o muestra (kgm^{-3}), ε es la porosidad del lecho, y es el contenido del extracto en la fase fluida $\left(kg \cdot kg_{CO_2}^{-1}\right)$, t es el tiempo de extracción (s).

En lo referente al balance de masa diferencial de masa en la fase fluida:

$$\rho\varepsilon\frac{\partial y}{\partial t} + \rho U\frac{\partial y}{\partial h} = J(x,y) \qquad \text{(Ecuación 1.13)}$$

Donde h es la coordenada axial a lo largo del lecho de extracción (m), ρ es la densidad del CO_2 $\left(kg_{CO_2} \cdot m^{-3}\right)$, U es la velocidad superficial $(m \cdot s^{-1})$, y x es el contenido de extracto en la fase sólida $(kg \cdot kg^{-1})$. El término a la izquierda de la ecuación (1.13) representa la acumulación del extracto y el segundo término se refiere a la convección. El

símbolo a la derecha representa la tasa de transferencia de masa desde la superficie de la partícula al disolvente ($kg \cdot m^{-3}s^{-1}$):

$$J = k_f a_0 \rho (Y^* - Y) \quad \text{(Ecuación 1.14)}$$

Donde Y^* es el contenido de extracto en la fase fluida en la superficie de la partícula $\left(kg \cdot kg_{CO_2}^{-1}\right)$ y $\left(k_f a_0\right)$ es el coeficiente volumétrico de transferencia de masa en la fase fluida (s^{-1}).

Las ecuaciones del modelo BIC que permiten obtener el rendimiento en masa de extracto (m) en función del tiempo (t) en los diferentes periodos se describen a continuación [93]:

Periodo CER: $m = QY^*[1 - exp(-Z)]t$ (Ecuación 1.15)

Periodo FER: $m = QY^*[t - t_{CER} exp(Z_W - Z)]$ (Ecuación 1.16)

Periodo DC: $m = m_{SI}\left\{X_0 - \frac{Y^*}{W} ln\left[1 + \left[exp\left(\frac{WX_0}{Y^*}\right) - 1\right] exp\left[\frac{WQ(t_{CER}-t)}{m_{SI}}\right]\left(\frac{X_k}{X_0}\right)\right]\right\}$ (Ecuación 1.17)

Donde:

$$Z = \frac{m_{SI} k_{YA} \rho}{Q(1-\varepsilon)\rho_s} \quad \text{(Ecuación 1.18)}$$

$$W = \frac{m_{SI} k_{XA}}{Q(1-\varepsilon)} \quad \text{(Ecuación 1.19)}$$

$$Z_W = \frac{ZY^*}{WX_0} ln\left\{\frac{X_0 exp[WQ(t-t_{CER})/m_{SI}] - X_k}{X_0 - X_k}\right\} \quad \text{(Ecuación 1.20)}$$

$$m_{SI} = X_0 F \quad \text{(Ecuación 1.21)}$$

$$t_{CER} = \frac{m_{SI}(X_0 - X_k)}{Y^* ZQ} \quad \text{(Ecuación 1.22)}$$

$$t_{FER} = t_{CER} + \frac{m_{SI}}{QW} ln\left[\frac{X_k + X_p exp(WX_0/Y^*)}{X_0}\right] \quad \text{(Ecuación 1.23)}$$

La relación másica del material extraído a la salida del lecho de extracción (Y_{CER}) en el periodo CER se obtiene mediante la siguiente ecuación:

$$Y_{CER} = \frac{m_{(t=t_{CER})}}{Qt_{CER}} \quad \text{(Ecuación 1.24)}$$

De este modo la tasa de extracción en el periodo CER se calcula:

$$M_{CER} = Y_{CER} Q \qquad \text{(Ecuación 1.25)}$$

Los parámetros de proceso que se requieren para aplicar el modelo BIC son: la porosidad del lecho (ε), la masa inicial de la muestra (F) y su densidad (ρ_s), la densidad del CO_2 (ρ), y el caudal (Q). Además de estos parámetros, el modelo BIC requiere el conocer la solubilidad del extracto en el disolvente supercrítico (Y^*) y el rendimiento global de extracción (X_0). Existen otros parámetros que son optimizados durante la ejecución del modelo a partir de los datos cinéticos experimentales y son: la relación intra-partícula del soluto (X_k) y los coeficientes volumétricos de transferencia de masa en la fase fluida y sólida, $k_{YA} = k_f \cdot a_0$ y $k_{XA} = k_s \cdot a_0$, donde k_f y k_s son los coeficientes de transferencia de masa en la fase fluida y sólida, respectivamente, y a_0 es el área superficial de la partícula, la cual ya se ha definido previamente. El parámetro que define el soluto de fácil acceso (X_p) se calcula mediante la diferencia: $(X_0 - X_k)$.

Algunas de las aplicaciones del modelo BIC se han acompañado de comparaciones con modelos teóricos basados en la transferencia de masa, por ejemplo, Huang y col. (2011) desarrollaron un proceso SFE para la obtención de extractos a partir de rizomas de *Atractylodis macrocephalae* Koidz, a las condiciones de 15 a 45 MPa y temperaturas de 313 a 333 K. Los resultados experimentales fueron ajustados en base a diferentes modelos matemáticos: desde los modelos teóricos propuestos por Naik y col. (1989), el modelo de Barton propuesto por Nguyen y col. (1991), una analogía al modelo de Crank (1975) desarrollada por Esquivel y col. (1999) [77] y Reverchon y col. (1993) [95], hasta el modelo BIC propuesto por Sovová (1994) [93] y el Modelo Multicomponentes, el cual es una modificación al modelo de Sovová y que fue desarrollada por Martínez y col. (2003) [48]. Los resultados indicaron que el modelo que mejor se ajustó a los datos experimentales fue el modelo BIC al presentar las menores desviaciones relativas absolutas (1.62 %) [96].

Recientemente algunos autores han aplicado el modelo BIC en combinación con las reglas de pulgar de la ingeniería que se han incorporado a procesos SFE las cuales ya han sido descritas previamente en este capítulo, y cuyo enfoque es el de generar estrategias de escalado en procesos *batch*.

Fernández-Ponce y col. (2016) desarrollaron una estrategia de escalado para la producción de extractos de hojas de mango (*Mangifera indica*) aplicando reglas de pulgar

que implicaban a la relación caudal másico de solvente y la masa de la muestra, e incluyendo además el diámetro de la celda de extracción $(Q \times D/F)$. Los resultados demostraron que el modelo BIC, además de ajustarse adecuadamente a los datos experimentales predijo satisfactoriamente el comportamiento cinético al efectuar el cambio de escala proyectado [23].

Todas estas consideraciones sobre el modelo BIC reflejan su gran ventaja para ser aplicado en numerosos procesos de SFE en los que se pueden incluir diferentes tipos de biomasas desde hojas, flores, raíces, cortezas o frutas, además de resultar adecuado en la descripción del comportamiento en la extracción de compuestos como los aceites esenciales, ácidos grasos, ceras, etc. [73,87,94]

1.3.3 Correlaciones Generalizadas

Un parámetro importante de la curva OEC es el coeficiente de transferencia de masa en la fase fluida, según muestran los diferentes modelos matemáticos descritos en la sección anterior. Las correlaciones generalizadas son ecuaciones que, mediante el uso de números adimensionales característicos del proceso, permiten estimar el coeficiente de transferencia de masa de la extracción. A este respecto, algunos autores han propuesto para la SFE algunas correlaciones generalizadas basadas en los números adimensionales tradicionales de la ingeniería para describir los procesos de transferencia de masa: Sherwood (Sh), Reynolds (Re), y Schmidt (Sc) [97].

1.3.3.1 Números Adimensionales

Los números adimensionales permiten comparar sistemas diferentes mediante la combinación de variables de proceso fundamentales. Los más utilizados en el desarrollo de correlaciones generalizadas, aplicadas a la transferencia de masa de un proceso SFE se describen a continuación:

Número de Reynolds (Re). Relacionado con las propiedades de flujo del disolvente:

$$Re = \frac{u d_p \rho_{CO_2}}{\mu_{CO_2}} \qquad \text{(Ecuación 1.26)}$$

Donde u es la velocidad del SC-CO_2, d_p es el diámetro medio de la partícula, ρ_{CO2} es la densidad del CO_2 y μ es su viscosidad.

Número de Schmidt (Sc). Vinculado a la difusividad del soluto en SC-CO_2 y que se describe según la ecuación:

$$Sc = \frac{\mu_{CO_2}}{\rho_{CO_2} D_{12}} \quad \text{(Ecuación 1.28)}$$

Donde D_{12} es el correspondiente coeficiente de difusión.

Número de Sherwood (Sh). Se encuentra relacionado con el coeficiente de transferencia de masa (k_f) así como con el coeficiente de difusión, y viene dado por la siguiente ecuación.

$$Sh = \frac{k_f d_p}{D_{12}} \quad \text{(Ecuación 1.29)}$$

Los números adimensionales se emplean a menudo para correlacionar la transferencia de masa en el proceso de extracción supercrítica y de acuerdo con Norjuda y Mohd (2009), citando a Lim y col. (1989), las correlaciones generalizadas abordadas para la transferencia de masa entre un fluido supercríticos y un sólido en un lecho empacado son de la forma [98,99]:

$$Sh = f(Re, Sc) \quad \text{(Ecuación 1.30)}$$

Sobre la base de algunos estudios publicados, la forma más aplicada es [97]:

$$Sh = m\left(Re^{1/2} Sc^{1/3}\right)^n \quad \text{(Ecuación 1.31)}$$

O en forma más general:

$$Sh = a\left(Re^b Sc^{1/3}\right) \quad \text{(Ecuación 1.32)}$$

Donde los coeficientes a y b son parámetros de la correlación, y su aplicación se encuentra limitada a un rango de valores que pueden tomar los números de *Re* y de *Sc*.

Norhuda y Mohd (2009) obtuvieron tres correlaciones generalizadas para modelar la transferencia de masa en un lecho empacado en la extracción supercrítica de almendra de palma en las condiciones de 27.6 a 48.3 MPa y de 323, 333 y 343 K. Las correlaciones presentaron coeficientes de correlación (R^2) entre 0.97 y 0.98, y la validación estadística del número *Sh* encontró una fuerte correlación entre los datos predichos y los datos experimentales, generando la siguiente correlación: $Sh = 0.980 ReSc^{1/3}$ [98].

En la tabla 1.2 se presentan las correlaciones más relevantes que se han publicado y que se desarrollaron para describir la transferencia de masa en condiciones supercríticas.

Tabla 1.2. Correlaciones generalizadas de la bibliografía empleadas para correlacionar la transferencia de masa en SFE.

Correlación	Rango (Re, Sc)	Referencia
$Sh = 0.82\ Re^{0.66}Sc^{1/3}$	$1 \leq Re \leq 70$ $3 \leq Sc \leq 11$	[100]
$Sh = 0.2548\ Re^{0.5}Sc^{1/3}$	$1 \leq Re \leq 70$ $3 \leq Sc \leq 11$	[101]
$Sh = 0.206\ Re^{0.8}Sc^{1/3}$	$10 \leq Re \leq 100$ $Sc < 10$	[102]
$Sh = 0.3954Re^{0.58}Sc^{1/3}$	$3 < Re < 19$ $3 < Sc < 19.3$	
$Sh = 0.38\ Re^{0.83}Sc^{1/3}$	$2 \leq Re \leq 40$ $2 \leq Sc \leq 20$	[103]
$Sh = 3.173Re^{-0.06}Sc^{-0.85}$	ND	[104]
$Sh = 0.085\ Re^{-0.298}Sc^{1/3}$	ND	
$Sh = 0.135Re^{0.5}Sc^{1/3}$	ND	
$Sh = 0.98ReSc^{1/3}$	$38.4 < Re < 47.9$ $0.262 < Sc < 0.384$	[98]
$Sh = 0.13\ Re1.4Sc^{0.75}$	$Re < 0.6$ $5 < Sc < 40$	[105]
$Sh = 0.0234Re^{1.02}7Sc^{1/3}$	$0.73 < Re < 17.63$	[106]
$Sh = 0.0122(Re^{1/2}Sc^{1/3}-0.412)^2$	$0.73 < Re < 17.63$ $Sc = 12.67$	
$Sh = 0.0506Re0.859Sc^{1/3}$	$2.25 < Re < 17.63$	
$Sh = 0.0123(Re^{1/2}Sc^{1/3}+0.875)^2$	$2.25 < Re < 17.63$ $Sc = 12.67$	

ND: No determinado

1.3.3.2 Coeficiente de Difusión

De acuerdo con Crank (1975), la difusión es el proceso mediante el cual la materia es transportada desde una parte de un sistema a otra como resultado de movimientos

moleculares aleatorios. Teniendo en cuenta la hipótesis planteada para la descripción de la transferencia de calor, en la cual la transferencia de calor por conducción se debe a movimientos moleculares aleatorios, en 1855 Fick reconoció este patrón y planteó que el fenómeno de difusión se podía describir como una forma análoga a la transferencia de calor. De esta forma logró establecer las bases matemáticas de la transferencia de masa en forma similar a la conducción de calor, las que habían sido derivadas por Fourier en 1822. De esta forma, la teoría matemática sobre la difusión de sustancias isotrópicas, es decir, aquellas sustancias cuyas características físicas son iguales en todas direcciones, se basa en la hipótesis de que la velocidad de difusión por unidad de área es proporcional al gradiente de concentración con respecto a la normal de tal sección, así [85]:

$$J = -D\,\partial C/\partial x \qquad \text{(Ecuación 1.35)}$$

Donde *J* es la velocidad de transferencia por unidad de área de la sección, *C* es la concentración de la sustancia que difunde, *x* es la coordenada espacial normal a la sección y *D* es el coeficiente de difusión. Si *J* se refiere a la cantidad de material que difunde y *C* a la concentración, y si ambas se expresan en términos de la misma unidad de cantidad, por ejemplo, gramos o gramos de moléculas, entonces en la Ecuación 1.37, *D* es independiente de estas unidades y tendrá las dimensiones de $(longitud)^2 \cdot (tiempo)^{-1}$, (ej. $cm^2 \cdot s^{-1}$). El signo negativo en la Ecuación 1.37 se debe a que la difusión ocurre en la dirección opuesta en la que la concentración de la sustancia se incrementa [85].

En este orden de ideas, el coeficiente de difusión binario (D_{12}) representa la facilidad con la que un soluto (2) se desplaza en el disolvente (1) y depende del tamaño, morfología y naturaleza del soluto, así como de la temperatura, viscosidad y naturaleza del disolvente [85].

El coeficiente de difusión binario (D_{12}) es un propiedad de gran importancia en el transporte de fluidos y resulta de gran importancia su determinación, ya sea en forma experimental mediante técnicas instrumentales, o calculado a partir de ecuaciones o modelos matemáticos [107]. Además, existe una demanda por parte de procesos SFE de expresiones simples y precisas para conocer el coeficiente de difusión en un amplio rango de temperaturas y presiones [108].

El coeficiente de difusión de un soluto en el fluido supercrítico (D_{12}) depende del tamaño y forma del soluto, la interacción molecular con el solvente supercrítico, y las

condiciones de temperatura y presión. En general, solutos con grandes masas moleculares y solutos que pueden presentar interacciones químicas difunden de forma más lenta. Adicionalmente, la presión y la temperatura determinan la densidad y la viscosidad del disolvente, los cuales tienen un efecto importante sobre la difusión del soluto. En general, el coeficiente de difusión aumenta de forma proporcional a la temperatura a presión constante, sufriendo menores efectos a elevadas presiones. Con respecto a la presión, el coeficiente de difusión disminuye con el incremento de esta. Altas presiones significan alta densidad del disolvente y por ende el proceso de difusión se hace más difícil debido al incremento en el número de colisiones moleculares. Además, las interacciones intermoleculares aumentan debido a la reducción en la distancia media intermolecular como causa del aumento en la densidad [109].

La medición o determinación de D_{12} puede realizarse en un gas, en un líquido y en fluidos supercríticos mediante el uso de diferentes técnicas. Algunas de estas técnicas que se encuentran disponibles en la literatura incluyen: espectroscopía de correlación de fotones [110,111], métodos geométricos [112–114], Resonancia Magnética Nuclear (RMN) [115–117], técnicas cromatográficas como la cromatografía de ensanchamiento de picos (*Chromatographic Peak Broadening* - CPB) también denominado método de Taylor [118–121], y la respuesta al impulso cromatográfico (*Chromatographic Impulse Response* - CIR) [122–124].

Actualmente existe en la bibliografía datos e información referente a la determinación de D_{12} para numerosos compuestos, obtenidos de forma experimental empleando algunas de las técnicas anteriormente descritas, a través de simulaciones computarizadas o mediante el uso de modelos macroscópicos. La aplicación de las diferentes técnicas que se han desarrollado para para la determinación experimental del coeficiente de difusión, se han enfocado a la medición de un componente puro. Sin embargo, para un extracto, este tipo de información es limitada o no se encuentra disponible, debido a que los extractos obtenidos a partir de fuentes naturales poseen una composición que normalmente incluye un gran número de compuestos.

Por otro lado, gran parte de las correlaciones que se han propuesto y que se encuentran disponibles, requieren el conocimiento de muchos parámetros del soluto, tales como la masa molecular, el volumen crítico, y el volumen molar en el punto de ebullición, entre otros. Estas correlaciones también demandan de la incorporación de propiedades físico-químicas

del disolvente supercrítico como son la densidad, viscosidad, parámetros críticos, etc., en general, en la medida que aumenta la predicción del modelo para la determinación del coeficiente de difusión, aumenta el número de parámetros necesarios para el cálculo.

Se han propuesto muchas ecuaciones, las que pueden encontrarse en la bibliografía, para predecir o correlacionar el D_{12}. En la tabla 1.3 se muestra un resumen de algunas de las correlaciones desarrolladas para la determinación del coeficiente de difusión en SC-CO_2, así como los parámetros o datos de entrada que requiere cada una de ellas. Una de las ecuaciones más precisas es la propuesta por Magalhães y col. (2013) [125]. Sin embargo, como se expuso anteriormente, esta gran variedad de correlaciones han facilitado la determinación del D_{12} en compuestos puros pero no se han aplicado a mezclas multicomponentes. Para determinar y/o predecir el D_{12} de un extracto, sería necesario conocer su composición así como establecer reglas de mezclado.

Tabla 1.3 Correlaciones para determinar el coeficiente de difusión de sustancias puras en SC-CO_2 y los parámetros requeridos para cada una.

Denominación	Correlación	Parámetros	Referencia
Scheibel	$D_{12}(cm^2/s) = \frac{8.2x10^{-8}T}{\mu_1 V_{bp,2}^{1/3}}\left[1+\left(\frac{3V_{bp,1}}{V_{bp,2}}\right)^{2/3}\right]$	$V_{bp,2}$	[126]
Reddy-Doraiswamy	$D_{12}(cm^2/s) = \beta \times \frac{T\sqrt{M_1}}{\mu_1\left(V_{bp,1}V_{bp,2}\right)^{1/3}}$ $\beta=1.0\times10^{-8}$ ($V_{bp,1}/V_{bp,2} \leq 1.5$) or $\beta=8.5\times10^{-8}$ ($V_{bp,1}/V_{bp,2} > 1.5$)	$V_{bp,2}$	[127]
Lusis-Ratcliff	$D_{12}(cm^2/s) = \frac{8.52\times10^{-8}T}{\mu_1 V_{bp,1}^{1/3}}\left[1.40\left(\frac{V_{bp,1}}{V_{bp,2}}\right)^{1/3}+\left(\frac{V_{bp,1}}{V_{bp,2}}\right)\right]$	$V_{bp,2}$	[128]
Lai-Tan	$D_{12}(cm^2/s) = 2.50\times10^{-7}\frac{T\sqrt{M_1}}{(10x\mu_1)^{0.688}V_{c,2}^{1/3}}$	$V_{c,2}$	[129]
Wilke-Chang	$D_{12}(cm^2/s) = 7.4x10^{-8}\left(\frac{T\sqrt{xM_1}}{\mu_1 V_{bp,2}^{0.6}}\right); x = \begin{cases}1\ para\ disolventes\ no\ asociados\ solvents\\ 2.6\ para\ agua\end{cases}$	x, $V_{bp,2}$	[130]
Stokes-Einstein Ecuación 1 Modificada	$D_{12}(cm^2/s) = A\left(\frac{T}{\mu_1}\right)^{\alpha}\frac{1}{\left(M_2V_{bp,2}\right)^{\beta}}$	M_2, $V_{bp,2}$	[131]
Stokes-Einstein Ecuación 2 Modificada	$D_{12}(cm^2/s) = A\left(\frac{T}{\mu_1}\right)^{\alpha}\frac{1}{\left(M_2V_{bp,2}\sigma_{bp,2}^{1/4}\right)^{\beta}}$	M_2, $V_{bp,2}$, $\sigma_{bp,2}$	[131]
Schiebel Modificada	$D_{12}(cm^2/s) = A\left(\frac{T}{\mu_1}\right)^{\alpha}\frac{1}{V_{c,2}^{\beta}}\left[1+\left(\frac{3V_{c,1}}{V_{c,2}}\right)^{2/3}\right]$	$V_{c,2}$	[132]
Lusis-Ratcliff Modificada	$D_{12}(cm^2/s) = A\left(\frac{T}{\mu_1}\right)^{\alpha}\left[\beta\left(\frac{V_{c,1}}{V_{c,2}}\right)^{1/3}+\left(\frac{V_{c,1}}{V_{c,2}}\right)\right]$	$V_{c,2}$	[132]
Tyn-Calus Modificada	$D_{12}(cm^2/s) = A\left(\frac{T}{\mu_1}\right)^{\alpha}\frac{\left(V_{bp,2}\sigma_{bp,2}^{1/4}\right)^{\beta}}{V_{c,2}^{\gamma}}$ $\sigma_{bp,2}(g/s^2) = P_{c,2}^{2/3}T_{c,2}^{1/3}\left(0.132\alpha_{c,2}-0.279\right)\left(1-T_{bp,2}\right)^{11/9}$	$V_{c,2}$, $\sigma_{bp,2}$, $P_{c,2}$, $T_{c,2}$, $\alpha_{c,2}$, $T_{bp,2}$	[132]
Wilke-Chang Modificada	$D_{12}(cm^2/s) = A\left(\frac{T}{\mu_1}\right)^{\alpha}\frac{1}{V_{c,2}^{\beta}}$	a, b, $V_{c,2}$	[132]
Magalhães y col. (2013)	$D_{12} = T\left(a\rho_1+\frac{b}{\mu_1}\right)$	a, b	[125]

1: disolvente (CO_2); 2: soluto; T: temperatura; P: presión; μ: viscosidad; ρ: densidad; σ: tensión superficial; V_{bp}: volumen molar en el punto de ebullición; M: masa molar; V_c: volumen molar crítico; x: parámetro de asociación en la ecuación de Wilke–Chang; A, α, β and γ: constantes específicas en las respectivas correlaciones.

1.4 Materiales de origen vegetal utilizados en esta Tesis para los estudios de escalado

Durante las últimas décadas se ha evidenciado un creciente interés por la utilización de sustancias de origen vegetal, considerando que muchas plantas producen una gran variedad de metabolitos que resultan de interés para la industria de alimentos, farmacéutica y cosmética [133–136]. La extracción de compuestos activos utilizando fluidos supercríticos empleando dióxido de carbono es una tecnología que ha demostrado ventajas significativas en relación a los métodos de extracción convencionales [38]. Estas ventajas han propiciado la investigación de numerosas fuentes vegetales, dando lugar a una gran producción científica. En este sentido, de Melo y col. (2014) recopilaron en un estudio los materiales vegetales más utilizados en la extracción supercrítica a partir de trabajos publicados entre 2000 y 2013. En la Figura 1.2 se observa que el tipo de material empleado es bastante heterogéneo predominando las semillas (28 %), y las hojas (17%) como biomasas de extracción; por su parte, las frutas y las flores representaron un 10 % y un 5 %, respectivamente.

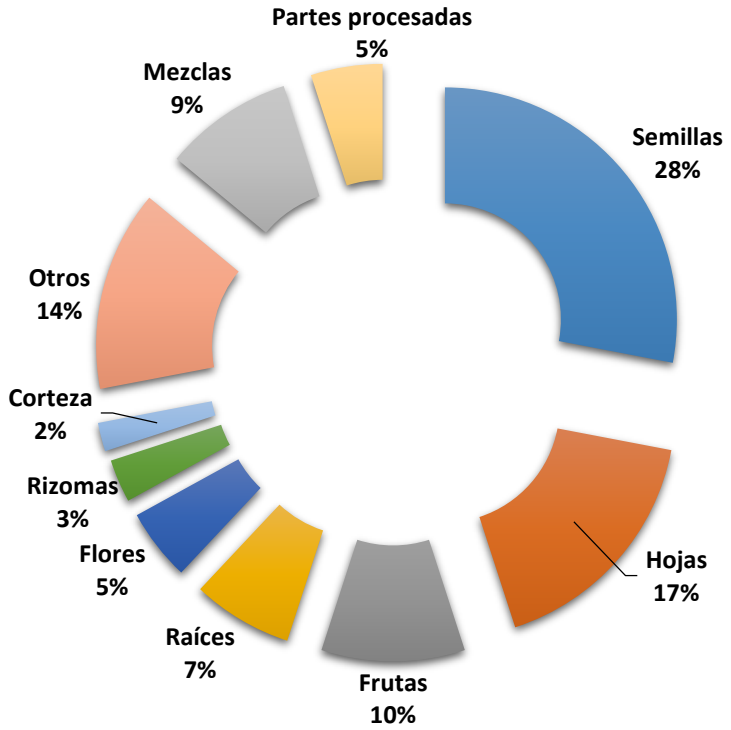

Figura 1.2 Clasificación de los materiales vegetales más utilizados en la SFE (adaptado de de Melo y col. 2014) [35].

Esta recopilación permite suponer que la extracción SFE presenta un amplio rango de aplicaciones a partir de materias primas de origen vegetal, tanto en investigación básica como aplicada al desarrollo de productos a nivel industrial, motivando así a continuar explorando la inmensa diversidad disponible.

A continuación, se describirán las materias primas que se emplearon en el desarrollo de esta Tesis, que comprenden frutos deshidratados del mortiño (*Vaccinium meridionale* Swartz) procedentes de Medellín (Colombia) y flores de caléndula (*Calendula officinalis*) procedentes de Murcia (España), con especial énfasis en el mortiño debido a la poca información científica que se encuentra disponible respecto de esta especie.

1.4.1 Mortiño (*Vaccinium meridionale* Swartz)

El género *Vaccinium* comprende un grupo de plantas que incluye alrededor de 450 especies dispersas por todo el mundo, las cuales poseen actividades biológicas, antiinflamatorias, inhibitorias del crecimiento de células cancerígenas, de efectos beneficiosos sobre la visión, desórdenes cardiovasculares, enfermedades degenerativas, y envejecimiento, entre otras [137–141]. Sus bayas se caracterizan por contener varios fitonutrientes, incluyendo compuestos fenólicos tales como flavonoides, ácidos fenólicos, lignanos y taninos poliméricos [142].

Los frutos del género *Vaccinium* han sido empleados tradicionalmente por muchas comunidades indígenas con fines nutricionales y terapéuticos. Actualmente, la creciente preocupación de los consumidores sobre su salud y la necesidad de llevar una alimentación saludable ha propiciado un incremento en el consumo de este tipo de frutos, aumentando con ello la producción anual en diferentes formatos (fruto fresco, congelado, fruta procesada) convirtiéndose así en una fuente importante de componentes nutracéuticos o de suplementos alimentarios. En los Estados Unidos, las especies más comercializadas son *V. corymbosum* L., *V. angustifolium* Ait., *V. asheireade* y *V. macrocarpon*. Dentro del conjunto de suplementos alimentarios, el extracto de *V. macrocarpon*, ocupa el puesto 14 en el ranking de popularidad y es utilizado de forma frecuente debido a sus efectos benéficos sobre el tracto urinario; por otro lado, el extracto de *V. myrtillus* L. se ubica en el puesto 21 debido a sus efectos benéficos sobre el sistema vascular y la retina. Para el año 2006 se encontraron más de 180 productos fitofarmacéuticos disponibles en el mercado mundial, los cuales contenían en sus ingredientes extractos de frutos del género *Vaccinium* [143,144].

Particularmente, la especie *Vaccinium meriodionale* Swartz se cultiva en la región andina de América del Sur (Colombia, Venezuela y Ecuador) a una altura entre 2300 y 3300 metros sobre el nivel del mar, específicamente entre los Trópicos de Cáncer y Capricornio (23°30'N-23°30'S) [145]. En Colombia, se conoce como "agraz", "mortiño", "uvito de monte" o "arándano azul", siendo básicamente una especie que crece de forma espontánea en la región andina (ver figura 1.3), uno de los pocos lugares donde se producen dos cosechas en el año (junio y diciembre) [146].

Figura 1.3. Mortiño (*Vaccinium meridionale* Swartz)

1.4.1.1 Características físicas

El mortiño es un arbusto de hojas simples, alternas, deformas elípticas y ovales, que crece de forma silvestre con un tamaño que oscila entre 1 y 4 metros de altura, aunque ocasionalmente se pueden encontrar algunos de hasta 8 metros. En Colombia se cosecha en dos épocas del año, la primera entre abril y mayo, y la segunda -más abundante- entre septiembre y diciembre [147].

Sus frutos son bayas globosas de aproximadamente 1 cm de diámetro y un peso fresco de 1,6 a 6,8 g cuyo color es verde cuando está inmaduro y púrpura oscuro cuando alcanza la madurez [148,149]. La pulpa de estas bayas es comestible, tiene un sabor ligeramente ácido y presenta pequeñas y numerosas semillas. La madurez fisiológica del fruto se alcanza entre 60 y 80 días después de su floración. Dependiendo de las características de la zona donde se realice su cultivo como el terreno y la temperatura, la cantidad de bayas en cada racimo pueden variar entre cinco y diez [149].

1.4.1.2 Aplicaciones

Uno de los usos más comunes que se le ha dado al mortiño ha sido en la elaboración de zumos [150] y derivados lácteos [151], sin embargo, ha despertado un interés agroindustrial en la última década debido al alto contenido de polifenoles, especialmente antocianinas como delfinidina y cianidina, además de ácidos fenólicos como ferúlico, cafeico y clorogénico, formando parte de los metabolitos secundarios responsables de sus efectos benéficos [139]. Actualmente existen muchos estudios sobre el cultivo y el manejo agrícola del mortiño, sin embargo, se encuentran pocos estudios publicados sobre las posibles aplicaciones del mortiño como ingrediente funcional.

Algunos de los estudios más relevantes se han centrado en el efecto del tratamiento de secado sobre la actividad antioxidante del mortiño [152]. Gaviria Montoya y col. (2009) estudiaron la actividad antioxidante y la inhibición de la peroxidación lipídica de los extractos de mortiño en aceite de maíz, donde reportaron valores de actividad antioxidante similares y superiores a otras especies de *Vaccinium*, además de una buena eficiencia inhibitoria frente a la oxidación lipídica de aceites vegetales al compararse con un antioxidante comercial como el BHT (Butil hidroxitolueno) [153]. Lopera y col. (2013) encontraron un efecto cardioprotector en los extractos no alcohólicos y fermentados de mortiño que fueron suministrados en roedores [154]; Maldonado y col. (2014) encontraron unos valores de actividad antioxidante similares a otras especies, así como efectos citotóxicos y antiproliferativos en un modelo *in vitro* de cáncer de colon, sugiriendo que los extractos de mortiño poseen un gran potencial para ser utilizados en la prevención de este tipo de cáncer [155]. Por otra parte, Zapata y col. (2015) estudiaron el efecto de disoluciones de mortiño en la estabilización del aceite de Sacha inchi (*Plukenetia volubilis* L.) encontrando que el aditivo desarrollado con extractos de mortiño era eficaz en la estabilización del aceite de Sacha inchi [156].

1.4.2 Caléndula (*Calendula officinalis*)

La caléndula (*Caléndula officinalis*) es una planta ornamental originaria del sur de Europa la que, debido a la actividad biológica que han presentados sus compuestos, posee un amplio interés por la industria farmacéutica siendo cultivada a escala comercial a nivel mundial [157,158]. Las flores de *C. officinalis* se han utilizado en la medicina tradicional y

popular debido a la actividad biológica que poseen sus extractos tales como efectos anti-inflamatorios, anti-tumorgénicos, propiedades antivirales y cicatrizantes [159–163].

Estas características hacen que la flor de caléndula resulte de gran interés para la producción de extractos por diferentes industrias que incluyen la cosmética, farmacéutica y de alimentos. Por esta razón, se dispone en la bibliografía de muchas publicaciones sobre la extracción SFE de *C. offinalis* empleando diversas condiciones y escalas de proceso [160,164–169].

1.5 Equipos de extracción supercrítica de la Plataforma Novalindus del CIAL (UAM+CSIC)

La **Plataforma NOVALINDUS** (In**NOV**ación **ALI**mentaria **INDUS**trial) es una planta piloto especializada en el desarrollo de procesos de obtención de productos alimentarios funcionales, así como en la producción piloto de dichos productos. Se trata de una plataforma de servicios de investigación y desarrollo para organismos públicos de investigación y empresas, que tiene como principal filosofía la investigación alimentaria útil, en constante evolución, para obtener resultados transferibles a la sociedad sin olvidar el papel fundamental de la empresa.

La Plataforma Novalindus se encuentra ubicada en la Planta Piloto del Instituto de Investigación en Ciencias de la Alimentación CIAL (UAM-CSIC) en el campus de la Universidad Autónoma de Madrid (Madrid, España). Se encuentra dotada de una serie de equipos singulares cuyos objetivos se centran en la investigación científica y el asesoramiento tecnológico.

En la plataforma ya se han desarrollado varios procesos SFE, utilizando materias primas como el romero (*Rosmarinus officinalis*) [16,170], espinacas (*Spinacia oleracea*) [171], tomillo (*Thymus zygis*) [170,172,173], Orégano (*Origanum vulgare*) [170], Salvia (*Salvia officinalis*) [170], Milenrama (*Achilea millenfolium*) [164,174,175], Melisa (*Melisa officinalis*) [164], flor de caléndula (*Calendula officinalis*) [164,165], corteza de plátano (*Platanus acerifolia* L.)[17] té verde (*Camellia sinensis*) [176] y mortiño (*Vaccinium meridionale* Swartz) [22]. Además, se han realizado en Novalindus una serie de trabajos de asesoramiento y extracción de otras materias primas de origen vegetal cuyos resultados se encuentran vinculados a servicios a empresas y no se encuentran publicados.

1.5.1 Planta de Extracción SFE de Escalas Laboratorio y Piloto

En las figuras 1.4 a 1.7 se muestran y describen las plantas de extracción supercrítica empleadas en el desarrollo de esta Tesis las cuales forman parte de las infraestructuras disponibles en la Plataforma Novalindus. La figura 1.4 corresponde a una planta de extracción Thar SF2000 (Pittsburgh, Pensilvania, Estados Unidos), esta planta posee una configuración que le permite llevar a cabo experimentos a pequeña escala utilizando una celda de extracción de 2.7×10^{-4} m^3 y a escala piloto mediante una celda de 1.35×10^{-3} m^3, el caudal de CO_2 se mide a través de un caudalímetro Siemens AIS, modelo Sitrans FC Mass

2100 DI 1.5 (Nordborgvej, Dinamarca), puede operar en un rango de presión de 0.1 a 6.9 MPa, la temperatura de entrada del CO_2 en la celda de extracción se controla mediante un intercambiador de calor eléctrico y el control de temperatura de la celda de extracción se realiza mediante una camisa calefactora, el CO_2 puede ser bombeado entre un rango de caudal de 0.2 a 12 $kg \cdot h^{-1}$, la presión se controla mediante una válvula BPR automática y la corriente de CO_2 puede ser recirculada al tanque de almacenamiento pasando primero por un Demister con un volumen de 1.71×10^{-3} m^3 de Proycon Pirineo S.L. (Huesca, España), en el cual se separan partículas sólidas o líquidas de la corriente de salida del CO_2, los extractos se recolectan en dos separadores ciclónicos de 5×10^{-4} m^3. En la figura 1.5 se presenta un diagrama esquemático detallado de esta planta cuya operación se controla mediante un sistema de control PLC conectado a un ordenador.

Figura 1.4 Planta de extracción SFE configurada para escalas laboratorio y piloto (Thar SF2000, Thar Technologies, Pittsburgh, Pensilvania, USA).

En la figura 1.5 se describe la planta Thar SFE2000 mediante un diagrama esquemático.

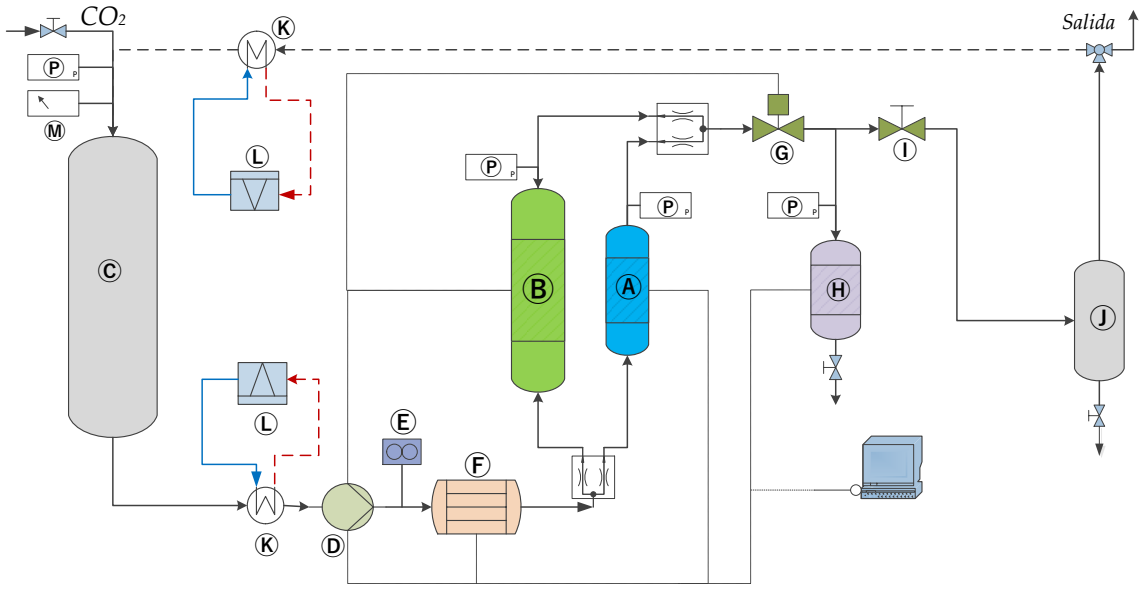

Figura 1.5 Diagrama esquemático de la planta SFE Thar SF2000 y su configuración para escalas de laboratorio y piloto. Donde A= Celda de extracción (2.7×10^{-4} m^3); B= Celda de extracción (1.35×10^{-3} m^3); C= Tanque de almacenamiento de CO_2; D= Bomba de CO_2; E= Caudalímetro; F= Intercambiador de calor; G= Válvula automática BPR; H= Separador ciclónico; I= Válvula BPR manual; J= Demister; K= Condensadores; L= Sistema de enfriamiento; M= Indicador de volumen; P= Manómetros; (⋯) líneas punteadas indican sistema de control PLC; (---) líneas con guiones indican recirculación.

1.5.2 Planta de Extracción SFE de Escala Semi-industrial

La figura 1.6 presenta la planta de extracción ZEAN, la cual posee una configuración para realizar experimentos a escala semi-industrial con una celda de extracción (C) de 5.19×10^{-3} m^3 y su calentamiento se realiza mediante una camisa calefactora. Esta planta puede operar en un rango de presión de 0.1 a 44 MPa, el CO_2 puede ser bombeado en un rango de 2.2 a 147 $kg\cdot h^{-1}$ mediante una bomba LEWA LDE1 de LEWA GmbH (Leonberg, Alemania), la temperatura del CO2 se controla mediante un intercambiador de calor de tubos enlazado a un baño termostático Huber Hotbox HB120 de Peter Huber Kältemaschinenbau GmbH (Offenbur, Alemania), la presión en la celda de extracción se controla mediante una válvula BPR RCV-2945 de Badger Meter Inc. (Tulsa, Estados Unidos). Los extractos se recolectan en dos separadores con un volumen de 1.57×10^{-3}, cada uno con control de presión independiente el cual se regula mediante válvulas BPR manuales y control de temperatura

controlado mediante resistencias eléctricas. Para recircular el CO_2 utilizado en la extracción hasta el tanque de almacenamiento de 8.8×10^{-2} m^3, la corriente pasa primero por un Demister de Proycon Pirineo S.L. (Huesca, España) con volumen de 1.5×10^{-2} m^3 y más adelante por un filtro de carbon activado con un volumen de 5×10^{-2} m^3. La operación de esta planta se controla mediante un sistema PLC diseñado por Invensys S.L. (Madrid, España).

En la figura 1.7 se describe la planta Zean mediante un diagrama esquemático.

Figura 1.6 Planta de extracción SFE configurada para escalas laboratorio y piloto (ZEAN Engineering, Madrid, España).

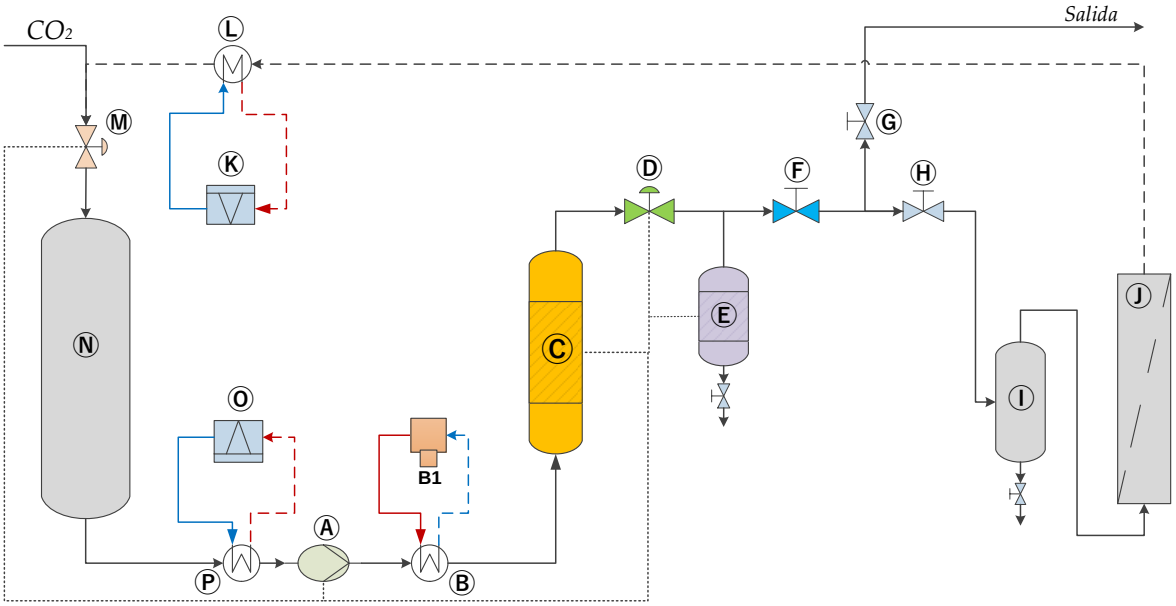

Figura 1.7 Diagrama esquemático de la planta ZEAN y su configuración para escala semi-industrial. Donde: A= bomba de CO_2; B= Intercambiador de calor; B1= Baño termostático; C= Celda de extracción; D= Válvula BPR automática; E= Separador ciclónico; F= Válvula BPR manual; G,H= Válvulas de paso; I= Demister; J= Filtro; K,O= Sistema de enfriamiento; L,P= Condensadores; M= Válvula neumática; N= Tanque de almacenamiento de CO_2; (…) líneas de puntos indican sistema de control PLC; (---) líneas con guiones indican sistema de recirculación.

CAPÍTULO 2.

OBJETIVOS Y PLAN DE TRABAJO

2. OBJETIVOS Y PLAN DE TRABAJO

2.1 Objetivo General

El objetivo general del trabajo de la Tesis Doctoral ha sido estudiar el escalado de la extracción de materiales de origen vegetal con dióxido de carbono (CO_2) supercrítico, desarrollando un procedimiento sencillo y de fácil aplicación que permita correlacionar el comportamiento cinético del proceso de extracción, abarcando diferentes materias primas y diferentes condiciones de extracción.

2.1.1 Objetivos específicos

a. Estudiar y analizar los procedimientos teóricos (modelos de transferencia de materia) y semi-empíricos (reglas de pulgar de la ingeniería, correlaciones de números adimensionales) ya utilizados en la bibliografía para el escalado de procesos de extracción supercrítica con lecho fijo en *batch*.

b. Estudiar experimentalmente el escalado de procesos de extracción supercrítica de diferentes matrices vegetales, utilizando las unidades de diferente escala disponibles en la Plataforma Novalindus (CIAL, UAM-CSIC).

c. Desarrollar un procedimiento simple, considerando los fundamentos teóricos y la información experimental, que permita estimar el caudal de CO_2 necesario en celdas de diferentes escalas para reproducir la misma cinética de extracción.

2.2 Plan de Trabajo

Según los objetivos propuestos en esta Tesis Doctoral, en la figura 2.1 se resume los modelos teóricos y semi-empíricos estudiados y aplicados para el escalado de procesos de extracción con fluidos supercríticos (SFE).

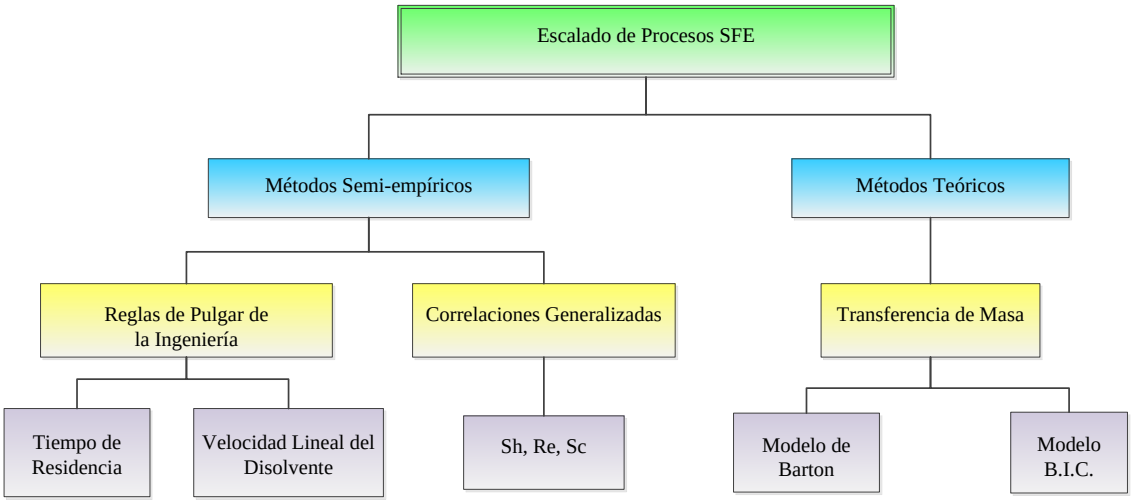

Figura 2.1 Modelos teóricos y semi-empíricos utilizados en esta tesis.

Para estudiar el cambio de escala, en lo referente a los métodos semi-empíricos se aplicaron dos reglas de pulgar de la ingeniería:

a. mantener constante el tiempo de residencia.
b. mantener la velocidad lineal del disolvente constante

En cuanto al desarrollo de correlaciones generalizadas, se tuvieron en cuenta los números adimensionales de Reynolds, Schmidt y Sherwood, los cuales describen el régimen de flujo, la difusión y la transferencia de masa en el interior de la celda de extracción.

En el caso de los métodos teóricos, se estudiaron varios modelos basados en la transferencia de materia disponibles en la bibliografía [30,78,86,177] y se aplicaron dos de ellos: el modelo cinético de Barton [78] y el modelo BIC (*Broken and Intact Cells*) propuesto por Sovová [30,75].

La aplicación de estos criterios o reglas para el escalado de un proceso SFE se llevó a cabo experimentalmente en la Plataforma Novalindus, utilizando dos materias primas de origen vegetal:

- *Vaccinium meridionale* Swartz (Mortiño) procedente de Colombia, a través de un acuerdo de colaboración con el Instituto de Ciencia y Tecnología Alimentaria (INTAL) con sede en Medellín, Colombia.
- *Calendula officinalis* (caléndula), originaria de Murcia, España.

Cada uno de estos materiales fueron acondicionados previamente al proceso de extracción según se muestra en la figura 2.2.

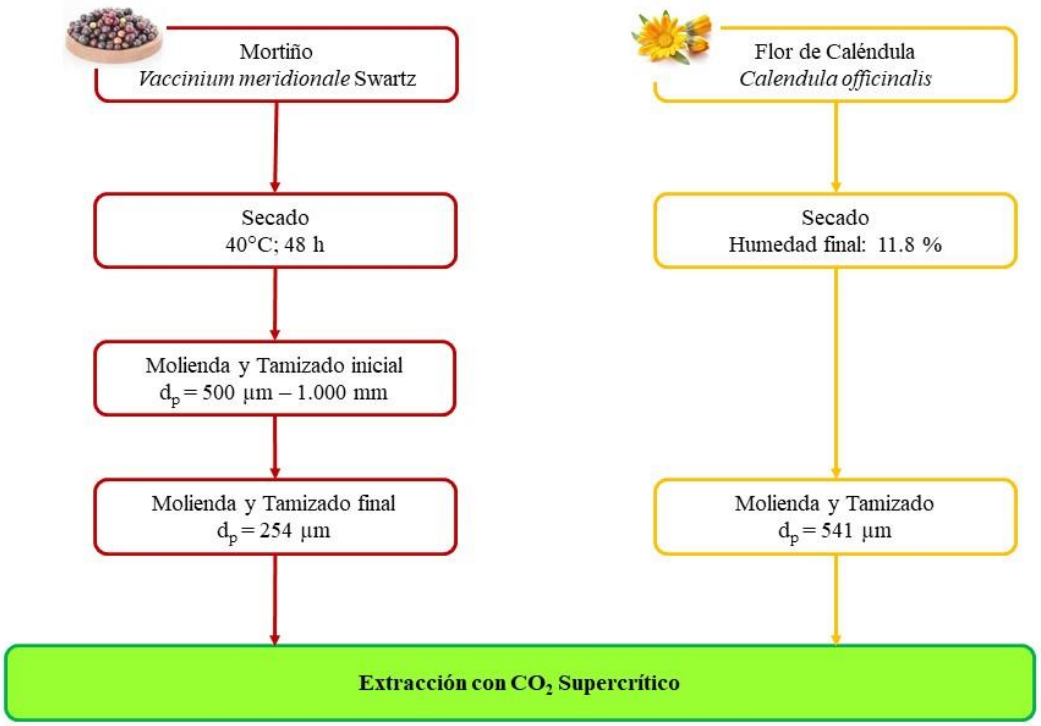

Figura 2.2 Pretratamiento de los materiales vegetales utilizados en esta Tesis.

Las unidades de extracción utilizadas se describieron en la Introducción y sus características se resumen en la Tabla 2.1.

Tabla 2.1. Características de las plantas de extracción SFE de la Plataforma Novalindus utilizadas para los estudios de escalado de esta Tesis.

	Escala Laboratorio	**Escala Piloto**	**Escala Semi-industrial**
L: Altura celda (m)	0.188	0.388	0.570
D: Diámero celda (m)	0.043	0.07	0.107
Volumen de celda (m^3)	2.7×10^{-4}	1.35×10^{-3}	5.19×10^{-3}
Area de flujo (m^2)	1.45×10^{-3}	3.53×10^{-3}	8.99×10^{-3}
Relación L/D	4.372	5.716	5.327
Volumen separador (m^3)	5×10^{-4}	5×10^{-4}	1.57×10^{-3}
Capacidad bomba ($kg\cdot h^{-1}$)	0.2 - 12	0.2 - 12	2.2 - 147
Presión de operación (MPa)	0.1 - 69	0.1 - 69	0.1 - 44
Temperatura de operación de la bomba (°C)	5 - 40	5 - 40	5 - 40
Volumen Demister (m^3)	1.71×10^{-3}	1.71×10^{-3}	1.5×10^{-2}
Volumen Filtro (m^3)	No	No	5×10^{-2}
Volumen tanque CO_2 (m^3)	1.5×10^{-2}	1.5×10^{-2}	8.8×10^{-2}
Sistema de recirculación	Si	Si	Si
BPR autómatica	Si	Si	Si
Caudalímetro	Si	Si	No
Control PLC	Si	Si	Si

Para el cálculo del coeficiente de difusión, el que forma parte del número de Schmidt, se realizó una recopilación y análisis de más de 1100 datos experimentales sobre coeficientes de difusión de compuestos puros disponibles en la literatura y mediante la aplicación de Regresiones Múltiples Lineales (MLRA, *Multiple Linear Regression Analysis*), se desarrollaron correlaciones generalizadas por familia de compuestos (tipo de extracto): (i) aceites volátiles; (ii) ácidos grasos; (iii) aceites fijos. Estas correlaciones permitieron el cálculo del coeficiente de difusión en función únicamente de la temperatura y presión, y de propiedades fisicoquímicas del CO_2, como la densidad y la viscosidad, las que a su vez dependen de la temperatura y presión de extracción.

En la figura 2.2 se resume el plan de trabajo desarrollado.

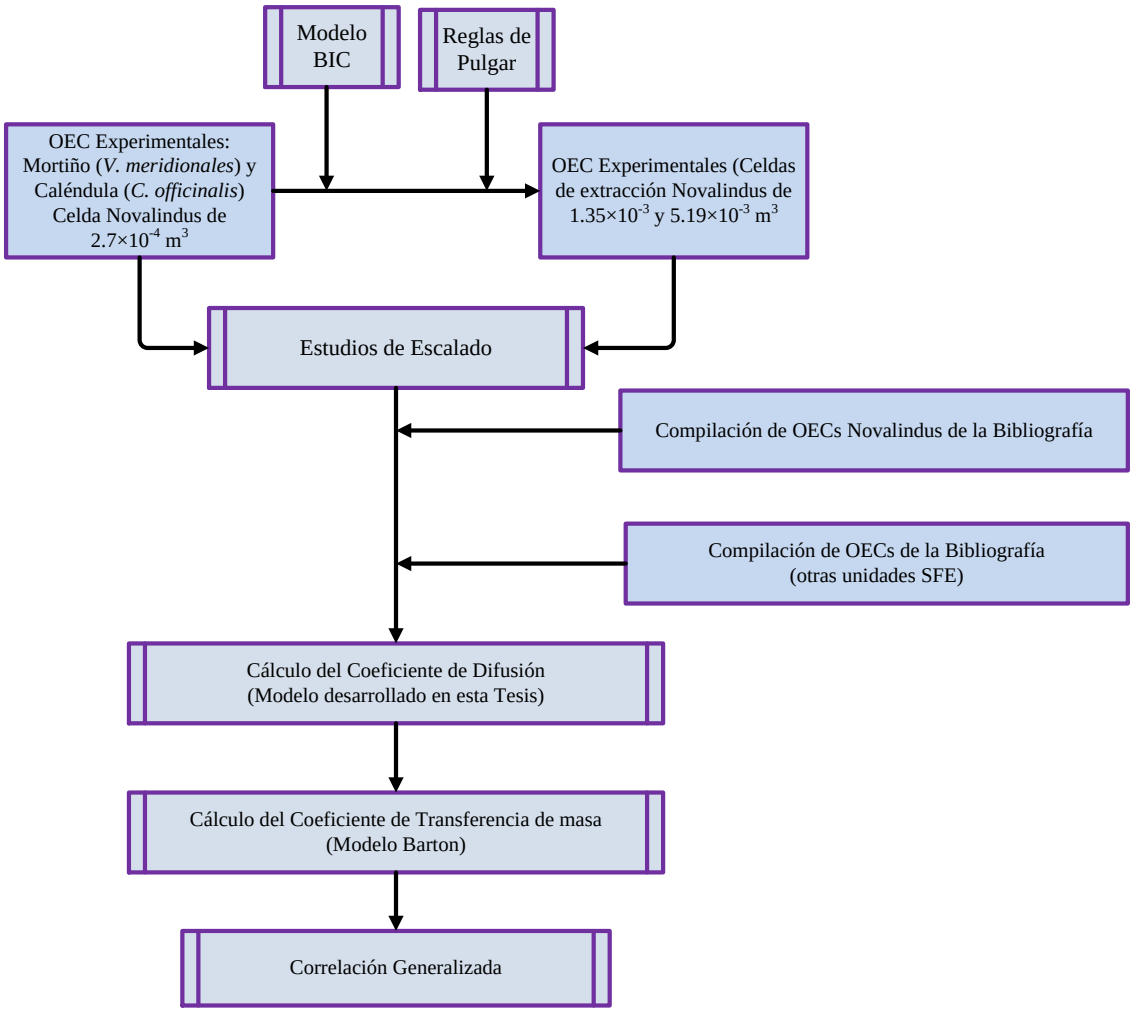

Figura 2.2 Esquema del Plan de Trabajo desarrollado en esta Tesis.

CAPÍTULO 3.

RESULTADOS

3. RESULTADOS

3.1 Prefacio

Como se describió en la introducción de esta memoria, la extracción con fluidos supercríticos utilizando dióxido de carbono se ha consolidado como una tecnología versátil, eficaz y respetuosa con el medio ambiente. Una prueba de ello es la extensión extraordinaria de sus aplicaciones en la investigación, desarrollo e innovación, siendo particularmente destacables las orientadas a la producción de ingredientes alimentarios funcionales.

Se estima que, sólo en la última década, se ha estudiado la obtención mediante tecnología supercrítica de extractos de más de 300 especies diferentes de plantas, con un gran número de aplicaciones a escala analítica y/o semi-preparativa para la obtención de ingredientes bioactivos [1,4,35,177–179].

Sin embargo, la velocidad con la que la academia ha adaptado y aplicado la SFE ha ocurrido de una forma mucho mayor que en la industria y el resultado puede verse reflejado en el número de plantas industriales (aproximadamente 150) de las que se tiene registro y que se han construido a nivel mundial con volúmenes de extracción superior a los 0.5 m^3 [27,28]. Los factores que han afectado el crecimiento de la SFE a nivel industrial se basan en los altos costes de inversión iniciales asociados a los procesos de extracción con fluidos supercríticos, así como a la escasez de trabajos y bibliografía sobre procedimientos confiables de escalado. Con respecto a los primeros, este concepto ha ido cambiando en los últimos años, debido a la expansión en la fabricación de equipos de alta presión, la variabilidad de los costos de producción en función de la aplicación específica y la alta calidad de los productos que se obtienen [27].

Por otro lado, si bien la información sobre procedimientos de escalado y diseño de plantas son fundamentales para que las empresas productoras puedan optimizar el tamaño y la configuración de plantas industriales desde un punto de vista económico, las herramientas actualmente disponibles no son todavía muy fiables, no son muy comprensibles o se encuentran parcialmente disponibles [28].

En particular, para el diseño adecuado de los procesos *batch* de extracción con fluidos supercríticos, es esencial tener un buen conocimiento del mecanismo de transferencia de

masa y una representación matemática apropiada de este proceso. Esto permitirá un diseño mucho más confiable de los diversos componentes del equipo al pasar de una escala analítica y/o semi-preparativa a una escala piloto y/o industrial [11-13].

En el Laboratorio de Extractos Naturales del CIAL (UAM-CSIC) se han estado desarrollando numerosos proyectos de investigación donde la extracción con CO_2 supercrítico ha sido el punto partida, aplicándose a diversas materias primas vegetales y en operaciones que van desde la escala analítica, laboratorio, piloto y semi-industrial mediante la utilización de la Plataforma Novalindus. Muchos de los resultados obtenidos hasta ahora se han enfocado a la caracterización, identificación, cuantificación y aplicación de los compuestos presentes en los extractos obtenidos como ingredientes alimentarios funcionales. Sin embargo, los estudios no han abordado de forma rigurosa las posibles estrategias de aumento de escala, para obtener mayor información del proceso SFE, haciéndolo más viable a la hora de extrapolar los resultados a un entorno comercial.

Teniendo en cuenta lo anteriormente expuesto, y sobre la base de los antecedentes analizados y descritos en la Introducción en esta Tesis Doctoral, se estudió el escalado en la extracción supercrítica de materiales de origen vegetal empleando CO_2 supercrítico, para desarrollar un procedimiento sencillo, eficaz y de fácil aplicación que permitiera correlacionar el comportamiento cinético de los procesos SFE llevados a cabo en la Plataforma Novalindus, empleando diferentes materias primas de origen vegetal y diferentes condiciones de extracción.

En la sección 3.2 se presentan los resultados del estudio experimental del proceso de escalado SFE en *batch* llevado a cabo con mortiño (*V. meridionale* Swartz) empleando las celdas de extracción de la Plataforma Novalindus de 2.7×10^{-4} m^3 y 1.35×10^{-3} m^3 y titulado "*Vaccinium meridionale Swartz Supercritical CO_2 Extraction: Effect of Process Conditions and Scaling Up*" de López-Padilla y col. publicado en la revista Materials 2016, 9 (519); doi:10.3390/ma9070519.

La sección 3.3 presenta los resultados obtenidos en el estudio del escalado SFE utilizando celdas de extracción con volúmenes de 2.7×10^{-4} m^3, 1.35×10-3 m^3 y 5.19×10^{-3} m^3 utilizando como materia prima la flor de caléndula (*C. officinalis*) titulado "*Supercritical carbon dioxide extraction of Calendula officinalis: kinetic modeling and scaling up study*". De López-Padilla y col. publicado en la revista Journal of Supercritical Fluids, 2017 (en prensa).

Los resultados de ambos estudios comprobaron que, habiendo aplicado únicamente dos criterios de escaldo, y al igual que en otros estudios de la bibliografía, no existe un único criterio de escalado aplicable a la SFE de las unidades de la Plataforma Novalindus. Así, con el objetivo de desarrollar una correlación general para todas las cinéticas de extracción obtenidas en Novalindus, se abordó el cálculo del coeficiente de difusión y del coeficiente de transferencia de masa, dos parámetros fundamentales de la extracción SFE.

En la sección 3.4 se presenta el trabajo titulado "*Study of the diffusion coefficient of solute-type extracts in supercritical carbon dioxide: Volatile oils, fatty acids and fixed oils*" de López-Padilla y col., publicado en la revista Journal of Supercritical Fluids, 2016, 109, 148-156. En este trabajo se desarrollan correlaciones semi-empíricas y simples para estimar el coeficiente de difusión de un extracto tipo (aceite esencial, ácidos grasos o aceites fijos) en función únicamente de la temperatura y la presión de operación. Estas correlaciones mantienen un alto grado de precisión en comparación con otros modelos y métodos de la bibliografía más costosos matemáticamente y que demandan parámetros, los que están disponibles para componentes puros, pero no disponibles para mezclas multicomponentes como son los extractos supercríticos.

A partir de los datos cinéticos obtenidos en esta Tesis Doctoral se desarrolló una correlación simple para el escalado SFE que permite estimar el caudal de SC-CO_2 necesario para efectuar un aumento de escala (manteniendo la temperatura y presión de operación) en función del número de Schmidt y de las variables geométricas del lecho fijo (diámetro y altura). Además, esta correlación pudo ser ampliada para incluir diferentes materiales de origen vegetal, incluyendo el diámetro de partícula y porosidad del lecho empacado. Estos resultados se presentan en la sección 3.5, en el trabajo titulado "*Supercritical extraction of solid materials: a practical correlation related with process scaling*" de López-Padilla y col. enviado a la revista Journal of Food Engineering en junio de 2017.

3.2 Vaccinium meridionale Swartz Supercritical CO_2 Extraction: Effect of Process Conditions and Scaling Up

Alexis López-Padilla, Alejandro Ruiz-Rodríguez, Claudia Estela Restrepo Flórez, Diana Marsela Rivero Barrios, Guillermo Reglero & Tiziana Fornari

Materials, 2016, 9(519);
DOI:10.3390/ma9070519.

materials

MDPI

Article

Vaccinium meridionale Swartz Supercritical CO_2 Extraction: Effect of Process Conditions and Scaling Up

Alexis López-Padilla [1], Alejandro Ruiz-Rodriguez [1], Claudia Estela Restrepo Flórez [2], Diana Marsela Rivero Barrios [2], Guillermo Reglero [1] and Tiziana Fornari [1,*]

[1] Institute of Food Science Research CIAL (CSIC-UAM)—CEI UAM + CSIC, Madrid 28049, Spain; alexis.lopez@estudiante.uam.es (A.L.-P.); alejandro.ruiz@uam.es (A.R.-R.); guillermo.reglero@uam.es (G.R.)

[2] INTAL Foundation Cra 50 G N° 12 Sur 91, Itagüí 050023, Colombia; crestrepo@fundacionintal.org (C.E.R.F.); vidautil@fundacionintal.org (D.M.R.B.)

* Correspondence: tiziana.fornari@uam.es; Tel.: +34-910-017-927

Academic Editor: Carlos Manuel Silva
Received: 11 March 2016; Accepted: 20 June 2016; Published: 25 June 2016

Abstract: *Vaccinium meridionale* Swartz (Mortiño or Colombian blueberry) is one of the *Vaccinium* species abundantly found across the Colombian mountains, which are characterized by high contents of polyphenolic compounds (anthocyanins and flavonoids). The supercritical fluid extraction (SFE) of *Vaccinium* species has mainly focused on the study of *V. myrtillus* L. (blueberry). In this work, the SFE of Mortiño fruit from Colombia was studied in a small-scale extraction cell (273 cm^3) and different extraction pressures (20 and 30 MPa) and temperatures (313 and 343 K) were investigated. Then, process scaling-up to a larger extraction cell (1350 cm^3) was analyzed using well-known semi-empirical engineering approaches. The Broken and Intact Cell (BIC) model was adjusted to represent the kinetic behavior of the low-scale extraction and to simulate the large-scale conditions. Extraction yields obtained were in the range 0.1%–3.2%. Most of the Mortiño solutes are readily accessible and, thus, 92% of the extractable material was recovered in around 30 min. The constant CO_2 residence time criterion produced excellent results regarding the small-scale kinetic curve according to the BIC model, and this conclusion was experimentally validated in large-scale kinetic experiments.

Keywords: supercritical fluid extraction; *Vaccinium meridionale* Swartz; extracts; scale-up

1. Introduction

The genus *Vaccinium* comprises a group of plants that includes up to 450 species with promising biological activities [1]. In different places its berries are being consumed as a part of a rich dietary source of various phytonutrients, including phenolic compounds such as flavonoids, phenolic acids, lignans and polymeric tannins [2]. In a recent study, Abreu et al. have reported medicinal uses for food uses of 36 *Vaccinium* species, mainly from North America, Asia and Europe [3]. The most commonly reported uses of *Vaccinium* extracts are as antioxidants due to their high content of anthocyanins and other antioxidants [4,5], but in addition to the antioxidant activity due to the anthocyanins, there is evidence of their antidiabetic [6], anti-hyperlipidemic [7], anti-tumorigenic [8] and neuroprotective effects [9].

Vaccinium meridionale Swartz (Mortiño or Colombian blueberry) is one of the *Vaccinium* species which grows in the Andean region of South America at 2300–3300 m above the sea level. Some authors have reported a cardioprotective effect of products obtained from Mortiño fermentation, suggesting that the consumption of Mortiño or its related products could be of importance not only in the maintenance of health but also in preventing cardiovascular diseases [10,11].

In the last decade, green technologies such as supercritical fluid extraction (SFE) have been used as alternatives to conventional solvent extraction in the recovery of plant extracts containing phenolic compounds, anthocyanins and other antioxidants [12,13]. Carbon dioxide (CO_2) is widely used for the extraction of natural compounds since it has moderate critical conditions (304.2 K, 7.38 MPa) and it is a colorless, odorless, nontoxic, non-flammable, safe, highly pure and cost-effective solvent [14–16]. Due to its low critical temperature, the thermal degradation of natural products and the subsequent generation of undesirable compounds are minimized or avoided. The low temperatures required, the absence of oxygen during extraction, and the advantage of recovering the extract with high purity, free of solvent, contribute to producing plant extracts of superior quality, i.e., better functional activity, in comparison with extracts produced using liquid solvents.

However, in the case of the genus *Vaccinium*, supercritical CO_2 extractions have been focused on *Vaccinium myrtillus* L. (blueberry), especially on the study of the extraction of phenolic compounds, anthocyanins and proanthocyanidins using ethanol and water as modifiers [17,18]. To our knowledge, no reports are available in the literature regarding the SFE of Mortiño fruits. Hence, the importance of the present study is based on the use of supercritical CO_2 extraction to recover bioactives from Mortiño, a widely distributed product in Colombia.

In this work, the SFE of Mortiño from Colombia, previously dehydrated until 12% of the moisture content remained and ground until a mean particle size of 240 µm was reached, was investigated in a small-scale extraction cell (273 cm^3) using different process conditions: pressures of 10 and 30 MPa, temperatures of 313 and 343 K, and CO_2 flows of 18 and 32 $g \cdot min^{-1}$. Extraction yields obtained were in a range of 1%–3%. Speedy extraction was observed studying the kinetic behavior of the process.

Theoretical and semi-empirical approaches were applied to study the SFE scaling-up to an extraction cell of 1350 cm^3 capacity. Pressure and temperature were preserved in both small- and large-scale experiments. Also, in order to make a comparison possible, the same particle size was used, as well as bed density and porosity. Two well-known scale-up criteria were tested [19]: maintaining the same linear velocity or maintaining the residence time of the solvent in the SFE bed. The model of Sovová [20] was adjusted to represent the kinetic behavior of the low-scale extraction and then was used to simulate the large-scale conditions and to evaluate the usefulness of the scale-up criteria.

2. Materials and Methods

2.1. Plant Material

Fresh and mature (between four and six years old plants) berries of *V. meridionale* were manually harvested in the farm "la Guija", "El Retiro" zone (2300 m altitude above sea level) belonging to the Antioquia region of Colombia. The berries where then transported to the Instituto de Ciencia y Tecnología Alimentaria (INTAL Foundation, Cra. 50 G N° 12 Sur 91, Itagüí, Colombia) where they were washed and disinfected with the organic disinfectant Citrosan® and then ground in a 15 L capacity cutting machine (Cruells, Girona, Spain) at a chopper speed of 1300 rpm. The disintegrated fruits were then arranged in aluminum trays of 40 × 60 cm containing about 1.5 kg of fruit per tray and subjected to a drying process in a forced convection oven (Binder FD115, Tuttlingen, Germany) to 318 K for 48 h. The product was then removed after 24 h and allowed to cool at room temperature of 296 ± 2 K for 4 h. A second size reduction process was performed using the same cutting machine as described before, and the final product with a particle size range of 500 µm–1.0 mm was vacuum packed in foil zipsealed pouches (BOPP/polyamide/LDPE) (Alico A.A., Medellin, Colombia) and sent it to the Universidad Autónoma de Madrid.

The plant material density (ρ_s) was determined using a helium pycnometer Ultrapyc 1200e (Quantachrome, Boynton Beach, FL, USA) and resulted to be of 1441.6 ± 0.4 $kg \cdot m^{-3}$.

2.2. Chemicals

Ethanol absolute (99.5% purity) was purchased from Panreac (Barcelona, Spain). The CO_2 (N-38) was obtained from Carburos Metalicos, S.A. (Madrid, Spain).

2.3. Supercritical Fluid Extraction

V. meridionale Sw. extracts were obtained using a pilot plant supercritical fluid extractor from Thar Technologies Inc (model SF2000; Pittsburgh, PA, USA) with two extraction vessels of 273 cm^3 (small-scale experiments) or 1350 cm^3 (large-scale experiments) of capacity.

The SFE devise comprises a cascade decompression system of two separators with independent temperature ($\pm$2 K) and pressure ($\pm$0.1 MPa) control. The extraction unit also includes a recirculation system, were the CO_2 is condensed and pumped up to the desired extraction pressure. The pressure in the extraction cell is controlled by an automated back pressure regulator valve. The CO_2 flow is measured using a flow meter from Siemens AIS (Model: Sitrans F C Mass 2100 DI 1.5, Nordborgvej, Denmark). The SFE PLC-based instrumentation and controls as well as the rest of the features have been described in detailed in previous works [21,22].

2.3.1. Small-Scale Extractions

First, small-scale kinetic behavior was studied using the 273 cm^3 cylindrical extraction vessel (internal diameter = 0.043 m; height = 0.188 m) packed with 0.160 kg of ground Mortiño with a mean particle size of 254 μm. The selected extraction conditions were of 30 MPa, 313 K and 32 $g \cdot min^{-1}$ of CO_2. The first data point was measured after 10 min of extraction, and the rest of the data were collected at intervals of 20 min until completing the total extraction time (180 min).

Then, in order to study the effect of process conditions on the overall extraction yield, small-scale extractions were accomplished using also 0.160 kg of Mortiño but at two different pressures (10 MPa and 30 MPa) and temperatures (313 K and 343 K). The overall extraction time was also set to 180 min and the CO_2 flow rate was 18 $g \cdot min^{-1}$.

In all experimental assays the supercritical stream was decompressed at a pressure of 6 MPa in both separators and CO_2 was recirculated during the whole extraction time. The solid, pasty extracts were recuperated and placed in vials. In order to ensure an accurate determination of the extraction yield with time, separators were washed with ethanol which was eliminated afterwards by evaporation at low temperature (313 K) in a rotavapor R210 (Büchi Labortechnik AG, Flawil, Switzerland).

2.3.2. Large-Scale Extractions

Kinetic data were obtained using the 1350 cm^3 cylindrical extraction vessel (internal diameter of 0.07 m; height of 0.388 m) loaded with 0.800 kg of ground Mortiño. The extraction pressure and temperature were the same as in the small-scale kinetic experiment (30 MPa and 313 K). The CO_2 flow rate was set to 158 $g \cdot min^{-1}$ according to the results of the BIC model process simulation. The material extracted at 15, 30, 100 and 160 min of extraction was collected from the separators the same way as described above.

2.4. Scaling Criteria and Mass Transfer Modeling

The objective of scaling up is to reproduce the kinetic behavior of the extraction curves obtained when using different extraction cells. Bed geometry is very important in SFE and can influence overall yield so as extract composition [23]. In general, extraction vessels are cylindrical and thus length (L) and bed diameter (D) of the cylinder are the variables which characterize bed geometry. Yet, to make the kinetic comparison possible, certain process variables such as extraction temperature and pressure should be maintained constant in both small- and large-scale extraction vessels. Also, the same particle size, as well as bed density and porosity, should be preserved. Thus, the key point is to determine the solvent flow necessary in the large-scale device (Q_{LS}) in order to attain similar kinetic profiles.

In this work two engineering approaches were applied to estimate Q_{LS} as a function of the solvent flow used in the small-scale experiment (Q_{SS}) and bed geometry. The first criterion was keeping the CO_2 velocity constant, thus:

$$Q_{LS} = \left(\frac{D_{LS}}{D_{SS}}\right)^2 Q_{SS} \quad (1)$$

Equation (1) was obtained considering that the same temperature and pressure (same CO_2 density) were preserved in both small- and large-scale experiments, and the cross-flow area of the cylindrical extraction vessels is $A = \pi D^2/4$.

The second criterion adopted was keeping the solvent residence time (t_R) constant. The t_R was calculated as the ratio between the bed volume accessible to CO_2 flow $\left(\pi D^2 L \varepsilon \rho/4\right)$ and the CO_2 flow rate (Q) [19]:

$$t_R = \frac{\pi D^2 L \varepsilon \rho}{4Q} \quad (2)$$

where D is the internal diameter of the extraction vessel; ε is the bed porosity and ρ is CO_2 density. Thus, the constant residence time criterion requires that:

$$Q_{LS} = \left(\frac{D_{LS}}{D_{SS}}\right)^2 \left(\frac{L_{LS}}{L_{SS}}\right) Q_{SS} \quad (3)$$

In this work, large-scale kinetic experiments were carried out preserving extraction temperature and pressure as those used in the small-scale kinetic assays (313 K and 30 MPa) and using in each experiment the CO_2 flow rate predicted by Equations (1) or (2).

Several scaling-up criteria were reported and analyzed in the literature, as described by Zabot et al. [24]. In general, there is no single criterion that can be effectively applied to all systems. For example, keeping the same residence time of the solvent inside the SFE bed (Equation (2)) was successfully applied for the SFE of clove buds but did not result adequate for the SFE of vetiver roots [19].

Vegetal matrices are complex and the type of extractable solutes and their location in the raw material affects the kinetics of extraction. For example, volatile oil is rather easy to extract by SFE, and its major part is obtained in the early stage of the extraction. In these cases, the broken and intact cells (BIC) mass transfer model has demonstrated good capability to represent the kinetic behavior [20]. In the BIC model, the solid phase is considered to be comprised by broken and intact cells and thus the total extractable oil is divided by easily accessible solute, which is available on the surface of the broken cells, and poorly accessible solute which is confined in the intact part of the cells.

The following assumptions are considered in the BIC model: temperature and pressure are constant during the whole extraction time; particle size and oil distributions are uniform in the packed bed; void fraction is constant during the extraction; CO_2 is solute free at the bed entrance; axial dispersion can be neglected (plug flow is assumed). Then, three different extraction periods can be distinguished:

1. The constant extraction rate (CER) period, in which the external surface of the particles is covered with easily accessible solute, and thus the extraction rate is constant during this period and determined by the convective solvent film resistance.
2. The falling extraction rate (FER) period, in which the intra-particle diffusion starts to become important. The remained accessible solute continues to be extracted but also the solute in the intact cells starts to be extracted. Thus, the extraction rate drops rapidly and at the end of this period, all the readily accessible solute has been removed from the vegetal matrix.
3. The diffusion controlled (DC) period, in which only the less accessible solute in intact cells is slowly extracted. Mass transfer is mainly dominated by slow diffusion inside the solid vegetal particles.

The BIC model equations to calculate the mass extracted (m) as a function of extraction time (t) in the different periods are the following [20]:

CER period:

$$m = Q\,Y*\left[1-\exp(-Z)\right]\,t \tag{4}$$

FER period:

$$m = Q\,Y*\left[t - t_{CER}\exp(Z_w - Z)\right] \tag{5}$$

DC period:

$$m = m_{SI}\left\{X_o - \frac{Y*}{W}\ln\left[1+\left[\exp\left(\frac{WX_o}{Y*}\right)-1\right]\exp\left[\frac{WQ(t_{CER}-t)}{m_{SI}}\right]\left(\frac{X_k}{X_o}\right)\right]\right\} \tag{6}$$

where,

$$Z = \frac{m_{SI}k_{YA}\rho}{Q(1-\varepsilon)\rho_s} \tag{7}$$

$$W = \frac{m_{SI}k_{XA}}{Q(1-\varepsilon)} \tag{8}$$

$$Z_W = \frac{ZY*}{WX_o}\ln\left\{\frac{X_o\exp\left[WQ(t-t_{CER})/m_{SI}\right]-X_k}{X_o-X_k}\right\} \tag{9}$$

$$t_{CER} = \frac{m_{SI}(X_o-X_k)}{Y*ZQ} \tag{10}$$

$$m_{SI} = X_oF \tag{11}$$

Process parameters required to apply the BIC model are the bed porosity (ε), mass (F) and density (ρ_s) of feed raw material, CO_2 density (ρ) and mass flow rate (Q). Additionally, the solubility of the extract in the supercritical solvent (Y^*) and the global extraction yield (X_o) have to be determined to apply the BIC model.

Parameters which are optimized according to the experimental kinetics are the intra-particle solute ratio (X_k) and the fluid phase and solid phase mass transfer coefficients (k_{YA} and k_{XA}). The ready accessible solute (X_p) is calculated as the difference ($X_o - X_k$).

3. Results

3.1. Small-Scale Extractions

The experimental conditions and yields obtained in the small-scale assays are given in Table 1. The extraction yield was calculated as the ratio between the mass extracted (m) and the mass of Mortiño used (F). As expected, the extraction yield increase with increasing pressure. With respect to temperature, the experimental results obtained follow the cross-over behavior observed for the solubility of solutes in supercritical CO_2: at low pressure (10 MPa) the yield decreased with the rise of temperature, but at higher pressure (30 MPa) the yield increased with increasing temperature.

Table 1. SFE of *Vaccinium meridionale* Swartz (Mortiño). Extraction cell capacity = 273 cm^3 (0.160 kg of Mortiño); CO_2 flow = 18 g· min^{-1}; Extraction time = 180 min.

Experiment	T (K)	P (MPa)	Yield (%)
1	313	10	1.03
2	343	10	0.08
3	313	30	2.67 *
4	343	30	3.16

* Standard Deviation = $\sqrt{\frac{\sum(x_1-x_2)^2}{2}}$; x_1 and x_2 are values of duplicate experiments (Experiment 3 was the only experiment that was carried out in duplicate).

Extraction yields of *Vaccinium meridionale* Swartz (Mortiño) were lower than 3.2% in the range of conditions explored. The supercritical CO_2 extraction of *Vaccinium myrtillus* (Blueberry) residues was recently reported by Paes et al. [17]. Although species are different, for the sake of comparison, the yields were around 2% from the fresh sample at 313 K and at pressures of 15–25 MPa. Higher yields were obtained (up to 7.6%) from freeze-dried samples but using water and ethanol as CO_2 cosolvents.

The kinetics of the overall extraction curve obtained in the small-scale cell at 313 K and 30 MPa is shown in Figure 1. The CO_2 mass flow was 32 g·min^{-1} during 180 min of extraction, with a solvent-to-raw material ratio of 36 kg·kg^{-1}. The experiment was carried out in duplicate; the mean values and standard deviations obtained in the accumulated yield are given in Table 2.

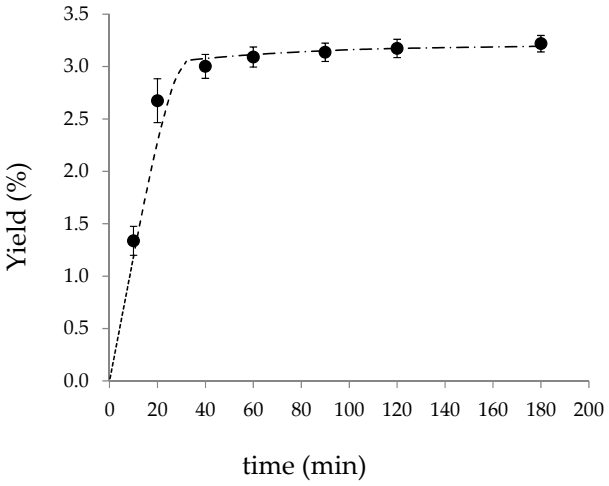

Figure 1. Kinetic behavior of Mortiño SFE at 313 K and 30 MPa in the small-scale extraction cell (273 cm^3) and with CO_2 mass flow Q_{SS} = 32 g·min^{-1}. (●) experimental data. Solid lines represent the BIC model fitting: (· · · · · ·) CER period; (- - -) FER period; (- · - ·) DC period.

Table 2. Experimental yield (%) obtained in the kinetic study of SFE of *Vaccinium meridionale* Swartz (Mortiño) at 313 K and 30 MPa in the low-scale extraction cell (273 cm^3). CO_2 flow = 32 g·min^{-1}.

Time (min)	Yield (%)			Standard Deviation (*SD*) *
	Kinetic 1	Kinetic 2	Mean Value	
10	1.24	1.44	1.34	0.14
20	2.53	2.82	2.67	0.21
40	2.92	3.08	3.00	0.11
60	3.02	3.16	3.09	0.09
90	3.07	3.20	3.14	0.09
120	3.11	3.23	3.17	0.09
180	3.16	3.27	3.22	0.08

* $SD = \sqrt{\frac{\sum(x_1 - x_2)^2}{2}}$ being x_1 and x_2 the corresponding values of duplicate experiments.

3.2. BIC Model Fitting of Small-Scale Experimental Kinetics

The BIC model was used to correlate the kinetic data obtained in the small-scale extraction cell. The Mortiño density (ρ_s) was 1441.6 kg·m^{-3}, and the bed porosity was determined on the basis of the corresponding apparent density (592.6 kg·m^{-3}) and resulted in ε = 0.5890. The CO_2 density at 30 MPa and 313 K was obtained from thermodynamic tables (ρ = 910 kg·m^{-3}) [25]. The solubility of the whole extract was estimated as the slope of a theoretical linear behavior of the extraction curve between t = 0 and t = 10 min (see data in Table 2) and resulted in Y^* = 0.006685 kg·kg^{-1} (apparent solubility). The global yield was assessed on the basis of the maximum yield attained (theoretically for $t \rightarrow \infty$) as 3% above the total amount extracted (X_o = 0.03315 kg·kg^{-1}).

Then, the intra-particle solute ratio (X_k) and the mass transfer coefficients in the fluid and solid phases (k_{YA} and k_{XA}) were adjusted to reproduce the experimental small-scale kinetic curve. The values obtained are X_k = 0.0018 kg· kg^{-1}, k_{YA} = 0.00490 s^{-1} and k_{XA} = 0.00016 s^{-1}. Table 3 reports the absolute relative deviation (ARD) between the experimental and calculated accumulated yields (the mean ARD was 2.10%).

Table 3. BIC model fitting of Mortiño SFE experimental kinetics at 30 MPa and 313 K in a small-scale extraction cell (273 cm^3).

T (min)	Experimental Yield Y_{exp} (%)	Calculated Yield Y_{cal} (%)	ARD *
10	1.34	1.30	2.73
20	2.67	2.48	7.39
40	3.00	3.02	0.57
60	3.09	3.14	1.65
90	3.14	3.17	1.01
120	3.17	3.17	0.02
180	3.22	3.18	1.35

* Absolute Relative Deviation = $100 \times \frac{|Yexp - Ycal|}{Yexp}$.

The optimal intra-particle solute ratio (X_k) was around 10 times lower than X_p, denoting that most of the solute is readily accessible and, thus, during the CER period (t_{CER} = 5.7 min) more than 23% of the extractable solute was recovered from Mortiño raw material. Moreover, after around 30 min (t_{FER} = 28.2 min) 94.5% of the extractable material was recovered. Accordingly, the optimal mass transfer coefficient in the fluid phase was 23 times higher than the mass transfer coefficient in the solid phase.

3.3. BIC Model Prediction of Large-Scale Mortiño SFE and Comparison with Experimental Large-Scale Extraction

The optimized parameters obtained in the BIC model fitting of the small-scale experimental Mortiño kinetics (273 cm^3 extraction cell, 32 g· min^{-1} CO_2) were applied to predict the kinetic behavior in the large-scale cell (1350 cm^3). The CO_2 density, solid density, apparent solubility and global extraction yield were kept constant. The mass of the raw material (F_{LS}) was calculated to be 0.800 kg according to the volume of the large-scale cell and to maintain the bed porosity constant (ε = 0.5890). The CO_2 mass flow rate (Q_{LS}) was calculated using the constant CO_2 residence time scaling-up criteria (Equation (1)). The Q_{LS} value that resulted was 158.2 g· min^{-1}. Table 4 and Figure 2 show a comparison between the two large-scale kinetics predicted by the BIC model. Certainly, the constant CO_2 residence time criterion (t_R = 4.58 min) produced the best results of the small-scale kinetic. The predicted t_{CER} and t_{FER} were very similar to the values corresponding to the small-scale extraction (see Table 4). Finally, as depicted in Figure 2, the experimental kinetic data obtained from the large-scale extraction also confirmed that maintaining a constant CO_2 residence time is a valid procedure to scaling-up Mortiño SFE.

Table 4. BIC model prediction of Mortiño SFE kinetics at 30 MPa and 313 K in a large-scale extraction cell (1350 cm^3).

Parameter	Small Scale (273 cm^3)	Large Scale (1350 cm^3)	
		Constant v	Constant t_R
F (g)	160	800	800
D (cm)	4.3	6.7	6.7
L (cm)	18.8	38.3	38.3
Q (g/min)	32	77.6	158.2
v (cm/min)	2.42	2.42	4.93

Table 4. *Cont.*

Parameter	Small Scale (273 cm^3)	Large Scale (1350 cm^3)	
		Constant v	Constant t_R
D/L	0.229	0.175	0.175
F/Q (min)	5.00	10.30	5.06
CO_2/F (g/g) t = 20 min	4.00	1.94	3.96
t_R (min)	4.58	9.32	4.58
t_{CER} (min)	5.70	5.63	5.63
t_{FER} (min)	28.2	52.9	28.4

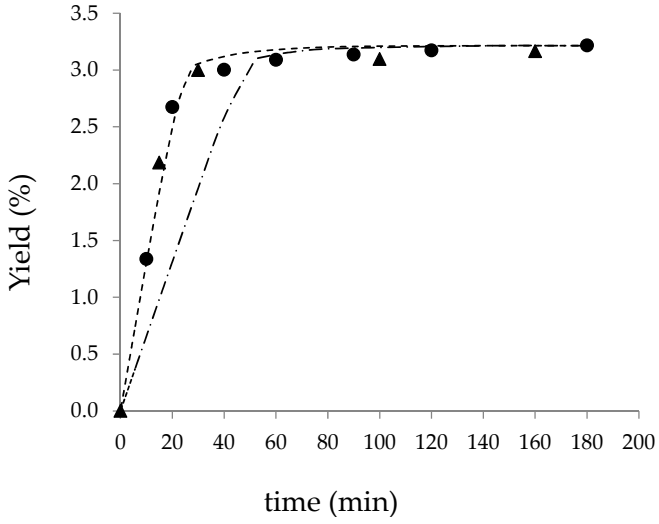

Figure 2. Scaling-up of Mortiño SFE at 40 °C and 30 MPa. Full symbols represent experimental data: (●) small-scale cell with Q_{SS} = 32 g·min^{-1}; (▲) large-scale cell with Q_{LS} = 158.0 g·min^{-1} (Equation (2)). Lines represent the different BIC model periods: (- · - ·) Q_{LS} = 77.6 g·min^{-1} and (- - -) Q_{LS} = 158.2 g·min^{-1}.

Duba and Fiori [26] recently discussed the effect of process parameters on the extraction kinetics of grape seed oil. Regarding the effect of the D/L ratio, they concluded that while keeping the ratio of the substrate mass to the CO_2 mass flow rate constant, the lower the D/L and the lower the specific CO_2 consumption. In this work, the D/L was 0.229 and 0.175, respectively, for the small- and large-scale extraction cells. The corresponding substrate mass to CO_2 mass flow rate (F/Q) are given in Table 4, together with the specific CO_2 consumption after 20 min of extraction. The constant F/Q (constant t_R criteria) denotes almost the same specific CO_2 consumption to attain the same kinetic behavior, with rather similar D/L values.

4. Conclusions

The supercritical CO_2 extraction of *Vaccinium meridionale* Swartz was studied to investigate the kinetic behavior, the effect of pressure and temperature on extraction yield and the potential scaling-up criteria.

A high extraction velocity was observed at 30 MPa and 313 K: around 95% of the extractable material was recovered in 30 min of extraction. Moreover, a significant effect of pressure and temperature on the overall extraction yield was determined. In the range of conditions studied, the cross-over behavior of the extraction yield with respect to pressure and temperature was observed.

An accurate representation of the overall extraction curve was obtained with the BIC model. Furthermore, a satisfactory scaling from the small-scale kinetic curve to a five-times-larger extraction vessel was obtained, maintaining constant CO_2 residence time as the scaling-up criterion.

The studies reported in this work provide preliminary and worthy fundamentals to develop supercritical CO_2 natural extracts from Colombian *Vaccinium meridionale* Swartz fruit.

Acknowledgments: Alexis López-Padilla thanks the Administrative Department of Science, Technology and Innovation—Colciencias (Call 568/2012) for his Ph.D. fellowship. This work was financed thanks to the ALIBIRD, S2013/ABI-2728 (Comunidad de Madrid) project.

Author Contributions: Alexis López-Padilla performed and designed the experiments as well as data analysis; Claudia Estela Restrepo Flórez and Diana Marsela Rivero Barrios made the pretreatment of the sample; Tiziana Fornari, Alejandro Ruiz-Rodriguez and Guillermo Reglero designed the experiments and provided guidance and all sorts of support during the work.

Conflicts of Interest: The authors declare no conflict of interest.

References

1. Schreckinger, M.E.; Wang, J.; Yousef, G.; Lila, M.A.; De Mejia, E.G. Antioxidant capacity and in vitro inhibition of adipogenesis and inflammation by phenolic extracts of *Vaccinium floribundum* and *Aristotelia chilensis*. *J. Agric. Food Chem.* **2010**, *58*, 8966–8976. [CrossRef] [PubMed]
2. Kšonžeková, P.; Mariychuk, R.; Eliašová, A.; Mudroňová, D.; Csank, T.; Király, J.; Marcinčáková, D.; Pistl, J.; Tkáčiková, L. In vitro study of biological activities of anthocyanin-rich berry extracts on porcine intestinal epithelial cells. *J. Sci. Food Agric.* **2016**, *96*, 1093–1100. [CrossRef] [PubMed]
3. Abreu, O.A.; Barreto, G.; Prieto, S. *Vaccinium* (ericaceae): Ethnobotany and pharmacological potentials, Emirates. *J. Food Agric.* **2014**, *26*, 577–591. [CrossRef]
4. Smeriglio, A.; Monteleone, D.; Trombetta, D. Health effects of *Vaccinium myrtillus* L.: Evaluation of efficacy and technological strategies for preservation of active ingredients. *Mini Rev. Med. Chem.* **2014**, *14*, 567–584. [CrossRef] [PubMed]
5. Gaviria Montoya, C.; Ochoa Ospina, C.; Sánchez Mesa, N.; Medina Cano, C.; Lobo Arias, M.; Galeano García, P.; Mosquera Martínez, A.; Tamayo Tenorio, A.; Lopera Pérez, Y.; Rojano, B. Actividad antioxidante e inhibición de la peroxidación lipídica de extractos de frutos de mortiño (*Vaccinium meridionale* Sw). *Bol. Latinoam. Caribe Plantas Med. Aromat.* **2009**, *8*, 519–528.
6. Güder, A.; Gür, M.; Engin, M.S. Antidiabetic and Antioxidant Properties of Bilberry (*Vaccinium myrtillus* Linn.) Fruit and Their Chemical Composition. *J. Agric. Sci. Technol.* **2015**, *17*, 401–414.
7. Asgary, S.; Rafieiankopaei, M.; Sahebkar, A.; Shamsi, F.; Goli-malekabadi, N. Anti-hyperglycemic and anti-hyperlipidemic effects of *Vaccinium myrtillus* fruit in experimentally induced diabetes (antidiabetic effect of *Vaccinium myrtillus* fruit). *J. Sci. Food Agric.* **2016**, *96*, 764–768. [CrossRef] [PubMed]
8. Lala, G.; Malik, M.; Zhao, C.; He, J.; Kwon, Y.; Giusti, M.M.; Magnuson, B.A. Anthocyanin-rich extracts inhibit multiple biomarkers of colon cancer in rats. *Nutr. Cancer.* **2006**, *54*, 84–93. [CrossRef] [PubMed]
9. Subash, S.; Essa, M.; Al-Adawi, S.; Memon, M.; Manivasagam, T.; Akbar, M. Neuroprotective effects of berry fruits on neurodegenerative diseases. *Neural Regen. Res.* **2014**, *9*, 1557–1566. [PubMed]
10. Ashour, O.M.; Elberry, A.A.; Alahdal, A.; Al Mohamadi, A.M.; Nagy, A.A.; Abdel-Naim, A.B.; Abdel-Sattar, E.A.; Mohamadin, A.M. Protective effect of bilberry (*Vaccinium myrtillus*) against doxorubicin-induced oxidative cardiotoxicity in rats. *Med. Sci. Monit.* **2011**, *17*, BR110–BR115. [CrossRef] [PubMed]
11. Lopera, Y.E.; Fantinelli, J.; Arbelaez González, L.F.; Rojano, B.; Ríos, J.L.; Schinella, G.; Mosca, S. Antioxidant Activity and Cardioprotective Effect of a Nonalcoholic Extract of *Vaccinium meridionale* Swartz during Ischemia-Reperfusion in Rats. *Evid. Based Complement. Altern. Med.* **2013**, *2013*, 1–10. [CrossRef] [PubMed]
12. Rodrigues Batista, C.D.C.; Santana De Oliveira, M.; Araújo, M.E.; Rodrigues, A.M.C.; Botelho, J.R.S.; Da Silva Souza Filho, A.P.; Machado, N.T.; Carvalho, R.N. Supercritical CO_2 extraction of açaí (*Euterpe oleracea*) berry oil: Global yield, fatty acids, allelopathic activities, and determination of phenolic and anthocyanins total compounds in the residual pulp. *J. Supercrit. Fluids* **2015**, *107*, 364–369. [CrossRef]
13. Vatai, T.; Škerget, M.; Knez, Ž. Extraction of phenolic compounds from elder berry and different grape marc varieties using organic solvents and/or supercritical carbon dioxide. *J. Food Eng.* **2009**, *90*, 246–254. [CrossRef]
14. Capuzzo, A.; Maffei, M.E.; Occhipinti, A. Supercritical fluid extraction of plant flavors and fragrances. *Molecules* **2013**, *18*, 7194–7238. [CrossRef] [PubMed]

15. Amandi, R.; Hyde, J.R.; Ross, S.K.; Lotz, T.J.; Poliakoff, M. Continuous reactions in supercritical fluids; A cleaner, more selective synthesis of thymol in supercritical CO_2. *Green Chem.* **2005**, *7*, 288–293. [CrossRef]
16. Pereira, C.G.; Meireles, M.A.A. Supercritical fluid extraction of bioactive compounds: Fundamentals, applications and economic perspectives. *Food Bioprocess Technol.* **2010**, *3*, 340–372. [CrossRef]
17. Paes, J.; Dotta, R.; Barbero, G.F.; Martínez, J. Extraction of phenolic compounds and anthocyanins from blueberry (*Vaccinium myrtillus* L.) residues using supercritical CO_2 and pressurized liquids. *J. Supercrit. Fluids* **2014**, *95*, 8–16. [CrossRef]
18. Babova, O.; Occhipinti, A.; Capuzzo, A.; Maffei, M.E. The Journal of Supercritical Fluids Extraction of bilberry (*Vaccinium myrtillus*) antioxidants using supercritical/subcritical CO_2 and ethanol as co-solvent. *J. Supercrit. Fluids* **2016**, *107*, 358–363. [CrossRef]
19. Martínez, J.; Rosa, P.T.V.; Meireles, M.A.A. Extraction of Clove and Vetiver Oils with Supercritical Carbon Dioxide: Modeling and Simulation. *Open Chem. Eng. J.* **2007**, *1*, 1–7. [CrossRef]
20. Sovová, H. Rate of the vegetable oil extraction with supercritical CO_2—I. Modelling of extraction curves. *Chem. Eng. Sci.* **1994**, *49*, 409–414. [CrossRef]
21. García-Risco, M.R.; Vicente, G.; Reglero, G.; Fornari, T. Fractionation of thyme (*Thymus vulgaris* L.) by supercritical fluid extraction and chromatography. *J. Supercrit. Fluids* **2011**, *55*, 949–954. [CrossRef]
22. Pinilla, J.M.; López-Padilla, A.; Vicente, G.; Fornari, T.; Quintela, J.C.; Reglero, G. Recovery of betulinic acid from plane tree (*Platanus acerifolia* L.). *J. Supercrit. Fluids* **2014**, *95*, 541–545. [CrossRef]
23. Zabot, G.L.; Moraes, M.N.; Meireles, M.A.A. Influence of the bed geometry on the kinetics of rosemary compounds extraction with supercritical CO_2. *J. Supercrit. Fluids* **2014**, *94*, 234–244. [CrossRef]
24. Zabot, G.L.; Moraes, M.N.; Petenate, A.J.; Meireles, M.A. Influence of the bed geometry on the kinetics of the extraction of clove bud oil with supercritical CO_2. *J. Supercrit. Fluids* **2014**, *93*, 56–66. [CrossRef]
25. NIST. Thermophysical Properties of Fluid Systems. *Natl. Inst. Stand. Technol.*; 2016. Available online: http://webbook.nist.gov/chemistry/fluid/ (accessed on 10 January 2015).
26. Duba, K.S.; Fiori, L. Supercritical CO_2 extraction of grape seed oil: Effect of process parameters on the extraction kinetics. *J. Supercrit. Fluids* **2015**, *98*, 33–43. [CrossRef]

3.3 Supercritical carbon dioxide extraction of *Calendula officinalis*: kinetic modeling and scaling up study

Alexis López-Padilla, Alejandro Ruiz-Rodríguez, Guillermo Reglero & Tiziana Fornari

Journal of Supercritical Fluids, 2017

DOI: 10.1016/j.supflu.2017.03.033.

Fecha: 22/06/17 [11:22:32 CEST]
De: Alejandro Ruiz <alejandro.ruiz@uam.es>
Para: alexis.lopez@predoc.uam.es, Tiziana Fornari <tiziana.fornari@uam.es>
Asunto: RV: Offprints Order form completed for your article [SUPFLU_3955]

-----Mensaje original-----
De: Elsevier - Author Forms [mailto:Article_Status@elsevier.com]
Enviado el: jueves, 22 de junio de 2017 11:21
Para: alejandro.ruiz@uam.es
Asunto: Offprints Order form completed for your article [SUPFLU_3955]

Please note this is a system generated email from an unmanned mailbox.
If you have any queries we really want to hear from you via our 24/7 support at http://service.elsevier.com

---

Article title: Supercritical carbon dioxide extraction of Calendula officinalis: kinetic modeling and scaling up study Article reference: SUPFLU3955 Journal title: The Journal of Supercritical Fluids Corresponding author: Dr Alejandro Ruiz-Rodriguez First author: Dr Alexis López-Padilla

Dear Dr Ruiz-Rodriguez,

Please find attached a copy of the "Offprints Order Form" which you completed online on 22-JUN-2017 If there are any details missing or incorrect on the Offprint Order Form, please alert us immediately.

If you have any questions, please do not hesitate to contact us. To help us assist you, please quote our article reference SUPFLU3955 in all correspondence.

We are committed to publishing your article as quickly as possible.

Kind regards,
Elsevier Author Support

HAVE QUESTIONS OR NEED ASSISTANCE?
For further assistance, please visit our Customer Support site where you search for solutions on a range of topics and find answers for frequently asked questions. You can also talk to our customer support team by hone 24 hours a day from Monday-Friday and 24/7 by live chat and email.
Get started at > http://service.elsevier.com

[T-5c-20150917]

OFFPRINTS ORDER

Article:	**Supercritical carbon dioxide extraction of Calendula officinalis: kinetic modeling and scaling up study**
Corresponding author:	**Dr Alejandro Ruiz-Rodriguez**
E-mail address:	**alejandro.ruiz@uam.es**
Journal:	**The Journal of Supercritical Fluids**
Our reference:	**SUPFLU3955**
PII:	**S0896-8446(17)30133-X**
DOI:	**10.1016/j.supflu.2017.03.033**

ORDER SUMMARY

Order number:	Order date:
OACSOSUPFLU39550	22nd June 2017

No paper offprints ordered at a charge

A Share Link with access to the final published article for sharing via e-mail and social media

22nd June 2017 T-offprint-v6

Supercritical carbon dioxide extraction of *Calendula officinalis*: kinetic modeling and scaling up study

Alexis López-Padilla, Alejandro Ruiz-Rodriguez*, Guillermo Reglero and Tiziana Fornari

Institute of Food Science Research CIAL (CSIC-UAM) – CEI UAM + CSIC, Madrid, 28049, Spain;

***** Correspondence: alejandro.ruiz@uam.es; Tel.: +34 -910-017-923

Abstract

The extraction of marigold (*Calendula officinalis*) oleoresin with supercritical carbon dioxide $SCCO_2$ was carried out in a small scale extraction vessel (2.7×10^{-4} m^3) studying different extraction pressures (14, 24 and 34 MPa) and different flow rates (15, 30 and 45 $g\cdot min^{-1}$) at 313 K. Then, using semi-empirical engineering scaling criterions (constant solvent lineal velocity or constant solvent residence time) and the Broken and Intact Cell (BIC) model, the scaling up to larger extraction vessels (1.35×10^{-3} m^3 and 5.16×10^{-3} m^3) was theoretically investigated.

According to the BIC model, by keeping constant the CO_2 residence time in the different size vessels a good reproduction of the kinetic behavior should be obtained. Nevertheless, experimental results did not confirm model predictions, and in fact none of the scaling criteria studied resulted adequate in the marigold supercritical extraction scaling up. Thus, using all the experimental overall extraction curves obtained, a new specific correlation was developed between the Schmidt number (Sc), CO_2 mass flow, bed geometry and the supercritical mass transfer coefficients k_{YA} with a good fit ($R^2 = 0.9767$) for scaling up the supercritical extraction of marigold.

Keywords: Supercritical fluid extraction; *Calendula officinalis*; Extracts; Scale up

1. Introduction

Marigold (*Calendula officinalis)* is an herbaceous ornamental plant native from the south of Europe. Due to its biological active compounds and its medicinal value it is cultivated all around the world on commercial scale [1,2]. *C. officinalis* flower is widely used in traditional and folk medicine and its extracts possess main biological activities such as anti-inflammatory, antitumorgenic, antiviral and cicatrizing properties [3–7]. Thus, the production of marigold extracts rich in bioactive compounds has great interest for different industries, including cosmetic, pharmacy and the food industry.

Under the concept of green processing, and considering the lipophilic character of most marigold bioactive compounds, supercritical fluid extraction (SFE) using carbon dioxide (CO_2) is one of the most efficient and promising alternatives to produce marigold extracts. SFE technology can be awarded as a superior extraction technique for biomolecules because it is organic solvent free, adequate for thermo-sensitive species, avoid oxidation damage, and can be applied from analytical scale (grams) to large industrial scale (tons) [8,9].

Regarding marigold SFE, there are many published works providing data about extraction yield, so as chemical and/or biological characterization of the extracts, obtained at different process conditions, from analytical to pilot scale. In this sense, Garcia-Risco et al. [10] studied the SFE of marigold flower on pilot scale with bed extraction volumes of 2×10^{-3} m^3 and extraction conditions of 14 MPa and 313 K, with CO_2 flow rates of 1.2×10^{-3} $kg\cdot s^{-1}$ and a total extraction time of 180 min. They reported a global extraction yield of around 3 % as well as good biological activities of the extracts, suggesting they might be used as a source of potential antiproliferative agents. Under the same experimental conditions Martin et al. [11] made the characterization of the extracts and observed a high bioaccesibility and an

79 improved antioxidant activity after *in vitro* digestion in the terpene fraction. On the other
80 hand, Hamburger et al. [12] described a method for triterpenoid esters purification from *C.*
81 *officinalis* flowers using a combination of SFE and chromatography. The SFE was carried
82 out on a pilot scale with bed extraction volumes of 7.0×10^{-3} m^3, at 50 MPa, and 323 K, with
83 CO_2 flow rates of 9.7×10^{-3} $kg \cdot s^{-1}$ and a total extraction time of 180 min. At the end of the
84 process, a global yield of 5 % and an extract that contained 85 % faradiol of the total ester
85 fraction were attained. One work from Baunmann et al. [13] reported the SFE of marigold
86 from a small scale (bed extraction volumes of 9×10^{-6} m^3, with temperature and pressures of
87 323 K and 30, 50 and 68.9 MPa, respectively, with extraction times of 90 – 180 min).The
88 global yields ranged from 5.5 % to 8.3 %, depending on the extraction pressure. The authors
89 also studied the effect of scaling up to a pilot plant scale with bed extraction volumes of 7.0
90 $\times 10^{-3}$ m^3, concluding that a qualitative and quantitative improvement can be obtained by
91 increasing the pressure and by adding a small amount of an extraction modifier, i.e. 0.5 %
92 (v/v) of ethanol; nevertheless, the extraction yield decreased when the scale up was made. An
93 analytical extraction of *C. officinalis* oleoresin (bed extraction = 1×10^{-5} m^3, P = 30, 35 and 40
94 MPa, T = 303, 408, 333, 348 K, extraction time = 240 min, average particle size = 190 – 220
95 μm) was described by Palumpitag et al. [14]. The authors recovered 87 % of lutein fatty acid
96 esters using palm oil as modifier (10 vol.%) and obtained up to 157 mg of free lutein/g
97 oleoresin after saponification. In the same way, Danielski et al. [4] carried out the SFE of an
98 oleoresin from marigold flowers coming from Brazil at laboratory scale with global yields
99 obtained in the range of 2.1 – 3.54 %, authors found that extraction yield were affected by the
100 origin of the plant and the extraction conditions. Finally, Baratto and Riva [15] described in
101 their patent application a process to obtain a supercritical CO_2 extract from European origin
102 *C. officinalis* flowers and its application in cosmetic and pharmaceutical products. The
103 inventors worked on industrial scale with 170 kg of dried marigold with 5 % of moisture
104 content and an average particle size between 2 and 5 mm, a pressure range between 60 and 70

105 MPa, and temperatures comprised between 333 and 343 K, with a total extraction time of 230
106 min, reporting a global extraction yield of 3 % (w/w).

107 Although SFE has been an important field of research within last decades, and a lot of
108 information about extracting bioactive compounds from natural resources has been published
109 [16,17], there is a need of more scientific studies about the influence of process variables on
110 the extraction kinetics, the modeling of extraction curves and, particularly, the progression of
111 scaling up strategies.

112 The SFE of solid materials is a semi-continuous process in which extraction time plays a
113 central role. The mass extracted varies with time and the plot of the extraction yield vs. time
114 is usually denoted as Overall Extraction Curve (OEC). Nevertheless, not only extraction
115 yield, but also composition, physicochemical and biological properties of the extract vary
116 along extraction time [18,19].

117 Regarding the OEC modeling, it can be pointed out that a number of kinetic models can be
118 found at present in specialized scientific literature, including semi-empirical, simplified and
119 comprehensive phenomenological models [16,20]. In this respect, Campos et al. [21] applied
120 several models to represent the kinetic behavior of the extraction of marigold oleoresin with
121 liquid and supercritical CO_2. These models include the Sovová model [22], the logistic model
122 presented by Martínez et al. [23], the desorption model proposed by Tan and Liou [24], the
123 simple single plate model of Gaspar et al. [25] and the diffusion model proposed by Crank
124 and presented by Reverchon [17]. Campos et al. [21] applied all these models to represent
125 experimental OECs, at pressures ranging from 12 to 20 MPa and temperatures from 293 to

313 K, and concluded that all models fitted reasonably well the marigold SFE experimental data.

On the other hand, more limited works are available in the literature regarding SFE scaling up studies and only a few of them described the five empirical criteria most used for scaling up processes which comprise keeping constant the following quantities: (i) ratio between the masses of spent CO_2 and biomass, (ii) ratio between CO_2 flow rate and biomass weight, (iii) a combination of both criteria (iv) a combination of both criteria plus the dimensionless Reynolds number and (v) bed geometrical relationships (height/diameter) [26]. Maintaining the same solvent linear velocity or the same solvent residence time in extraction vessels of different size, are criterions frequently investigated [27–30]. Bed geometry is considered an important factor in industrial extraction processes and the ratio between bed height (L) and bed diameter (D) has been used to validate some scale up process. For example, Carvalho et al. [31] and Zabot et al. [19, 22] applied the solvent to feed mass ratio criterion (Q/F) combined with the bed geometrical ratio (L/D), to compare the kinetic behavior in the SFE of rosemary (*Rosmarinus officinalis)* and clove buds (*Eugenia caryophyllus*), respectively, and found good results for maintaining the same (Q/F) criterion. On the other hand, Prado et al. [32] described the SFE scale up process from laboratory to pilot scale of grape seeds based on L/D ratio and found a good reproducibility of the extraction curves. Recently, Paula et al. [33] evaluated, at laboratory scale, the effect of bed geometry ratio combined with the empirical criterions of constant residence time and constant CO_2 velocity in the scaling up SFE process for *Baccharis dracunculifolia* and found that the second one was a suitable scale up criterion. And in the same year, Fernández-Ponce et al. [34] considered to keep constant

$\left(\frac{Q \times D}{F}\right)$ and found a suitable OEC kinetic reproduction from small scale to pilot scale supercritical extraction of *Mangifera indica* leaves. In general, there is not a single criterion for SFE scaling up that can be effectively applied to all systems. For example, keeping the same residence time of the solvent inside the packed bed was successfully applied for the SFE of *E. caryophyllus* but did not result adequate for the SFE of vetiver roots [28], showing that scale up data in SFE has a big variation and sometimes there is no an easy way to find a generalized conclusion between them. More studies are required to get more information about the applicability of SFE scale up criteria with different types of raw materials and taking account that mass transfer behavior could be affected by the origin, species and even the parts of the plant involved in the SFE process [35,36]. In this respect, as cited above, a few papers have been published regarding the SFE of marigold from laboratory to pilot or industrial scale but none of them describe or involve a scaling up process or criteria. In this work, the supercritical CO_2 extraction of marigold flowers was studied using three different volumes of extraction vessels. The modeling of the extraction curves and the correlation of parameters obtained were investigated in order to put forward a scaling up strategy.

2. Materials and Methods

2.1 Fundamentals

2.1.1 The Broken and Intact Cells model

One of the kinetic models most used to represent the OEC of SFE processes is the Broken and Intact Cells (BIC) model developed by Sovová [22]. In the BIC model the solid phase is

considered to be comprised by broken and intact cells and thus the total extractable material is distributed as easily accessible solute, which is available on the surface of the broken cells, and difficultly accessible solute which is confined in the intact part of the cells. Furthermore, in the BIC model it is assumed that temperature and pressure are constant during the whole extraction time, particle size and solute distribution are uniform in the packed bed, the void fraction is constant during the extraction, and axial dispersion can be neglected (plug flow is supposed). Then, three different extraction periods are distinguished:

1. The constant extraction rate (CER) period, in which the extraction rate is constant and determined by the convective solvent film resistance.
2. The falling extraction rate (FER) period, in which the intra-particle diffusion starts to become important and thus, the extraction rate drops rapidly. At the end of this period, all the readily accessible solute has been removed from the vegetal matrix.
3. The diffusion controlled (DC) period, in which mass transfer is mainly dominated by diffusion film resistance inside the solid vegetal particles.

The BIC model equations to calculate the cumulative mass of extract (m) as a function of time (t) in the different periods are the following [22]:

CER period: $$m = Q\,Y^{*}\left[1-\exp(-Z)\right]t \tag{1}$$

FER period: $$m = Q\,Y^{*}\left[t - t_{CER}\exp(Z_w - Z)\right] \tag{2}$$

DC period: $$m = m_{SI}\left\{X_o - \frac{Y^{*}}{W}\ln\left[1+\left[\exp\left(\frac{WX_o}{Y^{*}}\right)-1\right]\exp\left[\frac{WQ(t_{CER}-t)}{m_{SI}}\right]\left(\frac{X_k}{X_o}\right)\right]\right\} \tag{3}$$

where:

$$Z = \frac{m_{SI}k_{YA}\rho}{Q\,(1-\varepsilon)\rho_s} \tag{4}$$

191 $$W = \frac{m_{SI} k_{XA}}{Q\,(1-\varepsilon)} \quad (5)$$

192 $$Z_W = \frac{ZY^*}{WX_o} \ln\left\{ \frac{X_o \exp\left[WQ\,(t - t_{CER})/m_{SI}\right] - X_k}{X_o - X_k} \right\} \quad (6)$$

193 $$m_{SI} = X_o F \quad (7)$$

194 $$t_{CER} = \frac{m_{SI}(X_o - X_k)}{Y^* Z Q} \quad (8)$$

195 $$t_{FER} = t_{CER} + \frac{m_{SI}}{QW} ln\left[\frac{X_k + X_p \exp(WX_o/Y^*)}{X_o}\right] \quad (9)$$

196 The mass ratio of the extracted material at the bed outlet (Y_{CER}) in CER period is given by:

197 $$Y_{CER} = \frac{m_{(t=t_{CER})}}{Q t_{CER}} \quad (10)$$

198 Consequently, the extraction rate at CER period is:

199 $$M_{CER} = Y_{CER} Q \quad (11)$$

200 Process parameters required to apply BIC model are the bed porosity (ε), mass (F) and
201 density (ρ_s) of the raw material, CO_2 density (ρ) and mass flow rate (Q). Additionally, the
202 solubility of the extract in the supercritical solvent (Y^*) and the global extraction yield (X_o)
203 have to be determined to apply the BIC model. Parameters which are optimized according to
204 the experimental kinetic data are the intra-particle solute ratio (X_k) and the fluid phase and
205 solid phase volumetric mass transfer coefficients, $k_{YA} = k_f \cdot a_o$ and $k_{XA} = k_s \cdot a_o$. k_f and k_s are,
206 respectively, the fluid and solid mass transfer coefficients and a_o is the particles surface area
207 ($a_o = 6 \cdot (1-\varepsilon) \cdot d_p^{-1}$). The ready accessible solute (X_p) is calculated as the difference (X_o - X_k).

208 **2.1.2 Scaling up criterions**

209 Despite extraction temperature and pressure are crucial to establish the thermodynamic
210 boundaries of the extraction process, affecting fundamentally the supercritical solvent

density and the solubility and diffusivity of the solutes, the CO_2 flow (i.e. the solvent velocity through the extraction cell) is a determining factor regarding mass transfer. Of course, mass transfer is also greatly influenced by bed geometry and packing, since these variables determine the mass ratio of extracted material to spent CO_2 at bed outlet.

The objective of scaling up the SFE of solid materials is to reproduce the OEC in extraction vessels of different shape and/or capacity. In general, extraction vessels are cylindrical and thus length (L) and internal diameter (D) of the cylinder are the variables which characterize bed geometry. Yet, thermodynamic process variables, temperature and pressure, are maintained the same in the different volumes vessels. Furthermore, particle size, bed density and porosity, are intended to be preserved in SFE process scaling up. Thus, the key request is to determine the CO_2 flow rate necessary to attain the same OEC in the different scale systems.

Among different approaches, two engineering rules of thumb are often applied in SFE processes to estimate the relation between the CO_2 mass flow rate (Q) and the bed geometry [29,37,38]. One of these criteria is keeping the same solvent velocity (v) in the different scale vessels 1 and 2:

$$\frac{Q_1}{Q_2} = \left(\frac{D_1}{D_2}\right)^2 \tag{12}$$

Equation (12) was obtained considering that the same temperature and pressure (same CO_2 density) are preserved in the different scale experiments 1 and 2, and that the cross-flow area of each cylindrical extraction vessel is given by $A = \pi D^2/4$.

The second scaling up criteria usually used is keeping the solvent residence time (t_R) constant, which is calculated as the ratio between the mass of CO_2 fit in the extraction vessel ($\pi D^2 L\varepsilon\rho/4$) and the CO_2 flow mass rate (Q):

$$t_R = \frac{\pi D^2 L\varepsilon\rho}{4Q} \quad (13)$$

Considering, as in previous case, that the same temperature and pressure are preserved in the different scale experiments, the residence time criterion requires that:

$$\frac{Q_1}{Q_2} = \left(\frac{D_1}{D_2}\right)^2 \left(\frac{L_1}{L_2}\right) \quad (14)$$

2.2 Plant material

Dried marigold (*Calendula officinalis*) flowers with a moisture content of 11.8 % were obtained from Murciana Herboristería (Murcia, Spain). According to supplier, the origin of marigold plant was Egypt. Flowers were ground in a grind Premil 250 (Lleal S.A., Barcelona, Spain) to particles sizes in the range from 175 to 1340 μm, with a mean particle size of 541 μm, measured by light scattering with a laser diffraction system Mastersizer 3000 (Malvern Instruments Ltd., Malvern, UK), equipped with the Aero S dispersion unit at 0.5 bar of dispersion pressure. The plant material density (ρ_s) was determined using a helium pycnometer Ultrapyc 1200e (Quantachrome, Florida, USA) and resulted to be 1409 $kg \cdot m^{-3}$. Samples were packed and stored at room temperature until utilization.

2.3 Chemical

Ethanol absolute (99.5 % of purity) was purchased from Panreac (Barcelona, Spain). CO_2 was supplied by Carburos Metalicos, S.A. (Madrid, Spain) with a purity of 99.9 %.

2.4 Supercritical fluid extraction

Calendula officinalis extractions were carried out using three cylindrical extractor vessels of different capacities which were integrated in two supercritical extraction plants. Each plant

255 comprises a recirculation system where CO_2 is condensed, pumped up to the desired
256 extraction pressure and heated up to the desired extraction temperature.
257 One pilot supercritical plant (Figure 1a) is from Thar Technology (model SF2000;
258 Pittsburgh, Pensilvania, USA) with the possibility of being operated using two extraction
259 vessels, namely vessel A (V_A) of 2.7×10^{-4} m^3 (small scale experiments) and vessel B (V_B) of
260 1.35×10^{-3} m^3 (medium scale experiments). CO_2 flow is measured using a flow meter from
261 Siemens AIS (Model: Sitrans FC Mass 2100 DI 1.5, Nordborgvej, Denmark). The SFE
262 device has a computerized PLC-based instrumentation, including a separator with control of
263 temperature and pressure, where decompression up to recirculation pressure takes place. The
264 pressure in the extraction cell is controlled (± 0.1 MPa) by an automated back pressure
265 regulator (BPR) valve. Temperature is adjusted by electric heating and controlled by ± 2 K.
266 The other semi-industrial scale supercritical plant is from Zean Consultores S.L. (Madrid,
267 Spain) with an extraction vessel namely C (V_C) of 5.19×10^{-3} m^3 of capacity (large scale
268 experiments). The equipment comprises a LEWA LDE1 pump (LEWA GmbH, Leonberg,
269 Germany) with a maximum CO_2 flow rate of 146.93 $kg\cdot h^{-1}$. The pressure in the extraction
270 vessel is controlled by an automated BPR valve (RCV 2945) from Badger Meter Inc. (Tulsa,
271 USA). The cyclonic separator has a capacity of 1.57×10^{-3} m^3 with temperature and pressure
272 control from Link Industrial S.L. (Rubi, Spain). The cooling system connects the CO_2 pump
273 and the CO_2 recirculation system with two chillers Huber UC100T Advanced from Peter
274 Huber Kältemaschinenbau GmbH (Offenbur, Germany). A heating bath Huber Hotbox
275 HB120 from Peter Huber Kältemaschinenbau GmbH (Offenbur, Germany) is connected
276 on-line with the Heat Exchanger unit. The plant also comprises a demister unit with 1.5×10^{-2}
277 m^3 of capacity from Proycon Pirineo S.L. (Huesca, Spain) designed to separate liquid or solid
278 particles from the outgoing stream before driving CO_2 to the storage tank and on-line
279 connected with an activated carbon filter with a capacity of 5×10^{-2} m^3. The semi-industrial

supercritical device has a PLC-based instrumentation and control from Invensys S.L. (Madrid, Spain). A scheme of Zean supercritical plant is given in Figure 1b.

2.4.1 Small scale experiments

Kinetic behavior was studied in a small scale vessel (V_A), packed with 0.090 kg of grinded marigold flowers. OECs were obtained at 313 K and pressures of 14, 24 and 34 MPa, with a CO_2 flow of 5.0×10^{-4} kg·s^{-1}. Furthermore, additional OECs were obtained at constant pressure (14 MPa) and temperature (313 K) and CO_2 flows of 2.5×10^{-4}, 5.0×10^{-4} and 7.5×10^{-4} kg·s^{-1}, respectively. Extraction conditions of all OECs which were carried out in V_A are summarized in Table 1.

The first sample was collected after 15 min of extraction, second data point at 30 min, and the rest of the data were collected at intervals of 60 min until 180 min and the last one was collected at 270 min of total extraction time. Additionally, at 14 MPa, 313 K and 5.0×10^{-4} kg·s^{-1} CO_2 samples were collected in the separator until the vegetal material was completely extracted (750 min).

In all experimental assays the supercritical stream was decompressed at 5.4 MPa (i.e. the recirculation system pressure) in the separator. The different samples were collected with ethanol which was eliminated at low temperature (313 K) in a rotavapor R210 (Büchi Labortechnik AG, Flawil, Switzerland).

2.4.2 Medium scale experiments

V_B was used with 0.445 kg of ground marigold flowers, see Table 2. Extraction pressure and temperature were 14 MPa and 313 K, and the CO_2 flow rate was set to 6.0×10^{-4} kg·s^{-1} or 12.3×10^{-4} kg·s^{-1} according to the results of the scaling criterion adopted (Eq. 12 or Eq. 14,

302 respectively). Samples at 15, 30, 60, 120, 180 and 270 min of extraction were collected in the
303 separator with ethanol, and the solvent was eliminated at 313 K in the rotavapor.

304 **2.4.3 Large scale experiments**

305 Large scale experiments were carried out in extraction vessel V_C with 1.708 kg of marigold
306 flowers as can be observed in Table 2. The extraction pressure and temperature were
307 identical to those used for scaling studies (14 MPa and 313 K) in vessels A and B. The CO_2
308 flow rate was set to 21.2×10^{-4} kg·s^{-1} according to the constant linear velocity criterion (Eq.
309 12) or to 46.8×10^{-4} kg·s^{-1} considering the constant residence time scaling criterion (Eq. 14).
310 The extracts were collected from the separators at 60, 120, 180 and 270 min of total
311 extraction using ethanol which was evaporated after in a rotavapor.

312

313 **3. Results and Discussions**

314 **3.1 Apparent density and porosity of the packed beds**

315 Table 2 shows the geometrical characteristics of the different extraction vessels, together
316 with the mass of marigold used in each one. The mass of grinded marigold flowers (solid
317 density ρ_s = 1409 kg·m^{-3}) loaded in each extraction vessel was calculated in order to preserve
318 the same apparent density (ρ_{app} = 333 kg·m^{-3}) and porosity (ε = 0.763) in the three packed
319 beds. The vessel loading was carried out using the same protocol, and the calculated amount
320 of vegetal material satisfactory filled the corresponding extraction vessel.

321 **3.2 Small scale OECs**

322 The overall yields are reported in Table 1 and correspond to 313 K and 270 min of extraction
323 time. The shape of the OECs obtained at different pressures and solvent flow rates are shown
324 in Figure 2. Extraction yield was calculated as the ratio between the mass extracted (m) and
325 the mass of grinded calendula flowers feed into the extraction vessel (F).

As expected, extraction yield increases with increasing pressure at constant temperature (T = 313 K) and constant CO_2 flow rate ($Q = 5.0\times10^{-4}$ kg·s^{-1}). This behavior is due the increase of the supercritical solvent density, which enlarges the solubility of the solutes and thus enhances the extraction rate. However, slight increase of global yield was observed when pressure raised from 24 to 34 MPa (from 6.11 % to 6.28 %). Additionally, the effect of CO_2 flow rate on the global yield was important when Q increased from 2.5×10^{-4} to 7.5×10^{-4} kg·s^{-1} at 14 MPa (extraction yields were 4.56 and 6.11 %, respectively).

In general, the extractions yields of *Calendula officinalis* attained in this work were considerably higher than those obtained by Campos et al. [11], which were lower than 2.5 % for marigold flowers from Brazil at 313 K and pressures in the range 12-20 MPa and large extraction times (higher than 270 min). One reason could be the different origin of marigold plant, but also the lower Q/F ratios used by Campos et al. (0.46-0.70×10^{-3} s^{-1}) in comparison with those used in this work (2.78-8.33×10^{-3} s^{-1}).

3.3 Solubility determination

Solubility data is essential information for understanding the supercritical extraction process. Accordingly, the solubility of the solute in supercritical CO_2 (Y^*) is usually a parameter in SFE kinetic models, as is the case for the BIC model.

The thermodynamic concept of solubility refers to the amount of a pure compound which can be dissolved in supercritical CO_2 at a given temperature and pressure. There are many methods proposed [39] for the experimental determination of the solute solubility (static, dynamic and chromatographic methods) and also theoretical approaches have been proposed for solubility prediction, minimizing experimental efforts and costs [40]. When the solute is a multicomponent mixture such in the case of vegetal extracts, the concept of apparent solubility is utilized which is usually determined considering the kinetic data of the initial period of the OEC. In this period, the accessibility of the extractable material results in a constant extraction rate period and hence, the slope of the linear behavior (extracted mass vs.

mass of CO_2) is used to calculate the apparent solubility of the vegetal oleoresin at the temperature and pressure extraction conditions [29,42–45].

In this work the solubility of marigold extracts in supercritical CO_2 was determined at 313 K and 14 MPa using the first stages of the OECs obtained with the different solvent flow rates. Figure 3 shows these data plotted as mass of marigold oleoresin extracted vs. mass of spent CO_2. As can be observed in the figure, the data fit a good linear behavior ($R^2 = 0.9086$) for a CO_2 mass load lower than 0.8 kg. This means that in the first stage of the OECs obtained for the supercritical solvent was saturated with the marigold extractable material and thus, the slope of this linear trend is given in Figure 3 can be considered a reasonably estimation of marigold solubility. Then, Y^* was calculated to be 0.0032 kg of marigold extract per kg of CO_2 at 313 K and 14 MPa. This value is reasonably in accordance with the value reported by Danielski [46] at 313 K and 20 MPa (0.0028 kg/kg) which was used by Campos et al. due to the lack of solubility data [11].

3.4 Total extractable material

In order to apply BIC model, the total amount of extractable material (X_o) at a given extraction temperature and pressure, has to be determined. Then, a kinetic experiment was carried out at 313 K and 14 MPa extending extraction time until the vegetal material loaded in the extraction vessel was exhausted. Figure 2 shows the OEC obtained in vessel A with a CO_2 flow rate of 5.0×10^{-4} kg·s^{-1}. After 750 min of extraction, the amount of material recovered in the separator was lower than 0.1 % of the total material extracted. In view of that, the value of X_o was estimated to be 0.1 % higher than the total yield obtained after 750 min of extraction (X_o = 0.0745 kg/kg).

3.5 BIC model fitting of small scale OECs

BIC model was used to represent the experimental data obtained in the small scale V_A extraction vessel (see Table 1 and Figure 2). Table 3 shows the optimal mass transfer coefficients (k_{YA} and k_{XA}) for each of the five OECs. The intra-particle solute ratio (X_k) was

optimized as a unique value for all the OECs. The resulted value (see Table 3) indicates that only around 40 % of the extractable material is easily accessible. Also is included in Table 3 the average absolute relative deviation (*AARD*) of each OEC fitting (< 6.62 %). Figure 2 shows with dashed lines the BIC model fitting achieved.

For the sake of comparison, the values of the mass transfer coefficients obtained are compared with those reported by Campos et al. [21] for the BIC modeling of marigold OEC at 313 K and 15 MPa, which were $k_{YA} = 0.08\times10^{-2}$ s^{-1} and $k_{XA} = 0.001\times10^{-3}$ s^{-1}. The lower values obtained in the work of Campos et al. (2005) are in accordance with the lower yields obtained and can be explained by the lower apparent solubility and lower *Q/F* ratios used.

At constant temperature (313 K) and CO_2 flow rate (5.0×10^{-4} $kg\cdot s^{-1}$) the k_{YA} and k_{XA} values increase with increasing pressure and accordingly, higher extraction rates (M_{CER}) are obtained. At the three pressures investigated, the mass ratio of the extracted material at the bed outlet (Y_{CER}) is rather close to marigold oleoresin apparent solubility (i.e. the solvent is saturated with marigold extractable material), which was calculated as indicated in section 3.3 at 14 MPa ($Y^* = 0.0032$ $kg\cdot kg^{-1}$). At pressures of 24 MPa and 34 MPa, the Y^* values were considered fitting parameters and the optimal values (see Table 3) resulted very close to the slope of the corresponding OEC from t = 0 to t = 15 min, which were 0.0039 and 0.0050 $kg\cdot kg^{-1}$, respectively.

Regarding the effect of solvent flow rate, as expected, the k_{YA} values increase with increasing Q at constant pressure and temperature, and lower t_{CER} values are obtained. While Y_{CER} is very close to the extract apparent solubility, as mentioned before, increased solvent flow rates resulted in higher extraction rates (M_{CER}) and thus, the time in which ends the falling extraction rate period (t_{FER}) is shorter.

3.6 SFE scaling up study

3.6.1 BIC model prediction for marigold SFE scaling up

The BIC model was used to assess whether the solvent constant velocity (Eq. 12) or the solvent constant residence time (Eq. 14) were suitable criterions to calculate the CO_2 flow rate (Q) required for scaling up from vessel A to vessels B and C (scaling factors V_B/V_A = 4.95 and V_C/V_A = 19.04, respectively). The extraction conditions of the OEC target to be reproduced were 313 K, 14 MPa and 2.5×10^{-4} kg·s^{-1} (V_A). Bed porosity was kept constant (ε = 0.763) for all BIC simulations. The Q values calculated from Eq. (12) and (14) are given in Table 4 for each scaling case (V_B and V_C).

As can be observed in Table 4, t_{CER} is the same for all predictions regardless of the criterion applied to calculate Q. Nevertheless, the ratios $(M_{CER})_B/(M_{CER})_A$ and $(M_{CER})_C/(M_{CER})_A$ are equal to the corresponding scaling factors only when Eq. (14) was used to calculate Q. That is, according to the BIC model, the criterion given by Eq. (14) is suitable for marigold SFE scaling up from small scale (V_A) to both larger scales (V_B and V_C). Furthermore, it can be observed in Table 4 that the t_{FER} values obtained in the OEC simulations are similar only in the case of preserving the same residence time in the different scale units. That is, using Eq. (14) to Q scaling up and according to BIC simulation, the easy accessible material is completely extracted in around 73 min regardless the vessel scale.

The results of BIC simulation of the OECs at 313 K and 14 MPa in vessel B and vessel C with the different calculated Q values are depicted in Figures 5 (V_B/V_A = 4.95) and 6 (V_C/V_A = 19.04), respectively. Grey lines in the figures correspond to BIC simulation when Q is calculated according to Eq. (12), while black lines correspond to the use of Eq. (14). As can be observed for both vessel scales, black lines are the ones that fit reasonably well the experimental small scale OEC. Furthermore, in both cases, BIC model predicts that the CO_2 flow rate calculated according Eq. (12) (constant solvent lineal velocity) provides a significant delayed extraction.

3.6.2 Experimental marigold SFE scaling up

The SFE of marigold was experimentally carried out in vessels V_B and V_C with the CO_2 flow rates calculated according Eq. (12) or Eq. (14) and given in Table 4. The OECs obtained in each case are represented in Figure 4 (V_B) and Figure 5 (V_C), respectively. Despite BIC model predicts that Eq. (14) should be adequate for Q scaling up in both larger scale vessels, experimental data show important discrepancies.

In the case of V_B, similar OEC was obtained at the initial stages of the extraction when the solvent flow rate was the one provided by Eq. (14), but experimental results deviates from BIC model (and from the small scale experimental OEC) for increasing extraction time. Furthermore, the solvent flow rate obtained with Eq. (12) resulted in an OEC with significant lower yields, in comparison with BIC predictions and with the small scale experimental OEC.

On the other hand, the opposite tendency is observed when scaling from V_A to V_C. The solvent flow rate calculated using Eq. (14) resulted in significant larger yields than those obtained in V_A, while the OEC obtained using Eq. (12) is quite similar to the small scale experimental OEC.

3.6.3 Correlation of experimental data for scaling up

The theoretical fundamentals of the mass transfer correlations, which relate Sherwood (*Sh*) with Reynolds (*Re*) and Schmidt (*Sc*) dimensionless numbers [47], were used in order to assess a relation between the fluid phase mass transfer coefficients (k_{YA}) and the solvent flow rate (Q) of all experimental OECs obtained in this work for marigold SFE. The *Sc* number was included to take into account the most important physicochemical parameters of the extraction which depend on temperature and pressure:

$$Sc = \frac{\mu_{CO2}}{\rho_{CO2}\ D_{M-CO2}} \quad (15)$$

452 ρ_{CO2} and μ_{CO2} are, respectively, the solvent density and viscosity, and D_{M-CO2} is the
453 diffusion coefficient of marigold oleoresin in supercritical CO_2 which was calculated
454 following the general correlation recently proposed by López-Padilla et al. [48].
455 Figure 6 show the correlation obtained (R^2 = 0.9767) which also include vessel geometrical
456 dimensions (*D* and *L*). As can be observed in the figure, it satisfactory takes into account the
457 variation of some process variables, such as pressure and solvent flow rate, at constant
458 extraction temperature. Nevertheless, it has to be pointed out that other important variables,
459 such as particle diameter (d_p) and bed porosity (ε), were kept constant in all OECs used in the
460 development of this correlation. The effect of d_p and ε, and the potential extension of this
461 type of correlation to other vegetal raw materials is in progress, in order to set a practical
462 methodology for solid vegetal raw materials scaling up in the context of the different scale
463 SFE units available in our pilot plant.
464

465 **4. Conclusions**

466 SFE curves of *C. officinalis* at different extraction pressure, temperature and CO_2 mass flow
467 were measured at small scale, and were adequately represented by the BIC model. The model
468 was then used to assess the accuracy of scaling up criteria. According to BIC model the
469 constant CO_2 residence time criterion should provide good estimation of the CO_2 mass flow
470 for both scaling factors of 4.9 and 19. Nevertheless, experimental results do not agree with
471 the theoretical prediction: while the constant CO_2 residence time criterion looks quite
472 satisfactorily for a scaling factor of 4.9, the constant CO_2 velocity was the criterion suitable
473 for a larger scaling factor of 19.
474 The mass transfer coefficients in the supercritical fluid phase (k_{YA}) of all extraction curves
475 obtained in the different size cells and applying different extraction pressure, temperature
476 and CO_2 mass flow rate were satisfactorily correlated (R^2 = 0.9767) in terms of the CO_2 flow
477 rate (Q), the extraction cell geometric parameters (diameter D and length L) and the

dimensionless Schmidt number (Sc). This correlation should be tested in terms of parameters which were kept constant in this work, such as porosity and/or particle size.

Acknowledgments

López-Padilla A thanks to Administrative Department of Science, Technology and Innovation - Colciencias (Call 568/2012) for his Ph.D. fellowship. This work was financed thanks to ALIBIRD project: S2013/ABI-2728 (Comunidad de Madrid).

References

[1] D. Arora, A. Rani, A. Sharma, A review on phytochemistry and ethnopharmacological aspects of genus Calendula., Pharmacogn rev. 7 (2013) 179–187. http://dx.doi.org/10.4103/0973-7847.120520.

[2] R. Sausserde, K. Kampuss, Composition of Carotenoids in Calendula (*Calendula officinalis* L.) flowers, in: Foodbalt 2014, Jelgava, Latvia, 2014: pp. 13–18. http://agris.fao.org/agris-search/search.do?recordID=LV2014000480.

[3] M. Miguel, L. Barros, C. Pereira, R.C. Calhelha, P.A. García, M.A. Castro, et al., Chemical characterization and bioactive properties of two aromatic plants : *Calendula officinalis* (flowers) and *Mentha cervina* (leaves), Food Funct. 7 (2016) 2223–2232. http://pubs.rsc.org/en/content/articlepdf/2016/fo/c6fo00398b..

[4] L. Danielski, L.M.A.S. Campos, L.F. V Bresciani, H. Hense, R.A. Yunes, S.R.S. Ferreira, Marigold (*Calendula officinalis* L.) oleoresin: Solubility in SC-CO2 and composition profile, Chem. Eng. Process: Process Intensification. 46 (2007) 99–106. http://dx.doi.org/10.1016/j.cep.2006.05.004.

[5] Z. Kalvatchev, R. Walder, D. Garzaro, Anti-HIV activity of extracts from *Calendula officinalis* flowers, Biomed. Pharmacother. 51 (1997) 176–180. http://dx.doi.org/10.1016/S0753-3322(97)85587-4.

[6] A. Ramos, A. Edreira, A. Vizoso, J. Betancourt, M. López, M. Décalo, Genotoxicity of an extract of *Calendula officinalis* L., J. Ethnopharmacology. 61 (1998) 49–55. http://dx.doi.org/10.1016/S0378-8741(98)00017-8.

[7] M. Wang, R. Tsao, S. Zhang, Z. Dong, R. Yang, J. Gong, et al., Antioxidant activity,

511 mutagenicity/anti-mutagenicity, and clastogenicity/anti-clastogenicity of lutein from
512 marigold flowers, Food Chem. Toxicol. 44 (2006) 1522–1529.
513 http://dx.doi.org/10.1016/j.fct.2006.04.005.
514 [8] M.A. McHugh, V.J. Krukonis, Supercritical Fluid Extraction: Principles and Practice,
515 Butterworths, Boston, 1994.
516 [9] M. Mukhopadhyay, Natural Extracts Using Supercritical Carbon Dioxide, CRC Press,
517 New York, 2000.
518 [10] M.R. García-Risco, L. Mouhid, L. Salas-pérez, A. López-padilla, S. Santoyo, L.
519 Jaime, et al., Biological Activities of Asteraceae (*Achillea millefolium* and *Calendula*
520 *officinalis*) and Lamiaceae (*Melissa officinalis* and *Origanum majorana*) Plant
521 Extracts, Plant Foods Hum. Nutr. (2017) 1–7.
522 http://dx.doi.org/10.1016/j.supflu.2010.09.030.
523 [11] D. Martin, J. Navarro del Hierro, D. Villanueva Bermejo, R. Fernández-Ruiz, T.
524 Fornari, G. Reglero, Bioaccessibility and Antioxidant Activity of *Calendula*
525 *officinalis* Supercritical Extract as Affected by in Vitro Codigestion with Olive Oil, J.
526 Agr. Food Chem. 64 (2016) 8828–8837.
527 http://pubs.acs.org/doi/abs/10.1021/acs.jafc.6b04313.
528 [12] M. Hamburger, S. Adler, D. Baumann, A. Förg, B. Weinreich, Preparative
529 purification of the major anti-inflammatory triterpenoid esters from Marigold
530 (*Calendula officinalis*), Fitoterapia. 74 (2003) 328–338.
531 http://dx.doi.org/10.1016/S0367-326X(03)00051-0.
532 [13] D. Baumann, S. Adler, S. Grüner, F. Otto, B. Weinreich, M. Hamburger, Supercritical

carbon dioxide extraction of marigold at high pressures: Comparison of analytical and pilot-scale extraction, Phytochem. Analysis. 15 (2004) 226–230. http://dx.doi.org/doi/10.1002/pca.772.

[14] W. Palumpitag, P. Prasitchoke, M. Goto, A. Shotipruk, Supercritical Carbon Dioxide Extraction of Marigold Lutein Fatty Acid Esters: Effects of Cosolvents and Saponification Conditions, Sepa. Sci. Technol. 46 (2011) 605–610. http://dx.doi.org/10.1080/01496395.2010.533739.

[15] G. Baratto, E. Riva, Process for preparing an inflorescence extract of *Calendula officinalis* by means of extraction with supercritical carbon dioxide and compositions containing said extract, EP2520306A1, 2012.

[16] M.M.R. de Melo, A.J.D. Silvestre, C.M. Silva, Supercritical fluid extraction of vegetable matrices: Applications, trends and future perspectives of a convincing green technology, J. Supercrit. Fluid. 92 (2014) 115–176. http://dx.doi.org/10.1016/j.supflu.2014.04.007.

[17] E. Reverchon, I. De Marco, Supercritical fluid extraction and fractionation of natural matter, J. Supercrit. Fluid. 38 (2006) 146–166. http://dx.doi.org/10.1016/j.supflu.2006.03.020.

[18] G.L. Zabot, M.N. Moraes, M.A.A. Meireles, Influence of the bed geometry on the kinetics of rosemary compounds extraction with supercritical CO2, J. Supercrit. Fluid. 94 (2014) 234–244. http://dx.doi.org/10.1016/j.supflu.2014.07.020.

[19] M.R. García-Risco, E.J. Hernández, G. Vicente, T. Fornari, F.J. Señoráns, G. Reglero, Kinetic study of pilot-scale supercritical CO2 extraction of rosemary (*Rosmarinus*

555 *officinalis*) leaves, J. Supercrit. Fluid. 55 (2011) 971–976.
556 http://dx.doi.org/10.1016/j.supflu.2010.09.030.
557 [20] Z. Huang, X.-H. Shi, W.-J. Jiang, Theoretical models for supercritical fluid
558 extraction., J. Chromatogr. A. 1250 (2012) 2–26.
559 http://dx.doi.org/10.1016/j.chroma.2012.04.032.
560 [21] L.M.A.S. Campos, E.M.Z. Michielin, L. Danielski, S.R.S. Ferreira, Experimental data
561 and modeling the supercritical fluid extraction of marigold (*Calendula officinalis*)
562 oleoresin, J. Supercrit. Fluids¡. 34 (2005) 163–170.
563 http://dx.doi.org/10.1016/j.supflu.2004.11.010.
564 [22] H. Sovová, Rate of the vegetable oil extraction with supercritical CO2—I. Modelling
565 of extraction curves, Chem. Eng. Sci. 49 (1994) 409–414.
566 http://dx.doi.org/10.1016/0009-2509(94)87012-8.
567 [23] J. Martinez, A.R. Monteiro, P.T.V. Rosa, M.O.M. Marques, M.A. Meireles,
568 Multicomponent model to describe extraction of ginger oleoresin with supercritical
569 carbon dioxide, Ind. Eng. Chem. Res. 42 (2003) 1057–1063.
570 http://pubs.acs.org/doi/abs/10.1021/ie020694f.
571 [24] C.-S. Tan, D.-C. Liou, Modeling of desorption at supercritical conditions, AIChE J. 35
572 (1989) 1029–1031. http://onlinelibrary.wiley.com/doi/10.1002/aic.690350616/epdf.
573 [25] F. Gaspar, T. Lu, R. Santos, B. Al-Duri, Modelling the extraction of essential oils with
574 compressed carbon dioxide, J. Supercrit. Fluid. 25 (2003) 247–260.
575 http://dx.doi.org/10.1016/S0896-8446(02)00149-3.
576 [26] M.M.R. De Melo, R.M.A. Domingues, M. Sova, E. Lack, H. Seidlitz, F. Lang, et al.,

577 Scale-up studies of the supercritical fluid extraction of triterpenic acids from
578 *Eucalyptus globulus* bark, J. Supercrit Fluid. 95 (2014) 44–50.
579 http://dx.doi.org/10.1016/j.supflu.2014.07.030.
580 [27] G.L. Zabot, M.N. Moraes, A.J. Petenate, M.A. Meireles, Influence of the bed
581 geometry on the kinetics of the extraction of clove bud oil with supercritical CO_2, J.
582 Supercrit. Fluid. 93 (2014) 56–66. http://dx.doi.org/10.1016/j.supflu.2013.10.001.
583 [28] J. Martínez, P.T.V. Rosa, M.A.A. Meireles, Extraction of Clove and Vetiver Oils with
584 Supercritical Carbon Dioxide: Modeling and Simulation, Open Chem. Eng. J. 1
585 (2007) 1–7. https://benthamopen.com/ABSTRACT/TOCENGJ-1-1.
586 [29] A. López-Padilla, A. Ruiz-Rodriguez, C. Restrepo Flórez, D. Rivero Barrios, G.
587 Reglero, T. Fornari, *Vaccinium meridionale* Swartz Supercritical CO_2 Extraction:
588 Effect of Process Conditions and Scaling Up, Materials. 9 (2016) 519.
589 http://www.mdpi.com/1996-1944/9/7/519.
590 [30] T. Hatami, M.A.A. Meireles, G. Zahedi, Mathematical modeling and genetic
591 algorithm optimization of clove oil extraction with supercritical carbon dioxide, J.
592 Supercrit. Fluid. 51 (2010) 331–338. http://dx.doi.org/10.1016/j.supflu.2009.10.001.
593 [31] R.N. Carvalho, L.S. Moura, P.T. V Rosa, M.A.A. Meireles, Supercritical fluid
594 extraction from rosemary (*Rosmarinus officinalis*): Kinetic data, extract's global
595 yield, composition, and antioxidant activity, J. Supercrit. Fluid. 35 (2005) 197–204.
596 http://dx.doi.org/10.1016/j.supflu.2005.01.009.
597 [32] J.M. Prado, I. Dalmolin, N.D.D. Carareto, R.C. Basso, A.J. a. Meirelles, J. Vladimir
598 Oliveira, et al., Supercritical fluid extraction of grape seed: Process scale-up, extract

599 chemical composition and economic evaluation, J. Food Eng. 109 (2012) 249–257.
600 http://dx.doi.org/10.1016/j.jfoodeng.2011.10.007.
601 [33] J.T. Paula, A.C. Aguiar, I.M.O. Sousa, P.M. Magalhães, M.A. Foglio, F.A. Cabral,
602 Scale-up study of supercritical fluid extraction process for *Baccharis dracunculifolia*,
603 J. Supercrit. Fluid. 107 (2016) 219–225.
604 http://dx.doi.org/10.1016/j.supflu.2015.09.013.
605 [34] M.T. Fernández-Ponce, B.R. Parjikolaei, H.N. Lari, L. Casas, C. Mantell, E.J.
606 Martínez de la Ossa, Pilot-plant scale extraction of phenolic compounds from mango
607 leaves using different green techniques: Kinetic and scale up study, Chem. Eng. J. 299
608 (2016) 420–430. http://dx.doi.org/10.1016/j.cej.2016.04.046.
609 [35] J.M. Prado, G.H.C. Prado, M.A.A. Meireles, Scale-up study of supercritical fluid
610 extraction process for clove and sugarcane residue, J. Supercrit. Fluid. 56 (2011) 231–
611 237. http://dx.doi.org/10.1016/j.supflu.2010.10.036.
612 [36] E. Reverchon, C. Marrone, Supercritical extraction of clove bud essential oil: Isolation
613 and mathematical modeling, Chem. Eng. Sci. 52 (1997) 3421–3428.
614 http://dx.doi.org/10.1016/S0009-2509(97)00172-3.
615 [37] M.T. Fernández-Ponce, L. Casas, C. Mantell, E.J.M. De La Ossa, Potential Use of
616 mango leaves extracts obtained by high pressure technologies in cosmetic,
617 pharmaceutics and food industries, Chem. Eng. Trans. 32 (2013) 1147–1152.
618 http://www.aidic.it/cet/13/32/192.pdf.
619 [38] L. Casas, C. Mantell, M. Rodríguez, A. Torres, F.A. Macías, E.J.M. de la Ossa, SFE
620 kinetics of bioactive compounds from *Helianthus annuus* L, J. Sep. Sci. 32 (2009)

621 http://onlinelibrary.wiley.com/doi/10.1002/jssc.200800663/epdf.
622 [39] R. Dohrn, J.M.S. Fonseca, S. Peper, Experimental methods for phase equilibria at high
623 pressures., Ann Rev Chem Biomol. 3 (2012) 343–67.
624 https://doi.org/10.1146/annurev-chembioeng-062011-081008.
625 [40] D.E. Knox, Solubilities in supercritical fluids, Pure Appl. Chem. 77 (2005) 513–530.
626 https://doi.org/10.1351/pac200577030513.
627 [41] U. Salgın, S. Salgın, Effect of main process parameters on extraction of pine kernel
628 lipid using supercritical green solvents: Solubility models and lipid profiles, J.
629 Supercrit. Fluid. 73 (2013) 18–27. http://dx.doi.org/10.1016/j.supflu.2012.11.002.
630 [42] K.S. Duba, L. Fiori, Supercritical CO_2 extraction of grape seed oil: Effect of process
631 parameters on the extraction kinetics, J. Supercrit Fluid. 98 (2015) 33–43.
632 http://dx.doi.org/10.1016/j.supflu.2014.12.021.
633 [43] S.G. Özkal, U. Salgin, M.E. Yener, Supercritical carbon dioxide extraction of hazelnut
634 oil, J. Food Eng. 69 (2005) 217–223.
635 http://dx.doi.org/10.1016/j.jfoodeng.2004.07.020.
636 [44] U. Salgin, Extraction of jojoba seed oil using supercritical CO_2+ethanol mixture in
637 green and high-tech separation process, J. Supercrit. Fluid. 39 (2007) 330–337.
638 http://dx.doi.org/10.1016/j.supflu.2006.03.013.
639 [45] U. Salgin, H. Korkmaz, A green separation process for recovery of healthy oil from
640 pumpkin seed, J. Supercrit Fluid. 58 (2011) 239–248.
641 http://dx.doi.org/10.1016/j.supflu.2011.06.002.
642 [46] L. Danielski, Solubilidade das Oleoresinas de Calendula (*Calendula officinalis* L.) e

643 Cavalinha (*Equisetum arvense*) em CO2 Supercrítico, Universidade Federal de Santa
644 Catarina, 2002.
645 [47] R.B. Bird, W.E. Stewart, E.N. Lightfoot, Transport Phenomena, in: 2nd ed., John
646 Wiley & Sons, Inc., New York, NY, 2002: p. 914.
647 [48] A. López-Padilla, A. Ruiz-Rodriguez, G. Reglero, T. Fornari, Study of the diffusion
648 coefficient of solute-type extracts in supercritical carbon dioxide: Volatile oils, fatty
649 acids and fixed oils, J. Supercrit. Fluid. 109 (2016) 148–156.
650 http://dx.doi.org/10.1016/j.supflu.2015.11.017.
651 [49] NIST, Thermophysical properties of fluid systems, National Institute of Standards and
652 Technology. (2016). http://webbook.nist.gov/chemistry/fluid/ (accessed December
653 18, 2016).
654
655

656 **Table 1.** Total extraction yield (extraction time = 270 min) obtained in the SFE of *Calendula*
657 *officinalis* at 313 K and different pressures and CO_2 mass flow rates and extraction vessels
658 with a bed porosity of $\varepsilon = 0.763$.
659

Run order	Scale	$Q \times 10^4$ (kg·s^{-1})	P (MPa)	Yield (%)
1	V_{A1}	2.5	14	4.56
2	V_{A2}	5.0	14	5.61
3	V_{A3}	7.5	14	6.11
4	V_{A4}	5.0	24	6.28
5	V_{A5}	5.0	34	6.48
6	V_{B1}	6.0	14	3.08
7	V_{B2}	12.3	14	4.15
8	V_{C1}	15.5	14	4.77
9	V_{C2}	47.0	14	7.38

Extraction vessels volume: V_{A1} to $V_{A5} = 2.7\times10^{-4}$ m^3; V_{B1} and $V_{B2} = 1.35\times10^{-3}$ m^3; V_{C1} and $V_{C2} = 5.19\times10^{-3}$ m^3.

660
661

662 **Table 2.** Geometrical characteristics of the cylindrical extraction vessels used in this work
663 and mass of grinded marigold flowers loaded in each extraction vessel.
664

	V_A	V_B	V_C
Internal diameter, D (m)	0.043	0.067	0.107
Length, L (m)	0.188	0.383	0.570
L/D ratio	4.372	5.716	5.327
Cross-flow area, A (m^2)	0.00145	0.00353	0.00899
Volume, V (m^3)	0.00027	0.00135	0.00519
Mass loaded, F (kg)	0.090	0.445	1.708

665

Table 3. Optimal parameters obtained in the OEC fitting (BIC model) of the small scale (vessel V_A) marigold SFE at 313 K and different CO_2 flow rates and extraction pressures. V_A = 2.7×10^{-4} m^3; F = 0.090 kg; ε = 0.763; X_o = 0.0745; X_k = 0.0450.

	P = 14 MPa			P = 24 MPa	P = 34 MPa
Run order	1	2	3	4	5
$Q\times10^4$ ($kg\cdot s^{-1}$)	2.5	5.0	7.5	5.0	5.0
ρ_{CO2}* ($kg\cdot m^3$)	763.2	763.2	763.2	872.5	930.2
Y* ($kg\cdot kg^{-1}$)	0.0032	0.0032	0.0032	0.0038**	0.0049**
$k_{YA}\times10^2$ (s^{-1})	0.420	0.570	0.940	0.97	1.50
$k_{XA}\times10^3$ (s^{-1})	0.010	0.021	0.027	0.039	0.055
t_{CER} (mim)	15.98	11.78	7.14	5.10	2.40
t_{FER} (mim)	72.34	40.08	25.75	30.3	22.17
Y_{CER} (kg/kg)	0.0031	0.0028	0.0029	0.0036	0.0048
$M_{CER}\times10^7$ ($kg\cdot s^{-1}$)	7.68	14.2	21.8	18.3	24.3
*AARD**** *(%)*	6.62	3.67	2.06	2.47	5.06

* [49]

** fitting parameter

*** $AARD = \frac{1}{N}\sum\left|\frac{calculated\ yield - experimental\ yield}{experimental\ yield}\right|$

Table 4. Marigold SFE scaling up (BIC model predictions) at 14 MPa and 313 K from the small extraction vessel (V_A) to two larger scale vessels (V_B and V_C) preserving bed porosity (ε = 0.763). CO_2 flow rates were calculated according to Eq. (12) (equal CO_2 linear velocity) or Eq. (14) (equal CO_2 residence time) scaling criteria.

	V_A	V_B		V_C	
		Eq. (12)	Eq. (14)	Eq. (12)	Eq. (14)
Run order	1	6	7	8	9
L/D	4.372	5.716	5.716	5.327	5.327
Q $\times 10^4$ (kg·s^{-1})	2.5	6.0	12.3	15.5	47.0
$v \times 10^4$ (m·s^{-1})	2.25	2.25	4.58	2.25	6.85
t_R (min)	10.6	21.8	10.6	32.1	10.6
t_{CER} (min)	15.98	15.98	15.98	15.98	15.98
t_{FER} (min)	72.3	145.3	73.1	221.6	72.9
$M_{CER} \times 10^7$ (kg·s^{-1})	7.68	19.2	38.0	49.7	145
Fitting of the experimental OEC:					
$k_{YA} \times 10^2$ (s^{-1})	0.42	0.45	0.35	0.33	0.75
$k_{XA} \times 10^3$ (s^{-1})	0.010	0.003	0.007	0.010	0.134
AARD (%)*	6.62	11.4	8.02	10.3	6.62

$^{*}AARD = \frac{1}{N}\sum\left|\frac{experimental\ \ yield - calculated\ \ yield}{experimental\ \ yield}\right|$

Figure 1. Schematic diagram of Thar SFE pilot and semi industrial plants (1a = laboratory and pilot plant; 1b= semi-industrial plant). Nomenclature: A, B and C are extraction cells with volumes of = 2.7×10^{-4} m^3, B= 1.35×10^{-3} m^3 and 5.19×10^{-3} m^3, respectively; D= CO_2 storage tank; E= CO_2 Pump; F= Heat Exchanger; G= Automatic BPR Valve; H= Cyclonic Separator; I= BPR Valve; J= Pass valves; K= Condensers; L= Cooling System; M= Demister; N= Filter; P= Manometers; Q = Volume indicator; R= Flowmeter; (⋯) Dotted line means PLC control; (---) Dashed lines means recycling.

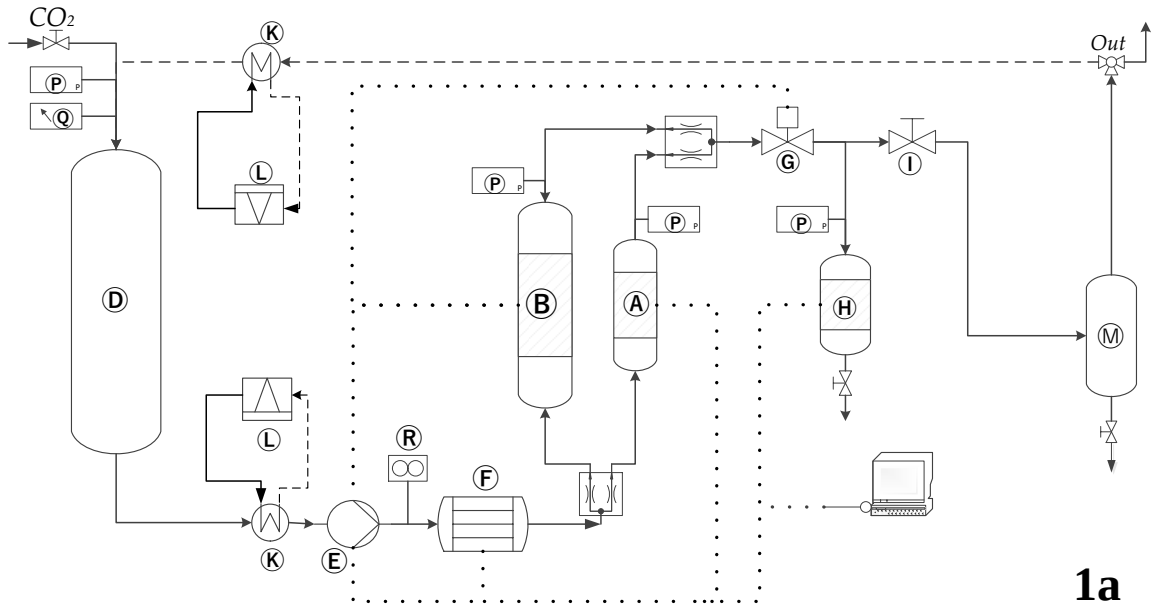

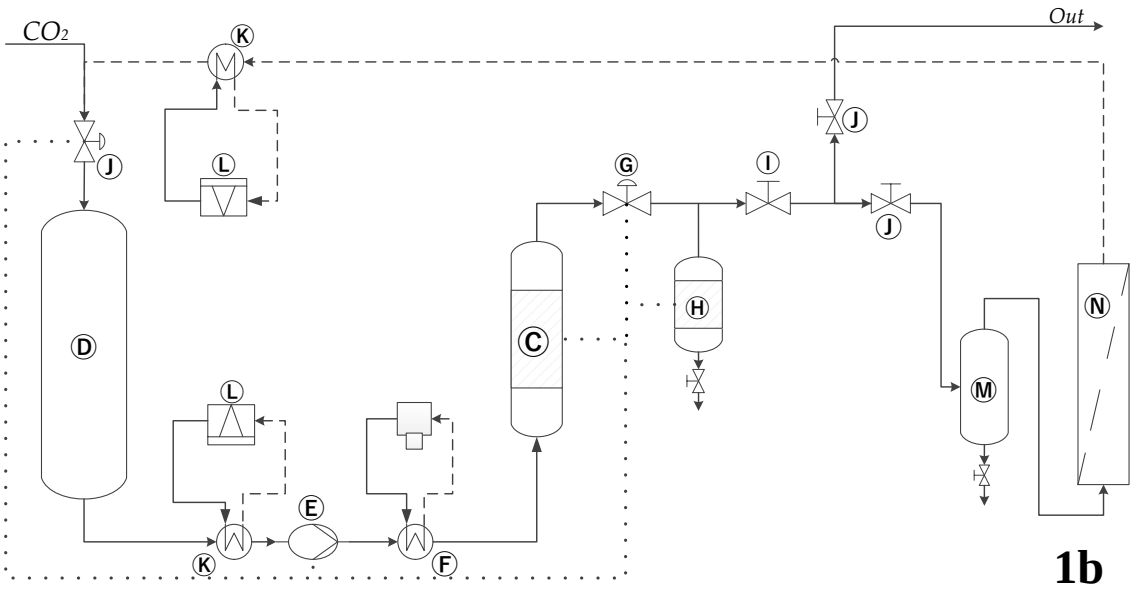

Figure 2. Overall extraction curves obtained using vessel V_A (2.7×10^{-4} m^3) and 0.090 kg of marigold flowers. Extraction temperature was 313 K and total extraction time was 270 min. (■) 14 MPa, 2.5×10^{-4} kg·s^{-1}; (▲) 14 MPa, 5.0×10^{-4} kg·s^{-1}; (●) 14 MPa, 7.5×10^{-4} kg·s^{-1}; (□) 24 MPa, 5.0×10^{-4} kg·s^{-1}; (△) 34 MPa, 5.0×10^{-4} kg·s^{-1}. Dashed lines represent the BIC model fitting.

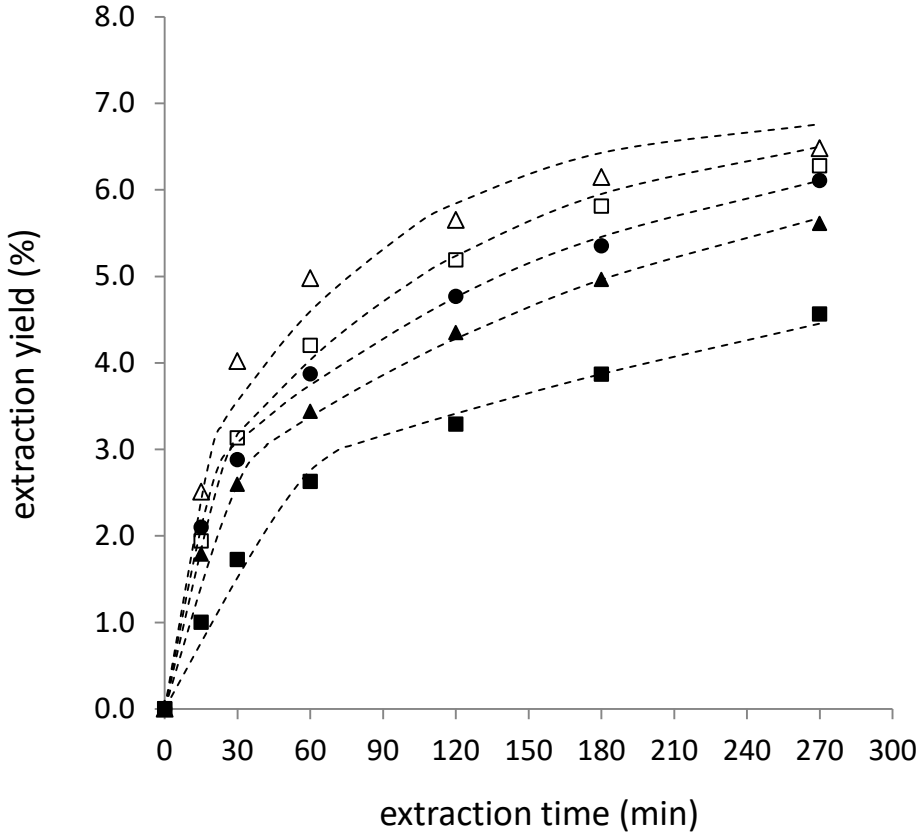

Figure 3. Total extractable material (X_o) and marigold solubility (Y^*) in supercritical CO_2 at 313 K and 14 MPa. Data represent the OECs obtained at 313 K and 14 MPa in V_A ($2.7x10^{-4}$ m^3) with different CO_2 flow rates Q = (■) 2.5×10^{-4} $kg\cdot s^{-1}$, (▲) 5.0×10^{-4} $kg\cdot s^{-1}$ and (●) 7.5×10^{-4} $kg\cdot s^{-1}$.

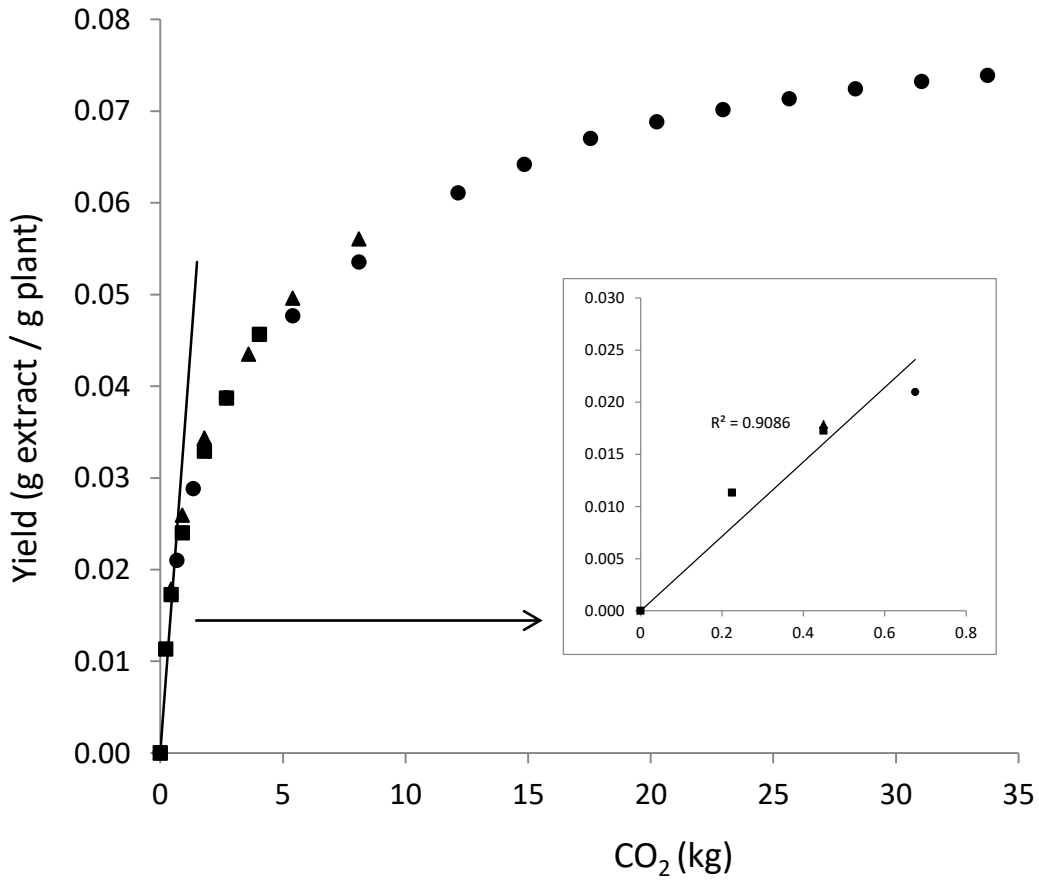

Figure 4. Marigold SFE scaling up at 313 K, 14 MPa and constant bed porosity (ε = 0.763) from V_A to V_B (scaling factor = 4.95). Grey and black lines represent BIC predictions using the criterions of keeping constant solvent velocity (Eq. (12)) and by keeping constant residence time (Eq. (14)), respectively: (---) CER period; (––) FER period; (–·–) DC period. Symbols represent experimental data: (■) laboratory scale V_A, $Q = 2.5\times10^{-4}$ kg·s^{-1}; (▲) pilot scale, V_B, using Eq. (12); (△) pilot scale, V_B, using Eq. (14).

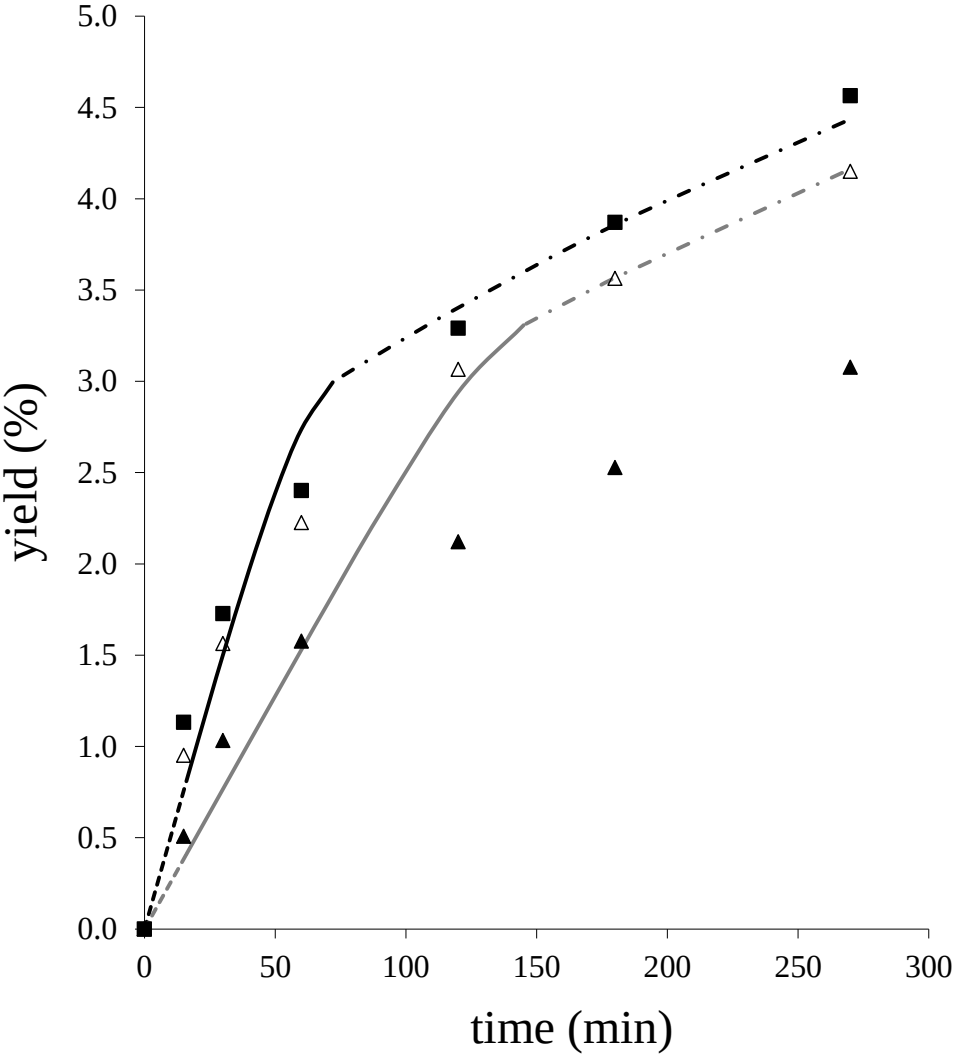

Figure 5. Marigold SFE scaling up at 313 K, 14 MPa and constant bed porosity (ε = 0.763) from V_A to V_C (scaling factor = 19.08). Grey and black lines represent BIC predictions using Eq. (12) and Eq. (14), respectively: (---) CER period; (––) FER period; (–·–) DC period. Symbols represent experimental data: (■) V_A, $Q = 2.5\times10^{-4}$ kg·s^{-1}; (○) V_C, Eq. (12); (●) V_C, Eq. (14).

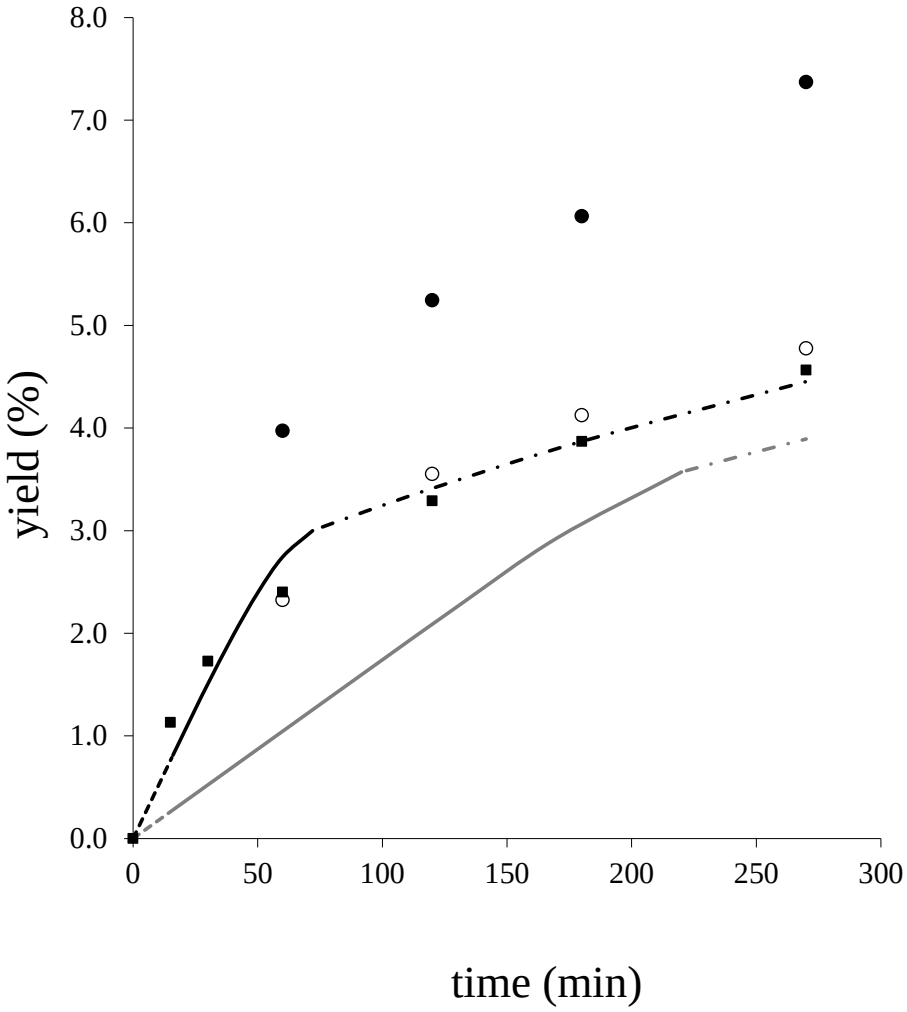

Figure 6. Correlating the fluid phase mass transfer coefficients k_{YA} of marigold experimental OECs with process parameters (Q and Sc number) and vessel geometrical constants (D and L). (△) V_A, 14 MPa; (▲) V_A, 24 and 34 MPa; (■) V_B, 14 MPa; (●) V_C, 14 MPa.

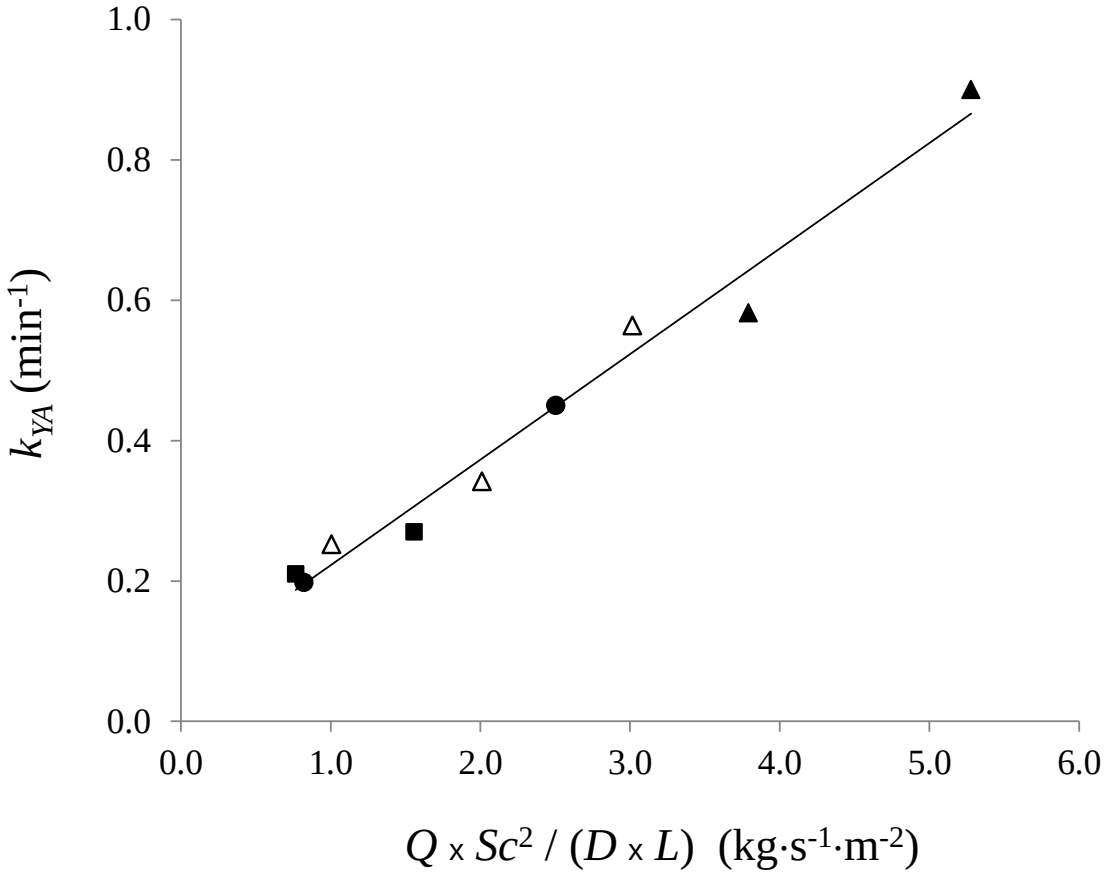

3.4 Study of the diffusion coefficient of solute-type extracts in supercritical carbon dioxide: Volatile oils, fatty acids and fixed oils

Alexis López-Padilla, Alejandro Ruiz-Rodríguez,
Guillermo Reglero & Tiziana Fornari

Journal of Supercritical Fluids, 109 (2016) 148-156.
DOI: 10.1016/j.supflu.2015.11.017

J. of Supercritical Fluids 109 (2016) 148–156

Contents lists available at ScienceDirect

The Journal of Supercritical Fluids

journal homepage: www.elsevier.com/locate/supflu

Study of the diffusion coefficient of solute-type extracts in supercritical carbon dioxide: Volatile oils, fatty acids and fixed oils

Alexis López-Padilla, Alejandro Ruiz-Rodriguez, Guillermo Reglero, Tiziana Fornari *

Institute of Food Science Research CIAL (CSIC-UAM) CEI UAM+CSIC, C/Nicolás Cabrera 9, Campus de Cantoblanco 28049 Madrid, Spain

ARTICLE INFO

Article history:
Received 13 August 2015
Received in revised form
17 November 2015
Accepted 18 November 2015
Available online 23 November 2015

Keywords:
Diffusion coefficients
Carbon dioxide
Correlation
Volatile oils
Fatty acids
Triglycerides

ABSTRACT

Supercritical carbon dioxide ($SCCO_2$) extraction is an innovative and efficient method to recover valued substances from vegetal materials. The diffusion behavior of the extract in the supercritical solvent is an important parameter to understand the mass transfer behavior of the process. In this work, experimental data from the literature were utilized to analyze the diffusivity of lipophilic chemically similar solutes in $SCCO_2$.

Substances with similar chemical structure, molecular weight and volatility, have also very similar diffusion coefficients, which are mainly determined by temperature, pressure and, in turn, by the corresponding physicochemical properties of the supercritical solvent (density and viscosity). Based on this premise, general correlations were derived to represent the diffusion coefficient of volatile oils, fatty acids and its esters, and fixed oils (triglycerides) in $SCCO_2$ as a function solely of pressure and temperature. The diffusion coefficients obtained were satisfactory compared with those calculated with theoretical and semi-empirical models from the literature, which require pure component parameters.

1. Introduction

The supercritical fluid extraction (SFE) of vegetable materials is a semi-continuous process in which the high pressure solvent dissolves and extracts substances, while flowing through a fixed bed of particles of the solid raw material. This technology is being extensively applied using supercritical carbon dioxide ($SCCO_2$) to extract lipophilic substances such as carotenoids, fatty acids, fatty acid esters, volatile oils, fixed oils, antioxidants, etc. from a wide variety of plants and herbs, seeds, algae and microalgae, wastes and by-products of the agrochemical and food industry.

One important parameter to describe mass transfer in SFE is the diffusion coefficient of the different substances extracted (solutes) in $SCCO_2$. Most of experimental data so as predictive and/or correlative models were determined for binary systems [1,2]. Equations available in the literature, demand pure solute parameters (molar mass, critical volume, molar volume at normal boiling point, surface tension, etc.), the physicochemical properties of the supercritical solvent (density, viscosity, critical parameters) and sometimes specific correlation parameters. The higher the accuracy of the model, the higher the number of parameters required.

Wilke–Chang equation [3] is one of the most popular correlations to calculate the diffusion coefficient of a pure solute in $SCCO_2$, with average deviations around 10% for 600 experimental data points including different type of solutes [1]. Lately, Magalhães et al. [4] proposed two modified Stokes–Einstein equations and proved their accuracy using a large database comprehending extremely distinct molecules in terms of size, shape, molar mass and polarity. The global deviations achieved by these equations were lower than 7%. In general, temperature, solvent viscosity and solute size (introduced in equations via molar volume at normal boiling point and critical volume) were explicit parameters in this type of correlations. More recently, Magalhães et al. [5] developed novel correlations for the diffusion coefficient of a pure solute in liquids and supercritical fluids over wide ranges of temperature and density, which are based on expressions that depend only on temperature, and/or solvent density, and/or solvent viscosity. Also, the equations involved two fitting parameters specifically for each pure compound. The accuracy of these correlations was tested with a large database (539 binary systems and 8219 data points) with average deviation around 3%.

Even though good correlations are available in the literature to represent the diffusion of a pure solute in $SCCO_2$, supercritical plant extracts are in general multicomponent mixtures. Furthermore, depending on the vegetal material and the process conditions, the resulted extract may mainly contain certain type of solutes,

* Corresponding author. Tel.: +34 910017927.
E-mail address: tiziana.fornari@uam.es (T. Fornari).

http://dx.doi.org/10.1016/j.supflu.2015.11.017
0896-8446/

Table 1
Diffusion coefficient correlations from the literature and pure component solute parameters required.

Equation		Parameters	Ref.
Scheibel	$D_{12}\left(\mathrm{cm^2\,s^{-1}}\right) = \frac{8.2x10^{-8}T}{\mu_1 V_{bp,2}^{1/3}}\left[1+\left(\frac{3V_{bp,1}}{V_{bp,2}}\right)^{2/3}\right]$	$V_{bp,2}$	[21]
Reddy-Doraiswamy	$D_{12}\left(\mathrm{cm^2\,s^{-1}}\right) = \beta x\frac{T\sqrt{M_1}}{\mu_1(V_{bp,1}V_{bp,2})^{1/3}}$ $\beta = 1.0\times10^{-8}\ (V_{bp,1}/V_{bp,2}\le 1.5)$; $\beta = 8.5\times10^{-8}\ (V_{bp,1}/V_{bp,2} > 1.5)$	$V_{bp,2}$	[22]
Lusis-Ratcliff	$D_{12}\left(\mathrm{cm^2 s^{-1}}\right) = \frac{8.52x10^{-8}T}{\mu_1 V_{bp,1}^{1/3}}\left[1.40\left(\frac{V_{bp,1}}{V_{bp,2}}\right)^{1/3}+\left(\frac{V_{bp,1}}{V_{bp,2}}\right)\right]$	$V_{bp,2}$	[23]
Lai-Tan	$D_{12}\left(\mathrm{cm^2 s^{-1}}\right) = 2.50x10^{-7}\frac{T\sqrt{M_1}}{(10x\mu_1)^{0.688}V_{c,2}^{1/3}}$	$V_{c,2}$	[24]
Wilke–Chang	$D_{12}\left(\mathrm{cm^2 s^{-1}}\right) = 7.4x10^{-8}\left(\frac{T\sqrt{xM_1}}{\mu_1 V_{bp,2}^{0.6}}\right)$; $\begin{cases} x=1 \text{ for nonassociated solvents} \\ x=2.6 \text{ for water}\end{cases}$	$V_{bp,2}$	[3]
Modified Stokes–Einstein Equation 1	$D_{12}\left(\mathrm{cm^2 s^{-1}}\right) = A\left(\frac{T}{\mu_1}\right)^{\alpha}\frac{1}{(M_2 V_{bp,2})^{\beta}}$	M_2, $V_{bp,2}$	[4]
Modified Stokes–Einstein Equation 2	$D_{12}\left(\mathrm{cm^2 s^{-1}}\right) = A\left(\frac{T}{\mu_1}\right)^{\alpha}\frac{1}{\left(M_2 V_{bp,2}\sigma_{bp,2}^{1/4}\right)^{\beta}}$	M_2, $V_{bp,2}$, $\sigma_{bp,2}$	[4]
Modified Schiebel	$D_{12}\left(\mathrm{cm^2 s^{-1}}\right) = A\left(\frac{T}{\mu_1}\right)^{\alpha}\frac{1}{V_{c,2}^{\beta}}\left[1+\left(\frac{3V_{c,1}}{V_{c,2}}\right)^{2/3}\right]$	$V_{c,2}$	[20]
Modified Lusis–Ratcliff	$D_{12}\left(\mathrm{cm^2 s^{-1}}\right) = A\left(\frac{T}{\mu_1}\right)^{\alpha}\left[\beta\left(\frac{V_{c,1}}{V_{c,2}}\right)^{1/3}+\left(\frac{V_{c,1}}{V_{c,2}}\right)\right]$	$V_{c,2}$	[20]
Modified Wilke–Chang	$D_{12}\left(\mathrm{cm^2 s^{-1}}\right) = A\left(\frac{T}{\mu_1}\right)^{\alpha}\frac{1}{V_{c,2}^{\beta}}$	$V_{c,2}$	[20]

1: solvent (CO_2); 2: solute; T: temperature; P: pressure; μ: viscosity; σ: surface tension; V_{bp}: molar volume at normal boiling point; M: molar mass; V_c: molecular critical volume; x: association parameter in Wilke–Chang equation; A, α, β and γ: specific constants in the corresponding correlations.

such as volatile oils, fatty acid esters or triglycerides. Information in the literature regarding the diffusion behavior of these multicomponent extracts is scarce. In this work, the diffusivity of these families of lipophilic compounds in $SCCO_2$ was analyzed and represented.

Volatile oil plant extracts comprise monoterpenes and sesquiterpenes with normal boiling points from 150 °C to 230 °C and molecular weights are in the range of 100–250 g mol^{-1}. On the other hand, fatty acid chains in vegetal oils are between C13 and C21 carbon number. Their molecular weights are around 220–350 g mol^{-1} and have very low volatility (normal boiling points around 250–450 °C). Similarly to fatty acids, triglycerides or fixed oils have high normal boiling points (low volatility) but considerable larger molecular weights, around 750–950 g mol^{-1}.

Significant different diffusion coefficients at a given temperature and pressure were measured for volatile oil compounds, fatty acids and triglycerides. For example, the diffusion coefficient of citral at 313 K and 20 MPa is 8.10×10^{-5} cm^2 s^{-1}, which is rather similar to the diffusion coefficient of other volatile oil substances such as eugenol (7.69×10^{-5} cm^2 s^{-1}) or α-pinene (8.90×10^{-5} cm^2 s^{-1}) [6–8]. Nevertheless, at the same conditions of pressure and temperature, these values are 6.13×10^{-5} cm^2 s^{-1}, 6.06×10^{-5} cm^2 s^{-1} and 5.45×10^{-5} cm^2 s^{-1} for respectively, linolenic, oleic and docosahexaenoic acids [9–11], i.e., around 40% lower than those of volatile oil compounds. Regarding de diffusion coefficient of fixed oils at 313 K and 20 MPa, the value reported for e.g., triarachidonin is 3.96×10^{-5} cm^2 s^{-1} (around 30% lower than those corresponding to fatty acids) [12].

Thus, substances of the same chemical family, with similar molecular mass and volatility, have very similar diffusion coefficients. Yet, substantial differences were observed among the diffusion coefficient of a volatile oil, a fatty acid and a triglyceride. Based on these observations, three general and simple correlations were derived in this work to estimate the diffusion coefficient of type-extracts, namely (i) volatile oils, (ii) fatty acids and derived fatty acid esters and (iii) fixed oils, as a function solely of pressure and temperature. The equations obtained are based on the regression of experimental data from the literature. A total of 30 different solute-$SCCO_2$ binary systems (1191 data points) were considered to assess the capability of the correlations developed and deviations lower than 13% were obtained.

2. Overview of diffusion coefficient correlations

The diffusion coefficient of a solute in a supercritical fluid ($D_{i\text{-SCF}}$) is affected by the size and shape of the solute, the intermolecular interaction with the supercritical solvent and the temperature and pressure conditions. In general, solutes with large molecular mass and solutes which can present chemical interactions diffuse more slowly. Additionally, pressure and temperature define solvent density and viscosity, which have an important effect on the solute diffusion. In general, the diffusion coefficient increases with increasing temperature at constant pressure, being the effect less important at higher pressures. And with respect to pressure, $D_{i\text{-SCF}}$ decreases with increasing pressure. High pressure means high solvent density, and if solvent density increases diffusion becomes more difficult due to an increased number of molecular collisions. Furthermore, intermolecular interactions also increase because the average intermolecular distance is reduced as density increases.

Predictive and correlative models and equations available in the literature follow the above observed experimental behavior of diffusion coefficients with respect to temperature, pressure, solute and solvent properties. Table 1 show several mathematical expressions derived from the Stokes–Einstein formula which were frequently used in the literature. In general, the supercritical fluid properties in these equations are viscosity, molecular weight, molar volume at normal boiling point and critical volume. Particularly, the supercritical solvent viscosity is a strategic variable in all equations given in Table 1, connecting the effect of temperature and pressure on the solute diffusion coefficient. Despite the goodness of correlations available in the literature, all equations demand pure component solute physicochemical parameters or even fitting parameters, which are problematic to estimate in the case of multicomponent and complex SFE extracts.

Recently, Magalhães et al. [5] investigated the effect of the supercritical solvent viscosity and density by defining several equations in which the term $D_{i\text{-SCF}}/T$ depends explicitly on solvent viscosity, on solvent density and both viscosity and density. All equations demand two specific fitting parameters for each pure compound and, in general, presented excellent correlative capability. Particularly, the equation:

$$D_{12}\left(\mathrm{cm^2\,s^{-1}}\right) = T\left(a\cdot\rho+\frac{b}{\mu}\right) \tag{2.1}$$

Table 2
Experimental data (Taylor–Aris chromatographic peak broadening method) used in the diffusion coefficient $D_{VO\text{-}CO_2}$ correlation for volatile oil compounds in CO_2 (Eq. (4.1)).

Volatile oil compound	N	P (bar)	T (°C)	CO_2 density (g cm^{-3})	CO_2 viscosity (cP)	AARD[a] (%)	AARD[b] (%)	AARD[c] (%)	Ref.
Anisole	15	400–600	40–60	0.604–0.935	0.046–0.100	12.85	1.92	5.00	[25]
Citral	15	120–200	40–60	0.447–0.843	0.033–0.079	4.68	2.42	7.30	[6]
D-limonene	15	120–200	40–60	0.447–0.843	0.033–0.079	5.24	2.95	9.24	[6]
Eugenol	15	150–350	40–60	0.607–0.936	0.047–0.100	11.51	2.51	18.94	[7]
L-carvone	27	150–300	35–65	0.650–0.929	0.051–0,099	5.21	3.15	3.71	[26,27]
Linalol	15	120–200	40–60	0.447–0.843	0.033–0.079	2.71	2.75	2.94	[28]
L-Menthone	23	150–300	35–65	0.650–0.929	0.051–0.099	3.62	3.35	6.97	[26]
4-Methylanisole	15	150–350	40–60	0.700–0.936	0.057–0.100	2.58	2.03	16.51	[29]
α-Pinene	15	120–200	40–60	0.447–0.843	0.033–0.079	5.04	3.15	7.78	[8]
β-Pinene	15	120–200	40–60	0.447–0.843	0.033–0.079	8.70	3.23	12.31	[8]
					Mean AARD (%)	5.48	2.84	9.52	

[a] This work (Eq. (4.1)).
[b] Estimated by Magalhães et al. (Eq. (2.1)) [5].
[c] Estimated by Modified Wilke–Chang Equation as proposed by Vaz et al. [20].

where, T is the temperature in K, ρ is the density in g cm^{-3}, μ is the viscosity in cP, and a and b are regression parameters for each pure solute, was tested using 539 binary systems of molecules with different size and polarity, and presented deviations of 3%, when used in correlative mode, and lower than 5% in predictive mode [5].

3. Mathematical approach

3.1. Regression analysis

Multiple Linear Regression Analysis (MLRA) was used in this work to correlate the experimental diffusion coefficient D_{i-CO_2} of volatile oil compounds, fatty acids and fixed oils as a function of temperature, pressure and the corresponding CO_2 density and viscosity. The mathematical model is given by the following equation [13–16]:

$$D_{i-CO_2} = \beta_0 + \beta_1 X_1 + \beta_2 X_2 + \ldots + \beta_n X_n + \varepsilon \quad (3.1)$$

where,

X_i are the independent variables, β_i are the corresponding regression coefficients, and ε is an error to account for the discrepancy between predicted data and the observed data.

MLRA was carried out with a forward stepwise regression method, using the software Statgraphics v.15.2 (Statpoint Technologies Inc., USA). Differences were considered significant for p-values with values lower than 0.10 ($p < 0.10$).

3.2. Estimation of CO_2 density and viscosity

CO_2 density was calculated using an EoS specifically derived for this substance as proposed by Span and Wagner [17] and using the NIST Webbook [18]. The EoS employed is an empirical representation of the fundamental equation explicit in the Helmholtz energy (calculated as the sum of a gas ideal term and a residual contribution) with two independent variables (density and temperature). Relative deviations in comparison with experimental CO_2 density are lower than ±0.2% for pressures and temperatures in the range of supercritical extraction.

CO_2 viscosity $\left(\mu_{CO_2}\right)$ was calculated using a correlation of μ_{CO_2} as a function of temperature and pressure [19] specifically derived for carbon dioxide, which covers the temperature range

Table 3
Experimental data used in the diffusion coefficient $D_{FA\text{-}CO_2}$ correlation for fatty acids in CO_2 (Eq. (4.3)). TCR: tracer response technique with a poly(ethylene glycol)-coated capillary column; CPB; Taylor–Aris capillary peak broadening method; CIR: chromatographic impulse response technique.

Compound	N	P (bar)	T (°C)	CO_2 density (g cm^{-3})	CO_2 viscosity (cP)	AARD[a] (%)	AARD[b] (%)	AARD[c] (%)	Ref.	Method
Arachidonic acid	75	95–305	35–70	0.555–0.932	0.042–0.099	7.16	1.40	3.02	[9]	TCR
Arachidonic acid ethyl ester	47	84–300	35–65	0.496–0.850	0.036–0.081	3.22	0.83	5.79	[30]	CPB
Docosahexaenoic acid	63	93–301	35–70	0.569–0.930	0.043–0.099	10.75	0.97	5.19	[11]	TCR
Docosahexaenoic acid ethyl ester	47	84–300	35–65	0.496–0.850	0.036–0.081	3.58	0.83	6.43	[30]	CPB
Eicosapentaenoic acid	55	87–302	35–70	0.464–0.914	0.034–0.095	6.10	0.74	2.93	[11]	TCR
Eicosapentaenoic acid ethyl ester	47	84–300	35–65	0.496–0.850	0.036–0.081	3.52	0.74	5.80	[30]	CPB
Linoleic acid	69	90–303	35–70	0.555–0.932	0.042–0.099	7.24	2.34	3.42	[9]	TCR
γ-Linolenic acid ethyl ester	44	81–160	40–70	0.290–0.795	0.023–0.070	7.12	5.38	7.44	[31]	CIR
γ-Linolenic acid methyl ester	36	81–160	40–70	0.290–0.795	0.023–0.070	6.07	4.32	8.39	[31]	CIR
α-Linolenic acid	55	91–301	35–70	0.544–0.930	0.041–0.099	6.54	1.57	4.43	[11]	TCR
γ-Linolenic acid	141	87–305	35–70	0.457–0.913	0.034–0.094	5.86	1.24	3.22	[31]	CIR
Myristotelic acid	42	92–130	40–70	0.457–0.880	0.034–0.087	8.21	1.68	5.14	[32]	CIR
Myristotelic acid methyl ester	79	80–140	40–70	0.227–0.580	0.022–0.043	7.43	10.35	11.00	[32]	CIR
Oleic acid	19	95–300	40	0.581–0.910	0.043–0.094	2.61	1.68	3.52	[10]	CIR
Oleic acid ethyl ester	5	86–110	40	0.376–0.683	0.027–0.054	10.65	1.91	5.78	[10]	CIR
Oleic acid methyl ester	19	80–110	40	0.278–0.683	0.022–0.054	9.60	2.92	4.89	[10]	CIR
					Mean AARD (%)	6.60	2.43	5.40		

[a] This work (Eq. (4.3)).
[b] Estimated by Magalhães et al. (Eq. (2.1)) [5].
[c] Estimated by Modified Wilke–Chang Equation as proposed by Vaz et al. [20].

Table 4
Experimental data (chromatographic impulse response method) used in the diffusion coefficient $D_{FO\text{-}CO_2}$ correlation for fixed oils in CO_2 (Eq. (4.4)).

Compound	N	P (bar)	T (°C)	CO_2 density (g cm^{-3})	CO_2 viscosity (cP)	AARD[a] (%)	AARD[b] (%)	AARD[c] (%)	Ref.
Triarachidonin	28	100–302	40	0.629–0.911	0.048–0.094	8.31	0.69	5.23	[10,12]
Trierucin	101	83–301	35–50	0.567–0.930	0.042–0.099	2.18	2.47	9.43	[12]
Trinervonin	38	90–301	35–50	0.567–0.930	0.042–0.099	5.99	2.34	7.41	[12]
Triolein	11	91–40	40	0.518–0.763	0.040–0.065	12.33	2.04	9.83	[10]
					Mean AARD (%)	7.20	1.89	7.98	

[a] This work (Eq. (4.4)).
[b] Estimated by Magalhães et al. (Eq. (2.1)) [5].
[c] Estimated by Modified Wilke–Chang Equation as proposed by Vaz et al. [20].

from −73 °C to 1227 °C and densities up to 1400 kg m^{-3}. In terms of pressure, the viscosity representation is valid up to 3000 bar for temperatures below 727 °C. The uncertainties associated with the proposed correlation vary from ±0.3% for the viscosity of the dilute gas near room temperature to ±5.0% at the highest pressures (3000 bar).

4. Results and discussion

4.1. Diffusion coefficient of volatile oils

The correlation is based on experimental data comprising the diffusion coefficients of 10 isoprenoids, which are typical compounds present in the volatile oil obtained by supercritical CO_2 extraction of plants and herbs. Table 2 show the chemicals included in the correlation procedure and the number of data points (N) for each substance, with a total of 170 data points. Taylor–Aris chromatographic peak broadening method was used independently of the solute and the reference. A unique and general equation for all these isoprenoids was assessed, in order to develop a simple tool to predict reasonable diffusion coefficients of volatile oil (VO) of plants and herbs in CO_2 $\left(D_{VO\text{-}CO_2}\right)$ at a given temperature (T) and pressure (P). Since CO_2 density $\left(\rho_{CO_2}\right)$ and viscosity $\left(\mu_{CO_2}\right)$ are very dependent on temperature and pressure, especially at supercritical conditions, these two properties were also selected as independent variables in the correlation procedure and the Eq. (4.1) was obtained from the regression procedure:

$$D_{VO\text{-}CO_2} = 3.5400x10^{-4} + 1.1129x10^{-3}\mu - 4.3036x10^{-4}\rho + 1.64x10^{-7}T \quad (4.1)$$

where, $D_{VO\text{-}CO_2}$ is given in cm^2 s^{-1}, μ is given in cP, ρ in g cm^{-3} and T in °C.

Table 3 report the Average Absolute Relative Deviation (AARD) which was calculated according to the following equation:

$$\text{AARD} = \frac{100}{N}\sum_{i=1}^{N}\frac{\left|D^{exp}_{i-CO_2} - D^{cal}_{i-CO_2}\right|}{D^{exp}_{i-CO_2}} \quad (4.2)$$

where, $D^{exp}_{i-CO_2}$ is the experimental diffusion coefficient of substance i at a given temperature and pressure, and $D^{cal}_{i-CO_2}$ is the diffusion coefficient calculated using Eq. (4.1).

As can be observed in the table for all compounds considered, the AARD% was lower than 13%, being the mean AARD around 5.5%.

4.2. Diffusion coefficient of fatty acids and fatty acid esters

The correlation is based on experimental data comprising the diffusion coefficients of 16 fatty acids and some of their methyl or ethyl esters, which are typical in vegetal oils. Table 3 shows the substances included in the correlation procedure and the number of data points (N) for each substance, with more than 840 data points. A unique and general equation for all these substances was developed to correlate the diffusion coefficient of fatty acids and fatty acid esters (FA) in CO_2 $\left(D_{FA\text{-}CO_2}\right)$ as a function of temperature and pressure. As in the case of volatile oil compounds, CO_2 density $\left(\rho_{CO_2}\right)$ and viscosity $\left(\mu_{CO_2}\right)$ were considered independent variables. Eq. (4.3) resulted from the regression procedure:

$$D_{FA\text{-}CO_2} = 2.3239x10^{-4} + 3.9332x10^{-3}\mu - 5.6372x10^{-4}\rho + 1.20x10^{-6}T - 2.71x10^{-7}P \quad (4.3)$$

where, D_{FA-CO_2} is given in cm^2 s^{-1}, μ is given in cP, ρ in g cm^{-3}, T in °C and P in bar.

The AARD% (see Table 3) was lower than 11% for all compounds considered, being the mean value 6.6%.

4.3. Diffusion coefficient of fixed oils

The correlation is based on experimental data comprising the diffusion coefficients of 4 triglycerides as reported in Table 4, with a total of 178 data points. It should be noticed that the experimental data includes high molecular triglycerides (fatty acid chains of C21 and C24) because data related with the most common triglycerides present in vegetal materials (mainly C16 and C18 fatty acid chains) is scarce. As in previous cases, a unique equation to predict the diffusion coefficient of fixed oils (FO) of plants and herbs

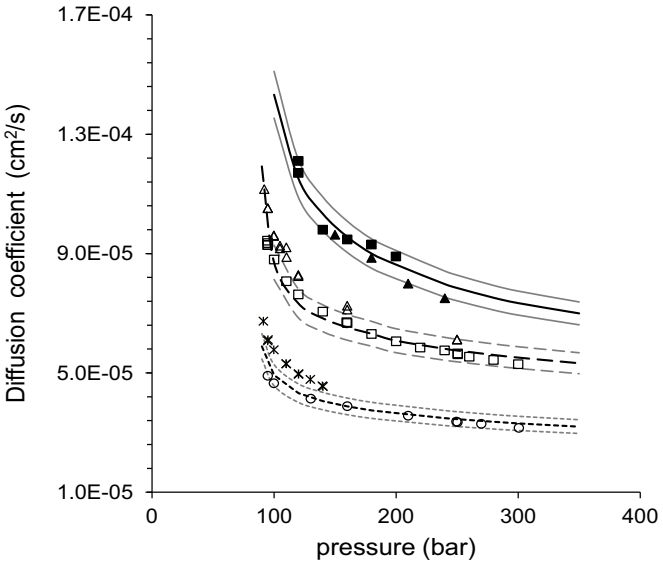

Fig. 1. Comparison between the correlations developed in this work for the diffusion coefficient of volatile oils (solid line), fatty acids (dashed line) and fixed oils (dotted line) in $SCCO_2$ and experimental values from the literature: (■) α-pinene; (▲) carvone; (□) oleic acid; (△) myristoleic acid; (*) triolein; (○) trierucin. Gray lines represent AARD of the corresponding correlations (5.48%, 6.60% and 7.20% for VO, FA and FO, respectively).

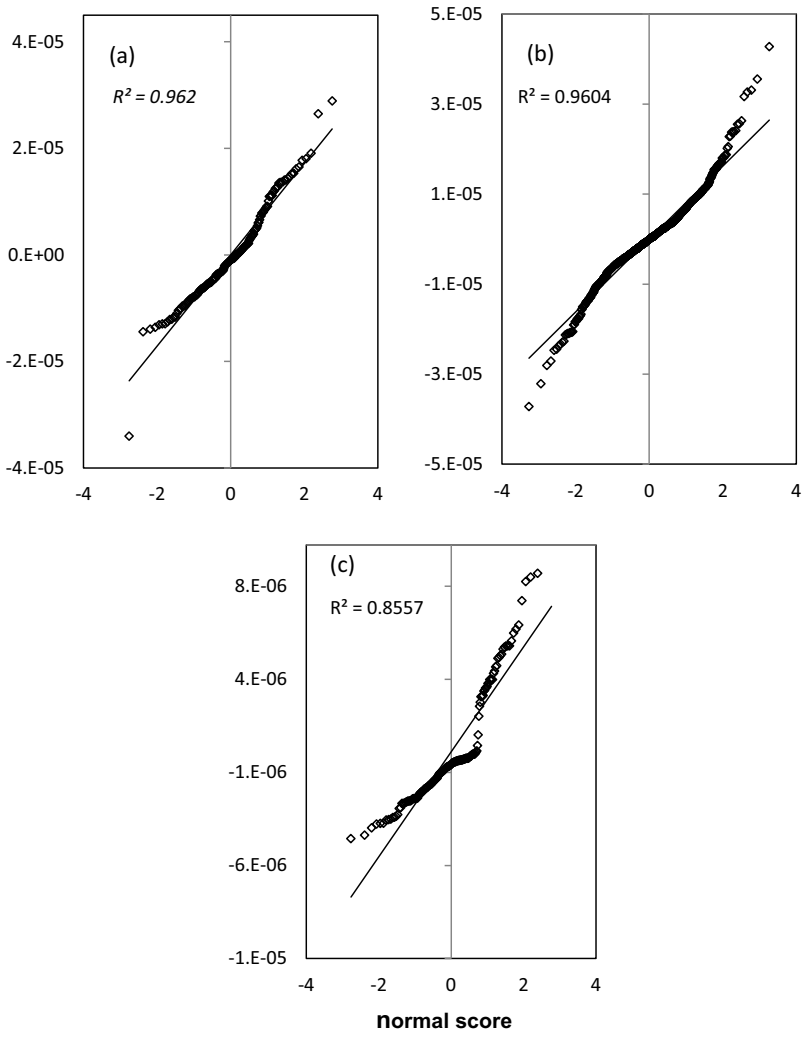

Fig. 2. Normal probability plot for (a) VO (Eq. (4.1)), (b) FA (Eq. (4.3)) and (c) fixed oils (Eq. (4.4)) diffusion coefficient residuals obtained in the correlations developed in this work.

in CO_2 $\left(D_{FO\text{-}CO_2}\right)$ as function of temperature and pressure was developed:

$$D_{FO-CO_2} = 8.5244x10^{-5} + 1.4097x10^{-4}\mu - 8.0482x10^{-5}\rho + 1.9613x10^{-7}T \quad (4.4)$$

where, D_{VO-CO_2} is given in $cm^2\ s^{-1}$, μ is given in cP, ρ in $g\ cm^{-3}$ and T in °C.

As reported in Table 4, the AARD% was lower than 13% for all compounds considered, being the mean AARD value of 7.2%.

4.4. Validation of the proposed correlations

Fig. 1 shows the variation at 40 °C of D_{VO-CO_2}, D_{FA-CO_2} and D_{FO-CO_2} with pressure as predicted, respectively, by Eqs. (4.1), (4.3) and (4.4). The figure also depicts the experimental diffusion coefficients of some VO (α-pinene and carvone), FA (oleic and myristoleic acids) and FO (triolein and trierucin). As expected, the equations developed in this work provide a distinct diffusion coefficient function for VO, FA and FO, and the experimental values follow the same tendency. In this respect, Fig. 1 is supporting the hypothesis that diffusion coefficient of chemically similar solute-type substances is predominantly determined by temperature, pressure, and the corresponding physicochemical properties

Table 5
Statistical details for each regression model.

Constant	Independent variable	Volatile oils	Fatty acids	Fixed oils
β_0		3.5400×10^{-4}	2.3239×10^{-4}	8.5244×10^{-5}
β_1	μ (cP)	1.1129×10^{-3}	3.9332×10^{-3}	1.4097×10^{-4}
β_2	ρ (g·cm^{-3})	-4.3036×10^{-4}	-5.6372×10^{-7}	-8.0482×10^{-5}
β_3	T (°C)	1.64×10^{-7}	1.20×10^{-6}	1.9613×10^{-7}
β_4	P (bar)	–	-2.71×10^{-7}	–
Mean value		1.08×10^{-4}	8.95×10^{-5}	4.29×10^{-5}
Standard deviation		8.73×10^{-6}	8.53×10^{-6}	2.74×10^{-6}
R^2		0.9187	0.9555	0.8192

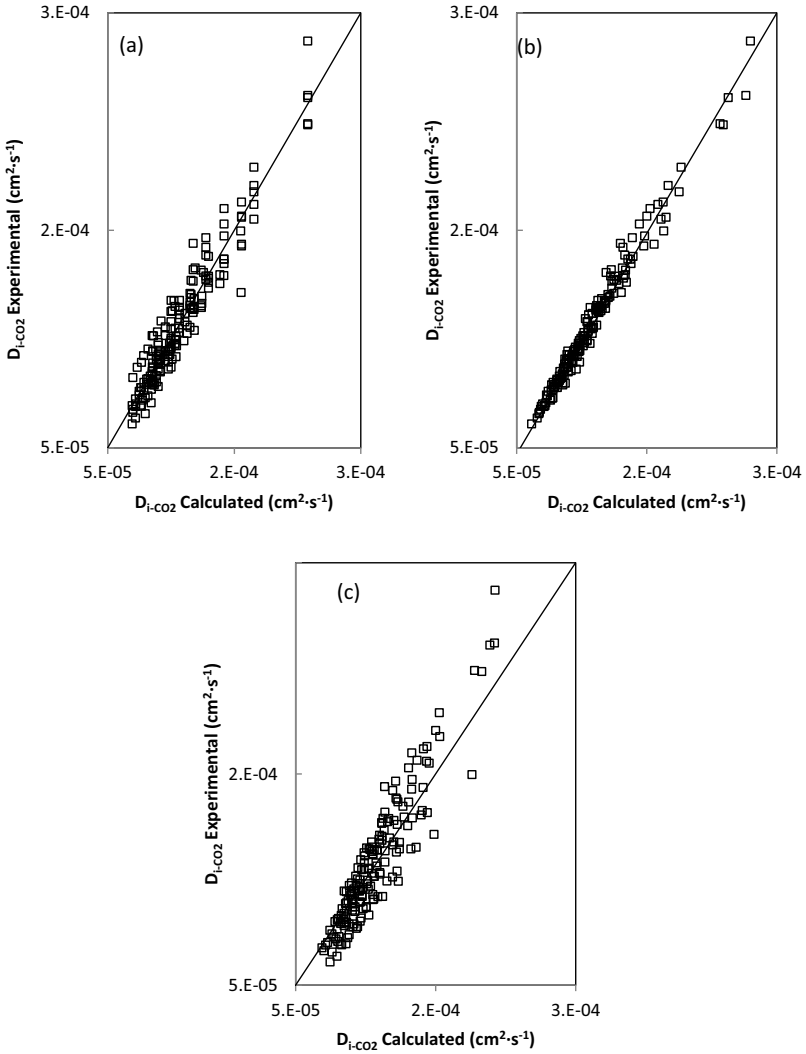

Fig. 3. Calculated vs. experimental diffusion coefficient of volatile oil compounds according to: (a) correlation proposed in this work (Eq. (4.1)); (b) Magalhães et al. model (Eq. (2.1)) [5] and (c) modified Wilke–Chang equation [20].

of the supercritical solvent (density and viscosity) which in turn, depend on temperature and pressure.

Regarding the accuracy of the correlations developed, Fig. 2 shows the normal probability plots of the residuals from the model fit (i.e., $D_{VO\text{-}CO_2}$, $D_{FA\text{-}CO_2}$ and $D_{FO\text{-}CO_2}$ correlations). As can be observed in the figure there is a linear trend in all cases (R^2 value of 0.9620 for VO, 0.9604 for FA and 0.8557 for FO) indicating that the residuals are approximately normally distributed. Additionally, the residual mean values are, respectively, 1.50×10^{-13}, 3.86×10^{-13} and 6.87×10^{-13} (i.e., very close to zero).

Table 5 gives the regression statistics of each diffusion models based on the independents variables considered in terms of the corresponding p-values. In all cases, the p-value corresponding to density resulted very low, indicating a decisive effect of $SCCO_2$ density in the regression procedure. The term related with temperature was also significant in all cases ($p < 0.10$). However, the term related with pressure was neglected for VO and FO (p values of 0.2857 and 0.6701, respectively) but was significant for FA ($p < 0.10$). In this respect, it can be observed that, in comparison with the VO or FO data, the FA data set include experimental points with pressures closer to the critical pressure of carbon dioxide, and the pressure effect in the range of pressures close to the critical point is in general more significant.

Additionally, as can be observed in Table 5, the standard error of the VO, FA and FO diffusion coefficient models were, respectively, 8.73×10^{-6}, 8.53×10^{-6} and 2.74×10^{-6}, which are satisfactory considering the diffusion coefficient mean value.

With respect to the correlation parameters (β_i) it can be observed that β_0 decreases when the molecular weight of the solutes increase, indicating lower diffusion coefficients for higher molecular size, according to theoretical considerations. Furthermore, negative β_2 represent that an increase in density produce a decrease in the diffusion coefficient, also in agreement with fundamentals. Nevertheless, and except for β_0, the rest of correlation parameters do not present a direct relation with the molecular size of the solutes studied.

4.5. Comparison of equations derived with diffusion coefficient models

Two diffusion coefficient models were selected for comparison: the predictive hydrodynamic expression of Wilke–Chang modified by Vaz et al. [20] and Eq. (2.1) proposed by Magalhães et al. [5].

The hydrodynamic equation of Wilke–Chang [8] was modified by Vaz et al. [20] improving its predictive capability at supercritical conditions. The dependence of the original model on the molar volumes at normal boiling point of both solute and solvent ($V_{bp,i}$) was

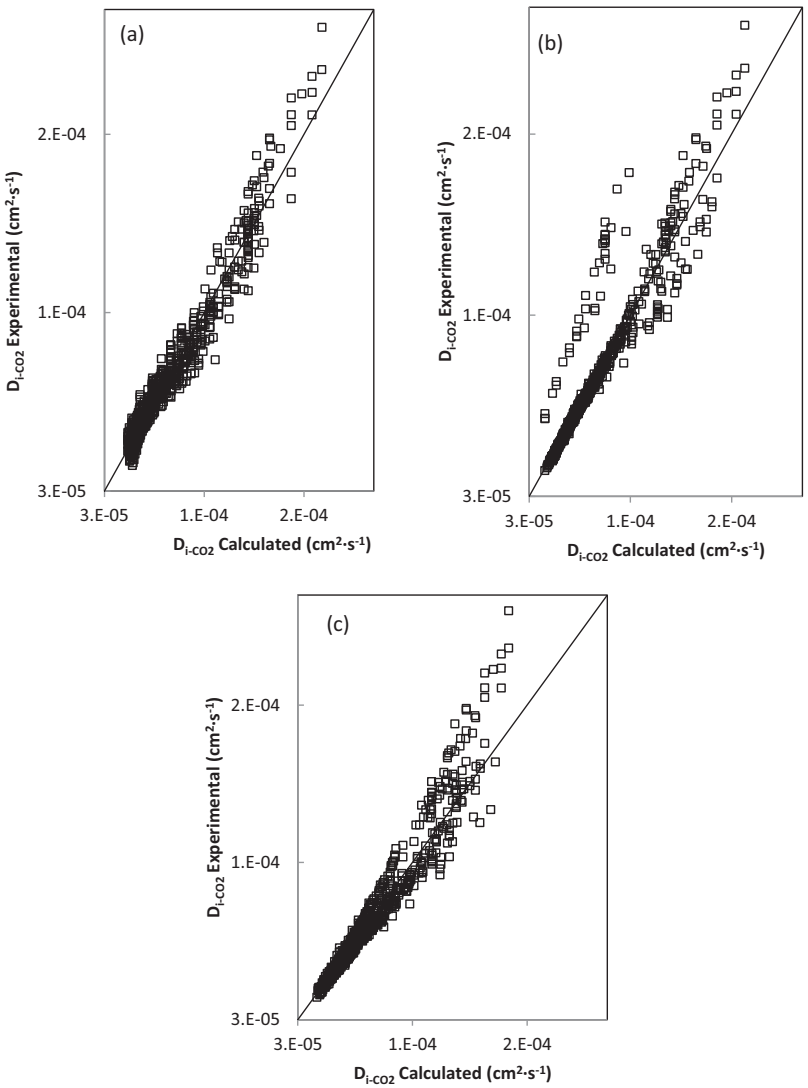

Fig. 4. Calculated vs. experimental diffusion coefficient of fatty acids according to: (a) correlation proposed in this work (Eq. (4.3)); (b) Magalhães et al. model (Eq. (2.1)) [5] and (c) modified Wilke–Chang equation [20].

replaced by analogous dependencies upon critical molar volumes ($V_{c,i}$). The modified Wilke–Chang (mWC) model contains three universal constants (A, α and β) and one pure-solute parameter ($V_{c,2}$) [20]. The mathematical expression is given in Table 1.

As mentioned previously, the Magalhães et al. [5] equation used for comparison was regressed on the basis of a large set of experimental diffusion coefficients data, and demand two specific regression parameters for each pure solute.

A detailed comparison of the three models is given in Table 2 (volatile oils), 3 (fatty acids and esters) and 4 (fixed oils), where the AARD% values obtained for each pure component and each model are indicated.

The results obtained in the case of volatile oil compounds are given in Table 2 and the mean AARD value resulted with Eq. (4.1) is 5.48. The method proposed by Magalhães et al. [5] resulted in lower AARD% values (mean value 2.84%) but it has to be taken into account that in this correlation two parameters for each pure compound are necessary while no pure-compound parameters were used in Eq. (4.1). Furthermore, in the case of the modified Wilke–Chang equation (one pure component parameter, $V_{c,2}$) some of the resulted AARD% values were higher than those obtained by the correlation developed in this work, being the mean value 9.52%.

Tables 3 and 4 permit, respectively, the comparison of AARD values in the case of fatty acids and fixed oils. Conclusions similar to those attained for volatile oil compounds can be derived from the AARD% values obtained, i.e., the method proposed by Magalhães et al. [5] provides a more accurate correlation of the data using two pure component parameters for each solute, and the modified Wilke–Chang equation provides similar or even worse results than the correlations presented in this work, in which no pure component parameters were utilized.

A general picture of the accuracy obtained with each of the models employed can be observed in Fig. 3 (volatile oil compounds), Fig. 4 (fatty acids) and Fig. 5 (fixed oils) where is represented the calculated diffusion coefficients vs. the experimental values. As can be observed from the figures, good correlation can be obtained considering an equation depending explicitly on temperature, pressure, solvent density and viscosity. Thus, the equations proposed in this work are good tools to estimate the diffusion coefficient of solute-type extracts, i.e., volatile oils, fatty acid and fatty acid ester mixtures and fixed oils, regardless of information about the exact composition of the extract.

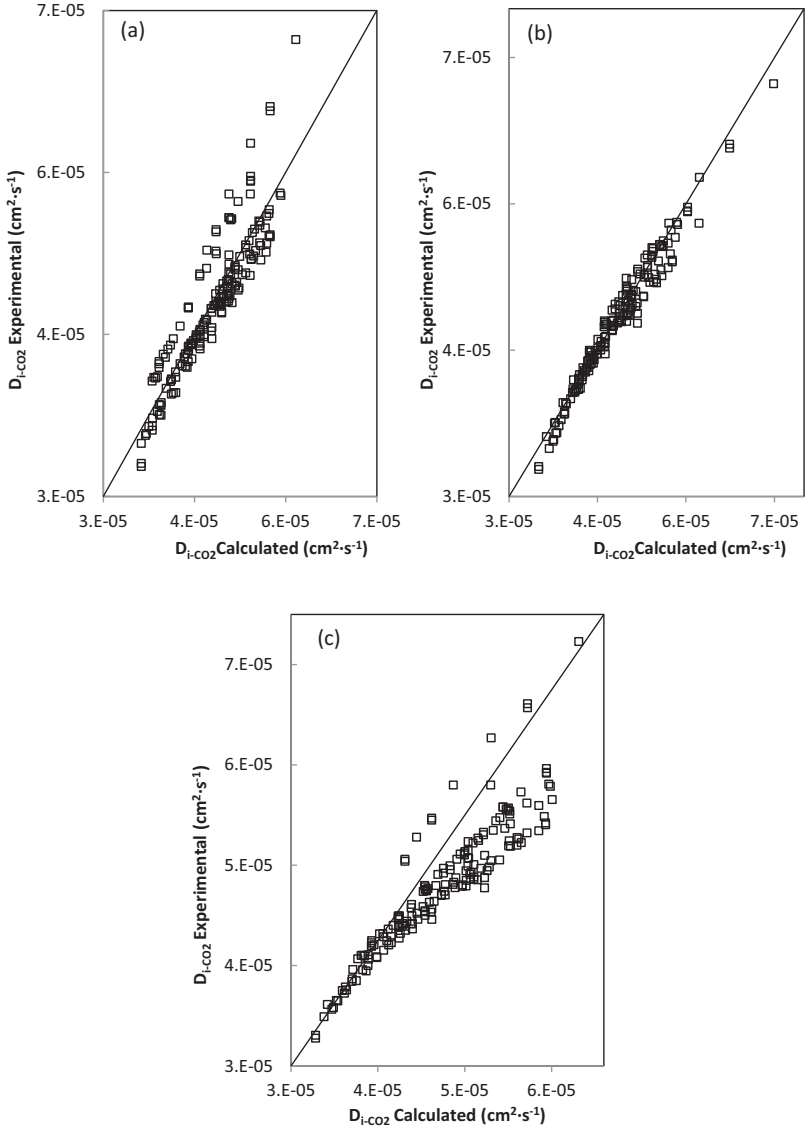

Fig. 5. Calculated vs. experimental diffusion coefficient of fixed oils according to: (a) correlation proposed in this work (Eq. (4.4)); (b) Magalhães et al. model (Eq. (2.1)) [5] and (c) modified Wilke–Chang equation [20].

5. Conclusions

The dominant effect of pressure and temperature and in turn, solvent density and viscosity, on solute diffusivity, permitted to postulate a parameter-less relationship to estimate the diffusion coefficient of a $SCCO_2$ type-extract which is mainly comprised by solutes with similar physicochemical properties.

Three correlations were derived in this work, one for each type-extract analyzed (i.e., volatile oils, fatty acid mixtures or triglycerides) proving good correlative capability in comparison with other models from the literature which demand pure component parameters. Since these equations demand only temperature and pressure to estimate the diffusion coefficient of a solute-type supercritical extract, they can be straightforwardly implemented in computer-aided tools and may contribute to the mass transfer simulation of plant SFE processes.

Acknowledgments

López-Padilla A thanks to COLCIENCIAS (568–2012) and Medellin Mayor's Office (Sapiencia/Enlaza Mundos Program, 2013) for the Ph.D. fellowship. This work was financed thanks ALIBIRD, S2013/ABI-2728 (Comunidad de Madrid) project.

References

[1] I. Medina, Determination of diffusion coefficients for supercritical fluids, J. Chromatogr. A 1250 (2012) 124–140.
[2] K.K. Liong, P.A. Wells, N.R. Foster, Diffusion in supercritical fluids, J. Supercrit. Fluids 4 (1991) 91–108.
[3] C.R. Wilke, P. Chang, Correlation of diffusion coefficients in dilute solutions, AIChE J. 1 (1995) 264–270.
[4] A.L. Magalhães, R.V. Vaz, R.M.G. Gonçalves, F.A. Da Silva, C.M. Silva, Accurate hydrodynamic models for the prediction of tracerdiffusivities in supercritical carbon dioxide, J. Supercrit. Fluids 83 (2013) 15–27.
[5] A.L. Magalhães, P.F. Lito, F.A. Da Silva, C.M. Silva, Simple and accurate correlations for diffusion coefficients of solutes in liquids and supercritical fluids over wide ranges of temperature and density, J. Supercrit. Fluids 76 (2013) 94–114.
[6] C.A. Filho, C.M. Silva, M.B. Quadri, E.A.E.A. Macedo, Tracer diffusion coefficients of citral and d-limonene in supercritical carbon dioxide, Fluid Phase Equilibria 204 (2003) 65–73.
[7] O. Suárez-Iglesias, I. Medina, C. Pizarro, J.L. Bueno, Limiting diffusion coefficients of ethyl benzoate, benzylacetone, and eugenol in carbon dioxide at supercritical conditions, J. Chem. Eng. Data 53 (2008) 779–784.

[8] C.M. Silva, C.A. Filho, M.B. Quadri, E.A. Macedo, Binary diffusion coefficients of α-pinene and β-pinene in supercritical carbon dioxide, J. Supercrit. Fluids 32 (2004) 167–175.
[9] T. Funazukuri, C. Kong, T. Kikuchi, S. Kagei, Measurements of binary diffusion coefficient and partition ratio at infinite dilution for linoleic acid and arachidonic acid in supercritical carbon dioxide, J. Chem. Eng. Data 48 (2003) 684–688.
[10] T. Funazukuri, C.Y. Kong, S. Kagei, Effects of molecular weight and degree of unsaturation on binary diffusion coefficients for lipids in supercritical carbon dioxide, Fluid Phase Equilibria 219 (2004) 67–73.
[11] T. Funazukuri, C.Y. Kong, S. Kagei, Binary diffusion coefficient, partition ratio, and partial molar volume for docosahexaenoic acid, eicosapentaenoic acid and α-linolenic acid at infinite dilution in supercritical carbon dioxide, Fluid Phase Equilibria 206 (2003) 163–178.
[12] C.Y. Kong, N.R.W. Withanage, T. Funazukuri, S. Kagei, Binary diffusion coefficients and retention factors for long-chain triglycerides in supercritical carbon dioxide by the chromatographic impulse response method, J. Chem. Eng. Data 50 (2005) 1635–1640.
[13] J.O. Rawlings, S.G. Pantula, D.A. Dickey, Applied Regression Analysis: A Research Tool, 2nd ed., Springer-Verlag, New York, 1998, pp. 658.
[14] A. Giacomino, O. Abollino, M. Malandrino, E. Mentasti, The role of chemometrics in single and sequential extraction assays: a review. Part II. Cluster analysis, multiple linear regression, mixture resolution, experimental design and other techniques, Anal. Chim. Acta 688 (2011) 122–139.
[15] S. Uhlig, M.M. Jestoi, A. Kristin Knutsen, B.T. Heier, Multiple regression analysis as a tool for the identification of relations between semi-quantitative LC-MS data and cytotoxicity of extracts of the fungus *Fusarium avenaceum* (syn. *F. arthrosporioides*), Toxicon 48 (2006) 567–579.
[16] N. Fumo, M.A. Rafe Biswas, Regression analysis for prediction of residential energy consumption, Renew. Sustain. Energy Rev. 47 (2015) 332–343.
[17] R. Span, W. Wagner, A new equation of state for carbon dioxide covering the fluid region from the triple-point temperature to 1100 K at pressures up to 800 MPa, J. Phys. Chem. Ref. Data 25 (1999) 1509–1596.
[18] NIST, Thermophysical properties of fluid systems, 21 may 2015. Available from: ⟨http://webbook.nist.gov/chemistry/fluid/⟩.
[19] A. Fenghour, W.A. Wakeham, V. Vesovic, The viscosity of carbon dioxide, J. Phys. Chem. Ref. Data 27 (1998) 31–44.
[20] R.V. Vaz, A.L. Magalhães, C.M. Silva, Improved hydrodynamic equations for the accurate prediction of diffusivities in supercritical carbon dioxide, Fluid Phase Equilibria 360 (2013) 401–415.
[21] E.G. Scheibel, Correspondence. Liquid Diffusivities. Viscosity of Gases, Ind. Eng. Chem. 46 (1954) 2007–2008.
[22] K.A. Reddy, L.K. Doraiswamy, Estimating Liquid Diffusivity, Ind. Eng. Chem. Fundam. 6 (1967) 77–79.
[23] M.A. Lusis, C.A. Ratcliff, Diffusion in binary liquid mixtures at infinite dilution, Can. J. Chem. Eng. 46 (1968) 385–387.
[24] C.C. Lai, C.S. Tan, Measurement of molecular diffusion coefficients in supercritical carbon dioxide using a coated capillary column, Ind. Eng. Chem. Res. 34 (1995) 674–680.
[25] L.M. González, J.L. Bueno, I. Medina, Determination of binary diffusion coefficients of anisole 2,4-dimethylphenol, and nitrobenzene in supercritical carbon dioxide, Ind. Eng. Chem. Res. 40 (2001) 3711–3716.
[26] X. Dong, B. Su, H. Xing, Y. Yang, Q. Ren, Diffusion coefficients of l-menthone and l-carvone in mixtures of carbon dioxide and ethanol, J. Supercrit. Fluids 55 (2010) 86–95.
[27] X. Dong, B. Su, H. Xing, Z. Bao, Y. Yang, Q. Ren, Cosolvent effects on the diffusions of 1 3-dichlorobenzene, l-carvone, geraniol and 3-fluorophenol in supercritical carbon dioxide, J. Supercrit. Fluids 58 (2011) 216–225.
[28] C.A. Filho, C.M. Silva, M.B. Quadri, E.A. Macedo, Infinite dilution diffusion coefficients of linalool and benzene in supercritical carbon dioxide, J. Chem. Eng. Data 47 (2002) 1351–1354.
[29] C. Pizarro, O. Suárez-Iglesias, I. Medina, J.L. Bueno, Binary diffusion coefficients for 2 3-dimethylaniline, 2,6-dimethylaniline, 2-methylanisole, 4-methylanisole and 3-nitrotoluene in supercritical carbon dioxide, J. Supercrit. Fluids 48 (2009) 1–8.
[30] Y.S. Han, Y.W. Yang, P.D. Wu, Binary diffusion coefficients of arachidonic acid ethyl ester, cis-5,8,11,14,17-eicosapentaenoic acid ethyl ester, and cis-4,7,10,13,16,19-docosahexanenoic acid ethyl ester in supercritical carbon dioxide, J, Chem. Eng. Data 52 (2007) 555–559.
[31] C.Y. Kong, N.R.W. Withanage, T. Funazukuri, S. Kagei, Binary diffusion coefficients and retention factors for γ-linolenic acid and its methyl and ethyl esters in supercritical carbon dioxide, J. Supercrit. Fluids 37 (2006) 63–71.
[32] C.Y. Kong, M. Mori, T. Funazukuri, K.K. Seiichiro, Measurements of binary diffusion coefficients, retention factors and partial molar volumes for myristoleic acid and its methyl ester in supercritical carbon dioxide, Anal. Sci. 22 (2006) 1431–1436.

3.5 Supercritical extraction of solid materials: a practical correlation related with process scaling

Alexis López-Padilla, Alejandro Ruiz-Rodríguez,
Guillermo Reglero & Tiziana Fornari

Enviado al Journal of Food Engineering, enviado Junio de 2017

Fecha: 15/06/17 [13:09:47 CEST]
De: Alejandro Ruiz <alejandro.ruiz@uam.es>
Para: guillermo.reglero@uam.es, Tiziana Fornari <tiziana.fornari@uam.es>, alexis.lopez@predoc.uam.es
Cc: Alejandro Ruiz <alejandro.ruiz@uam.es>
Asunto: RV: Submission Confirmation

Paper submitted...

-----Mensaje original-----
De: eesserver@eesmail.elsevier.com [mailto:eesserver@eesmail.elsevier.com]
Enviado el: jueves, 15 de junio de 2017 13:09
Para: alejandro.ruiz@uam.es
Asunto: Submission Confirmation

Dear Alejandro,

Your submission entitled "Supercritical extraction of solid materials: a practical correlation related with process scaling" has been received by Journal of Food Engineering

You may check on the progress of your paper by logging on to the Elsevier Editorial System as an author. The URL is https://ees.elsevier.com/jfoodeng/.

Your username is: alejandro.ruiz@uam.es
If you need to retrieve password details, please go to:
http://ees.elsevier.com/jfoodeng/automail_query.asp

Your manuscript will be given a reference number once an Editor has been assigned.

Thank you for submitting your work to this journal.

Kind regards,

Elsevier Editorial System
Journal of Food Engineering

For further assistance, please visit our customer support site at http://help.elsevier.com/app/answers/list/p/7923. Here you can search for solutions on a range of topics, find answers to frequently asked questions and learn more about EES via interactive tutorials. You will also find our 24/7 support contact details should you need any further assistance from one of our customer support representatives.

Supercritical extraction of solid materials: a practical correlation related with process scaling

Alexis López-Padilla, Alejandro Ruiz-Rodriguez*, Guillermo Reglero and Tiziana Fornari

Institute of Food Science Research CIAL (CSIC-UAM) – CEI UAM + CSIC,

Madrid, 28049, Spain

* Correspondence: alejandro.ruiz@uam.es; Tel.: +34 -910-017-923

Abstract

The supercritical fluid extraction (SFE) of vegetal raw materials is a large field of research, innovation and entrepreneurial developments. Optimization of process conditions is usually accomplished in analytical or laboratory scale equipment. Although SFE scaling is essential to attain industrial applications, studies in the literature are scarce. In this work, the kinetic behavior of 19 overall extraction curves (OEC's), obtained by the authors in previous works using NOVALINDUS Platform SFE facilities, and a set of 34 OEC's published by other authors, were considered all together to study SFE scaling. A general trend between the solvent flow rate and Barton kinetic constant was obtained for all extraction curves included in the data base, which comprise 10 different plant materials, temperatures in the range 298-333 K, pressures of 10-30 MPa, extractor volumes from 50 to 5200 cm^3, particle diameters from 250 to 1400 µm and bed porosity in the range 0.59-0.97.

Keywords: *Supercritical fluid extraction; Overall extraction curve; Mass transfer; Barton model; Scaling up.*

1. Introduction

The kinetic behavior of the Supercritical Fluid Extraction (SFE) of solid materials is usually represented by the plot of the mass extracted as a function of time or as a function of the mass of spent solvent. This representation is commonly called the Overall Extraction Curve (OEC). Not only mass yield varies along extraction time, but also composition, physicochemical and biological properties of the extract (García-Risco et al., 2011a; Zabot et al., 2014a). SFE scaling aims to reproduce the same kinetic behavior in extraction vessels with different shape and/or capacity.

A large number of kinetic models can be found in the literature, which were developed to represent the OEC of SFE processes, including simple correlations based on first order kinetics, such as the Barton model (Barton et al., 1992; Cháfer and Berna, 2014; Silva et al., 2011, 2008), to comprehensive phenomenological models based on mass transfer differential occurring in the cell extraction (De Melo et al., 2014; Huang et al., 2012; Oliveira et al., 2011). Yet, more limited approaches and studies are available in the literature regarding SFE scaling. Studies are mainly based on some thumb rules or semi-empirical approaches based on traditional chemical engineering fundamentals and adapted for high pressure SFE process. For example, keeping constant the ratio between solvent flow rate and biomass weight, or keeping constant the ratio between the mass weight of solvent spent and of biomass weight (Prado et al., 2012, 2011; Yesil-Celiktas et al., 2009), or maintaining constant the solvent linear velocity, or the solvent residence time, among others, are very common scaling criterions applied in SFE (López-Padilla et al., 2016b).

SFE vessels are in general cylindrical. Vessel length and internal diameter are usually used to describe bed geometry, which also affects significantly the extraction. Furthermore, the ratio

between height and diameter of the packed bed has been used to validate some scaling approaches (Prado et al., 2012).

For example, Carvalho et al. (2005) and Zabot et al. (2014a, 2014b) found good scaling results in the SFE of rosemary and clove buds by applying the solvent to feed mass ratio criterion combined with maintaining the height/diameter ratio. Paula et al. (2016) evaluated the effect of bed geometry using the criterions of constant residence time or constant CO_2 velocity in the scaling up SFE process for *Baccharis dracunculifolia* and found that the second one was appropriate. Recently, López-Padilla et al. (2017) studied the SFE scaling of *Calendula officinalis* and the experiments proved that constant CO_2 residence time was an adequate scaling criterion for a scaling factor around 5, while the constant CO_2 velocity was the criterion suitable for a larger scaling factor close to 20.

Thus, in general, there is not a single criterion effective for SFE scaling and more studies are required to get more information about the influence of the large set of variables that can affect the extraction kinetics. In this respect, López-Padilla et al. (2017) have recently correlated the mass transfer coefficients (Broken and Intact Cell model) of calendula OECs obtained in cells of diverse size, at different extraction pressures and temperatures, in terms of the CO_2 flow rate, the extraction cell geometric parameters (diameter and length) and the dimensionless Schmidt number. The correlation was derived by keeping constant bed porosity and mean particle size of calendula raw material.

In this work, this correlation was extended to consider a variety of plant raw materials of different apparent density, porosity and particle size. First, a set of 19 OECs obtained by the authors in previous works using their SFE facilities (NOVALINDUS Platform) were considered, and then the correlation developed was tested using a set of 34 OECs reported by other authors in the literature.

2. Fundamentals and data base

In the SFE of solid raw materials, the mass extracted and thus the extraction yield (mass extracted / mass loaded in the extraction vessel) increases with time, defining the typical shape of the overall extraction curve (OEC) (see Figure 1). The rate of solutes mass transfer from the surface of the solid particles to the core of the supercritical solvent depends significantly on the mass transfer coefficient and the interfacial area. The objective of this work is to investigate the relation between these process variables and the solvent flow rate, considering a large set of OEC data, related with the SFE of different plant materials, and taking into account the variability of process conditions (temperature and pressure), extraction cell dimensions (diameter and height) and packed bed characteristics (apparent density, porosity).

The mass transfer coefficient of a specific OEC can be estimated using a variety of kinetic models. Although accurate and theoretical-based models are available in the literature, these models usually demand several fitting parameters besides the mass transfer coefficient, and require specific software and mathematical routines for the fitting procedure. On the other side, Barton et al. (1992) presented a single model to express the mass rate out of a solid matrix, by describing the solutes extraction as a first-order-type reaction. Because of its simplicity, Barton model was used in this work to estimate the mass transfer coefficient of all OEC data compiled from the literature, as described in the following section.

2.1 Barton model

The overall extraction curve (OEC) according to Barton model can be described as a first-order-type reaction:

$$Y = Y_\infty[1 - \exp(-kt)] \quad (1)$$

Where Y is the extraction yield (mass extracted / mass loaded in the extraction vessel), Y_∞ is the extraction yield when $t \to \infty$ and k is Barton kinetic constant. The accumulated mass of extract versus time (Y vs. t) of a OEC can be represented using Eq. (1) by the $\ln(1 - Y/Y_\infty)$ vs. t linear regression, and considering the simultaneous fitting of parameters k and Y_∞ to minimize the corresponding regression coefficient (R^2).

Barton kinetic constant (k) can be related to the fluid-phase mass transfer coefficient (k_f) by means of the specific interfacial area (a_0):

$$k_f = k \,/\, a_0 \quad (2)$$

Where:

$$a_0 = 6(1 - \varepsilon)/d_p \quad (3)$$

Being ε the porosity of the packed bed and d_p the mean diameter of the spherical solid particles.

2.2 Kinetic data compiled

2.2.1 OECs from NOVALINDUS Platform

NOVALINDUS is a technological platform comprising SFE facilities of diverse capacities which were used by the authors in previous works (Fornari et al., 2012; García-Risco et al., 2011b; López-Padilla et al., 2016b; Villanueva-Bermejo et al., 2017) to extract a variety of vegetal materials. Table 1 reports the characteristics of the facilities and extractor vessels available in NOVALINDUS Platform.

The extraction conditions of different SFE experiments are given in Table 2 and comprise 19 OECs concerning the extraction of seven different plants: oregano, sage, thyme, rosemary,

yarrow, calendula and mortiño. For each OEC, Table 2 reports the diameter (D) and length (L) of the corresponding cylindrical extraction vessel, the characteristics of the packed bed (type of plant, mass loaded F, particle diameter d_p, plant density ρ_B and bed porosity ε) and the SFE extraction conditions (temperature T, pressure P and CO_2 flow rate Q).

CO_2 density ρ_{CO_2} and viscosity μ_{CO_2} were calculated using an equation of state proposed by Span and Wagner (Tegeler et al., 1999) and involved in an open web source by NIST Webbook (NIST, 2017). This equation resulted from an empirical representation of the fundamental equation based on Helmholtz energy in dependence on density and temperature. This equation shows lower relative deviations between experimental and predicted values $\pm 0.2\ \%$ under supercritical pressures and temperatures extraction processes. CO_2 viscosity μ_{CO_2} was calculated using a correlation of $D_{E_{CO2}}$ as a function of temperature and pressure (Fenghour et al., 1998) specifically derived for carbon dioxide and linked by the NIST Webbook. The diffusion coefficient of the extract in CO_2 (D_{E-CO2}) was estimated using the equation recently given by López-Padilla et al. (2016a) for plant essential oils in supercritical CO_2:

$$D_{E-CO2} = 3.5400x10^{-4} + 1.1129x10^{-3}\mu - 4.3036x10^{-4}\rho + 1.64x10^{-7}T \qquad (4)$$

Where D_{E-CO2} is given in $cm^2 \cdot s^{-1}$, μ is given in cP, ρ in $g \cdot cm^{-3}$ and T in °C.

The Schmidt dimensionless number was also calculated according to:

$$S_c = \frac{\mu_{CO2}}{\rho_{CO2}\, D_{E-CO2}} \qquad (5)$$

The values obtained are given in Table 2.

2.2.2 OECs from the literature

Similarly to Table 2, Table 3 gives the data corresponding to 34 OECs reported by different authors concerning the SFE of red pepper (Silva and Martínez, 2014), chamomile (Povh et al.,

2001) and ginger (Martinez et al., 2003; Zancan et al., 2002). CO_2 density (ρ_{CO2}) and viscosity (μ_{CO2}), the diffusion coefficient (D_{E-CO2}) and Schmidt number (S_c) were calculated as described in previous section. Bed porosity (ε) is according the value reported in the corresponding literature source, but the value was checked to satisfy the following equation:

$$\varepsilon = 1 - \frac{\rho_{app}}{\rho_B} = 1 - \frac{4F}{\pi D^2 L \rho_B} \quad (5)$$

Where ρ_{app} is the apparent density of the packed bed.

3. Results and Discussion

3.1 Correlation of Barton kinetic constants of calendula OECs obtained in NOVALINDUS Platform

In previous work, the scaling of calendula SFE was studied (López-padilla et al., 2017). Nine OECs were obtained using the extraction cells of different size available in NOVALINDUS Platform (Table 1) and were represented using the Broken and Intact Cell (BIC) model (Sovová, 2017; Sovová, 1994) . With the purpose of developing a scaling correlation applicable among NOVALINDUS facilities, the regressed BIC mass transfer coefficients in the supercritical fluid phase (k_{YA}) were correlated with the CO_2 flow rate (Q). The scaling correlation (see Figure 2) includes the extractor diameter and length, and the dimensionless Schmidt number (S_c). Bed porosity and particle size were not included in the correlation because these parameters were kept constant during calendula SFE.

In this work, the same nine calendula OECs of previous work (López-padilla et al., 2017) were represented using Barton model (Eq. 1), and the type of relation depicted in Figure 2 was tested using Barton kinetic constant (k) instead of BIC mass transfer coefficient (k_{YA}).

Tables 4 gives the values obtained for k, together with the Y_∞ value which minimize the regression coefficient (R^2), which is also given in the table. In general, Barton k values were one order of magnitude lower than BIC k_{YA} values (López-padilla et al., 2017). As sake of comparison, Figure 3 show BIC and Barton model representations for two selected calendula OECs. Figure 3(a) correspond to OEC 11 in Table 2, for which BIC model resulted better than Barton model, while the opposite resulted in the case of Figure 3(b) corresponding to OEC 17 in Table 2 (worse R^2 value of Barton model fitting).

Figure 4 shows the same relation depicted in Figure 2 using the regressed Barton k values. It can be clearly stated from the figure that the correlation reported in previous work (Figure 2) is still valid and effective in the case of using Barton kinetic constants instead of BIC mass transfer coefficients. The regression coefficient obtained in Figure 4 is $R^2 = 0.9906$, slightly higher than the one obtained in Figure 2 $(R^2 = 0.9767)$.

3.2 Extension of the correlation to other OECs obtained in NOVALINDUS Platform

As mentioned in previous section, the correlation presented in Figures 2 and 4 do not include bed porosity or mean particle diameter of plant material, because all calendula OECs were carried out keeping constant these two variables.

With the objective of analyze the influence of ε and d_p in the SFE scaling correlation, the 19 OECs obtained in the three different scale supercritical plants available in NOVALINDUS Platform (Table 2) were considered all together. These OECs include extractions with bed porosity in the range of 0.59-0.82 and particle diameter in the range of 250-1000 µm.

198 It was observed that the inclusion of the specific interfacial area (a_0) resulted in a good
199 correlation of all OEC Barton k values regressed (which are reported in Table 3) with $R^2 =$
200 0.9647. Then, CO_2 density was also included with the aim of attain a dimensionless relation
201 between the abscissa and ordinate of the correlation. Figure 5 shows the final result, with a
202 regression coefficient $R^2 = 0.9624$, very similar to the previous one. Then, the correlation
203 depicted in Figure 5 provides a fundamental relation between the main variables affecting
204 the kinetic behavior of the SFE extractions carried out in NOVALINDUS Platform (Table 2)
205 and can be a useful tool for SFE scaling.

206 **3.3 Applying the scaling correlation to OECs from the literature**

207 The correlation developed considering the OEC data produced by the authors in
208 NOVALINDUS Platform was tested using the OEC data from the literature given in Table 3. A
209 total of 34 OECS were compiled. Although a larger number was originally considered, many
210 were discarded due to the lack of information, mainly bed porosity, extraction cell
211 dimensions, plant material density, or the kinetic data was insufficient and/or do not allow
212 an accurate estimation of Y_∞.

213 In order to fit the Barton kinetic constant for each OEC, in several cases and due to the
214 absence of numerical data, the experimental OECs ($Y\ vs\ t$ points) were taken from the plots
215 available in the corresponding published works, using the open software Plot Digitizer v.
216 2.6.6 (Huwaldt and Steinhorst, 2014). The Barton k values regressed, together with the Y_∞
217 and R^2 values obtained are given in Table 4.

218 Figure 5 shows the correlation between the Barton k values and solvent flow rate for the 19
219 NOVALINDUS OECs plus the 34 OECs from the literature. Despite the regression coefficient
220 obtained is somewhat smaller ($R^2 = 0.8651$) the general trend of the scaling correlation
221 proposed in this work is confirmed.

Conclusions

The relation between the solvent flow rate (Q) in plant material SFE and the mass transfer coefficient was studied. A large set of OECs was compiled from the literature, including 19 OECs obtained by the authors in NOVALINDUS Platform and 34 OECs from the literature. OEC data comprise 10 different plant materials, temperatures in the range 298-333 K and pressures in the range 10-30 MPa. Additionally, particle diameter varied from 250 to 1400 µm, extractor volume from 50 to 5200 cm^3 and bed porosity was in the range 0.59-0.97. All OECs were correlated using Barton model, by fitting the Barton kinetic constant k and achieving regression coefficients higher than 0.90.

A relation between the solvent flow rate and Barton kinetic constant observed in previous work (López-padilla et al., 2017), which was developed for a single plant material and an unique particle diameter and bed porosity, was reasonably extended to cover the wider extraction conditions and materials covered in the 53 OECs compiled in this work, and demonstrated a general trend which can be used for estimating the solvent flow rate required in SFE scaling.

Acknowledges

López-Padilla A. Thanks to COLCIENCIAS (568–2012) and Medellin Mayor's Office (Sapiencia/Enlaza Mundos Program, 2013 Call) for the Ph.D. fellowship. This work was financed thanks ALIBIRD, S2013/ABI-2728 (Comunidad de Madrid) project.

References

Barton, P., Hughes, R.E., Hussein, M.M., 1992. Supercritical Carbon Dioxide Extraction of Peppermint and Spearmint. The Journal of Supercritical Fluids 5, 157–162. https://doi.org/10.1016/0896-8446(92)90002-2.

Carvalho, R.N., Moura, L.S., Rosa, P.T. V, Meireles, M.A.A., 2005. Supercritical fluid extraction from rosemary (*Rosmarinus officinalis*): Kinetic data, extract's global yield, composition, and antioxidant activity. Journal of Supercritical Fluids 35, 197–204. https://doi.org/10.1016/j.supflu.2005.01.009.

Cháfer, A., Berna, A., 2014. Study of kinetics of the d-pinitol extraction from carob pods using supercritical CO2. Journal of Supercritical Fluids 94, 212–215. https://doi.org/10.1016/j.supflu.2014.07.015.

De Melo, M.M.R., Silvestre, A.J.D., Silva, C.M., 2014. Supercritical fluid extraction of vegetable matrices: Applications, trends and future perspectives of a convincing green technology. The Journal of Supercritical Fluids 92, 115–176. https://doi.org/10.1016/j.supflu.2014.04.007.

Fenghour, A., Wakenham, W.A., Vesovic, V., 1998. The Viscosity of Carbon Dioxide. Journal of Physical and Chemical Reference Data 27, 31–44. doi:10.1098/rspa.1912.0058

Fornari, T., Ruiz-Rodriguez, A., Vicente, G., Vázquez, E., García-Risco, M.R., Reglero, G., 2012. Kinetic study of the supercritical CO2 extraction of different plants from Lamiaceae family. The Journal of Supercritical Fluids 64, 1–8. https://doi.org/10.1016/j.supflu.2012.01.006.

García-Risco, M.R., Hernández, E.J., Vicente, G., Fornari, T., Señoráns, F.J., Reglero, G., 2011a. Kinetic study of pilot-scale supercritical CO2 extraction of rosemary (*Rosmarinus officinalis*) leaves. Journal of Supercritical Fluids 55, 971–976. https://doi.org/10.1016/j.supflu.2010.09.030.

García-Risco, M.R., Vicente, G., Reglero, G., Fornari, T., 2011b. Fractionation of thyme (*Thymus vulgaris* L.) by supercritical fluid extraction and chromatography. The Journal of Supercritical Fluids 55, 949–954. https://doi.org/10.1016/j.supflu.2010.10.008.

Huang, Z., Shi, X.-H., Jiang, W.-J., 2012. Theoretical models for supercritical fluid extraction. Journal of chromatography. A 1250, 2–26. https://doi.org/10.1016/j.chroma.2012.04.032.

Huwaldt, J.A., Steinhorst, S., 2014. Plot Digitizer.

López-padilla, A., Ruiz-Rodriguez, A., Reglero, G., Fornari, T., 2017. Supercritical carbon dioxide extraction of Calendula officinalis : kinetic modeling and scaling up study. Journal of Supercritical Fluids, In press.

López-Padilla, A., Ruiz-Rodriguez, A., Reglero, G., Fornari, T., 2016a. Study of the diffusion coefficient of solute-type extracts in supercritical carbon dioxide: Volatile oils, fatty

283 acids and fixed oils. Journal of Supercritical Fluids 109, 148–156.
284 https://doi.org/10.1016/j.supflu.2015.11.017.

285 López-Padilla, A., Ruiz-Rodriguez, A., Restrepo Flórez, C., Rivero Barrios, D., Reglero, G.,
286 Fornari, T., 2016b. *Vaccinium meridionale* Swartz Supercritical CO2 Extraction: Effect
287 of Process Conditions and Scaling Up. Materials 9, 519. Doi:10.3390/ma9070519.

288 Martinez, J., Monteiro, A.R., Rosa, P.T.V., Marques, M.O.M., Meireles, M.A., 2003.
289 Multicomponent model to describe extraction of ginger oleoresin with supercritical
290 carbon dioxide. Industrial & Engineering Chemistry Research 42, 1057–1063.
291 doi:10.1021/Ie020694f.

292 NIST, 2017. Thermophysical properties of fluid systems [WWW Document]. National
293 Institute of Standards and Technology. URL http://webbook.nist.gov/chemistry/fluid/
294 (accessed 5.16.17).

295 Oliveira, E.L.G., Silvestre, A.J.D., Silva, C.M., 2011. Review of kinetic models for supercritical
296 fluid extraction. Chemical Engineering Research and Design 89, 1104–1117.
297 https://doi.org/10.1016/j.cherd.2010.10.025.

298 Paula, J.T., Aguiar, A.C., Sousa, I.M.O., Magalhães, P.M., Foglio, M.A., Cabral, F.A., 2016.
299 Scale-up study of supercritical fluid extraction process for *Baccharis dracunculifolia*.
300 Journal of Supercritical Fluids 107, 219–225.
301 https://doi.org/10.1016/j.supflu.2015.09.013.

302 Povh, N.P., Marques, M.O.M., Meireles, M.A., 2001. Supercritical CO2 extraction of essential
303 oil and oleoresin from chamomile (*Chamomilla recutita* [L.] Rauschert). Journal of
304 Supercritical Fluids 21, 245–256. https://doi.org/10.1016/S0896-8446(01)00096-1.

305 Prado, J.M., Dalmolin, I., Carareto, N.D.D., Basso, R.C., Meirelles, A.J.A., Vladimir Oliveira, J.,
306 Batista, E. a. C., Meireles, M.A.A., 2012. Supercritical fluid extraction of grape seed:
307 Process scale-up, extract chemical composition and economic evaluation. Journal of
308 Food Engineering 109, 249–257. https://doi.org/10.1016/j.jfoodeng.2011.10.007.

309 Prado, J.M., Prado, G.H.C., Meireles, M.A.A., 2011. Scale-up study of supercritical fluid
310 extraction process for clove and sugarcane residue. Journal of Supercritical Fluids 56,
311 231–237. doi: https://doi.org/10.1016/j.supflu.2010.10.036.

312 Silva, C.F., Mendes, M.F., Pessoa, F.L.P., Queiroz, E.M., 2008. Supercritical carbon dioxide
313 extraction of macadamia (*Macadamia integrifolia*) nut oil: experiments and modeling.
314 Brazilian Journal of Chemical Engineering 25, 175–181.
315 http://dx.doi.org/10.1590/S0104-66322008000100018.

316 Silva, C.F., Moura, F.C., Mendes, M.F., Pessoa, F.L.P., 2011. Extraction of citronella
317 (*Cymbopogon nardus*) essential oil using supercritical CO2: Experimental data and
318 mathematical modeling. Brazilian Journal of Chemical Engineering 28, 343–350.
319 http://dx.doi.org/10.1590/S0104-66322011000200019.

320 Silva, L.P.S., Martínez, J., 2014. Mathematical modeling of mass transfer in supercritical fluid
321 extraction of oleoresin from red pepper. Journal of Food Engineering 133, 30–39.
322 https://doi.org/10.1016/j.jfoodeng.2014.02.013.

Sovova, H., 2017. Broken and intact cell model for supercritical fluid extraction: its origin and limits. The Journal of Supercritical Fluids, In press. https://doi.org/10.1016/j.supflu.2017.02.014

Sovová, H., 1994. Rate of the vegetable oil extraction with supercritical CO2—I. Modelling of extraction curves. Chemical Engineering Science 49, 409–414. https://doi.org/10.1016/0009-2509(94)87012-8.

Tegeler, C., Span, R., Wagner, W., 1999. A New Equation of State for Argon Covering the Fluid Region for Temperatures From the Melting Line to 700 K at Pressures up to 1000 MPa. Journal of Physical and Chemical Reference Data 28, 779–850. http://dx.doi.org/10.1063/1.556037.

Villanueva-Bermejo, D., Zahran, F., García-Risco, M.R., Reglero, G., Fornari, T., 2017. Supercritical fluid extraction of Bulgarian Achillea millefolium. The Journal of Supercritical Fluids 119, 283–288. https://doi.org/10.1016/j.supflu.2016.10.005.

Yesil-Celiktas, O., Otto, F., Gruener, S., Parlar, H., 2009. Determination of extractability of pine bark using supercritical CO2 extraction and different solvents: Optimization and prediction. Journal of Agricultural and Food Chemistry 57, 341–347. Doi:10.1021/jf8026414

Zabot, G.L., Moraes, M.N., Meireles, M.A., 2014a. Influence of the bed geometry on the kinetics of rosemary compounds extraction with supercritical CO2. Journal of Supercritical Fluids 94, 234–244. https://doi.org/10.1016/j.supflu.2014.07.020.

Zabot, G.L., Moraes, M.N., Petenate, A.J., Meireles, M.A., 2014b. Influence of the bed geometry on the kinetics of the extraction of clove bud oil with supercritical CO2. The Journal of Supercritical Fluids 93, 56–66. https://doi.org/10.1016/j.supflu.2013.10.001.

Zancan, K.C., Marques, M.O.M., Petenate, A.J., Meireles, M.A., 2002. Extraction of ginger (*Zingiber officinale* roscoe) oleoresin with CO2 and co-solvents: A study of the antioxidant action of the extracts. Journal of Supercritical Fluids 24, 57–76. https://doi.org/10.1016/S0896-8446(02)00013-X.

352 **Table 1.** NOVALINDUS facilities for the SFE of solid materials.

353

Characteristics	**Lab Scale 1**	**Lab Scale 2**	**Pilot Scale**
L: Bed length (m)	0.188	0.388	0.570
D: Bed diameter (m)	0.043	0.07	0.107
Bed volume (m^3)	2.7×10^{-4}	1.35×10^{-3}	5.19×10^{-3}
Cross flow area (m^2)	1.45×10^{-3}	3.53×10^{-3}	8.99×10^{-3}
Ratio L/D	4.372	5.716	5.327
Cyclone volume (m^3)	5×10^{-4}	5×10^{-4}	1.57×10^{-3}
Pump capacity (kg/h)	0.2 - 12	0.2 - 12	2.2 - 147
Pressure work (MPa)	0.1 - 69	0.1 - 69	0.1 - 44
Temperature work (°C)	5 - 40	5 - 40	5 - 40
Demister (m^3)	1.71×10^{-3}	1.71×10^{-3}	1.5×10^{-2}
Filter (m^3)	No	No	5×10^{-2}
Storage tank (m^3)	1.5×10^{-2}	1.5×10^{-2}	8.8×10^{-2}
Recycler system CO_2	Yes	Yes	Yes
Automated BPR	Yes	Yes	Yes
Flowmeter	Yes	Yes	No
PLC control	Yes	Yes	Yes

354

355

356

357

358

359

360

361

362 **Table 2.** SFE data of different OECs obtained in NOVALINDUS Platform.

	Raw Material	D (m)	L (m)	F (kg)	$d_p \times 10^4$ (m)	ρ_B (kg/m^3)	ε	$Q \times 10^3$ (kg/s)	T (K)	P (bar)	ρ_{CO2} (kg/m^3)	$\mu_{CO2} \times 10^5$ (kg/m·s)	$D_{E\text{-}CO2} \times 10^8$ (m^2/s)	S_c	Ref.
1	Origanum	0.076	0.416	0.60	5.0	1020	0.69	1.00	313	300	909.9	9.38	1.18	8.725	(Fornari et al., 2012)
2	Sage	0.076	0.416	0.60	5.0	1050	0.70	1.00	313	300	909.9	9.38	1.18	8.725	(Fornari et al., 2012)
3	Thyme	0.076	0.416	0.60	10.0	1580	0.80	1.00	313	300	909.9	9.38	1.18	8.725	(Fornari et al., 2012)
4	Rosemary	0.076	0.416	0.60	10.0	1046	0.70	1.00	313	300	909.9	9.38	1.18	8.725	(Fornari et al., 2012)
5	Rosemary	0.076	0.416	0.60	10.0	1046	0.70	1.00	314	300	909.9	9.38	1.18	8.713	(García-Risco et al., 2011a)
6	Rosemary	0.076	0.416	0.60	10.0	1046	0.70	1.00	315	300	909.9	9.38	1.19	8.701	(García-Risco et al., 2011a)
7	Thyme	0.076	0.416	0.55	4.0	1580	0.82	0.67	313	300	910.0	9.62	1.21	8.752	(García-Risco et al., 2011a)
8	Yarrow	0.067	0.383	0.40	5.0	1015	0.71	1.20	313	140	763.0	6.50	1.49	5.705	(Villanueva-Bermejo et al., 2017)
9	Calendula	0.043	0.188	0.09	5.0	1409	0.76	0.25	313	140	763.0	6.50	1.49	5.702	(López-padilla et al., 2017)
10	Calendula	0.043	0.188	0.09	5.0	1409	0.76	0.50	313	140	763.0	6.50	1.49	5.702	(López-padilla et al., 2017)
11	Calendula	0.043	0.188	0.09	5.0	1409	0.76	0.75	313	140	763.0	6.50	1.49	5.702	(López-padilla et al., 2017)
12	Calendula	0.043	0.188	0.09	5.0	1409	0.76	0.50	313	240	872.5	8.51	1.25	7.829	(López-padilla et al., 2017)
13	Calendula	0.043	0.188	0.09	5.0	1409	0.76	0.50	313	340	930.2	9.91	1.15	9.238	(López-padilla et al., 2017)
14	Calendula	0.067	0.383	0.45	5.0	1409	0.76	0.60	313	140	763.0	6.50	1.49	5.702	(López-padilla et al., 2017)
15	Calendula	0.067	0.383	0.45	5.0	1409	0.76	1.23	313	140	763.0	6.50	1.49	5.702	(López-padilla et al., 2017)
16	Calendula	0.107	0.570	1.71	5.0	1409	0.76	1.54	313	140	763.0	6.50	1.49	5.702	(López-padilla et al., 2017)
17	Calendula	0.107	0.570	1.71	5.0	1409	0.76	4.70	313	140	763.0	6.50	1.49	5.702	(López-padilla et al., 2017)
18	Mortiño	0.043	0.188	0.16	2.5	1440	0.59	0.53	313	300	909.9	9.38	1.18	8.724	(López-Padilla et al., 2016b)
19	Mortiño	0.067	0.383	0.80	2.5	1440	0.59	2.63	313	300	909.9	9.38	1.18	8.724	(López-Padilla et al., 2016b)

363

364

365 **Table 3.** SFE data of OECs obtained from the literature.

	Raw Material	D (m)	L (m)	F (kg)	$d_p \times 10^4$ (m)	ρ_B (kg/m³)	ε	$Q \times 10^3$ (kg/s)	T (K)	P (bar)	ρ_{CO2} (kg/m³)	$\mu_{CO2} \times 10^5$ (kg/m·s)	$D_{E\text{-}CO2} \times 10^8$ (m²/s)	S_c	Ref.
1	Red pepper	0.030	0.075	0.024	9.3	1320	0.66	0.402	313	150	780.2	6.77	0.93	9.289	(Silva and Martínez, 2014)
2	Red pepper	0.030	0.129	0.042	9.3	1320	0.66	0.402	313	150	780.2	6.77	0.93	9.289	(Silva and Martínez, 2014)
3	Red pepper	0.054	0.125	0.128	9.3	1320	0.66	0.402	313	150	780.2	6.77	0.93	9.289	(Silva and Martínez, 2014)
4	Red pepper	0.054	0.125	0.125	4.3	1320	0.67	0.402	313	150	780.2	6.77	0.93	9.289	(Silva and Martínez, 2014)
5	Red pepper	0.054	0.125	0.125	4.3	1320	0.67	0.285	313	150	780.2	6.77	0.93	9.289	(Silva and Martínez, 2014)
6	Red pepper	0.054	0.125	0.125	4.3	1320	0.67	0.170	313	150	780.2	6.77	0.93	9.289	(Silva and Martínez, 2014)
7	Red pepper	0.030	0.129	0.040	4.3	1320	0.67	0.170	313	150	780.2	6.77	0.93	9.289	(Silva and Martínez, 2014)
8	Red pepper	0.030	0.129	0.042	9.3	1320	0.66	0.170	313	150	780.2	6.77	0.93	9.289	(Silva and Martínez, 2014)
9	Red pepper	0.030	0.129	0.041	14.1	1320	0.67	0.170	313	150	780.2	6.77	0.93	9.289	(Silva and Martínez, 2014)
10	Red pepper	0.030	0.075	0.023	4.3	1320	0.68	0.285	313	150	780.2	6.77	0.93	9.289	(Silva and Martínez, 2014)
11	Red pepper	0.030	0.075	0.024	9.3	1320	0.66	0.285	313	150	780.2	6.77	0.93	9.289	(Silva and Martínez, 2014)
12	Red pepper	0.030	0.075	0.024	14.1	1320	0.67	0.285	313	150	780.2	6.77	0.93	9.289	(Silva and Martínez, 2014)
13	Red pepper	0.030	0.129	0.041	14.1	1320	0.67	0.285	313	150	780.2	6.77	0.93	9.289	(Silva and Martínez, 2014)
14	Red pepper	0.030	0.075	0.023	4.3	1320	0.68	0.402	313	150	780.2	6.77	0.93	9.289	(Silva and Martínez, 2014)
15	Red pepper	0.030	0.129	0.040	4.3	1320	0.67	0.402	313	150	780.2	6.77	0.93	9.289	(Silva and Martínez, 2014)
16	Red pepper	0.030	0.129	0.041	14.1	1320	0.67	0.402	313	150	780.2	6.77	0.93	9.289	(Silva and Martínez, 2014)
17	chamomile	0.040	0.166	0.075	3.0	1346	0.72	0.067	303	100	771.5	6.61	1.45	5.897	(Povh et al., 2001)
18	chamomile	0.040	0.166	0.075	3.0	1346	0.72	0.067	303	120	808.9	7.24	1.36	6.572	(Povh et al., 2001)
19	chamomile	0.040	0.166	0.075	3.0	1346	0.72	0.067	303	160	857.1	8.17	1.26	7.579	(Povh et al., 2001)
20	chamomile	0.040	0.166	0.075	3.0	1346	0.72	0.067	303	200	890.5	8.91	1.20	8.364	(Povh et al., 2001)
21	chamomile	0.040	0.166	0.075	3.0	1346	0.72	0.067	313	100	628.7	4.02	1.80	3.563	(Povh et al., 2001)
22	chamomile	0.040	0.166	0.075	3.0	1346	0.72	0.033	313	120	717.8	5.85	1.62	5.046	(Povh et al., 2001)

Table 3. SFE data of OECs obtained from the literature (Continuation).

	Raw Material	D (m)	L (m)	F (kg)	$d_p \times 10^4$ (m)	ρ_B (kg/m^3)	ε	$Q \times 10^3$ (kg/s)	T (K)	P (bar)	ρ_{CO2} (kg/m^3)	$\mu_{CO2} \times 10^5$ (kg/m·s)	$D_{E\text{-}CO2} \times 10^8$ (m^2/s)	S_c	Ref.
23	chamomile	0.040	0.166	0.075	3.0	1346	0.72	0.067	313	120	717.8	5.12	1.53	4.651	(Povh et al., 2001)
24	chamomile	0.040	0.166	0.075	3.0	1346	0.72	0.067	313	160	792.2	6.69	1.39	6.082	(Povh et al., 2001)
25	chamomile	0.040	0.166	0.075	3.0	1346	0.72	0.033	313	160	794.9	7.02	1.41	6.245	(Povh et al., 2001)
26	chamomile	0.040	0.166	0.075	3.0	1346	0.72	0.067	313	200	839.9	7.79	1.31	7.103	(Povh et al., 2001)
27	Ginger	0.028	0.375	0.080	10.2	1300	0.74	0.056	313	250	881.0	8.82	1.24	8.049	(Martinez et al., 2003)
28	Ginger	0.028	0.375	0.080	10.2	1300	0.74	0.056	303	150	847.0	7.86	1.27	7.326	(Martinez et al., 2003)
29	Ginger	0.028	0.375	0.080	10.2	1300	0.74	0.056	313	200	841.0	7.79	1.30	7.119	(Martinez et al., 2003)
30	Ginger	0.028	0.375	0.080	10.2	1300	0.74	0.056	313	150	841.0	6.36	1.14	6.621	(Martinez et al., 2003)
31	Ginger	0.028	0.387	0.008	3.9	1524	0.97	0.059	298	200	914.2	9.97	1.20	9.056	(Zancan et al., 2002)
32	Ginger	0.028	0.387	0.008	3.9	1524	0.97	0.060	298	250	943.5	10.3	1.11	9.793	(Zancan et al., 2002)
33	Ginger	0.028	0.387	0.008	3.9	1524	0.97	0.059	308	200	866.2	8.46	1.26	7.757	(Zancan et al., 2002)
34	Ginger	0.028	0.387	0.008	3.9	1524	0.97	0.059	308	250	901.8	9.17	1.18	8.582	(Zancan et al., 2002)

373 **Table 4.** Barton kinetic constants of OECs obtained in NOVALINDUS Platform.

	Raw Material	k (min^{-1})	Y_∞	R^2	Ref.
1	Origanum	0.0182	0.048	0.980	(Fornari et al., 2012)
2	Sage	0.0177	0.047	0.995	(Fornari et al., 2012)
3	Thyme	0.0099	0.033	0.995	(Fornari et al., 2012)
4	Rosemary	0.0094	0.038	0.969	(Fornari et al., 2012)
5	Rosemary	0.0078	0.049	0.959	(García-Risco et al., 2011a)
6	Rosemary	0.0085	0.043	0.988	(García-Risco et al., 2011a)
7	Thyme	0.0132	0.032	0.999	(García-Risco et al., 2011a)
8	Yarrow	0.0151	0.030	0.963	(Villanueva-Bermejo et al., 2017)
9	Calendula	0.0091	0.050	0.984	(López-padilla et al., 2017)
10	Calendula	0.0112	0.059	0.974	(López-padilla et al., 2017)
11	Calendula	0.0127	0.063	0.963	(López-padilla et al., 2017)
12	Calendula	0.0143	0.064	0.985	(López-padilla et al., 2017)
13	Calendula	0.0175	0.065	0.969	(López-padilla et al., 2017)
14	Calendula	0.0081	0.035	0.986	(López-padilla et al., 2017)
15	Calendula	0.0095	0.045	0.988	(López-padilla et al., 2017)
16	Calendula	0.0082	0.053	0.973	(López-padilla et al., 2017)
17	Calendula	0.0113	0.078	0.998	(López-padilla et al., 2017)
18	Mortiño	0.0429	0.032	0.925	(López-Padilla et al., 2016b)
19	Mortiño	0.0511	0.032	0.909	(López-Padilla et al., 2016b)

374

375

376 **Table 5.** Barton kinetic constants of OECs obtained from the literature.

	Raw Material	k (min^{-1})	Y_∞	R^2	Ref.
1	Red pepper	0.0270	0.5300	0.917	(Silva and Martínez, 2014)
2	Red pepper	0.0216	0.5947	0.953	(Silva and Martínez, 2014)
3	Red pepper	0.0118	0.0553	0.996	(Silva and Martínez, 2014)
4	Red pepper	0.0141	0.0912	0.951	(Silva and Martínez, 2014)
5	Red pepper	0.0105	0.0778	0.953	(Silva and Martínez, 2014)
6	Red pepper	0.0076	0.0475	0.959	(Silva and Martínez, 2014)
7	Red pepper	0.0124	0.0860	0.989	(Silva and Martínez, 2014)
8	Red pepper	0.0153	0.0535	0.993	(Silva and Martínez, 2014)
9	Red pepper	0.0122	0.0409	0.996	(Silva and Martínez, 2014)
10	Red pepper	0.0295	0.0875	0.980	(Silva and Martínez, 2014)
11	Red pepper	0.0263	0.0568	0.981	(Silva and Martínez, 2014)
12	Red pepper	0.0235	0.0423	0.966	(Silva and Martínez, 2014)
13	Red pepper	0.0148	0.0460	0.971	(Silva and Martínez, 2014)
14	Red pepper	0.0416	0.1046	0.950	(Silva and Martínez, 2014)
15	Red pepper	0.0244	0.0958	0.968	(Silva and Martínez, 2014)
16	Red pepper	0.0220	0.0510	0.982	(Silva and Martínez, 2014)
17	chamomile	0.0053	0.0339	0.996	(Povh et al., 2001)
18	chamomile	0.0049	0.0320	0.994	(Povh et al., 2001)
19	chamomile	0.0058	0.0390	0.995	(Povh et al., 2001)
20	chamomile	0.0075	0.0391	0.994	(Povh et al., 2001)
21	chamomile	0.0046	0.0219	0.994	(Povh et al., 2001)
22	chamomile	0.0030	0.0528	0.998	(Povh et al., 2001)
23	chamomile	0.0063	0.0324	0.998	(Povh et al., 2001)
24	chamomile	0.0052	0.0376	0.984	(Povh et al., 2001)
25	chamomile	0.0039	0.0539	0.996	(Povh et al., 2001)
26	chamomile	0.0079	0.0440	0.985	(Povh et al., 2001)
27	Ginger	0.0037	0.6465	0.985	(Martinez et al., 2003)
28	Ginger	0.0025	0.0450	0.958	(Martinez et al., 2003)
29	Ginger	0.0038	0.0494	0.964	(Martinez et al., 2003)
30	Ginger	0.0033	0.0421	0.978	(Martinez et al., 2003)
31	Ginger	0.0084	0.0342	0.994	(Zancan et al., 2002)
32	Ginger	0.0078	0.0375	0.982	(Zancan et al., 2002)
33	Ginger	0.0070	0.0251	0.992	(Zancan et al., 2002)
34	Ginger	0.0086	0.0208	0.980	(Zancan et al., 2002)

377

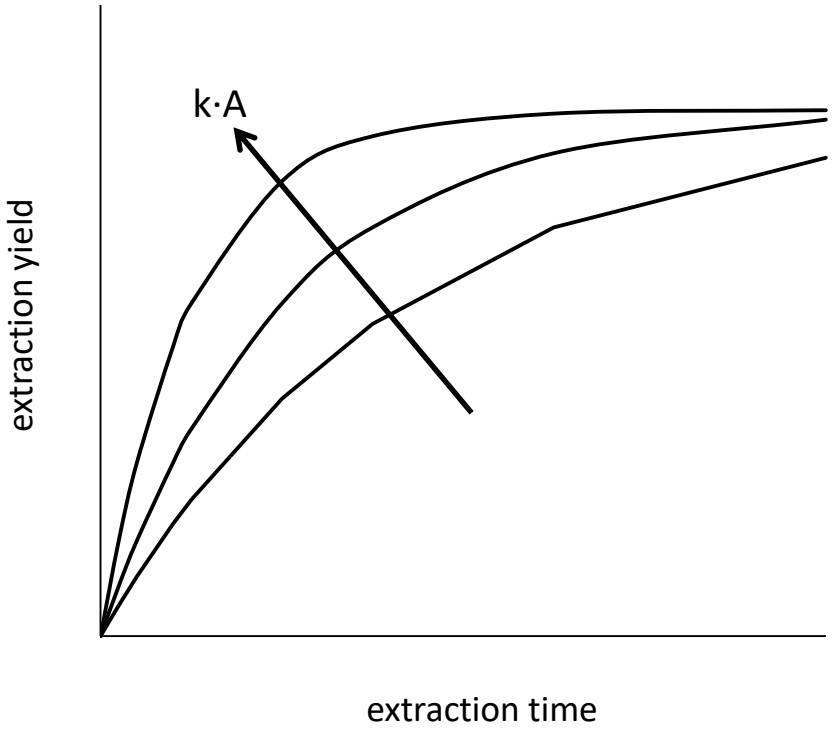

Figure 1. General shape of the Overall Extraction Curve (OEC): effect of mass transfer coefficient and interfacial area.

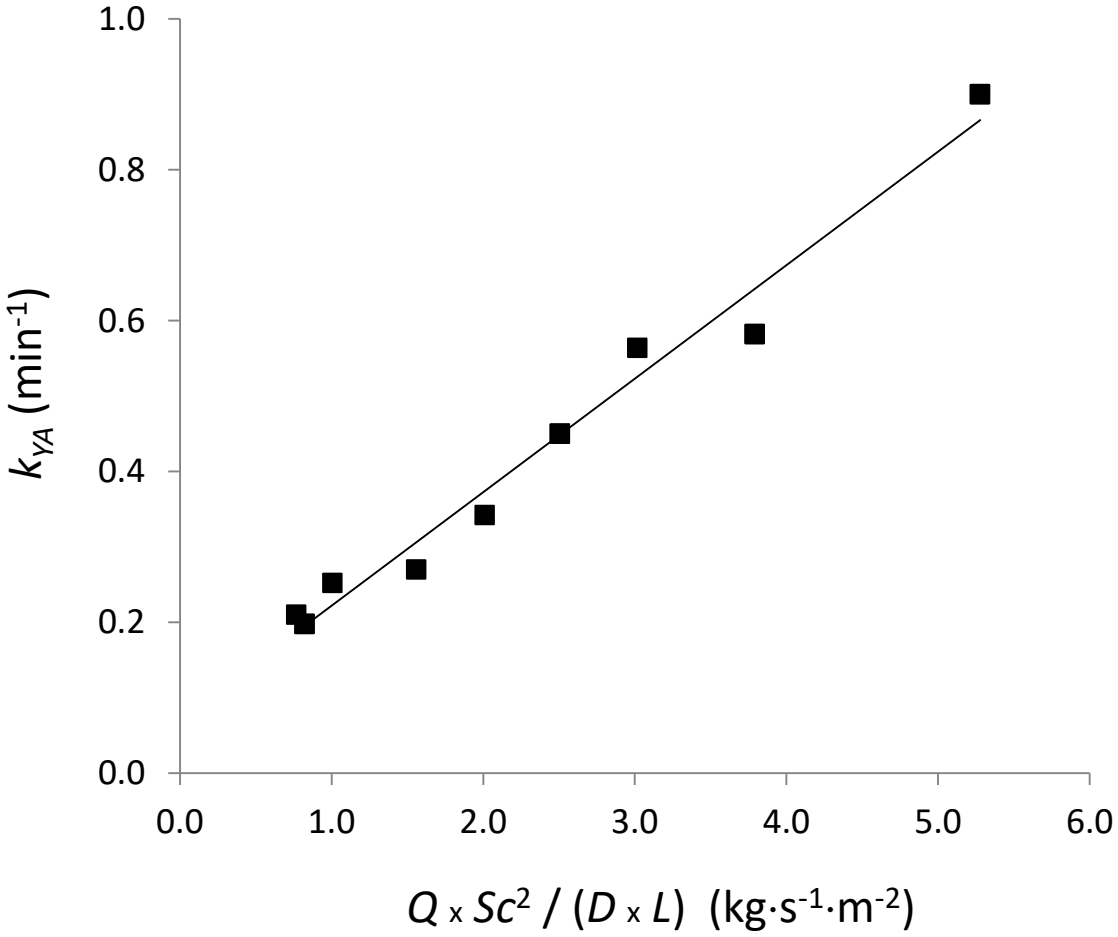

Figure 2. Correlation between BIC model mass transfer coefficient in the supercritical fluid phase (k_{YA}) and the CO_2 flow rate (Q) of nine OECs corresponding to calendula SFE (López-padilla et al., 2017) at constant bed porosity and constant mean particle diameter ($R^2 = 0.9676$).

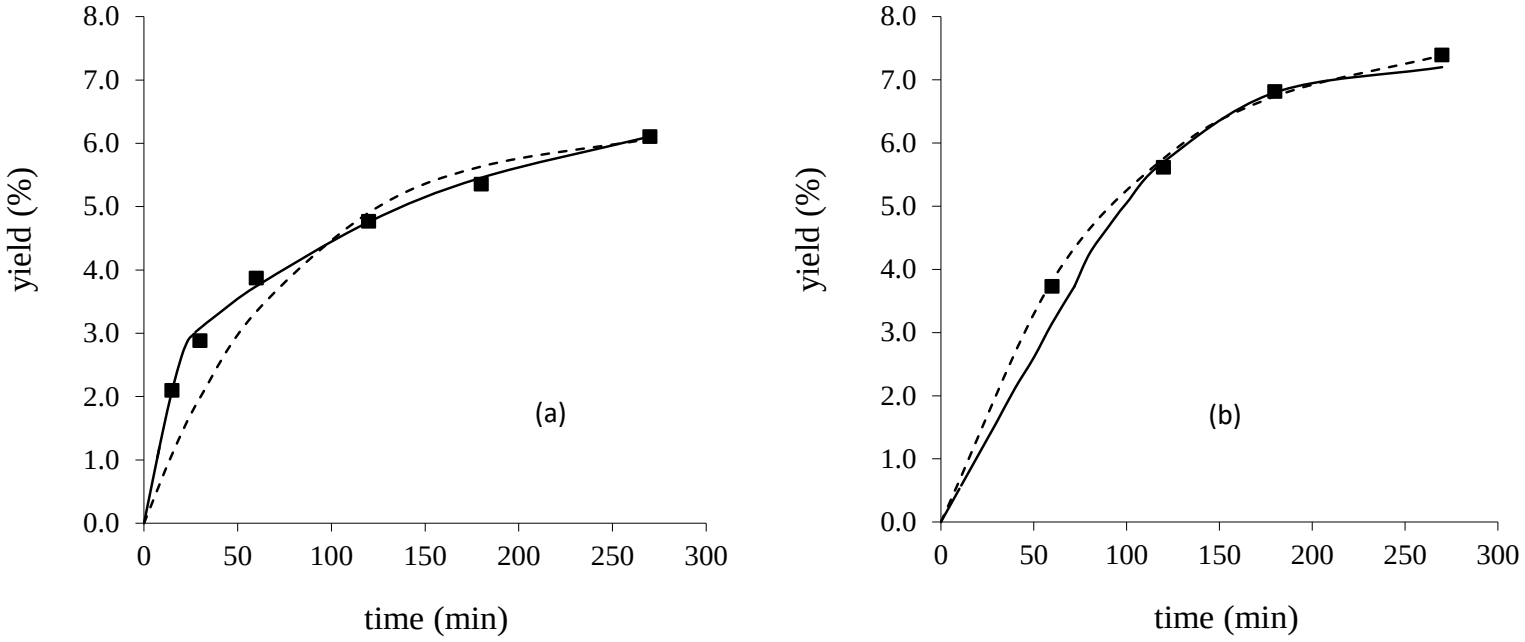

Figure 3. Comparison between BIC and Barton models in the fitting of calendula OECs 11 and 17 of Table 2.

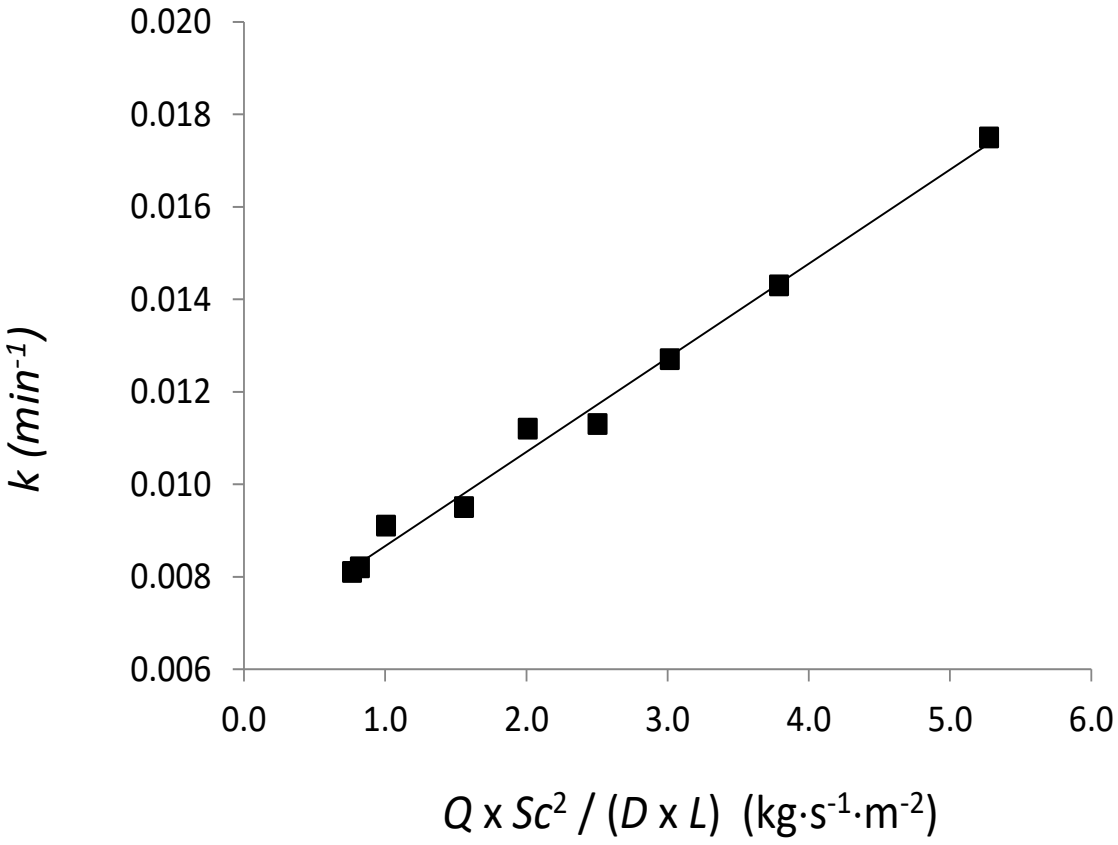

Figure 4. Correlation between Barton model kinetic constant (k) and the CO_2 flow rate (Q) of nine OECs corresponding to calendula SFE at constant bed porosity and constant mean particle diameter ($R^2 = 0.9906$).

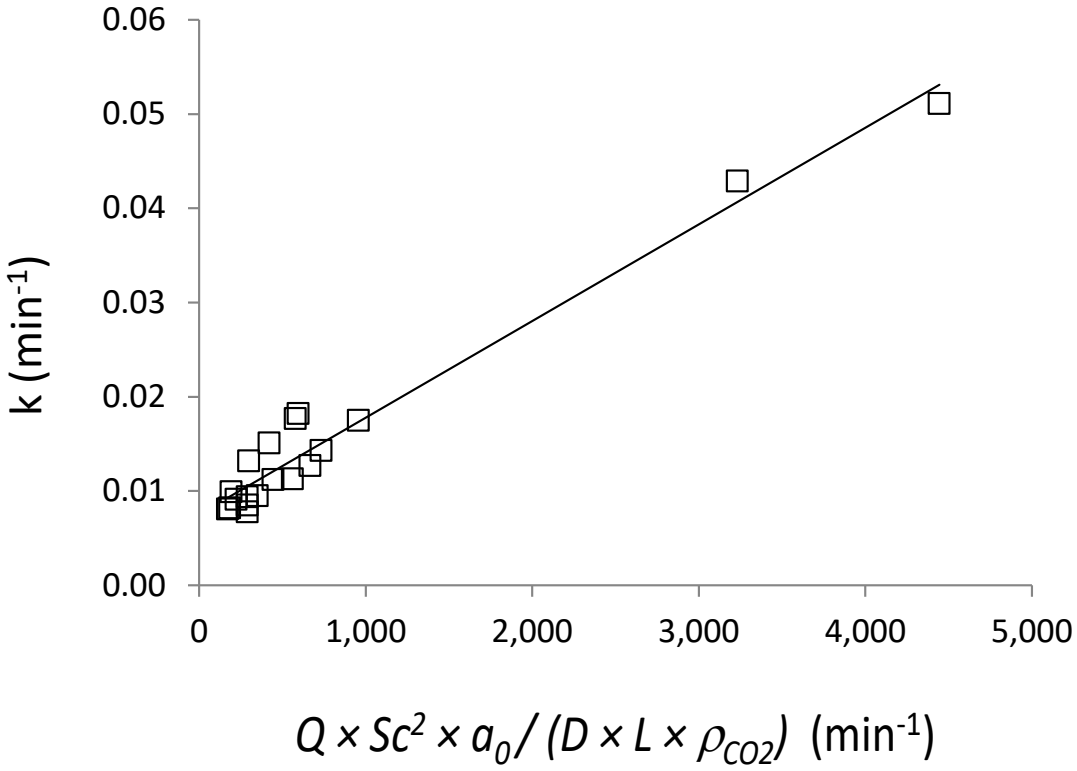

Figure 5. Correlation between Barton model kinetic constant (k) and the CO_2 flow rate (Q) of OECs obtained in NOVALINDUS Platform (Table 2) with bed porosity in the range of 0.59-0.82 and particle diameter in the range of 250-1000 µm. $R^2 = 0.9624$.

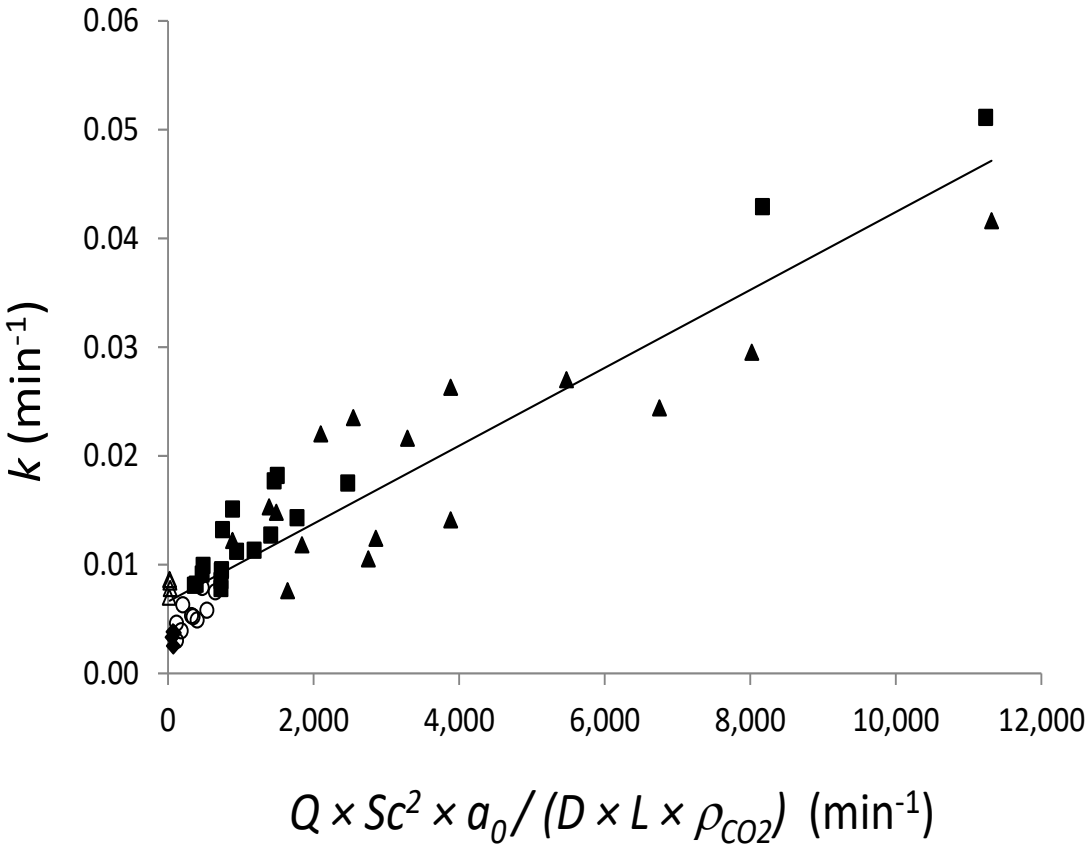

Figure 6. Correlation between Barton model kinetic constant (k) and the CO_2 flow rate (Q) of OECs of Tables 2 and 3. (■) NOVALINDUS (Fornari et al., 2012; García-Risco et al., 2011a; López-padilla et al., 2017; López-Padilla et al., 2016b; Villanueva-Bermejo et al., 2017); (▲) Red pepper (Silva and Martínez, 2014); (○) Chamomile (Povh et al., 2001); (△) Ginger (Martinez et al., 2003; Zancan et al., 2002). $R^2 = 0.8651$.

CAPÍTULO 4.

DISCUSIÓN GENERAL

4. DISCUSIÓN GENERAL

La SFE es una tecnología muy valorada en sectores diversos como la alimentación, la cosmética y la farmacia, debido a su capacidad de recuperar de forma eficiente y sostenible una gran cantidad de sustancias con actividades biológicas presentes en los materiales de origen natural. Frente a otras tecnologías de extracción posee la ventaja de emplear un disolvente GRAS (*General Recognized As Safe*) como es el dióxido de carbono, puro o mezclado con cosolventes, haciendo de la SFE una tecnología versátil, eficaz y respetuosa con el medio ambiente, siendo prueba de ello la gran variedad de sus aplicaciones en investigación, desarrollo e innovación, destacándose particularmente las orientadas a la producción de ingredientes alimentarios funcionales [27,180,181].

Usualmente, un proceso de SFE se estudia en primer lugar a escala analítica y/o laboratorio, con el fin de optimizar las condiciones de extracción, tales como temperatura, presión, caudal de disolvente, tamaño de partículas, porosidad del lecho, para lograr el objetivo deseado (máximo rendimiento, máxima concentración de un determinado componente, máxima acción biológica, etc.). En este sentido, el estudio de la cinética de extracción (*overall extraction curve*, OEC) es muy importante para determinar el tiempo óptimo de extracción. El tiempo de extracción fija la productividad del proceso y, consecuentemente, es esencial para estimar su beneficio económico

El escalado de un proceso de producción SFE significa esencialmente reproducir la misma cinética de extracción en celdas de diferente tamaño y/o forma. En general, las celdas de extracción son cilíndricas, por lo que los parámetros que determinan la geometría del proceso son el diámetro y la longitud de la celda. Asimismo, las condiciones de extracción que no dependen de la cantidad de material procesado, como son la temperatura y la presión, se mantienen constantes en las distintas escalas de producción, puesto que ellas determinan las propiedades intensivas de la extracción, como son la densidad y viscosidad del disolvente, así como la solubilidad de los solutos. Otras propiedades como tamaño de partícula y porosidad del lecho empacado se intentan reproducir al pasar de pequeña a gran escala, aunque el control de esas variables en el cambio de escala muchas veces no es fácil. Por ejemplo, se ha descrito en algunos trabajos de escalado que las aglomeraciones del material a extraer y la consecuente canalización del flujo del disolvente supercrítico, se producen más fácilmente en celdas grandes que en celdas pequeñas, aun manteniendo el mismo tamaño de partícula del material vegetal [42]. En cambio, otros

autores han reportado en ciertos procesos de extracción SFE un incremento en el rendimiento de extracción al aumentar la escala de producción [41,182].

La cinética de la extracción se caracteriza principalmente por los siguientes parámetros: el coeficiente de transferencia masa del proceso (k) y el área superficial accesible al disolvente (a_0). El aumento de k y/o de a_0 significa un aumento de la velocidad de extracción. Asimismo, es necesaria una buena difusión de los solutos en el fluido supercrítico para garantizar la eliminación de los mismos en las cercanías de la superficie de las partículas, contribuyendo así al proceso de extracción. Para determinar estos parámetros básicos que describen la SFE hay una gran variedad de modelos matemáticos, cada uno con más o menos hipótesis, complejidad de cálculo, fiabilidad, así como capacidad predictiva. En la sección 1.3.2 de la Introducción de esta Tesis se presenta una revisión de los modelos teóricos disponibles en la bibliografía para calcular el coeficiente de transferencia de masa, así como de los métodos publicados para el cálculo del coeficiente de difusión.

El Instituto de Investigación en Ciencias de la Alimentación (CIAL UAM-CSIC) dispone de la Plataforma de In**nova**ción **Ali**mentaria **Indus**trial (Novalindus), que cuenta con varias plantas de extracción SFE de diferentes escalas de producción. En esta plataforma se ha venido trabajando intensamente en la extracción de una gran variedad de materiales de origen vegetal, para la obtención de ingredientes alimentarios funcionales. Entre estos extractos con actividad biológica se investigaron en Novalindus los procedentes de romero (*Rosmarinus officinalis*), con propiedades inhibitorias de la proliferación de células cancerígenas en el hígado [16]; el fraccionamiento de extractos de romero (*R. officinalis*) para mejorar su actividad antioxidante [183]; la obtención de extractos de espinaca (*Spinacea olearecea*) y la evaluación de su actividad antioxidante y propiedades antiinflamatorias [184]; la extracción simultánea de romero (*R. officinalis*) y espinaca (*S. oleracee*) y la posterior evaluación de la actividad antioxidante de sus extractos [171]; los extractos de tomillo (*Thymus zygis*) y orégano (*Origanum vulgare*), con propiedades antimicrobianas [170]; la extracción de diferentes especies de tomillo (*Thymus vulgaris, Thymus hyemalis* y *Thymus zygis*) para obtener extractos con efectos antivirales [185]; los extractos de milenrama (*Achillea milefolium*) y su efecto antiproliferativo en células cancérigenas pancreáticas [164], los procedentes del brezo (*Calluna vulgaris*) con efecto antiviral frente el virus de la hepatitis C [186], la extracción y recuperación del ácido betulínico a partir de la corteza del plátano (*Platanus acerifolia* L.) [17] entre otros.

En este sentido, es de gran importancia para la Plataforma Novalindus el estudio del escalado de procesos SFE de lecho fijo en batch, con el objetivo de desarrollar un método práctico y confiable para pasar de una escala a otra dentro de la misma plataforma, así como para desarrollar herramientas que permitan estimar la escala industrial, contribuyendo al análisis y evaluación de la productividad y el balance beneficio-costo del proceso de extracción. Estas herramientas significan una contribución adicional a los servicios que la Plataforma Novalindus puede ofrecer al sector industrial y a empresas de base tecnológica.

La discusión de los trabajos llevados a cabo en esta Tesis para lograr desarrollar estas herramientas de escaldo puede organizarse según se indica a continuación:

(1) Obtención de datos experimentales de cinéticas de extracción en la Plataforma Novalindus y recopilación de datos de la bibliografía
(2) Desarrollo de un método simple para calcular el coeficiente de difusión del extracto en SC-CO_2 (cálculo del número de Schmidt)
(3) Criterios semi-empíricos de escalado y modelos teóricos para el cálculo del coeficiente de transferencia de masa
(4) Desarrollo de una correlación generalizada para relacionar el coeficiente de transferencia de masa del proceso de extracción con el caudal de CO_2

La discusión de los desarrollos y resultados alcanzados en cada uno de estos apartados se presenta a continuación.

4.1 Obtención de datos experimentales de cinéticas de extracción en la Plataforma Novalindus y recopilación de datos de la bibliografía

En esta tesis se ha estudiado el escalado de procesos SFE llevados a cabo en las plantas de extracción de la Plataforma Novalindus, utilizando tres diferentes escalas de producción según se ha indicado en el plan de trabajo. Se llevaron a cabo cinéticas de extracción (OEC) de los siguientes materiales (a) mortiño (*Vaccinium meridionales* Swartz) y (b) flor de Caléndula (*Calendula officinalis*). Las condiciones de extracción, características de la celda de extracción y material utilizado en cada caso se muestran en la Tabla 4.1. No obstante, para el desarrollo de una correlación generalizada, también se incluyeron en este trabajo los estudios cinéticos de otros materiales vegetales, llevados a cabo en la Plataforma Novalindus con anterioridad a esta tesis (ver Tabla 4.2).

Tabla 4.1. OECs obtenidas en la Plataforma Novalindus durante el desarrollo de esta Tesis.

	Material vegetal	D (m)	L (m)	V×10^3 (m^3)	F (kg)	Q×10^3 (kg/s)	T (K)	P (bar)	Referencia
1	Origanum	0.076	0.416	1.89	0.60	1.00	313	300	[170]
2	Sage	0.076	0.416	1.89	0.60	1.00	313	300	[170]
3	Thyme	0.076	0.416	1.89	0.60	1.00	313	300	[170]
4	Rosemary	0.076	0.416	1.89	0.60	1.00	313	300	[170]
5	Rosemary	0.076	0.416	1.89	0.60	1.00	314	300	[14]
6	Rosemary	0.076	0.416	1.89	0.60	1.00	315	300	[14]
7	Thyme	0.076	0.416	1.89	0.55	0.67	313	300	[14]
8	Yarrow	0.067	0.383	1.35	0.40	1.20	313	140	[175]
9	Calendula	0.043	0.188	0.27	0.09	0.25	313	140	[187]
10	Calendula	0.043	0.188	0.27	0.09	0.50	313	140	[187]
11	Calendula	0.043	0.188	0.27	0.09	0.75	313	140	[187]
12	Calendula	0.043	0.188	0.27	0.09	0.50	313	240	[187]
13	Calendula	0.043	0.188	0.27	0.09	0.50	313	340	[187]
14	Calendula	0.067	0.383	1,35	0.45	0.60	313	140	[187]
15	Calendula	0.067	0.383	1,35	0.45	1.23	313	140	[187]
16	Calendula	0.107	0.570	5.13	1.71	1.54	313	140	[187]
17	Calendula	0.107	0.570	5.13	1.71	4.70	313	140	[187]
18	Mortiño	0.043	0.188	0.27	0.16	0.53	313	300	[22]
19	Mortiño	0.067	0.383	1.35	0.80	2.63	313	300	[22]

Tabla 4.2. OECs de la Plataforma Novalindus previas a esta Tesis

	Material vegetal	D (m)	L (m)	V×10^3 (m^3)	F (kg)	Q×10^3 (kg/s)	T (K)	P (bar)	Referencia
1	Origanum	0.076	0.416	1.89	0.60	1.00	313	300	[170]
2	Sage	0.076	0.416	1.89	0.60	1.00	313	300	[170]
3	Thyme	0.076	0.416	1.89	0.60	1.00	313	300	[170]
4	Rosemary	0.076	0.416	1.89	0.60	1.00	313	300	[170]
5	Rosemary	0.076	0.416	1.89	0.60	1.00	314	300	[14]
6	Rosemary	0.076	0.416	1.89	0.60	1.00	315	300	[14]
7	Thyme	0.076	0.416	1.89	0.55	0.67	313	300	[14]
8	Yarrow	0.067	0.383	1.35	0.40	1.20	313	140	[175]

Asimismo, se consideraron 34 OECs compiladas de la bibliografía, las que corresponden a cinéticas de extracción llevadas a cabo en otras plantas de extracción diferentes a las disponibles en Novalindus y con otros materiales de extracción (ver Tabla 4.3).

Tabla 4.3. OECs compiladas de la bibliografía y obtenidas en unidades de extracción diferentes a las de la Plataforma Novalindus.

	Material vegetal	D (m)	L (m)	V×10^4 (m^3)	F (kg)	Q×10^3 (kg/s)	T (K)	P (bar)	Referencia
1	Red pepper	0.030	0.075	0.53	0.024	0.402	313	150	[106]
2	Red pepper	0.030	0.129	0.91	0.042	0.402	313	150	[106]
3	Red pepper	0.054	0.125	2.86	0.128	0.402	313	150	[106]
4	Red pepper	0.054	0.125	2.86	0.125	0.402	313	150	[106]
5	Red pepper	0.054	0.125	2.86	0.125	0.285	313	150	[106]
6	Red pepper	0.054	0.125	2.86	0.125	0.170	313	150	[106]
7	Red pepper	0.030	0.129	0.91	0.040	0.170	313	150	[106]
8	Red pepper	0.030	0.129	0.91	0.042	0.170	313	150	[106]
9	Red pepper	0.030	0.129	0.91	0.041	0.170	313	150	[106]
10	Red pepper	0.030	0.075	0.53	0.023	0.285	313	150	[106]
11	Red pepper	0.030	0.075	0.53	0.024	0.285	313	150	[106]
12	Red pepper	0.030	0.075	0.53	0.024	0.285	313	150	[106]
13	Red pepper	0.030	0.129	0.91	0.041	0.285	313	150	[106]
14	Red pepper	0.030	0.075	0.53	0.023	0.402	313	150	[106]
15	Red pepper	0.030	0.129	0.91	0.040	0.402	313	150	[106]
16	Red pepper	0.030	0.129	0.91	0.041	0.402	313	150	[106]
17	chamomile	0.040	0.166	2.09	0.075	0.067	303	100	[188]
18	chamomile	0.040	0.166	2.09	0.075	0.067	303	120	[188]
19	chamomile	0.040	0.166	2.09	0.075	0.067	303	160	[188]
20	chamomile	0.040	0.166	2.09	0.075	0.067	303	200	[188]
21	chamomile	0.040	0.166	2.09	0.075	0.067	313	100	[188]
22	chamomile	0.040	0.166	2.09	0.075	0.033	313	120	[188]
23	chamomile	0.040	0.166	2.09	0.075	0.067	313	120	[188]
24	chamomile	0.040	0.166	2.09	0.075	0.067	313	160	[188]
25	chamomile	0.040	0.166	2.09	0.075	0.033	313	160	[188]
26	chamomile	0.040	0.166	2.09	0.075	0.067	313	200	[188]
27	Ginger	0.028	0.375	2.31	0.080	0.056	313	250	[48]
28	Ginger	0.028	0.375	2.31	0.080	0.056	303	150	[48]
29	Ginger	0.028	0.375	2.31	0.080	0.056	313	200	[48]
30	Ginger	0.028	0.375	2.31	0.080	0.056	313	150	[48]
31	Ginger	0.028	0.387	2.38	0.008	0.059	298	200	[189]
32	Ginger	0.028	0.387	2.38	0.008	0.060	298	250	[189]
33	Ginger	0.028	0.387	2.38	0.008	0.059	308	200	[189]
34	Ginger	0.028	0.387	2.38	0.008	0.059	308	250	[189]

4.2 Desarrollo de un método simple para calcular el coeficiente de difusión del extracto en SC-CO_2 (cálculo del número de Schmidt)

En un proceso de extracción SFE, el número de Schmidt (Sc) caracteriza el flujo conectivo, vinculando el coeficiente de difusión de los solutos en el disolvente (D_{12}) con las propiedades fisicoquímicas del medio (densidad ρ y viscosidad μ de la fase fluida):

$$Sc = \frac{\mu}{\rho D_{12}} \qquad \text{(Ecuación 1.28)}$$

Para estimar el coeficiente de difusión de solutos en SC-CO_2 existen muchos modelos teóricos y semi-teóricos disponibles en la bibliografía, todas orientados al cálculo del coeficiente de difusión de compuestos puros. No sólo las ecuaciones de la bibliografía sino también los datos experimentales disponibles corresponden a sistemas binarios componente + CO_2 [190,191].

Estas ecuaciones contienen parámetros puros del soluto (masa molar, volumen crítico, volumen molar a punto de ebullición normal, tensión superficial, etc.) así como propiedades fisicoquímicas del disolvente supercrítico (densidad, viscosidad, parámetros críticos), además de los parámetros específicos de la correlación. En general, cuanto mayor es la precisión del modelo, mayor es el número de parámetros requeridos.

Por ejemplo, la ecuación de Wilke-Chang [130] es una de las correlaciones más populares, con desviaciones promedio de un 10% para 600 datos experimentales de coeficientes de difusión de diferentes tipos de solutos en SC-CO_2. Asimismo, las ecuaciones propuestas recientemente por Magalhães y col. [192] , aplicables a moléculas extremadamente distintas en términos de tamaño, forma y polaridad, presentan desviaciones globales inferiores al 3%, habiendo sido probadas con una gran base de datos (539 sistemas binarios y 8219 datos). Estas ecuaciones se basan en expresiones que dependen únicamente de la temperatura y/o densidad y/o viscosidad del disolvente. No obstante, las ecuaciones implican dos parámetros de ajuste específicos para cada compuesto puro.

A pesar de que existen buenas correlaciones en la bibliografía para representar la difusión de un soluto puro en SC-CO_2, no hay información experimental ni métodos desarrollados para extractos de materiales de origen vegetal, los que, en general, son mezclas multicomponentes.

En esta tesis se estudió las variaciones del coeficiente de difusión de familias de compuestos con afinidad lipídica, presentes en los materiales de origen vegetal y fácilmente extraíbles con SC-CO_2, en función de la temperatura y presión del proceso de extracción. Se estudiaron los monoterpenos y sesquiterpenos, representando a los aceites esenciales, los ácidos grasos, y los triglicéridos representando a los aceites fijos. Cada una de estas familias de compuestos presentan propiedades distintivas en cuanto a tamaño molecular y volatilidad, tal y cómo se resumen en la Tabla 4.4.

Tabla 4.4. Propiedades fisicoquímicas de las familias de compuestos estudiadas en esta Tesis para el cálculo del coeficiente de difusión en SC-CO_2

Familia de compuestos	**Punto normal de ebullición (ºC)**	**Peso molecular ($g \cdot mol^{-1}$)**
Monotepenos y sesquiterpenos (aceites esenciales)	150 - 230	108 - 165
Ácidos grasos	169-450	280 - 356
Triglicéridos (aceites fijos)	> 800	885 - 1137

La recopilación de una gran cantidad de datos experimentales de coeficientes de difusión de componentes puros en SC-CO_2 (170 datos de monoterpenos y sesquiterpenos, 843 datos de ácidos grasos y 178 de triglicéridos) permitió demostrar que las sustancias de la misma familia química, con masa molecular y volatilidad similares, tienen coeficientes de difusión muy similares. Sin embargo, se observaron diferencias significativas entre el coeficiente de difusión de un aceite volátil, un ácido graso y un triglicérido.

Sobre la base de estas observaciones, en esta Tesis se derivaron tres correlaciones generales y simples para estimar el coeficiente de difusión de extractos vegetales tipo, aceites volátiles, ácidos grasos y aceites fijos, en función exclusivamente de la presión y temperatura de extracción. Se consideró un total de 30 diferentes sistemas binarios soluto + SC-CO_2 (1191 datos) y se obtuvieron en todos los casos desviaciones inferiores al 13%.

La figura 4.1 permite interpretar gráficamente los conceptos demostrados en esta Tesis. Se observan los resultados de las correlaciones desarrolladas (líneas punteadas) a temperatura constante de 40 °C (313 K) por familia de compuesto, y se comparan con los datos experimentales de algunas sustancias puras de la familia correspondiente. Como puede

observarse en la figura, a temperatura constante, existen diferencias significativas en función de la presión de los coeficientes de difusión de compuestos de diferente familia, mientras que son mucho menores las diferencias correspondientes a compuestos de una misma familia.

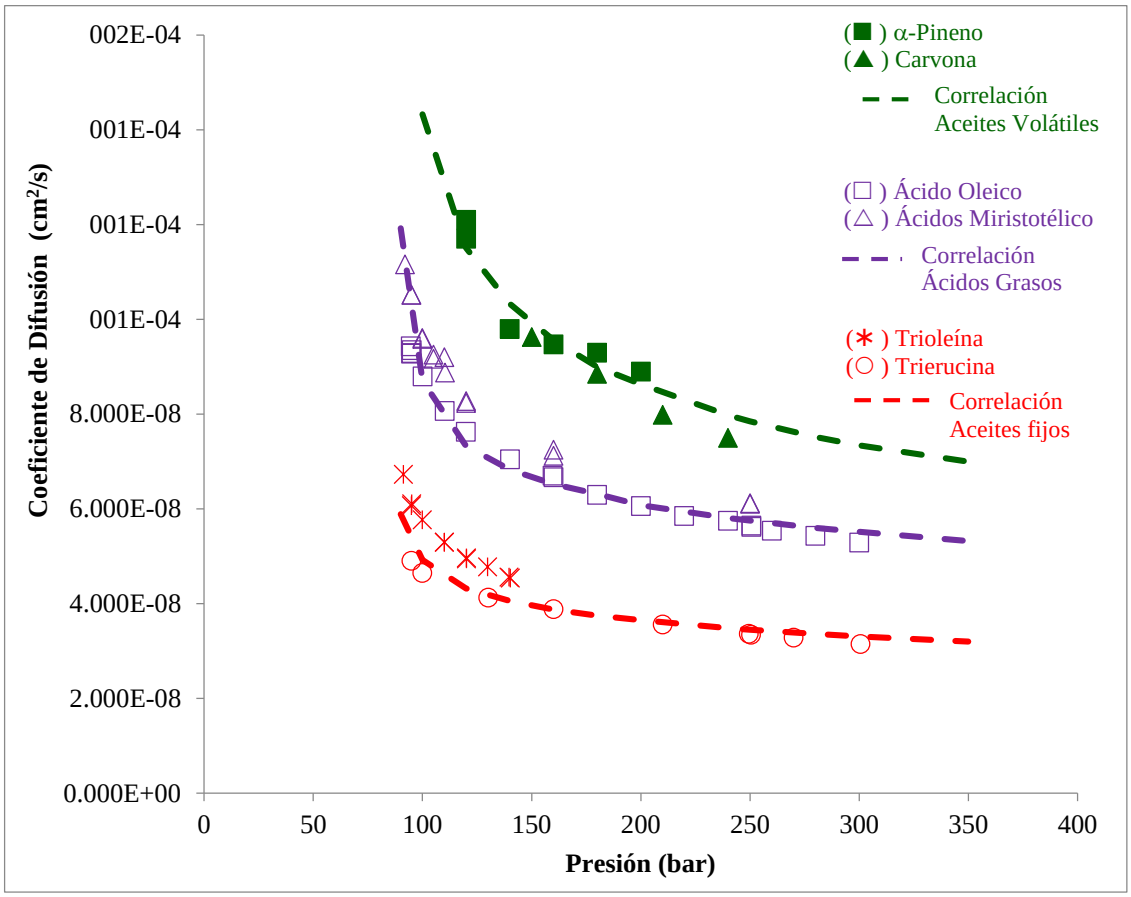

Figura 4.1 Correlaciones generalizadas para la predicción de coeficientes de difusión en CO_2 supercrítico según familia de compuestos a 313 K.

Las correlaciones desarrolladas en esta Tesis para el cálculo del coeficiente de difusión de extractos tipo (aceites esenciales, ácidos grasos y aceites fijos) se encuentran publicadas en el trabajo "Study of the diffusion coefficient of solute-type extracts in supercritical carbon dioxide: Volatile oils, fatty acids and fixed oils" en el Journal of Supercritical Fluids, 109 (2016) 148–156 [109].

4.3 Criterios semi-empíricos de escalado y modelos teóricos para el cálculo del coeficiente de transferencia de masa

El modelo BIC [75,93] se aplicó para representar las cinéticas de extracción de mortiño y caléndula, obtenidas experimentalmente en la Plataforma Novalindus. Las condiciones de extracción de las distintas OECs y los correspondientes coeficientes de transferencia de masa en la fase fluida (k_{YA}) obtenidos, se muestran en la tabla 4.5 para el mortiño y en las tablas 4.6 y 4.7 para la caléndula.

En el procedimiento de escalado, se aplicaron dos reglas de pulgar de la ingeniería, muy utilizadas en la bibliografía, con el objetivo de estimar el caudal de SC-CO_2 necesario al pasar a una celda de extracción pequeña a un mayor tamaño, manteniendo la presión y temperatura de operación, así como el tamaño de partícula del material a extraer y la porosidad del lecho fijo. Los criterios de escalado analizados fueron: (i) mantener la velocidad lineal del SC-CO_2 constante; (ii) mantener el tiempo de residencia del SC-CO_2 constante.

Tabla 4.5 Coeficientes de transferencia de masa en la fase fluida (k_{YA}) ajustados mediante el modelo BIC de las OECs de mortiño obtenidas a 313 K y 300 bar en la unidad de pequeña escala (2.7×10^{-4} m^3) de la Plataforma Novalindus. $\varepsilon = 0.589$; $X_o = 0.0332$; $X_k = 0.0180$.

Volumen (m^3)	2.7×10^{-4}	1.35×10^{-3}	
		velocidad constante	tiempo de residencia constante
F (kg)	0.160	0.800	0.800
Q $\times10^4$ ($kg\cdot s^{-1}$)	5.33	0.13	0.26
$k_{YA} \times 10^2$ (s^{-1})	0.00490	-	0.00490

Tabla 4.6 Coeficientes de transferencia de masa en la fase fluida (k_{YA}) ajustados mediante el modelo BIC de las OECs de caléndula obtenidas a 313 K y diferentes condiciones de presión y caudales de SC-CO_2 en la unidad de pequeña escala de la Plataforma Novalindus. ε = 0.763; X_o = 0.0745; X_k = 0.0450.

Volumen (m^3)	2.7×10^{-4}				
	P = 140 bar			P = 240 bar	P = 340 bar
F (kg)	0.090	0.090	0.090	0.090	0.090
$Q\times10^4$ ($kg\cdot s^{-1}$)	2.5	5.0	7.5	5.0	5.0
$k_{YA}\times10^2$ (s^{-1})	0.420	0.570	0.940	0.97	1.50

Tabla 4.7 Coeficientes de transferencia de masa en la fase fluida (k_{YA}) ajustados mediante el modelo BIC de las OECs de caléndula obtenidas a 140 bar, 313 K y diferentes caudales de SC-CO_2 en las unidades de mayor escala 1.35×10^{-3} y 5.19×10^{-3} m^3 de la Plataforma Novalindus. ε = 0.763; X_o = 0.0745; X_k = 0.0450.

Volumen (m^3)	1.35×10^{-3}		5.19×10^{-3}	
	velocidad constante	tiempo de residencia constante	velocidad constante	tiempo de residencia constante
F (kg)	0.450	0.450	1.710	1.710
$Q\times10^4$ ($kg\cdot s^{-1}$)	6.0	12.3	15.5	47.0
$k_{YA}\times10^2$ (s^{-1})	0.45	0.35	0.33	0.75

Mientras que el modelo BIC predice que el criterio de mantener el tiempo de residencia constante debería ser adecuado para el escaldo de la SFE de ambos materiales (mortiño y caléndula), los resultados experimentales obtenidos en celdas de extracción de escala mayor, demuestras discrepancias con las predicciones del modelo teórico en el caso del escaldo SFE de caléndula. Esto es, al igual que en estudios realizados por otros autores [40,59,63,65], de este análisis se comprueba que, aun habiendo evaluado únicamente dos criterios semi-empíricos para predecir el caudal de SC-CO_2 necesario para ampliar la escala de producción, y habiendo analizado sólo dos materiales vegetales diferentes, no existe un único criterio válido para el escalado SFE.

En el caso del mortiño, el cambio de escala fue de una celda de 2.7×10^{-4} m^3 a una de 1.35×10^{-3} m^3 (factor de escalado = 5). El criterio de mantener el tiempo de residencia constante resultó excelente, reproduciendo muy satisfactoriamente los tiempos de los periodos o etapas de extracción según el modelo BIC (CER, FER, DC) en la celda de extracción de mayor tamaño (ver Figura 3.2).

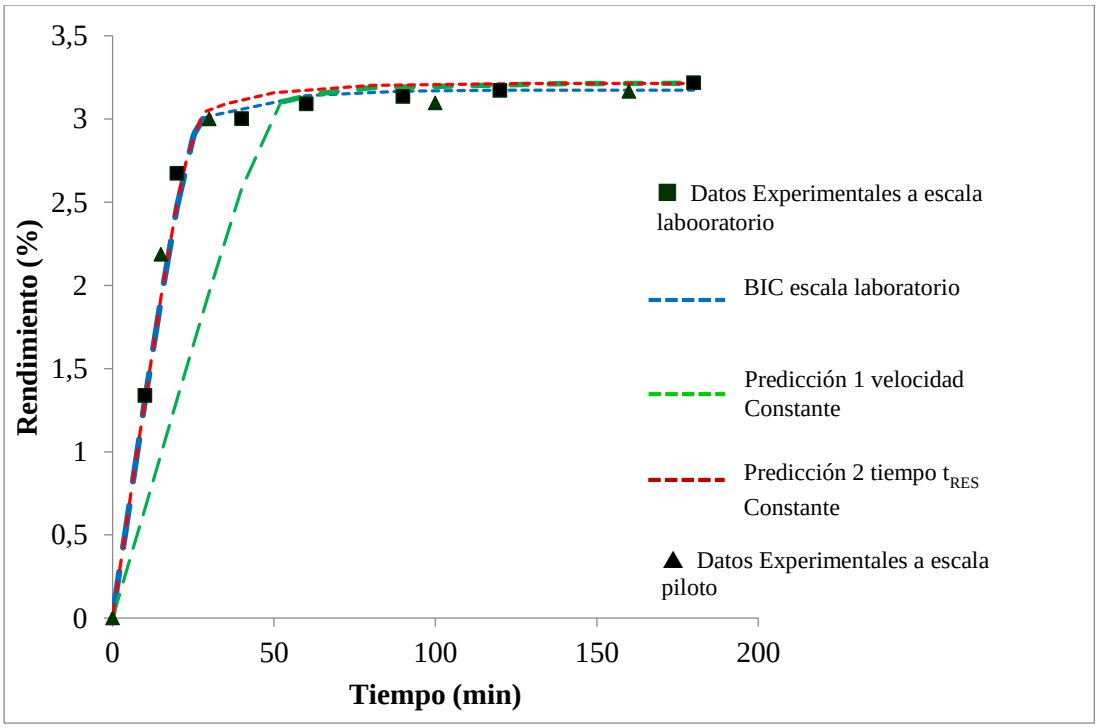

Figura 4.2 Escalado de la SFE de mortiño (*Vaccinium meridionale* Swartz) desde una celda de extracción de 2.7×10^{-4} m^3 (escala laboratorio) a una de 1.35×10^{-3} m^3 (escala piloto). Las líneas corresponden al ajuste y/o predicciones del modelo BIC y los símbolos a los datos experimentales obtenidos en cada una de las unidades.

Los resultados del escalado de mortiño se publicaron en el artículo "*Vaccinium meridionale* Swartz Supercritical CO_2 Extraction: Effect of Process Conditions and Scaling Up" Materials, 9:519 (2016) 1-10 [193].

En cuanto a los ensayos SFE de caléndula obtenidos a escala laboratorio (2.7×10^{-4} m^3) se observó un notable efecto de la presión sobre el rendimiento de extracción a temperatura y caudal de CO_2 constantes, con rendimientos de extracción considerablemente mayores a los reportados por otros autores, como el caso de Campos y col. [194], en el mismo rango de temperatura y presión. Las diferencias encontradas en estos resultados pueden ser consecuencia una mayor relación entre el caudal de CO_2 y la cantidad de materia prima

utilizada, así como el origen de la planta y el proceso de acondicionamiento previo a la extracción. Todas las cinéticas de extracción experimentales de caléndula, obtenidas en las diferentes escalas de producción, se ajustaron satisfactoriamente al modelo BIC con errores menores a 11.4%, y obteniéndose los correspondientes coeficientes de transferencia de masa en fase fluida (k_{YA}).

En el estudio del escaldo, se aplicaron también los criterios de velocidad constante o tiempo de residencia constante, y se llevó a cabo experimentalmente a 140 bar y 313 K desde la celda de extracción pequeña de 2.7×10^{-4} m^3 a celdas de mayor tamaño, de 1.35×10^{-3} m^3 (factor de escalado = 5) y 5.16×10^{-3} m^3 (factor de escalado = 19) respectivamente. Si bien según el modelo BIC, el criterio de mantener constante el tiempo de residencia del SC-CO_2 debería proporcionar una muy buena estimación del caudal de disolvente para ambos factores de escalado (igual que en el caso del mortiño), los resultados experimentales de SFE de caléndula no concuerdan en ninguna de las dos escalas con la predicción teórica. Más aún, en el caso de un factor de escala de 5 el criterio de tiempo de residencia constante resultó ser el más aproximado, mientras que el criterio de mantener constante la velocidad del SC-CO_2 fue más acertado para el factor de escala de 19. Las figuras 3.3. y 3.4 muestran gráficamente estos resultados.

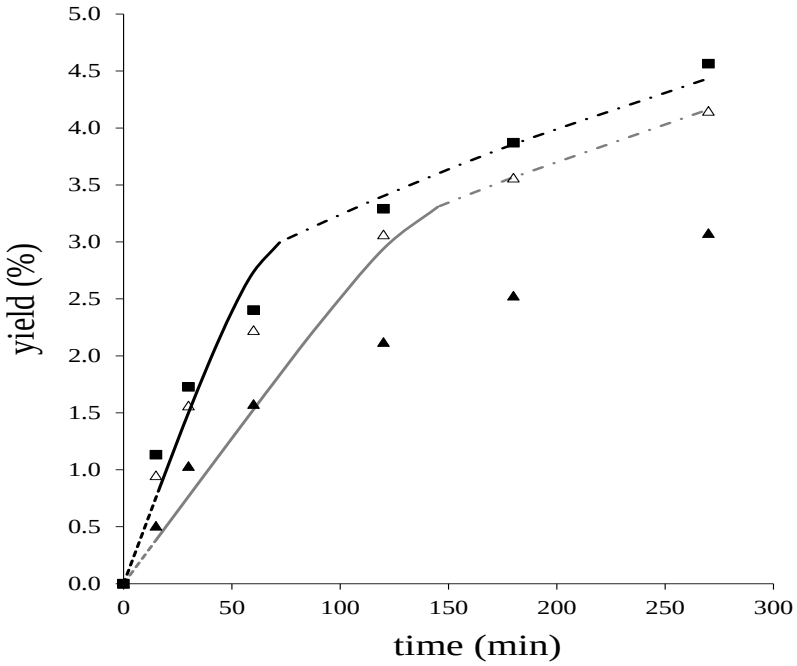

Figura 4.3 Estudio del escalado SFE de caléndula a 313 K, 14 MPa y porosidad del lecho constante (ε = 0.763) a partir de una celda V_A (2.7×10^{-4} m^3) hasta una V_B (1.35×10^{-3} m^3), empleando un factor de escalado de 4.95. Líneas grises y negras representan las predicciones del modelo BIC utilizando los criterios de mantener la velocidad lineal constante (Ecuación (1.6)) y mantener constante el tiempo de residencia (Ecuación (1.5)), respectivamente: (---) etapa CER; (––) etapa FER; (–·–) etapa DC. Símbolos representan los datos experimentales: (■) escala laboratorio V_A, $Q = 2.5\times10^{-4}$ $kg\cdot s^{-1}$; (▲) escala piloto, V_B, utilizando la Ecuación (1.5); (△) escala piloto, V_B, utilizando la Ecuación (1.6).

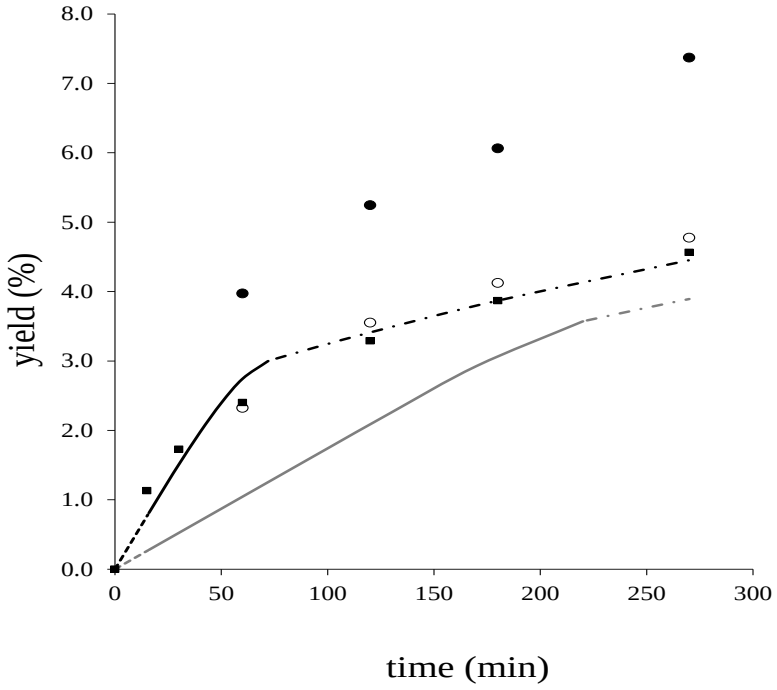

Figura 4.4 Escalado SFE de caléndula a 313 K, 14 MPa y porosidad del lecho constante (ε = 0.763) desde una celda V_A (2.7×10^{-4} m^3) hasta V_C (5.16×10^{-3} m^3), utilizando un factor de escalado de 19.08). Líneas grises y negras representan las predicciones del modelo BIC utilizando la Ecuación 1.6 y 1.5, respectivamente: (---) etapa CER; (––) etapa FER; (–·–) etapa DC. Símbolos representan datos experimentales: (■) V_A, $Q = 2.5\times10^{-4}$ $kg\cdot s^{-1}$; (○) V_C, Ecuación. (1.5); (●) V_C, Ecuación (1.6).

Los resultados vinculados al estudio del escalado SFE de caléndula han sido publicados en el artículo "Supercritical carbon dioxide extraction of Calendula officinalis: kinetic modeling and scaling up study", Journal of Supercritical Fluids (2017) (en prensa) [187].

4.4 Desarrollo de una correlación generalizada para relacionar el coeficiente de transferencia de masa del proceso de extracción con el caudal de CO_2

Teniendo en cuenta que ninguno de los criterios semi-empíricos utilizados para predecir el caudal de SC-CO_2 en los procesos de escalado estudiados (mortiño y caléndula) fue completamente satisfactorio, se planteó generar una correlación generalizada entre el coeficiente de transferencia de masa del proceso de extracción y el caudal de CO_2, teniendo en cuenta también otras importantes variables de la extracción, tales como la geometría de

la celda y las condiciones de temperatura y presión, que definen la densidad y viscosidad del SC-CO_2, así como el comportamiento difusivo del extracto.

En primer lugar, se consideraron todas las cinéticas de extracción obtenidas para la caléndula (nueve en total), en las diferentes condiciones de temperatura y presión de extracción experimentales, y en las tres diferentes escalas de producción utilizadas. Los coeficientes de trasferencia de masa del modelo BIC (k_{YA}) pudieron ser vinculados con el caudal de SC-CO_2 (Q) con un alto grado de correlación ($R^2 = 0.9767$) cuando se consideraron también las variables geométricas de la celda de extracción (D y L) así como el número de Schmidt. Estos resultados se incluyen en el trabajo publicado y citado anteriormente ("Supercritical carbon dioxide extraction of Calendula officinalis: kinetic modeling and scaling up study", Journal of Supercritical Fluids (2017) (en prensa) [187]).

No obstante, con miras a extender esta correlación a otros materiales y a otras unidades de extracción de la bibliografía, fue necesario aplicar un modelo más simple para determinar el coeficiente de transferencia de masa, puesto que el modelo BIC demanda el conocimiento de ciertas propiedades del material vegetal muchas veces no disponibles en las OECs reportadas en la bibliografía, como por ejemplo la densidad del material vegetal y/o el grado de rotura de la pared exterior (células rotas).

Así, se utilizó el modelo de Barton, descrito en la Introducción de esta Tesis, como un método sencillo matemáticamente y muy práctico (sólo demandara los datos cinéticos) para estimar el coeficiente de transferencia de masa:

$$Y = Y_\infty(1 - exp\{-kt\}) \qquad \text{(Ecuación 1.8)}$$

Donde $\boldsymbol{Y}$ es el rendimiento de extracción (kg/kg), t es el tiempo, Y_∞ es el valor de rendimiento para un tiempo de extracción infinito ($t \to \infty$) y k es la constante cinética de Barton. Al representar gráficamente $ln(1 - Y/Y_\infty)$ vs t es posible mediante una regresión lineal ajustar simultáneamente los parámetros k y Y_∞ para minimizar el coeficiente de la regresión. Así, se ajustaron al modelo de Barton todas las OECs obtenidas experimentalmente en esta Tesis, así como las obtenidas de la bibliografía, determinando en cada caso los correspondientes parámetros k y Y_∞.

Se demostró que la correlación desarrollada utilizando los k_{YA} del modelo BIC para las OECs de caléndula ($R^2 = 0.9767$) mantuvo un alto grado de correlación ($R^2 = 0.9906$)

cuando los k_{YA} fueron reemplazados por los coeficiente k de Barton ajustados (ver figura 3.5).

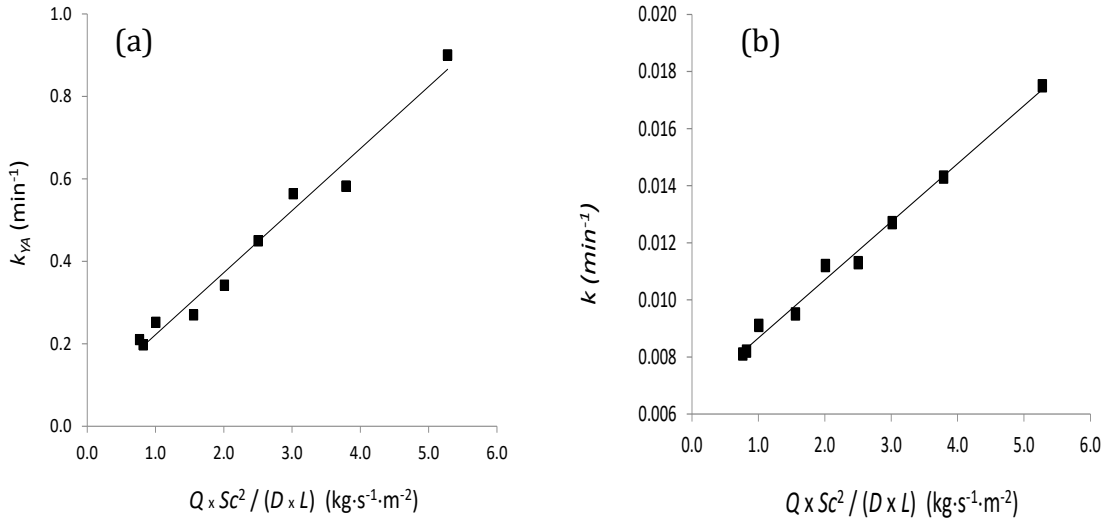

Figura 4.5 Correlación entre el coeficiente de trasferencia de masa y el caudal de SC-CO_2 (Q) de nueve OECs de caléndula obtenidas en diferentes condiciones de extracción y en diferentes escalas de producción, pero manteniendo constante el tamaño de partícula del material y la porosidad del lecho fijo. (a) Coeficientes de transferencia de masa según el modelo BIC ($R^2 = 0.9767$); (b) Coeficientes de transferencia de masa según el modelo de Barton ($R^2 = 0.9906$).

Para extender esta correlación a otras cinéticas de extracción obtenidas en la Plataforma Novalindus para otros materiales vegetales (en total 19 OECs) fue necesario considerar tanto el tamaño de partícula (d_p) como la porosidad del lecho fijo (ε), tal y como se muestra en la figura 3.6.

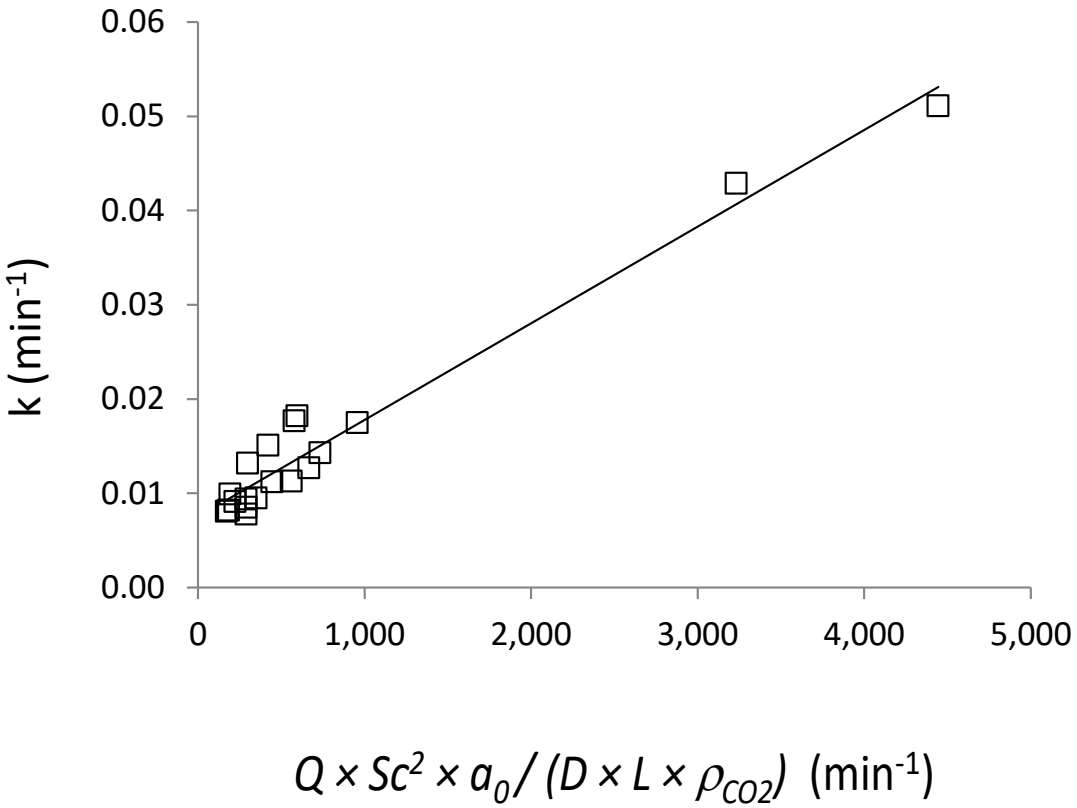

Figura 4.6 Correlación entre la constante cinética de Barton (k) y el caudal de SC-CO_2 (Q) de 19 OECs obtenidas en la Plataforma Novalindus, en diferentes condiciones de extracción y escalas de producción, de 7 materiales vegetales diferentes, porosidades en el rango 0.59-0.82 y tamaños de partícula entre 250 y 1000 µm. $R^2 = 0.9624$.

El alto grado de correlación obtenido ($R^2 = 0.9624$) permiten suponer que esta correlación puede ser una herramienta útil en el escalado de la SFE dentro de las unidades de la Plataforma Novalindus. No obstante, la extensión de la correlación a otras 34 OECs obtenidas de la bibliografía, abarcando 10 materiales vegetales diferentes, temperaturas en el rango de 298-333 K, presiones de 100-300 bar, tamaños de partícula entre 250 a 1400 µm, celdas de extracción entre 50 y 5200 cm^3 y porosidades en el rango de 0.59-0.97, redujo el coeficiente de regresión a $R^2 = 0.8651$.

CAPÍTULO 5.

CONCLUSIONES

5. CONCLUSIONES

Sobre los estudios de escaldo de mortiño y caléndula

En esta Tesis se ha estudiado el escalado del proceso en *batch* de la extracción supercrítica con SC-CO_2 de dos materiales vegetales (mortiño y caléndula) utilizando tres escalas de producción de la Plataforma Novalindus del CIAL (UAM-CSIC), combinando el modelo teórico BIC, para representar y predecir la transferencia de materia y el comportamiento cinético, con dos reglas de pulgar de la ingeniería, mantener la velocidad lineal o el tiempo de residencia del SC-CO_2 constante.

➔ El modelo BIC ha sido capaz de representar satisfactoriamente todas las cinéticas de extracción obtenidas experimentalmente, para los dos materiales estudiados, abarcando lechos fijos de 0.27 a 5.20 litros, presiones de 140 a 340 bar, caudales de SC-CO_2 de 15 a 280 g/min, con errores inferiores a 11%.

➔ Aunque el modelo BIC predice que el criterio de mantener constante el tiempo de residencia del SC-CO_2 debería ser apropiado para escalar cualquiera de los dos procesos estudiados, los resultados experimentales demuestran que sólo en el caso del mortiño el criterio es adecuado, mientras que en el escalado de caléndula existen diferencias significativas respecto de cualquiera de los dos criterios aplicados.

Sobre el cálculo del coeficiente de difusión y el coeficiente de transferencia de masa

Con el objetivo de desarrollar una correlación con capacidad de abarcar ambos estudios de escalado se desarrollaron métodos simples para estimar los principales parámetros del proceso de extracción: el coeficiente de difusión y el coeficiente de transferencia de masa (k) del extracto en SC-CO_2.

➔ Se ha demostrado que el coeficiente de difusión de los solutos en SC-CO_2 depende fuertemente del tipo de sustancias que se extrae, así como de la temperatura y de la presión de extracción. Así, se han desarrollado en esta Tesis correlaciones generalizadas para calcular el coeficiente de difusión de un extracto tipo (aceites esenciales, ácidos grasos o aceites fijos) en función únicamente de la temperatura y de la presión. Estas correlaciones simples conservan buena precisión cuando se las compara con otros métodos más complejos y/o que demandan varios parámetros.

➔ El modelo de Barton, por su simplicidad, permitió estimar el coeficiente de transferencia de masa utilizando únicamente los datos cinéticos, asimilando la curva de extracción (OEC) a una cinética de primer orden. Así, se calculó *k* para las 11 OECs obtenidas en esta Tesis y fue posible extender la base de datos, compilando de la bibliografía otras 8 OECs obtenidas en Novalindus en trabajos previos a esta Tesis y 34 OECs de otros autores.

Sobre el desarrollo de una correlación generalizada para el escaldo de la SFE

Utilizando las correlaciones generalizadas desarrolladas en esta Tesis para calcular el coeficiente de difusión, y ecuaciones de la bibliografía para la densidad y viscosidad del SC-CO_2, fue posible estimar el número de Schmidt (*Sc*) del proceso. Este número adimensional resultó fundamental para correlacionar el coeficiente de transferencia de masa de las OECs con el caudal de SC-CO_2 (Q) utilizado en el proceso de extracción, así como con las variables geométricas del lecho fijo, diámetro (D) y longitud (L) de la celda de extracción.

➔ Para las 9 OECs de caléndula, obtenidas en distintas condiciones y escalas, pero siendo constante el tamaño de partícula (d_p) y la porosidad del lecho (ε), se ha desarrollado en esta Tesis una relación entre el coeficiente de trasferencia de masa, sea calculado por el modelo BIC o por el modelo de Barton, con el caudal de SC-CO_2. La regresión lineal, k vs. $Q \times {S_C}^2/(D \times L)$, fue de R^2 = 0.9676 en el caso de correlacionar los coeficientes de transferencia de masa del modelo BIC y R^2 = 0.9906 para el modelo de Barton.

➔ La extensión de esta relación para abarcar las OECs de mortiño y de otros materiales extraídos en la Plataforma Novalindus (romero, tomillo, orégano, salvia y milenrama) pudo llevarse a cabo al incluir d_p y ε como variables característicos del material vegetal, manteniéndose un alto grado de correlación (R^2 = 0.9624). No obstante, si bien puede observarse una tendencia general positiva, la aplicación de esta correlación a toda la base de datos (19 OECs Novalindus + 34 OECs de otros autores) redujo el coeficiente de regresión a R^2 = 0.8651.

Así, como conclusión general, se deriva de esta Tesis una correlación práctica, matemáticamente simple de aplicar, que demanda pocos parámetros, con alto grado de regresión abarcando todas las cinéticas de extracción obtenidas en la Plataforma Novalindus, y que constituye una herramienta de base para continuar el análisis del escalado de procesos SFE de materiales de origen vegetal. Esta correlación podrá ser utilizada para estimar el caudal de SC-CO_2 para realizar un cambio de escala dentro de la Plataforma Novalindus, y será modulada conforme los resultados y la ampliación de la base de datos.

BIBLIOGRAFÍA

6. BIBLIOGRAFÍA

[1] M. V. Palmer, S.S.T. Ting, Applications for supercritical fluid technology in food processing, Food Chem. 52 (1995) 345–352. doi:10.1016/0308-8146(95)93280-5.

[2] J.J. a Barry, M.M.C.G. Silva, V.K. Popov, K.M. Shakesheff, S.M. Howdle, Supercritical carbon dioxide: putting the fizz into biomaterials., Philos. Trans. A. Math. Phys. Eng. Sci. 364 (2006) 249–261. doi:10.1098/rsta.2005.1687.

[3] E. Reverchon, Supercritical fluid extraction and fractionation of essential oils and related products, J. Supercrit. Fluids. 10 (1997) 1–37. doi:10.1016/S0896-8446(97)00014-4.

[4] G. Brunner, Supercritical fluids: Technology and application to food processing, J. Food Eng. 67 (2005) 21–33. doi:10.1016/j.jfoodeng.2004.05.060.

[5] R.C. Reid, J.M. Prausnitz, B.E. Poling, The properties of gases and liquids, 4th ed., McGraw-Hill, Inc, New York, 1987.

[6] M.A. Mchugh, V.J. Krukonis, Supercritical Fluid Extraction - Principals and Practice, 2nd ed., Butterworth-Heinemann, Newton, MA, 1994.

[7] D.R. Lide, Handbook of Chemistry and Physics, 84th ed., CRC Press, Boca Raton, FL, 2003. doi:10.1136/oem.53.7.504.

[8] G. Della Porta, R. Taddeo, E. D'Urso, E. Reverchon, Isolation of Clove Bud and Star Anise Essential Oil by Supercritical CO2Extraction, LWT - Food Sci. Technol. 31 (1998) 454–460. doi:10.1006/fstl.1998.0381.

[9] C. Tzia, G. Liadakis, Extraction Optimization in Food Engineering, Marcel Dekker, Inc., New York, NY, 2003. doi:10.1201/9780824756185.

[10] SFI, Le portal des fluides supercritiques, Superctitical Fluids Innov. Supercrit. Fluids Appl. (2017). http://www.supercriticalfluid.org/Applications.149.0.html (accessed March 6, 2017).

[11] E. Schütz, Supercritical fluids and applications - A patent review, Chem. Eng. Technol. 30 (2007) 685–688. doi:10.1002/ceat.200600297.

[12] G. L. Zabot, M. N. Moraes, M. Angela A. Meireles, Supercritical Technology Applied to the Production of Bioactive Compounds: Research Studies Conducted at LASEFI from 2009 to 2013, Food Public Heal. 4 (2014) 36–48. doi:10.5923/j.fph.20140402.04.

[13] S. Quispe-Condori, D. Sánchez, M. a. Foglio, P.T.V. Rosa, C. Zetzl, G. Brunner, M.A. a. Meireles, Global yield isotherms and kinetic of artemisinin extraction from Artemisia annua L leaves using supercritical carbon dioxide, J. Supercrit. Fluids. 36 (2005) 40–48. doi:10.1016/j.supflu.2005.03.003.

[14] M.R. García-Risco, E.J. Hernández, G. Vicente, T. Fornari, F.J. Señoráns, G. Reglero, Kinetic study of pilot-scale supercritical CO2 extraction of rosemary (Rosmarinus officinalis) leaves, J. Supercrit. Fluids. 55 (2011) 971–976. doi:10.1016/j.supflu.2010.09.030.

[15] L.S. Moura, R.N. Carvalho Jr., M.B. Stefanini, L.C. Ming, M.A. a. Meireles, Supercritical fluid extraction from fennel (Foeniculum vulgare): global yield, composition and kinetic data, J. Supercrit. Fluids. 35 (2005) 212–219. doi:10.1016/j.supflu.2005.01.006.

[16] G. Vicente, S. Molina, M. González-Vallinas, M.R. García-Risco, T. Fornari, G. Reglero, A.R. de Molina, Supercritical rosemary extracts, their antioxidant activity and effect on hepatic tumor progression, J. Supercrit. Fluids. 79 (2013) 101–108. doi:10.1016/j.supflu.2012.07.006.

[17] J.M. Pinilla, A. López-Padilla, G. Vicente, T. Fornari, J.C.- Quintela, G. Reglero, Recovery of betulinic acid from plane tree (*Platanus acerifolia* L.), J. Supercrit. Fluids. 95 (2014) 541–545. doi:10.1016/j.supflu.2014.09.001.

[18] M.M.R. De Melo, R.M.A. Domingues, M. Sova, E. Lack, H. Seidlitz, F. Lang, A.J.D. Silvestre, C.M. Silva, Scale-up studies of the supercritical fluid extraction of triterpenic acids from *Eucalyptus globulus* bark, J. Supercrit. Fluids. 95 (2014) 44–50. doi:10.1016/j.supflu.2014.07.030.

[19] A.R. Kamarei, Supercritical fluid extraction of animal derived materials, 4749522, 1981.

[20] H. Sovová, B.P. Nobre, A. Palavra, Modeling of the kinetics of supercritical fluid extraction of lipids from microalgae with emphasis on extract desorption, Materials (Basel). 9 (2016). doi:10.3390/ma9060423.

[21] J. Paes, R. Dotta, G.F. Barbero, J. Martínez, Extraction of phenolic compounds and anthocyanins from blueberry (*Vaccinium myrtillus* L.) residues using supercritical CO2 and pressurized liquids, J. Supercrit. Fluids. 95 (2014) 8–16. doi:10.1016/j.supflu.2014.07.025.

[22] A. López-Padilla, A. Ruiz-Rodriguez, C. Restrepo Flórez, D. Rivero Barrios, G. Reglero, T. Fornari, *Vaccinium meridionale* Swartz Supercritical CO2 Extraction: Effect of Process Conditions and Scaling Up, Materials (Basel). 9 (2016) 519. doi:10.3390/ma9070519.

[23] M.T. Fernández-Ponce, B.R. Parjikolaei, H.N. Lari, L. Casas, C. Mantell, E.J. Martínez de la Ossa, Pilot-plant scale extraction of phenolic compounds from mango leaves using different green techniques: Kinetic and scale up study, Chem. Eng. J. 299 (2016) 420–430. doi:10.1016/j.cej.2016.04.046.

[24] P.G.M. Haring, Process for the extraction of lactones from lipid material and use of the extract thus obtained for flavouring foodstuffs, EP87202559, 1989.

[25] Z. Zeković, O. Bera, S. Đurović, B. Pavlić, Supercritical fluid extraction of coriander seeds: Kinetics modelling and ANN optimization, J. Supercrit. Fluids. 125 (2017) 88–95. doi:10.1016/j.supflu.2017.02.006.

[26] C.M.P. Sarmento, S.R.S. Ferreira, H. Hense, Supercritical fluid extraction (SFE) of rice bran oil to obtain fractions enriched with tocopherols and tocotrienols, Brazilian J. Chem. Eng. 23 (2006) 243–249. doi:10.1590/S0104-66322006000200012.

[27] J.W. King, Modern supercritical fluid technology for food applications., Annu. Rev. Food Sci. Technol. 5 (2014) 215–38. doi:10.1146/annurev-food-030713-092447.

[28] J.M. Del Valle, Extraction of natural compounds using supercritical CO2: Going from the laboratory to the industrial application, J. Supercrit. Fluids. 96 (2014) 180–199. doi:10.1016/j.supflu.2014.10.001.

[29] G. Brunner, Gas extraction: an introduction to fundamentals of supercritical fluids and the application to separation process, Springer, Hamburg, 1994.

[30] H. Sovová, Rate of the vegetable oil extraction with supercritical CO2—I. Modelling of extraction curves, Chem. Eng. Sci. 49 (1994) 409–414. doi:10.1016/0009-2509(94)87012-8.

[31] M.A.A. Meireles, Extraction of Bioactive Compounds from Latin American Plants, in: J.L. Martínez (Ed.), Supercrit. Fluid Extr. Nutraceuticals Bioact. Compd., CRC Press, Boca Raton, FL, 2008: pp. 243–274.

[32] J.M. Del Valle, P. Napolitano, N. Fuentes, Estimation of relevant mass transfer parameters for the extraction of packed substrate beds using supercritical fluids, Ind. Eng. Chem. Res. 39 (2000) 4720–4728. doi:10.1021/ie000034f.

[33] E. Reverchon, C. Marrone, Modeling and simulation of the supercritical CO2 extraction of vegetable oils, J. Supercrit. Fluids. 19 (2001) 161–175. doi:10.1016/S0896-8446(00)00093-0.

[34] J. Martínez, Extração de Óleos Voláteis e Outros Compostos com CO 2 Supercrítico : Desenvolvimento de uma Metodologia de Aumento de Escala a partir da Modelagem Matemática do Processo e Avaliação dos Extratos Obtidos, Universidad Estadual de Campinas, 2005.

[35] M.M.R. De Melo, A.J.D. Silvestre, C.M. Silva, Supercritical fluid extraction of vegetable matrices: Applications, trends and future perspectives of a convincing green technology, J. Supercrit. Fluids. 92 (2014) 115–176. doi:10.1016/j.supflu.2014.04.007.

[36] M. Al-Jabari, Kinetic models of supercritical fluid extraction, J. Sep. Sci. 25 (2002) 477–489. doi:10.1002/1615-9314(20020601)25:8<477::AID-JSSC477>3.0.CO;2-C.

[37] C. Zetzl, G. Brunner, STANDARDIZED SFE- UNIT FOR UNIVERSITY EDUCATION AND RESEARCH, (n.d.).

[38] M.A. a. Meireles, Supercritical extraction from solid: process design data (2001–2003), Curr. Opin. Solid State Mater. Sci. 7 (2003) 321–330. doi:10.1016/j.cossms.2003.10.008.

[39] J.M. Del Valle, M. Jiménez, J.C. De la Fuente, Extraction kinetics of pre-pelletized jalapeño peppers with supercritical CO2, J. Supercrit. Fluids. 25 (2003) 33–44. doi:10.1016/S0896-8446(02)00090-6.

[40] T.M. Takeuchi, Supercritical extraction of macela, clove and vetiver: technological and economical aspects, State University of Campinas, 2009.

[41] J.M. Prado, I. Dalmolin, N.D.D. Carareto, R.C. Basso, A.J.A. Meirelles, J. Vladimir Oliveira, E. a. C. Batista, M.A.A. Meireles, Supercritical fluid extraction of grape seed: Process scale-up, extract chemical composition and economic evaluation, J. Food Eng. 109 (2012) 249–257. doi:10.1016/j.jfoodeng.2011.10.007.

[42] J.M. Del Valle, O. Rivera, M. Mattea, L. Ruetsch, J. Daghero, A. Flores, Supercritical CO2 processing of pretreated rosehip seeds: Effect of process scale on oil extraction kinetics, J. Supercrit. Fluids. 31 (2004) 159–174. doi:10.1016/j.supflu.2003.11.005.

[43] M. Perrut, J.-Y. Clavier, Supercritical Fluid Formulation: Process Choice and Scale-up, Ind. Eng. Chem. Res. 42 (2003) 6375–6383. doi:10.1021/ie030144x.

[44] P. Zacchi, A. Pietsch, S. Voges, A. Ambrogi, R. Eggers, P. Jaeger, Concepts of phase separation in supercritical processing, Chem. Eng. Process. Process Intensif. 45

(2006) 728–733. doi:10.1016/j.cep.2006.03.006.

[45] M. Perrut, Supercritical Fluid Applications: Industrial Developments and Economic Issues, Ind. Eng. Chem. Res. 39 (2000) 4531–4535. doi:10.1021/ie000211c.

[46] J.M. Del Valle, J.C. De la Fuente, D. a. Cardarelli, Contributions to supercritical extraction of vegetable substrates in Latin America, J. Food Eng. 67 (2005) 35–57. doi:10.1016/j.jfoodeng.2004.05.051.

[47] P. Kotnik, M. Škerget, Ž. Knez, Supercritical fluid extraction of chamomile flower heads: Comparison with conventional extraction, kinetics and scale-up, J. Supercrit. Fluids. 43 (2007) 192–198. doi:10.1016/j.supflu.2007.02.005.

[48] J. Martinez, A.R. Monteiro, P.T.V. Rosa, M.O.M. Marques, M.A. Meireles, Multicomponent model to describe extraction of ginger oleoresin with supercritical carbon dioxide, Ind. Eng. Chem. Res. 42 (2003) 1057–1063. doi:Doi 10.1021/Ie020694f.

[49] D.R. Woods, Rules of Thumb in Engineering Practice, Wiley-VCH, Weinheim, 2007. doi:10.1002/9783527611119.

[50] S. Hall, Rules of Thumb for Chemical Engineers, 5th ed., Elsevier Inc., Waltham, MA, 2012. doi:10.1016/B978-0-12-387785-7.00001-3.

[51] E. Merhej, S. Schockaert, M. De Cock, Repairing inconsistent answer set programs using rules of thumb: A gene regulatory networks case study, Int. J. Approx. Reason. 83 (2017) 243–264. doi:10.1016/j.ijar.2017.01.012.

[52] M. Athar, M.Y. Lone, P.C. Jha, First protein drug target's appraisal of lead-likeness descriptors to unfold the intervening chemical space, J. Mol. Graph. Model. 72 (2017) 272–282. doi:10.1016/j.jmgm.2016.12.019.

[53] N. Wyttenbach, M. Kuentz, Glass-forming ability of compounds in marketed amorphous drug products, Eur. J. Pharm. Biopharm. 112 (2017) 204–208. doi:10.1016/j.ejpb.2016.11.031.

[54] R.T. Driessen, P. Kamphuis, L. Mathijssen, R. Zhang, L.G.J. van der Ham, H. van den Berg, A.J. Zeeuw, Industrial Process Design for the Production of Aniline by Direct Amination, Chem. Eng. Technol. (2017) 1–10. doi:10.1002/ceat.201600635.

[55] A. Pecher, J.P. Kofoed, Handbook of Ocean Wave Energy, 2017. doi:10.1007/978-3-319-39889-1.

[56] J. Gali, J.D. Lopez-Salido, J. Valles, Rule-of-Thumb Consumers and the Design of Interest Rate Rules, J. Money, Credit Bank. 36 (2004) 739–763. doi:10.3386/w10392.

[57] J.D. Amato, T. Laubach, Rule-of-thumb behaviour and monetary policy, Eur. Econ.

Rev. 47 (2003) 791–831. doi:10.1016/S0014-2921(02)00270-2.

[58] N. Mezzomo, J. Martínez, S.R.S. Ferreira, Supercritical fluid extraction of peach (Prunus persica) almond oil: Kinetics, mathematical modeling and scale-up, J. Supercrit. Fluids. 51 (2009) 10–16. doi:10.1016/j.supflu.2009.07.008.

[59] G.L. Zabot, M.N. Moraes, M.A.A. Meireles, Influence of the bed geometry on the kinetics of rosemary compounds extraction with supercritical CO2, J. Supercrit. Fluids. 94 (2014) 234–244. doi:10.1016/j.supflu.2014.07.020.

[60] G.L. Zabot, M.N. Moraes, A.J. Petenate, M.A. Meireles, Influence of the bed geometry on the kinetics of the extraction of clove bud oil with supercritical CO2, J. Supercrit. Fluids. 93 (2014) 56–66. doi:10.1016/j.supflu.2013.10.001.

[61] L. Casas, C. Mantell, M. Rodríguez, A. Torres, F.A. Macías, E.J.M. de la Ossa, SFE kinetics of bioactive compounds from Helianthus annuus L, J. Sep. Sci. 32 (2009) 1445–1453. doi:10.1002/jssc.200800663.

[62] P.T.V. Rosa, M.A. a. Meireles, Rapid estimation of the manufacturing cost of extracts obtained by supercritical fluid extraction, J. Food Eng. 67 (2005) 235–240. doi:10.1016/j.jfoodeng.2004.05.064.

[63] R.N. Carvalho, L.S. Moura, P.T. V Rosa, M.A.A. Meireles, Supercritical fluid extraction from rosemary (Rosmarinus officinalis): Kinetic data, extract's global yield, composition, and antioxidant activity, J. Supercrit. Fluids. 35 (2005) 197–204. doi:10.1016/j.supflu.2005.01.009.

[64] J.M. Prado, Scale-up study of supercritical fluid extraction process in fixed bed, State University of Campinas, 2010.

[65] J. Martínez, P.T.V. Rosa, M.A.A. Meireles, Extraction of Clove and Vetiver Oils with Supercritical Carbon Dioxide: Modeling and Simulation, Open Chem. Eng. J. 1 (2007) 1–7. doi:10.2174/1874123100701010001.

[66] S. Quispe-Condori, M. a. Foglio, P.T.V. Rosa, M.A. a. Meireles, Obtaining β-caryophyllene from Cordia verbenacea de Candolle by supercritical fluid extraction, J. Supercrit. Fluids. 46 (2008) 27–32. doi:10.1016/j.supflu.2008.02.015.

[67] O. Yesil-Celiktas, F. Otto, S. Gruener, H. Parlar, Determination of extractability of pine bark using supercritical CO2 extraction and different solvents: Optimization and prediction, J. Agric. Food Chem. 57 (2009) 341–347. doi:10.1021/jf8026414.

[68] C.L.C. Albuquerque, M.A.A. Meireles, Defatting of annatto seeds using supercritical carbon dioxide as a pretreatment for the production of bixin: Experimental, modeling and economic evaluation of the process, J. Supercrit. Fluids. 66 (2012) 86–94.

doi:10.1016/j.supflu.2012.01.004.

[69] X. Han, L. Cheng, R. Zhang, J. Bi, Extraction of safflower seed oil by supercritical CO2, J. Food Eng. 92 (2009) 370–376. doi:10.1016/j.jfoodeng.2008.12.002.

[70] T. Hatami, M.A.A. Meireles, G. Zahedi, Mathematical modeling and genetic algorithm optimization of clove oil extraction with supercritical carbon dioxide, J. Supercrit. Fluids. 51 (2010) 331–338. doi:10.1016/j.supflu.2009.10.001.

[71] A. Berna, A. Tárrega, M. Blasco, S. Subirats, Supercritical CO2 extraction of essential oil from orange peel: effect of the height of the bed, J. Supercrit. Fluids. 18 (2000) 227–237.

[72] M. Perrut, J.-Y. Clavier, M. Poletto, E. Reverchon, Mathematical Modeling of Sunflower Seed Extraction by Supercritical CO2, Ind. Eng. Chem. Res. 36 (1997) 430–435. doi:10.1021/ie960354s.

[73] E.L.G. Oliveira, A.J.D. Silvestre, C.M. Silva, Review of kinetic models for supercritical fluid extraction, Chem. Eng. Res. Des. 89 (2011) 1104–1117. doi:10.1016/j.cherd.2010.10.025.

[74] L.S. Moura, Obtenção por extração supercrítica do extrato de funcho (Foeniculum vulgare): determinação das isotermas de rendimento global, de parâmetros cinéticos e do equilíbrio de fases, Universidad Estadual de Campinas, 2004.

[75] H. Sovova, Broken and intact cell model for supercritical fluid extraction: its origin and limits, J. Supercrit. Fluids. (2017) 1–14. doi:10.1016/j.supflu.2017.02.014.

[76] S.N. Naik, H. Lentz, R.C. Maheshwari, Extraction of perfumes and flavours from plant materials with liquid carbon dioxide under liquid-vapor equilibrium conditions, Fluid Phase Equilib. 49 (1989) 115–126. doi:10.1016/0378-3812(89)80009-3.

[77] M.M. Esquível, M.G. Bernardo-Gil, M.B. King, Mathematical models for supercritical extraction of olive husk oil, J. Supercrit. Fluids. 16 (1999) 43–58. doi:10.1016/S0896-8446(99)00014-5.

[78] P. Barton, R.E. Hughes, M.M. Hussein, Supercritical Carbon Dioxide Extraction of Peppermint and Spearmint, J. Supercrit. Fluids. 5 (1992) 157–162. doi:https://doi.org/10.1016/0896-8446(92)90002-2.

[79] A. Cháfer, A. Berna, Study of kinetics of the d-pinitol extraction from carob pods using supercritical CO2, J. Supercrit. Fluids. 94 (2014) 212–215. doi:10.1016/j.supflu.2014.07.015.

[80] B. Honarvar, S.A. Sajadian, M. Khorram, A. Samimi, Mathematical modeling of supercritical fluid extraction of oil from canola and sesame seeds, Brazilian J. Chem.

Eng. 30 (2013) 159–166. doi:10.1590/S0104-66322013000100018.

[81] C.F. Silva, M.F. Mendes, F.L.P. Pessoa, E.M. Queiroz, Supercritical carbon dioxide extraction of macadamia (macadamia integrifolia) nut oil: experiments and modeling, Brazilian J. Chem. Eng. 25 (2008) 175–181. doi:10.1590/S0104-66322008000100018.

[82] C.F. Silva, F.C. Moura, M.F. Mendes, F.L.P. Pessoa, Extraction of citronella (Cymbopogon nardus) essential oil using supercritical CO2: Experimental data and mathematical modeling, Brazilian J. Chem. Eng. 28 (2011) 343–350. doi:10.1590/S0104-66322011000200019.

[83] H. Sovová, Mathematical model for supercritical fluid extraction of natural products and extraction curve evaluation, J. Supercrit. Fluids. 33 (2005) 35–52. doi:10.1016/j.supflu.2004.03.005.

[84] H. Sovová, R.P. Stateva, Supercritical fluid extraction from vegetable materials, Rev. Chem. Eng. 27 (2011) 79–156. doi:10.1515/REVCE.2011.002.

[85] J. Crank, The mathematics of diffusion, 2nd ed., Oxford University Press, Bristol, England, 1975.

[86] C.-S. Tan, D.-C. Liou, Modeling of desorption at supercritical conditions, AIChE J. 35 (1989) 1029–1031. doi:10.1002/aic.690350616.

[87] Z. Huang, X.-H. Shi, W.-J. Jiang, Theoretical models for supercritical fluid extraction., J. Chromatogr. A. 1250 (2012) 2–26. doi:10.1016/j.chroma.2012.04.032.

[88] M. Goto, B.C. Roy, T. Hirose, Shrinking-core leaching model for supercritical-fluid extraction, J. Supercrit. Fluids. 9 (1996) 128–133. doi:10.1016/S0896-8446(96)90009-1.

[89] Z. Ahmed, M. Abdeslam-Hassan, L. Ouassila, B. Danielle, Extraction and modeling of Algerian Rosemary essential oil using supercritical CO2: Effect of pressure and temperature, Energy Procedia. 18 (2012) 1038–1046. doi:10.1016/j.egypro.2012.05.118.

[90] C.S.G. Kitzberger, R.H. Lomonaco, E.M.Z. Michielin, L. Danielski, J. Correia, S.R.S. Ferreira, Supercritical fluid extraction of shiitake oil: Curve modeling and extract composition, J. Food Eng. 90 (2009) 35–43. doi:10.1016/j.jfoodeng.2008.05.034.

[91] I. Zizovic, M. Stamenic, A. Orlovic, D. Skala, Supercritical carbon dioxide essential oil extraction of Lamiaceae family species: Mathematical modelling on the micro-scale and process optimization, Chem. Eng. Sci. 60 (2005) 6747–6756. doi:10.1016/j.ces.2005.03.068.

[92] I. Zizovic, M. Stamenic, A. Orlovic, D. Skala, Supercritical carbon dioxide extraction of essential oils from plants with secretory ducts: Mathematical modelling on the micro-scale, J. Supercrit. Fluids. 39 (2007) 338–346. doi:10.1016/j.supflu.2006.03.009.

[93] H. Sovová, Rate of the vegetable oil extraction with supercritical CO2 - I. Modeling of extraction curves, Chem. Eng. Sci. 49 (1994) 409–414.

[94] Z. Huang, Mass transfer models for supercritical fluid extraction, in: T. Fornari, R.P. Stateva (Eds.), High Press. Fluid Technol. Fro Green Food Process., Springer, 2015: p. 517.

[95] E. Reverchon, G. Donsi, L.S. Osseo, Modeling of supercritical fluid extraction from herbaceous matrices, Ind. Eng. Chem. Res. 32 (1993) 2721–2726. doi:10.1021/ie00023a039.

[96] Z. Huang, M.-J. Yang, S.-F. Liu, Q. Ma, Supercritical carbon dioxide extraction of Baizhu: Experiments and modeling, J. Supercrit. Fluids. 58 (2011) 31–39. doi:10.1016/j.supflu.2011.05.008.

[97] J. Shi, Y. Kakuda, X. Zhou, G. Mittal, Q. Pan, Correlation of mass transfer coefficient in the extraction of plant oil in a fixed bed for supercritical CO2, J. Food Eng. 78 (2007) 33–40. doi:10.1016/j.jfoodeng.2005.08.050.

[98] I. Norhuda, K.M. Omar, Mass Transfer Modeling in a Packed Bed of Palm Kernels under Supercritical Conditions, Eng. Technol. 3 (2009) 147–150.

[99] G.-B. Lim, G.D. Holder, Y.T. Shah, Solid-fluid mass transfer in a packed bed under supercritical conditions, Supercrit. Fluid Sci. Technol. ACS Symp. Ser. 406, Washingt. USA. (1989).

[100] M.B. King, O.J. Catchpole, Physico-chemical data required for the design of near-critical fluid extraction process, in: M.B. King, T.R. Bott (Eds.), Extr. Nat. Prod. Using Near-Critical Solvents, Springer, Netherlands, 1993: pp. 184–231.

[101] J.W. King, M. Cygnarowicz-Provost, F. Favati, Supercritical Fluid Extraction of Evening Primrose Oil Kinetic and Mass Transfer Effects, Ital. J. Food Sci. 9 (1997) 193–204.

[102] J. Puiggené, M.A. Larrayoz, F. Recasens, Free liquid-to-supercritical fluid mass transfer in packed beds, Chem. Eng. Sci. 52 (1997) 195–212. doi:10.1016/S0009-2509(96)00379-X.

[103] C.S. Tan, S.K. Liang, D.C. Liou, Fluid-solid mass transfer in a supercritical fluid extractor, Chem. Eng. J. 38 (1988) 17–22. doi:10.1016/0300-9467(88)80049-2.

[104] D. Mongkholkhajornsilp, S. Douglas, P.L. Douglas, A. Elkamel, W. Teppaitoon, S. Pongamphai, Supercritical CO2 extraction of nimbin from neem seeds - A modelling study, J. Food Eng. 71 (2005) 331–340. doi:10.1016/j.jfoodeng.2004.08.007.

[105] H. Taher, S. Al-Zuhair, A.H. Al-Marzouqi, Y. Haik, M. Farid, Mass transfer modeling of Scenedesmus sp. lipids extracted by supercritical CO2, Biomass and Bioenergy. 70 (2014) 530–541. doi:10.1016/j.biombioe.2014.08.019.

[106] L.P.S. Silva, J. Martínez, Mathematical modeling of mass transfer in supercritical fluid extraction of oleoresin from red pepper, J. Food Eng. 133 (2014) 30–39. doi:10.1016/j.jfoodeng.2014.02.013.

[107] C.M. Silva, H. Liu, Modelling of Transport Properties of Hard Sphere Fluids and Related Systems, and its Applications, in: A. Mulero (Ed.), Theory Simul. Hard-Sph. Fluids Relat. Syst., Springer, Heidelberg, Germany, 2008: pp. 383–492.

[108] C.M. Silva, H. Liu, E.A. Macedo, Models for self-diffusion coefficients of dense fluids, including hydrogen-bonding substances, Chem. Eng. Sci. 53 (1998) 2423–2429. doi:10.1016/S0009-2509(98)00037-2.

[109] A. López-Padilla, A. Ruiz-Rodriguez, G. Reglero, T. Fornari, Study of the diffusion coefficient of solute-type extracts in supercritical carbon dioxide: Volatile oils, fatty acids and fixed oils, J. Supercrit. Fluids. 109 (2016) 148–156. doi:10.1016/j.supflu.2015.11.017.

[110] H. Saad, E. Culari, Diffusion of Liquid Hydrocarbons in Supercritical CO2 by Photon Correlation Spectroscopy, Berichte Der Bunsengesellschaft Für Phys. Chemie. 88 (1984) 834–837. doi:10.1002/cjce.5450460519.

[111] K.K. Liong, P.A. Wells, N.R. Foster, Diffusion in supercritical fluids, J. Supercrit. Fluids. 4 (1991) 91–108. doi:10.1016/0896-8446(91)90037-7.

[112] Y.V. Tsekhanskaya, M.B. Iomtev, A method of measuring diffusion coefficients of solid substances in compressed gases, Inzhenerno-Fizicheskii Zhurnal. 5 (1962).

[113] P.G. Debenedetti, R.C. Reid, Diffusion and mass transfer in supercritical fluids, AIChE J. 32 (1986) 2034–2046. doi:10.1002/aic.690321214.

[114] O.J. Catchpole, M.B. King, Measurement and Correlation of Binary Diffusion Coefficients in Near Critical Fluids, Ind. Eng. Chem. Res. 33 (1994) 1828–1837. doi:10.1021/ie00031a024.

[115] E.S. Baker, D.R. Brown, J. Jonas, Self-diffusion in compressed supercritical ethylene, J. Phys. Chem. 88 (1984) 5425–5249. doi:10.1063/1.441097.

[116] J. Jonas, Nuclear Magnetic Resonance at High Pressure, Rev. Sci. Instrum. 43 (1972)

643–649. doi:10.1126/science.216.4551.1179.

[117] D.M. Lamb, S.T. Adamy, K.W. Woo, J. Jonas, Transport and relaxation of naphthalene in supercritical fluids, J. Phys. Chem. 93 (1989) 5002–5005.

[118] G. Taylor, Conditions under Which Dispersion of a Solute in a Stream of Solvent can be Used to Measure Molecular Diffusion, Proc. R. Soc. A Math. Phys. Eng. Sci. 225 (1954) 473–477. doi:10.1098/rspa.1954.0216.

[119] J.C. Giddings, S.L. Seager, Method for rapid determination of diffusion coefficients, Ind. Eng. Chem. Fundam. 1 (1962) 277–283. doi:10.1021/i160004a009.

[120] T. Funazukuri, C.Y. Kong, S. Kagei, Binary diffusion coefficients of acetone in carbon dioxide at 308.2 and 313.2 K in the pressure range from 7.9 to 40 MPa, Int. J. Thermophys. 21 (2000) 651–669. doi:10.1023/A:1006637401868.

[121] G. Madras, B.L. Hamilton, M. a. Matthews, Influence of adsorption on the measurement of diffusion coefficients by Taylor dispersion, Int. J. Thermophys. 17 (1996) 373–389. doi:10.1007/BF01443398.

[122] T. Funazukuri, C.Y. Kong, S. Kagei, Impulse response techniques to measure binary diffusion coefficients under supercritical conditions, J. Chromatogr. A. 1037 (2004) 411–429. doi:10.1016/j.chroma.2004.03.043.

[123] C.Y. Kong, T. Funazukuri, S. Kagei, G. Wang, F. Lu, T. Sako, Applications of the chromatographic impulse response method in supercritical fluid chromatography, J. Chromatogr. A. 1250 (2012) 141–156. doi:10.1016/j.chroma.2012.04.033.

[124] C.Y. Kong, T. Funazukuri, S. Kagei, Chromatographic impulse response technique with curve fitting to measure binary diffusion coefficients and retention factors using polymer-coated capillary columns, J. Chromatogr. A. 1035 (2004) 177–193. doi:10.1016/j.chroma.2004.02.067.

[125] A.L. Magalhães, P.F. Lito, F. a. Da Silva, C.M. Silva, Simple and accurate correlations for diffusion coefficients of solutes in liquids and supercritical fluids over wide ranges of temperature and density, J. Supercrit. Fluids. 76 (2013) 94–114. doi:10.1016/j.supflu.2013.02.002.

[126] Scheibel, E.G., Liquid Diffusivities, Ind. Eng. Chem. 46 (1954) 2007–2008. doi:10.1021/ie50537a062.

[127] K.A. Reddy, L.K. Doraiswany, Estimating Liquid Diffusivity, I&Ec Fundametals. 6 (1967) 77–79. doi:10.1021/i160021a012.

[128] M.A. Lusis, G.A. Ratcliff, Difision in Binary Liquid Mixtures at Infinite Dilution EyrinB, Can. J. Chem. Eng. 46 (1948) 385–387. doi:10.1002/cjce.5450460519.

[129] C.-C. Lai, C.-S. Tan, Measurement of molecular Diffusion Coefficient in Supercritical Carbon Dioxide Using a Coated Capillary Column, Ind. Eng. Chem. Res. 34 (1995) 674–680. doi:10.1021/ie00041a029.

[130] C.R. Wilke, P. Chang, Correlation of diffusion coefficients in dilute solutions, AIChE J. 1 (1955) 264–270. doi:10.1002/aic.690010222.

[131] A.L. Magalhães, R. V. Vaz, R.M.G. Gonçalves, F. a. Da Silva, C.M. Silva, Accurate hydrodynamic models for the prediction of tracer diffusivities in supercritical carbon dioxide, J. Supercrit. Fluids. 83 (2013) 15–27. doi:10.1016/j.supflu.2013.08.001.

[132] R. V. Vaz, A.L. Magalhães, C.M. Silva, Improved hydrodynamic equations for the accurate prediction of diffusivities in supercritical carbon dioxide, Fluid Phase Equilib. 360 (2013) 401–415. doi:10.1016/j.fluid.2013.09.052.

[133] M.M. Cowan, Plant products as antimicrobial agents., Clin. Microbiol. Rev. 12 (1999) 564–82. doi:0893-8512/99/$04.00‧0.

[134] D.E. Moerman, An analysis of the food plants and drug plants of native North America., J. Ethnopharmacol. 52 (1996) 1–22. doi:10.1016/0378-8741(96)01393-1.

[135] J.D. Phillipson, Phytochemistry and medicinal plants, Phytochemistry. 56 (2001) 237–243. doi:10.1016/S0031-9422(00)00456-8.

[136] I.B. Suffredini, H.S. Sader, A.G. Gonçalves, A.O. Reis, A.C. Gales, A.D. Varella, R.N. Younes, Screening of antibacterial extracts from plants native to the Brazilian Amazon Rain Forest and Atlantic Forest, Brazilian J. Med. Biol. Res. 37 (2004) 379–384. doi:10.1590/S0100-879X2004000300015.

[137] M.E. Schreckinger, J. Wang, G. Yousef, M.A. Lila, E.G. De Mejia, Antioxidant capacity and in Vitro inhibition of adipogenesis and inflammation by phenolic extracts of Vaccinium floribundum and Aristotelia chilensis, J. Agric. Food Chem. 58 (2010) 8966–8976. doi:10.1021/jf100975m.

[138] I. a-L. Persson, K. Persson, R.G.G. Andersson, Effect of Vaccinium myrtillus and its polyphenols on angiotensin-converting enzyme activity in human endothelial cells., J. Agric. Food Chem. 57 (2009) 4626–9. doi:10.1021/jf900128s.

[139] G.A. Garzón, C.E. Narváez, K.M. Riedl, S.J. Schwartz, Chemical composition, anthocyanins, non-anthocyanin phenolics and antioxidant activity of wild bilberry (Vaccinium meridionale Swartz) from Colombia, Food Chem. 122 (2010) 980–986. doi:10.1016/j.foodchem.2010.03.017.

[140] M. Kondo, S.L. Mackinnon, C.C. Craft, M.D. Matchett, R.A.R. Hurta, C.C. Neto,

Ursolic acid and its esters: Occurrence in cranberries and other Vaccinium fruit and effects on matrix metalloproteinase activity in DU145 prostate tumor cells, J. Sci. Food Agric. 91 (2011) 789–796. doi:10.1002/jsfa.4330.

[141] J. Ferrier, S. Djeffal, H.P. Morgan, S.P. Vander Kloet, S. Redžić, A. Cuerrier, M.J. Balick, J.T. Arnason, Antiglycation activity of Vaccinium spp. (Ericaceae) from the Sam Vander Kloet collection for the treatment of type II diabetes, Botany. 90 (2012) 401–406. doi:10.1139/b2012-026.

[142] P. Kšonžeková, R. Mariychuk, A. Eliašová, D. Mudroňová, T. Csank, J. Király, D. Marcinčáková, J. Pistl, L. Tkáčiková, In vitro study of biological activities of anthocyanin-rich berry extracts on porcine intestinal epithelial cells, J. Sci. Food Agric. 96 (2016) 1093–1100. doi:10.1002/jsfa.7181.

[143] L.J. Cseke, A. Kirakosyan, P.B. Kaufman, S.L. Warber, J.A. Duke, H.L. Brielmann, Natural Products from Plants, 2nd ed., CRC Press, Boca Raton, FL, 2006.

[144] W.E.E. Manrique, L.C.A.G. Salcedo, O.J.M. Vargas, Validación de una metodología analítica para la cuantificación de polifenoles totales , en procesos de extracción asistida por microondas sobre frutos de la especie colombiana Vaccinium meridionale Resumen Validation of an analytical method for quantifica, Rev. Colomb. Ciencias Químico Farm. 45 (2016) 109–126.

[145] J.L. Luteyn, P. Pedraza-Peñaloza, Blueberry relatives of the New World tropics (Ericaceae), New York Bot. Gard. (2012) 1. http://sweetgum.nybg.org/ericaceae/index.php (accessed March 28, 2017).

[146] N. Guzmán, D. Ramírez, ¿Qué tienen que ver el mortiño y el síndrome metabólico?, Univ. Antioquia - Cienc. (2016) 1. http://www.udea.edu.co/wps/portal/udea/web/inicio/udea-noticias/udea-noticia/!ut/p/z0/fYy7DsIwDEV_haVj5AAlwFgxICEGBoTaLMi0ERhau4-04vNJYYGFxTrn6vqChRQs40BX9CSMZfDMmvNqvZlNk1jvtYmNTswhXixn2_nxpGEH9n8hLNC9aWwCNhf27ukhraX1WPaFw0hj92s3qdyHxzth8ZQTdpF-fzMVMra-Y (accessed March 29, 2017).

[147] Hernán Guillermo Ávila Rodríguez, Julián Andrés Cuspoca Riveros, Gerhard Fischer, Gustavo Adolfo Ligarreto Moreno, Martha Cecilia Quicazán, Caracterización Fisicoquímica y Organoléptica del Fruto de Agraz (Vaccinium meridionale Swartz) Almacenado 1 a 2oC, Rev. Fac. Nac. Agron. Medellín. Vol.60 (2007) 4179–4193. http://www.scielo.org.co/pdf/rfnam/v60n2/a19v60n2.pdf.

[148] M.L. De Valencia, F. Ramírez, Notas Sobre la Morfología, Anatomía y Germinación del Agraz (Vaccinium meridionale Swartz.), Agron. Colomb. 10 (1993) 151–159.

[149] C.M. Buitrago Guacaneme, M.C. Rincón Soledad, H.E. Balaguera López, G.A. Ligarreto Moreno, Tipificación de Diferentes Estados de Madurez del Fruto de Agraz (*Vaccinium meridionale* Swartz), Rev. Fac. Nac. Agron. Medellín. 68 (2015) 7521–7531.

[150] M.F. Martínez Zambrano, Jose Jobanny; Rojas Sarmiento, Hugo Alfonso; Borda Guerra, Gloria del Cármen; Hastamorir Caro, Alba Nidia; Medina Riaño, Estabilidad de Antocianinas en Jugo y Concentrado de Agraz (*Vaccinium meridionale* Sw.), Rev. Fac. Nal. Agr. Medellín. 64 (2011) 6015–6022. http://www.revistas.unal.edu.co/index.php/refame/article/view/26410.

[151] I.C. Zapata, U. Sepúlveda-Valencia, B.A. Rojano, Efecto del tiempo de almacenamiento sobre las propiedades fisicoquímicas, probióticas y antioxidantes de yogurt saborizado con mortiño (*Vaccinium meridionale* Sw), Inf. Tecnol. 26 (2015) 17–28. doi:10.4067/S0718-07642015000200004.

[152] E.C. López-Vidaña, I. Pilatowsky Figueroa, F.B. Cortés, B.A. Rojano, A. Navarro Ocaña, Effect Of Temperature On Antioxidant Capacity During Drying Process Of Mortiño (*Vaccinium meridionale Swartz*), Int. J. Food Prop. 2912 (2016) 10942912.2016.1155601. doi:10.1080/10942912.2016.1155601.

[153] C. Gaviria Montoya, C. Ochoa Ospina, N. Sánchez Mesa, C. Medina Cano, M. Lobo Arias, P. Galeano García, A. Mosquera Martínez, A. Tamayo Tenorio, Y. Lopera Pérez, B. Rojano, Actividad antioxidante e inhibición de la peroxidación lipídica de extractos de frutos de mortiño (*Vaccinium meridionale* SW), Bol. Latinoam. Y Del Caribe Plantas Med. Y Aromat. 8 (2009) 519–528. http://www.redalyc.org/articulo.oa?id=85617461007.

[154] Y.E. Lopera, J. Fantinelli, L.F. Arbeláez González, B. Rojano, J.L. Ríos, G. Schinella, S. Mosca, Antioxidant Activity and Cardioprotective Effect of a Nonalcoholic Extract of *Vaccinium meridionale* Swartz during Ischemia-Reperfusion in Rats, Evidence-Based Complement. Altern. Med. 2013 (2013). doi:10.1155/2013/516727.

[155] M.E. Maldonado-Celis, S.S. Arango-Varela, B.A. Rojano, Free radical scavenging capacity and cytotoxic and antiproliferative effects of *Vaccinium meridionale* Sw. against colon cancer cell lines, Rev. Cuba. Plantas Med. 19 (2014) 172–184. http://scielo.sld.cu/scielo.php?script=sci_arttext&pid=S1028-47962014000200006&lng=es&nrm=iso.

[156] K. Zapata Acosta, A.M. Piedrahita, A.F. Alzate, F.B. Cortés, B.A. Rojano, Oxidative stabilization of Sacha Inchi (*Plukenetia Volubilis* Linneo) oil with Mortiño (*Vaccinium Meridionale* SW) suspensions addition, Rev. Cienc. En Desarro. 6 (2015) 141–153. doi:10.19053/01217488.3784.

[157] D. Arora, A. Rani, A. Sharma, A review on phytochemistry and ethnopharmacological aspects of genus Calendula., Pharmacogn. Rev. 7 (2013) 179–187. doi:10.4103/0973-7847.120520.

[158] R. Sausserde, K. Kampuss, Composition of Carotenoids in Calendula (*Calendula officinalis* L.) flowers, in: Foodbalt 2014, Jelgava, Latvia, 2014: pp. 13–18. http://agris.fao.org/agris-search/search.do?recordID=LV2014000480.

[159] M. Miguel, L. Barros, C. Pereira, R.C. Calhelha, P.A. García, M.A. Castro, C. Santos-Buelga, I.C.F.R. Ferreira, Chemical characterization and bioactive properties of two aromatic plants: *Calendula officinalis* (flowers) and *Mentha cervina* (leaves), Food Funct. 7 (2016) 2223–2232. doi:10.1039/c6fo00398b.

[160] L. Danielski, L.M.A.S. Campos, L.F. V Bresciani, H. Hense, R.A. Yunes, S.R.S. Ferreira, Marigold (*Calendula officinalis* L.) oleoresin: Solubility in SC-CO2 and composition profile, Chem. Eng. Process. Process Intensif. 46 (2007) 99–106. doi:10.1016/j.cep.2006.05.004.

[161] Z. Kalvatchev, R. Walder, D. Garzaro, Anti-HIV activity of extracts from *Calendula officinalis* flowers, Biomed. Pharmacother. 51 (1997) 176–180. doi:10.1016/S0753-3322(97)85587-4.

[162] A. Ramos, A. Edreira, A. Vizoso, J. Betancourt, M. López, M. Décalo, Genotoxicity of an extract of *Calendula officinalis* L., J. Ethnopharmacol. 61 (1998) 49–55. doi:10.1016/S0378-8741(98)00017-8.

[163] M. Wang, R. Tsao, S. Zhang, Z. Dong, R. Yang, J. Gong, Y. Pei, Antioxidant activity, mutagenicity/anti-mutagenicity, and clastogenicity/anti-clastogenicity of lutein from marigold flowers, Food Chem. Toxicol. 44 (2006) 1522–1529. doi:10.1016/j.fct.2006.04.005.

[164] M.R. García-risco, L. Mouhid, L. Salas-pérez, A. López-padilla, S. Santoyo, L. Jaime, A.R. De Molina, G. Reglero, Biological Activities of Asteraceae (*Achillea millefolium* and *Calendula officinalis*) and Lamiaceae (*Melissa officinalis* and *Origanum majorana*) Plant Extracts, Plant Foods Hum. Nutr. (2017) 1–7. doi:10.1007/s11130-016-0596-8.

[165] D. Martin, J. Navarro del Hierro, D. Villanueva Bermejo, R. Fernández-Ruiz, T. Fornari, G. Reglero, Bioaccessibility and Antioxidant Activity of *Calendula officinalis* Supercritical Extract as Affected by in Vitro Codigestion with Olive Oil, J. Agric. Food Chem. 64 (2016) 8828–8837. doi:10.1021/acs.jafc.6b04313.

[166] M. Hamburger, S. Adler, D. Baumann, A. Förg, B. Weinreich, Preparative purification of the major anti-inflammatory triterpenoid esters from Marigold (*Calendula officinalis*), Fitoterapia. 74 (2003) 328–338. doi:10.1016/S0367-326X(03)00051-0.

[167] D. Baumann, S. Adler, S. Grüner, F. Otto, B. Weinreich, M. Hamburger, Supercritical carbon dioxide extraction of marigold at high pressures: Comparison of analytical and pilot-scale extraction, Phytochem. Anal. 15 (2004) 226–230. doi:10.1002/pca.772.

[168] W. Palumpitag, P. Prasitchoke, M. Goto, A. Shotipruk, Supercritical Carbon Dioxide Extraction of Marigold Lutein Fatty Acid Esters: Effects of Cosolvents and Saponification Conditions, Sep. Sci. Technol. 46 (2011) 605–610. doi:10.1080/01496395.2010.533739.

[169] G. Baratto, E. Riva, Process for preparing an inflorescence extract of *Calendula officinalis* by means of extraction with supercritical carbon dioxide and compositions containing said extract, EP2520306A1, 2012.

[170] T. Fornari, A. Ruiz-Rodriguez, G. Vicente, E. Vázquez, M.R. García-Risco, G. Reglero, Kinetic study of the supercritical CO2 extraction of different plants from Lamiaceae family, J. Supercrit. Fluids. 64 (2012) 1–8. doi:10.1016/j.supflu.2012.01.006.

[171] E. Vázquez, M.R. García-Risco, L. Jaime, G. Reglero, T. Fornari, Simultaneous extraction of rosemary and spinach leaves and its effect on the antioxidant activity of products, J. Supercrit. Fluids. 82 (2013) 138–145. doi:10.1016/j.supflu.2013.07.004.

[172] M.R. García-Risco, G. Vicente, G. Reglero, T. Fornari, Fractionation of thyme (*Thymus vulgaris* L.) by supercritical fluid extraction and chromatography, J. Supercrit. Fluids. 55 (2011) 949–954. doi:10.1016/j.supflu.2010.10.008.

[173] D. Villanueva Bermejo, I. Angelov, G. Vicente, R.P. Stateva, M. Rodriguez García-Risco, G. Reglero, E. Ibañez, T. Fornari, Extraction of thymol from different varieties of thyme plants using green solvents, J. Sci. Food Agric. 95 (2015) 2901–2907. doi:10.1002/jsfa.7031.

[174] D. Villanueva-Bermejo, F. Zahran, D. Troconis, M. Villalva, G. Reglero, T. Fornari, Selective precipitation of phenolic compounds from *Achillea millefolium* L. extracts

by supercritical anti-solvent technique, J. Supercrit. Fluids. 120 (2017) 52–58. doi:10.1016/j.supflu.2016.10.011.

[175] D. Villanueva-Bermejo, F. Zahran, M.R. García-Risco, G. Reglero, T. Fornari, Supercritical fluid extraction of Bulgarian *Achillea millefolium*, J. Supercrit. Fluids. 119 (2017) 283–288. doi:10.1016/j.supflu.2016.10.005.

[176] D.V. Bermejo, E. Ibáñez, G. Reglero, T. Fornari, Effect of cosolvents (ethyl lactate, ethyl acetate and ethanol) on the supercritical CO2 extraction of caffeine from green tea, J. Supercrit. Fluids. 107 (2016) 507–512. doi:10.1016/j.supflu.2015.07.008.

[177] E. Reverchon, I. De Marco, Supercritical fluid extraction and fractionation of natural matter, J. Supercrit. Fluids. 38 (2006) 146–166. doi:10.1016/j.supflu.2006.03.020.

[178] J.W. King, Critical fluid technology for the processing of lipid-related natural products, Comptes Rendus Chim. 7 (2004) 647–659. doi:10.1016/j.crci.2004.02.008.

[179] B.A.S. Machado, C.G. Pereira, S.B. Nunes, F.F. Padilha, M.A. Umsza-Guez, Supercritical Fluid Extraction Using CO_2 : Main Applications and Future Perspectives, Sep. Sci. Technol. 48 (2013) 2741–2760. doi:10.1080/01496395.2013.811422.

[180] J.M. DeSimone, Practical Approaches to Green Solvents, Science (80). 297 (2002) 799–803. doi:10.1126/science.1069622.

[181] T. Fornari, R.P. Stateva, High Pressure Fluid Technology for Green Food Processing, Springer, 2015. doi:10.1007/978-3-319-10611-3.

[182] J.M. Prado, G.H.C. Prado, M.A.A. Meireles, Scale-up study of supercritical fluid extraction process for clove and sugarcane residue, J. Supercrit. Fluids. 56 (2011) 231–237. doi:10.1016/j.supflu.2010.10.036.

[183] G. Vicente, M.R. García-Risco, T. Fornari, G. Reglero, Supercritical fractionation of rosemary extracts to improve the antioxidant activity, Chem. Eng. Technol. 35 (2012) 176–182. doi:10.1002/ceat.201100367.

[184] L. Jaime, E. Vázquez, T. Fornari, M. del C. López-Hazas, M.R. García-Risco, S. Santoyo, G. Reglero, Extraction of functional ingredients from spinach (Spinacia oleracea L.) using liquid solvent and supercritical CO2extraction, J. Sci. Food Agric. 95 (2015) 722–729. doi:10.1002/jsfa.6788.

[185] S. Santoyo, L. Jaime, M.R. García-Risco, M. Lopez-Hazas, G. Reglero, Supercritical fluid extraction as an alternative process to obtain antiviral agents from thyme species, Ind. Crops Prod. 52 (2014) 475–480. doi:10.1016/j.indcrop.2013.10.028.

[186] M.R. García-Risco, E. Vázquez, J. Sheldon, E. Steinmann, N. Riebesehl, T. Fornari,

G. Reglero, Supercritical fluid extraction of heather (*Calluna vulgaris*) and evaluation of anti-hepatitis C virus activity of the extracts, Virus Res. 198 (2015) 9–14. doi:10.1016/j.virusres.2014.12.022.

[187] A. López-padilla, A. Ruiz-Rodriguez, G. Reglero, T. Fornari, Supercritical carbon dioxide extraction of *Calendula officinalis* : kinetic modeling and scaling up study, J. Supercrit. Fluids. (2017) DOI: 10.1016/j.supflu.2017.03.033.

[188] N.P. Povh, M.O.M. Marques, M.A. Meireles, Supercritical CO2 extraction of essential oil and oleoresin from chamomile (*Chamomilla recutita* [L.] Rauschert), J. Supercrit. Fluids. 21 (2001) 245–256. doi:10.1016/S0896-8446(01)00096-1.

[189] K.C. Zancan, M.O.M. Marques, A.J. Petenate, M.A.A. Meireles, Extraction of ginger (*Zingiber officinale* roscoe) oleoresin with CO2 and co-solvents: A study of the antioxidant action of the extracts, J. Supercrit. Fluids. 24 (2002) 57–76. doi:10.1016/S0896-8446(02)00013-X.

[190] I. Medina, Determination of diffusion coefficients for supercritical fluids, J. Chromatogr. A. 1250 (2012) 124–140. doi:10.1016/j.chroma.2012.04.052.

[191] K.K. Liong, P.A. Wells, N.R. Foster, Diffusion coefficients of long-chain esters in supercritical carbon dioxide, Ind. Eng. Chem. Res. 30 (1991) 1329–1335. doi:10.1021/ie00054a039.

[192] A.L. Magalhães, P.F. Lito, F.A. Da Silva, C.M. Silva, Simple and accurate correlations for diffusion coefficients of solutes in liquids and supercritical fluids over wide ranges of temperature and density (Supplementary Data), J. Supercrit. Fluids. 76 (2013) 94–114. doi:10.1016/j.supflu.2013.02.002.

[193] A. López-Padilla, A. Ruiz-Rodriguez, C.E.R. Flórez, D.M.R. Barrios, G. Reglero, T. Fornari, *Vaccinium meridionale* Swartz supercritical CO2 extraction: Effect of process conditions and scaling up, Materials (Basel). 9 (2016). doi:10.3390/ma9070519.

[194] L.M.A.S. Campos, E.M.Z. Michielin, L. Danielski, S.R.S. Ferreira, Experimental data and modeling the supercritical fluid extraction of marigold (*Calendula officinalis*) oleoresin, J. Supercrit. Fluids. 34 (2005) 163–170. doi:10.1016/j.supflu.2004.11.010.

ANEXOS

ANEXO A. Otras Publicaciones Derivadas De La Tesis

1. *Vaccinium meridionale* Swartz extracts and their addition in beef burgers as antioxidant ingredient

Alexis López-Padilla, Diana Martína, David Villanueva Bermejo, Laura Jaime, Alejandro Ruiz-Rodriguez, Claudia Estela Restrepo Flórez, Diana Marsela Rivero Barrios and Tiziana Fornari

Journal of the Science of Food and Agriculture. *En prensa*.
DOI: 10.1002/jsfa.8483

Martin Diana (Orcid ID: 0000-0002-1082-9280)

Vaccinium meridionale Swartz extracts and their addition in beef burgers as antioxidant ingredient

Running tittle: Mortiño extraction and use as meat product antioxidant

Alexis López-Padilla[a,b], Diana Martín[a,b*], David Villanueva Bermejo[a,b], Laura Jaime[a,b], Alejandro Ruiz-Rodriguez[a,b], Claudia Estela Restrepo Flórez[c], Diana Marsela Rivero Barrios[c] and Tiziana Fornari[a,b]

[a] Departamento de Producción y Caracterización de Nuevos Alimentos. Instituto de Investigación en Ciencias de la Alimentación (CIAL) (CSIC–UAM), 28049 Madrid, Spain

[b] Sección Departamental de Ciencias de la Alimentación. Facultad de Ciencias. Universidad Autónoma de Madrid, 28049 Madrid, Spain

[c] INTAL Foundation Cra 50 G N° 12 Sur 91, Itagüí, Colombia

*** Corresponding author**: Diana Martin. Instituto de Investigación en Ciencias de la Alimentación (CIAL), Campus de la Universidad Autónoma de Madrid, 28049 Madrid, Spain. Phone: +34 910017930. E-mail: diana.martin@uam.es; ORCID: 0000-0002-1082-9280

This article has been accepted for publication and undergone full peer review but has not been through the copyediting, typesetting, pagination and proofreading process which may lead to differences between this version and the Version of Record. Please cite this article as doi: 10.1002/jsfa.8483

Abstract

BACKGROUND: *Vaccinium meridionale Swartz* (mortiño) constitute a source of bioactive phytochemicals, but the studies related to its efficient and green production is scarce. Pressurized liquid extraction (PLE) and ultrasound assisted extraction were compared for mortiño extraction. Total phenolic compounds (TPC) and antioxidant capacity (ABTS•+) were determined. Beef burgers with 2% of mortiño (MM) or its PLE extract (ME) were manufactured. Lipid oxidation (TBARS) and instrumental color changes were measured after refrigerated storage.

RESULTS: High amounts of TPC (up to 72 g gallic acid/kg extract) were determined in mortiño extracts, which was positively correlated with the antioxidant activity. TBARS values of beef burgers containing either MM or ME did not change after refrigerated storage, whereas lipid oxidation of control burgers increased significantly. The color of the burgers was different from the control due to addition of either MM or ME (lower b* and a* values). However, the evolution of color after storage was similar between the control and ME samples.

CONCLUSION: Mortiño extracts with high TPC can be obtained by PLE and either mortiño or its PLE extract are able to control the lipid oxidation of beef burgers, but PLE extract is preferred from the color quality point of view.

Keywords: Pressurized liquid extraction, Ultrasound assisted extraction, mortiño, antioxidant, meat products

Introduction

The genus *Vaccinium* comprises a group of plants that includes up to 450 species; the fruits (berries) of many species are consumed by humans. The berries constitute a source of various bioactive phytonutrients, including phenolic compounds, such as flavonoids, phenolic acids, lignans and polymeric tannins. [1, 2] Certain beneficial properties have been associated to the consumption of these berries, such as antioxidant, anti-diabetic, anti-hyperlipidemic, antiproliferative and neuroprotective activity. [3-7]

Particularly, *Vaccinium meridionale* Swartz (mortiño or Colombian blueberry) is one of the *Vaccinium* species which grows in the Andean region of South America at 2300–3300 m above the sea level. Several biological properties have been attributed to mortiño, and more specifically to its phenolic content. Lopera et al [8] evaluated the antioxidant properties and the effects against myocardial reperfusion injury of an aqueous extract obtained by mortiño fermentation. Maldonado-Celis et al [9] studied the cytotoxic and antiproliferative effects of a mortiño extract obtained by simply dissolving a certain amount of mortiño into distillated water. Gaviria Montoya et al [10] and Sequeda-Castañeda et al [11] evaluated, respectively, the inhibition of lipid peroxidation and the cytotoxic activity in fibroblastoma cell lines of mortiño extracts obtained by sequential extraction with acidic methanol.

Despite all these health-promoting properties, there are no many studies related to the efficient and green production of *Vaccinium meridionale* extracts with high content of phenolic compounds. In this respect, Garzón et al [12] reported the chemical composition and phenolic profile of extracts obtained from mortiño by sequential extractions using methanol. Paes et al [13] studied the use of supercritical CO_2 for the extraction of phenolic compounds from another *Vaccinium* species (*Vaccinium myrtillus* L.), obtaining extracts with antioxidant activity higher than that of the extracts produced with liquid solvents. Recently, López-Padilla

et al [14] investigated the kinetic behavior and scaling-up of the supercritical CO_2 extraction of mortiño. Other efficient and green extraction technologies which are nowadays popular in the production of plant extracts, such as pressurized liquid extraction (PLE) or ultrasound assisted extraction (UAE) have not been previously reported for *Vaccinium meridionale* extracts.

On the other hand, the use of natural antioxidants from fruits rich in phenolic compounds is currently quite popular within the research field of meat products. [15, 16] This is because they have shown potent activities against lipid oxidation, which is one of their main causes of deterioration and quality loss. Together with lipid oxidation, changes in meat color due to oxidative damage of myoglobin are another of the important reasons of quality deterioration of meat and meat products. This decreasing tendency is due to a gradual oxidation of the myoglobin and the increase of the metamyoglobin in dependence of time, which is a characteristic behavior in meat and meat products. In this respect, previous studies have reported that diverse phenolic-rich extracts can also protect against myoglobin oxidation. [17, 18] Furthermore, phenolic-rich extracts included as food ingredients might have the additional advantage of contributing with the own bioactive properties of these compounds. [16] In this respect, diverse examples can be found in the scientific literature concerning the use of berries in foodstuffs for antioxidant and functional purposes, including meat products. [19-21] However, previous information on the potential use of mortiño as antioxidant ingredient in meat products has not been described.

In this work, the use of green solvents (ethanol and water) combined with efficient extraction technologies, in particular PLE and UAE, were investigated to produce *Vaccinium meridionale Swartz* (mortiño) extracts with high content of phenolic compounds, high antioxidant activity, and thus, with potential use as a food ingredient. Furthermore, the

possible use of mortiño as antioxidant ingredient in meat preparations, specifically beef burgers, was tested and the lipid oxidation and color of the resulting products was evaluated in dependence of storage time.

Materials and methods

Solvents and reagents

Ethanol (99.5 % purity), trichloroacetic acid (> 99 %) and sodium carbonate salt (≥ 99.5 %) were acquired from Panreac (Barcelona, Spain). Folin-Ciocalteu´s reagent, ABTS (2,20-azino-bis(3-ethylbenzothiaoline-6-sulphonic acid), potassium persulfate, Trolox (6-hydroxy-2,5,7,8-tetramethylchromane-2-carboxylic acid), TBA (2-thiobarbituric acid) (≥ 98 %) and gallic acid standard (≥ 97.5 %) were purchased from Sigma-Aldrich (St. Louis, MO, USA). Phosphate Buffered Saline 10X, pH 7.2 was acquired from Thermo Fisher (Waltham, MA, USA).

Mortiño vegetal material

Fresh and mature berries from plants between 4 and 6 years old of *V. meridionale* were manually harvested in the farm “La Guija” of “El Retiro” zone (2300 m altitude above sea level) belonging to Antioquia region in Colombia, and transported until Instituto de Ciencia y Tecnología Alimentaria (INTAL Foundation) where they were washed and disinfected with organic disinfectant Citrosan® and then ground in a 15 L capacity cutting machine (Cruells, Girona, Spain) at a chopper speed of 1300 rpm. The disintegrated fruits were then arranged in aluminum trays of 40 x 60 cm containing about 1.5 kg of fruit per tray and exposed to a drying process in a forced convection oven (Binder FD115, Tuttlingen, Germany) at 45 ºC for 48 h. The product was removed after 24 h and allowed to cool at room temperature of 23 ºC +/- 2 ºC for 4 h. A second size reduction process was performed using the same cutting machine as described before, and the final product with a particle size range of 500-1000

μm was vacuum packed in foil zip sealed pouches (BOPP/polyamide/LDPE) (Alico A.A., Medellin, Colombia) and sent to the Universidad Autónoma de Madrid (Madrid, Spain).

Extraction

Ultrasound assisted extraction (UAE)

Extractions were carried out in an ultrasonic device (Branson Digital Sonifier 450 model, Danbury, USA) with an electric power of 400 W, frequencies of 14 kHz and using an ½" extension tip. Experiments were carried out using 20 g of sample with 200 mL of ethanol during 30 min, and extraction temperatures were 25 and 75 °C. After extraction, supernatant was filtered through cellulose filter and solvent was removed by evaporation under vacuum. Finally, the extracts were dried up to constant weight in a stream of N_2. All experiments were carried out in duplicate. The dried samples obtained were stored at -18 °C in darkness until analysis.

Pressurized solvent extraction (PLE)

Extractions were carried out in an ASE 350 system from Dionex Corporation (Sunnyvale, CA, USA) equipped with a solvent controller unit. Each extraction cell (10 ml capacity) was loaded with 1 g of solid sample and 2 g of sea sand dispersed as a sandwich-type structure, and then placed into an oven. Then, the cell was filled with the corresponding solvent (ethanol or ethanol:water mixture 50:50) up to a pressure of 1500 psi and was heated-up to the desired temperature (50, 100, 150 and 200 °C). Static extractions were performed during 15 min. After extraction the cell was washed with the solvent and subsequently the solvent was purged from cell using N_2 gas until complete depressurization was accomplished. The extracts were recovered in glass vials and the solvent was eliminated (evaporation under vacuum and freeze-drying in the case of water) and then dried to constant weight in a

stream of N_2. All experiments were carried out by duplicate. The dried samples obtained were stored at -18 °C in darkness until analysis.

Content of total phenolic compounds (TPC)

The total phenolic content in the raw mortiño vegetal material and in mortiño PLE and UAE extracts was determined using Folin-Ciocalteu phenol reagent method. [22] Briefly 50 μl of extract dissolved in ethanol were mixed with 250 μl of Folin Ciocalteu reagent and 3 mL of milliQ water and allowed to stand at room temperature for 3 min; 750 μl of sodium carbonate (20%) solution and 950 μl of milliQ water were added to the mixture. After 2 hours at room temperature in darkness, absorbance was measured at 760 nm. Results were carried out by triplicate and expressed as g gallic acid equivalents per kg of extract (g GAE/kg extract).

Antioxidant activity by the ABTS test

The ABTS assay described by Re et al [23] was used to measure the antioxidant activity of the raw mortiño vegetal material and mortiño extracts. Trolox (6-hydroxi-2,5,7,8-tetramethylcromane-2-carboxilic acid) was used as reference standard and the results were expressed as Trolox equivalent antioxidant capacity (TEAC) values (mol Trolox/kg). $ABTS^{\bullet+}$ was produced by mixing ABTS stock solution (7 mM in water) with 2.45 mM potassium persulfate and the solution was held 16 h under darkness until used. Once the radical was formed, the solution absorbance was adjusted to 0.7 at 734 nm by PBS (when solution was used to measure the PLE samples) or ethanol (in the case of raw mortiño and UAE samples). After that, 1 mL $ABTS^{\bullet+}$ was added to 10 μL sample and the reaction mixture was allowed to stand at room temperature, under darkness, until the absorbance reached a plateau. Standard curves using Trolox were run with each set of samples. The absorbance was recorded at 734 nm. The TEAC value was calculated according to the Trolox and

sample concentrations that produce 70% ABTS•+ inhibition. All the analyses were carried out in triplicate.

Evaluation of Mortiño antioxidant activity in beef burgers

Manufacture of beef burgers

Beef burgers with 20 g/kg of raw mortiño material (MM) or a mortiño PLE extract (ME), as well as control burgers in absence of mortiño, were manufactured. Recently minced beef meat was acquired in a local supermarket. Sodium chloride (15 g/kg), water (15 g/kg), and MM or ME when corresponding, were added, and all the ingredients were manually mixed until a homogeneous raw batter was obtained. Six burgers per batch were formed by a domestic mold for mini-burgers manufacture (30 g/burger, 6 cm diameter and 1 cm thickness). Three samples per batch were analyzed after manufacturing, and the rest of the samples was kept refrigerated for 7 days.

TBARS analysis

Lipid oxidation of samples was assessed at 0 and 7 days of refrigerated storage by the thiobarbituric acid reactive substances (TBARS) method described by Salih et al [24] with slight modifications. Briefly, 2.5 g of sample were homogenized in 7.5 mL of trichloroacetic acid solution (TCA, 0.6 M) for 1 min at 11000 rpm. The homogenized sample was filtered and filled up to 10 mL with TCA. Then, 2 mL were mixed with 2 mL of TBA solution (0.02 M). The samples were kept at 90 ºC for 30 min and after that they were cooled down in ice/water bath for 10 min. The absorbance was measured at 532 nm. A stock solution of 1,1,3,3-tetraethoxypropane in TCA (equivalent to 2 µg MDA/mL) was used to plot a standard curve. The values were expressed as g MDA/kg sample.

Color measurement

Instrumental color of each burger at 0, 1, 2, 3, 6 and 7 days was measured at different points of the surface of each sample in triplicate using a Minolta Portable Spectrophotometer CM-508i (Minolta Co. LTD, Japan) with illuminant D_{65}, 10º observer and 8 mm of aperture size. Color was described as coordinates: lightness (L*), redness (a*, red-green) and yellowness (b*, yellow-blue). Nine replicate measurements were taken for each sample. Numerical total color differences (ΔE_M or ΔE_S) were calculated between control (C) and experimental samples (M), or between initial (*i*) and final (*f*) time of storage, respectively, as follows:

$$\Delta E_M = [(L_M - L_C)^2 + (a_M - a_C)^2 + (b_M - b_C)^2]^{1/2}$$

$$\Delta E_S = [(L_f - L_i)^2 + (a_f - a_i)^2 + (b_f - b_i)^2]^{1/2}$$

When the average ΔE difference between two samples was below 2.56, the samples were considered not discriminable from each other (Stokes et al. 1992). [25]

Data analysis

Results were analyzed by the Statgraphics Centurion XV software (Statpoint Technologies, Inc., USA). The multifactorial analysis of variance (ANOVA) was made on the data from extractions with PLE and UAE using the Least Significant Difference (LSD) test with significant $p \leq 0.05$ values to detect differences. Color mean data were analyzed by Generalized Linear Models (GLM), which are made to build a statistic model describing the impact of one or more factors in a dependent variable. Furthermore, for the discrimination of mean ($p \leq 0.05$) a one-way analysis of variance (ANOVA) was made using the LSD test.

Results and discussion

Extraction yield, content of phenolic compounds and antioxidant activity of the extracts

The total extraction yields (Y = mass of extract/mass of mortiño) obtained using the different extraction techniques, solvents and temperatures are given in Table 1. In case of PLE

extracts, the temperatures studied were selected to explore the range of temperatures with which the device allows for working. Both the used solvent and temperature significantly influenced the extraction yield (P=0.020 and P=0.012, respectively). Thus, the highest yields were obtained with ethanol:water (mean value = 665 g/kg) compared with ethanol (mean value = 544 g/kg), regardless of temperature. On the other hand, a trend to a higher yield with temperature was observed. Thus, the highest yields were obtained at 200ºC (mean value = 705 g/kg), and the lowest yields were obtained at 50ºC (mean value = 484 g/kg), regardless of the solvent. Therefore, the best yields were obtained by PLE with ethanol:water as solvent and at 200ºC. The observed effect due to temperature was in agreement with the typical behavior in PLE extracts, since the increase in temperature causes an increase in the solubility of compounds, diffusion rates, disruption of interactions with matrix components and a decrease in viscosity and surface tension of the solvents and, in turn, an increase in the yield of extracts. [26] Concerning the effect of the solvent, the higher yield obtained with more polar solvents (ethanol:water compared to ethanol) have been already described in previous studies related to the use of PLE and might suggest that mainly polar compounds were present in the sample. [27, 28] Previous studies about the extraction of mortiño by PLE has not been described. However, concerning other species of Vaccinium, Paes et al [13] described yields of 42 g/kg with ethanol and 54 g/kg with ethanol:water for PLE extracts at 40ºC from *Vaccinium myrtillus* L. Such values were much lower than those described in the present study, probably due to the lower temperatures applied.

In case of UAE yields, considering the results obtained with PLE at 50 ºC and 100 ºC, the solvent selected to carry out the extractions was ethanol. As for PLE, the aim was the study of the range of temperatures which can be applied in this extraction technique. In this case,

two temperatures were selected, one at ambient temperature (25 ºC) and the other one (75 ºC) at high temperature (close to the boiling point of the solvent used). A lack of effect of temperature was observed in the UAE yields (Table 1). Furthermore, the UAE yields were similar to those obtained by PLE with ethanol:water at 50ºC or with ethanol at 100ºC and 150ºC. However, the yield of mortiño extracts was not improved by the UAE, since the highest yields were obtained by PLE conditions (ethanol:water at 200ºC). These results demonstrated that PLE was a more suitable extraction technique than UAE for extraction of compounds from mortiño, probably due to the higher temperatures applied during PLE.

The content of total phenolic compounds (TPC) followed the same tendencies observed for total extraction yield for PLE (see Table 1), with higher concentration of TPC as temperature increased (mean value of 51 g GAE/kg at 200ºC compared to mean value of 18 g GAE/kg at 50ºC, regardless of solvent), and with ethanol:water used as solvent (mean value 46 g GAE/kg for ethanol:water compared to mean value of 20 g GAE/kg for ethanol, regardless of temperature). Therefore, extracts with up to 71.7 g GAE/kg were reached by PLE with ethanol:water as solvent and at 200ºC. In case of UAE, the content of TPC at 75 ºC was not different than the one obtained at 25 ºC. Furthermore, similarly to the yield values, the UAE did not improve the extraction of TPC compared to PLE.

For comparative purposes, the TPC of the raw mortiño were also analyzed, showing a value of 27.8 g GAE/kg. Therefore, according to Table 1, most PLE conditions led to extracts with higher TPC than the raw mortiño, whereas lower TPC were found for UAE samples. These results demonstrated that PLE was a more suitable extraction technique than UAE for recovering phenolic compounds from mortiño, probably due to the higher temperatures applied during PLE. The same reasons previously used to explain the differences on the extraction yield might explain the observed differences between treatments in the extraction

of TPC. Thus, higher temperatures combined with more polar solvent enhanced the extraction of TPC by PLE. On the contrary, the observed results for UAE suggested a negative impact of the ultrasonic conditions on TPC.

Regarding the antioxidant activity of the extracts (TEAC values, Table 1), the PLE extracts with ethanol:water were also the best antioxidants (mean value = 0.86 mol Trolox/kg) compared to ethanol extracts (mean value = 0.53 mol Trolox/kg), regardless of temperature. Additionally, a trend to a better antioxidant activity was observed with temperature (mean value = 0.53 mol Trolox/kg for 50ºC up to 0.87 mol Trolox/kg for 200ºC), regardless of the solvent. The UAE extracts showed a considerably lower antioxidant activity at both temperatures in comparison with PLE extracts.

Probably, the results obtained for antioxidant activity might be related to the TPC of the extracts. In this respect, Figure 1 shows the TEAC values as a function of the TPC content. All PLE extracts exhibited good linear correlation between the TPC content and the antioxidant activity, with a regression coefficient close to 0.90. Moreover, at the same extraction temperature, the ethanol:water extracts presented higher antioxidant activity than the ethanolic extracts, with TEAC values from 1.5 to 1.9 fold higher. On the other hand, UAE extracts seemed to be somewhat out of the linear correlation depicted in Figure 1, reducing the regression coefficient to 0.75 if these extracts are included in the regression procedure. Therefore, these results might suggest that the antioxidant activity of the PLE extracts might be mainly attributed to the phenolic compounds, whereas the observed antioxidant activity of UAE might be related to other different extracted molecules different to phenolic compounds.

It is important to remark that the TEAC values of raw mortiño were extremely low compared to the extracts from PLE and UAE. Thus, 0.007 mol Trolox/kg were obtained for raw mortiño, whereas the values for the extracts varied from 0.140 up to 1.034 mol Trolox/kg (Table 1).

These results demonstrated that both PLE and UAE were suitable extraction techniques to obtain mortiño extracts with antioxidant properties, but the PLE technique being superior than UAE, taking into account both the TEAC and TPC values.

For comparison, Namiesnik et al [29] obtained *V. corymbosum* and *V. macrocarpon* extracts using water and methanol (at room temperature for 24 h) with concentrations of TPC between 15.3-58.0 g GAE/kg and antioxidant activities in the range 0.065-0.255 mol TE/kg. Arancibia-Avila et al [30] obtained between 2.0-31.2 g GAE/kg and 0.01-0.26 mol TE/kg from *V. corymbosum* using water and acetone (3 h at room temperature). Therefore, the data reported in the literature for other *Vaccinium* species and other extraction procedures conform high TPC content and especially high antioxidant activity of the mortiño (*V. meridionale*) PLE extracts produced in this work.

Effect of Mortiño as natural antioxidant of beef burger

The PLE mortiño extract (ME) obtained with ethanol at 200 °C together with the raw mortiño material (MM) were investigated as natural antioxidant of beef burger. Lipid oxidation of beef burgers treated with ME and MM (20 g/kg) were compared with control burgers after refrigerated storage. According to Figure 2, the initial TBARS values (day 0) were different for the three samples, probably due to mortiño pigments which absorbed light in the same wavelength range of MDA. [18] Nevertheless, this does not hinder the comparison of the evolution of each sample between day 0 and day 7 of storage, in order to investigate the impact of mortiño on lipid oxidation. As shown in Figure 2, the TBARS values of beef burgers containing either MM or ME did not change after refrigerated storage, whereas lipid oxidation of control burgers increased significantly, closer to 200 %. Therefore, the preliminary results obtained in this work showed that both mortiño material and its PLE extract might be potential antioxidants in the control of lipid oxidation of beef burgers during refrigerated

storage. Nevertheless, taking into account the limitations of the TBARS method, further measurements of lipid oxidation by other procedures might be necessary in order to confirm the preliminary results about the potential of mortiño extracts. Previous studies about the use of mortiño as an antioxidant ingredient in foods is scarce. Zapata Acosta et al [31] and Gaviria Montoya et al [10] described the protection against lipid oxidation of mortiño after addition to edible oils. However, previous studies on the addition to complex food matrices such as meat preparations or meat products in general have not been found.

Together with lipid oxidation, changes in meat color due to oxidative damage of myoglobin are important factors determining a quality deterioration of meat and meat products. Previous studies have reported that diverse phenolic-rich extracts can protect against myoglobin oxidation. [17, 32] Therefore, the potential of mortiño as myoglobin antioxidant as well as its global contribution to the color or beef burgers was evaluated. As shown in Table 2, initial (day 0) a* and b* parameters for treated samples were lower than control samples, whereas L* values were not significantly different between samples. These results led to an evident total color difference value between treated samples and control (ΔE_M), especially for the MM samples (Table 2), and according to Stokes et al, [25] the treated samples would be clearly discriminable from the control.

When the burgers were kept refrigerated, the control samples suffered a deterioration on L*, b* and especially on a* values. This decreasing tendency is due to a gradual oxidation of the myoglobin and the increase of the metmyoglobin in dependence of time, which is a characteristic behavior in of raw meat and meat preparations. [33] However, in case of ME, despite the initial differences at day 0 with respect to the control (ΔE_S = 5.6), such differences attenuated during storage, and thus the evolution of color of ME and control was similar. This effect was reflected on a decrease on the ΔE_M values between ME and control

with increasing the number of days of storage. Thus, after 7 days of storage, the mean total color difference for ME samples was 2.25 (Table 2) showing that they would not be discriminable from each other. On the other hand, it is interesting to remark that the total color difference of control samples after storage (ΔE_S=6.8) was superior than the value for the samples treated with ME (ΔE_S=4.7) and slightly higher than those corresponding to MM samples (ΔE_S=6.0). Therefore, this result might suggest a potential lower rate of color deterioration of burgers due to mortiño and especially, due to mortiño PLE extract.

Conclusions

Mortiño extracts were produced in this work by PLE with ethanol and ethanol:water 50:50 mixtures (50-200 °C) and by UAE with ethanol (25 and 75 °C). PLE extracts obtained with ethanol:water presented the highest concentrations of total phenolic compounds and the highest TEAC values, presuming good antioxidant activity and even better than those obtained for other *Vaccinium* species.

Preliminary results were obtained in this work showing that both mortiño material and especially its PLE extract might be used as antioxidants in the control of lipid oxidation of beef burgers during refrigerated storage, although further studies would be necessary by other procedures in order to confirm such antioxidant effect. Additionally, regarding the instrumental color analysis, the results suggest a potential lower rate of color deterioration of burgers treated with mortiño and especially, with mortiño PLE extract.

Finally, future studies might be necessary in order to perform a sensorial analysis of the experimental beef burgers to evaluate the impact of mortiño or its PLE extracts on the organoleptic acceptation, and in turn, the potential use of mortiño extracts as ingredient of meat preparations.

Acknowledgements

Alexis López-Padilla thanks to the Administrative Department of Science, Technology and Innovation-Colciencias (Call 568/2012) for his Ph.D. fellowship. This work was supported by the Community of Madrid, Spain (ALIBIRD-CM S2013/ABI-2728)

References

1. Kšonžeková P, Mariychuk R, Eliašová A, Mudroňová D, Csank T, Király J, Marcinčáková D, Pistl J and Tkáčiková L, In vitro study of biological activities of anthocyanin-rich berry extracts on porcine intestinal epithelial cells. *J Sci Food Agric* **96:** 1093–1100 (2016).
2. Skrovankova S, Sumczynski D, Mlcek J, Jurikova T and Sochor J, Bioactive compounds and antioxidant activity in different types of berries. *Int J Mol Sci* **16:** 24673–24706 (2015).
3. Prior RL, Cao G, Martín A, Sofic E, McEwen J, O´Brien C, Lischner N, Ehlenfedlt M, Kalt W, Krewer G and Mailand CM, Antioxidant capacity as influenced by total phenolic and anthocyanin content, maturity, and variety of *Vaccinium* species. *J Agric Food Chem* **46:** 2686–2693 (1998).
4. Blueberry L, Aiton V, Grace MH, Ribnicky DM, Kuhn P, Poulev A, Logendra S, Yousef GG, Raskin I and Lila MA, Hypoglycemic activity of a novel anthocyanin-rich formulation from lowbush blueberry, *Vaccinium angustifolium* Aiton. *Phytomedicine* **16:** 406–415 (2009).
5. Kianbakht S, Abasi B and Dabaghian FH, Improved lipid profile in hyperlipidemic patients taking *Vaccinium arctostaphylos* fruit hydroalcoholic extract: a randomized double-blind placebo-controlled clinical trial. *Phytotherapy Res* **28:** 432–436 (2014).

6. Katsube N, Iwashita K, Tsushida T, Yamaki K and Kobori M, Induction of apoptosis in cáncer cells by bilberry (*Vaccinium myrtillus*) and the anthocyanins. *J Agric Food Chem* **51:** 68–75 (2003).
7. Subash S, Essa M, Al-Adawi S, Memon M, Manivasagam T and Akbar M, Neuroprotective effects of berry fruits on neurodegenerative diseases. *Neural Regener Res* **9:** 1557–1566 (2014).
8. Lopera YE, Fantinelli J, Arbeláez Gonzálex LF, Rojano B, Ríos JL, Schinella G and Mosca S, Antioxidant Activity and Cardioprotective Effect of a Nonalcoholic Extract of *Vaccinium meridionale* Swartz during Ischemia-Reperfusion in Rats. *J Evid Based Complementary Altern Med* **2013:** 1-10 (2013).
9. Maldonado-Celis ME, Arango-Varela SS amd Rojano BA, Free radical scavenging capacity and cytotoxic and antiproliferative effects of *Vaccinium meridionale* Sw. against colon cancer cell lines. *Revista Cubana de Plantas Medicinales* **19:** 172–184 (2014).
10. Gaviria Montoya C, Ochoa Ospina C, Sánchez Mesa N, Medina Cano C, Lobo Arias M, Galeano García P, Mosquera Martínez A, Tamayo Tenorio A, Lopera Pérez Y and Rojano B, Actividad antioxidante e inhibición de la peroxidación lipídica de extractos de frutos de mortiño (*Vaccinium meridionale* SW). *Boletin Latinoamericano Y Del Caribe de Plantas Medicinales Y Aromaticas* **8:** 519–528 (2009).
11. Sequeda-Castañeda LG, Barrera-Bugallo AR, Celis C, Iglesias J and Morales L, Evaluation of antioxidant and cytotoxic activity of extracts from fruits in fibroblastoma HT1080 cell lines: four fruits with commercial potential in Colombia. *Emirates J Food Agric* **28:** 143–151 (2016).

12. Garzón GA, Narváez CE, Riedl KM and Schwartz SJ, Chemical composition, anthocyanins, non-anthocyanin phenolics and antioxidant activity of wild bilberry (*Vaccinium meridionale* Swartz) from Colombia. *Food Chem* **122:** 980–986 (2010).
13. Paes J, Dotta R, Barbero GF and Martínez J, Extraction of phenolic compounds and anthocyanins from blueberry (*Vaccinium myrtillus* L.) residues using supercritical CO2 and pressurized liquids. *J Supercritical Fluids* **95:** 8–16 (2014).
14. López-Padilla A, Ruiz-Rodriguez A, Restrepo Flórez C, Rivero Barrios D, Reglero G and Fornari T, *Vaccinium meridionale* Swartz Supercritical CO2 Extraction: Effect of Process Conditions and Scaling Up. *Materials* **9:** 519, 1-10 (2016).
15. Ahmad SR, Gokulakrishnan P, Giriprasad R and Yatoo MA, Fruit-based natural antioxidants in meat and meat products: A review. *Crit Rev Food Sci Nutr* **55:** 1503–1513 (2015).
16. Jiang J and Xiong YL, Natural antioxidants as food and feed additives to promote health benefits and quality of meat products: A review. *Meat Sci* **120:** 107-117 (2016).
17. Utrera M, Morcuende D, Ganhão R and Estévez M, Role of phenolics extracting from Rosa canina L. on meat protein oxidation during frozen storage and beef patties processing. *Food Bioprocess Tech* **8**:4, 854–864 (2015).
18. Ganhão R, Estévez M and Morcuende D, Suitability of the TBA method for assessing lipid oxidation in a meat system with added phenolic-rich materials. *Food Chem* **126:** 772–778 (2011).
19. Bialek M, Rutkowska J, Bialek A and Adamska A, Oxidative stability of lipid fraction of cookies enriched with chokeberry polyphenols extract. *Polish J Food Nutr Sci* **6:** 77–84 (2016).

20. Aliakbarlu J and Mohammadi S, Effect of sumac (*Rhus coriaria* L.) and barberry (*Berberis vulgaris* L.) water extracts on microbial growth and chemical changes in ground sheep meat. *J Food Process Preserv* **39:** 1859–1866 (2015).
21. Ganhão R, Estévez M, Armenteros M and Morcuende D, Mediterranean berries as inhibitors of lipid oxidation in porcine burger patties subjected to cooking and chilled storage. *J Integr Agr* **12:** 1982–1992 (2013).
22. Singleton VL, Orthofer R and Lamuela-Raventós RM, Analysis of total phenols and other oxidation substrates and antioxidants by means of Folin-Ciocalteu reagent. *Method Enzymol* **299:** 152–178 (1999).
23. Re R, Pellegrini N, Proteggente A, Pannala A, Yang M and Rice-Evans C, Antioxidant activity applying an improved ABTS radical cation decolorization assay. *Free Radic Biol Med* **26:** 1231–1237 (1999).
24. Salih AM, Smith DM, Price JF and Dawson LE, Modified Extraction 2-Thiobarbituric Acid Method for Measuring Lipid Oxidation in Poultry. *Poultry Sci* **66:** 1483–1488 (1987).
25. Stokes M, Fairchild MD and Berns RS, Precision requirements for digital color reproduction. *Acm Transactions on Graphics* **11:** 406–422 (1992).
26. Giergielewicz-Możajska H, Dąbrowski Ł and Namieśnik J., Accelerated Solvent Extraction (ASE) in the Analysis of Environmental Solid Samples — Some Aspects of Theory and Practice. *Cr Rev Anal Chem* **31**: 3, 149–165 (2001).
27. Herrero H, Martín-Álvarez PJ, Señoráns FJ, Cifuentes A, and Ibáñez E, Optimization of accelerated solvent extraction of antioxidants from Spirulina platensis microalga. *Food Chem* **93**: 3, 417–423 (2005).

28. Jaime L, Vázquez E, Fornari T, López-Hazas M del C, García-Risco MR, Santoyo S and Reglero G, Extraction of functional ingredients from spinach (*Spinacia oleracea* L.) using liquid solvent and supercritical CO_2 extraction. *J Sci Food Agr* **95**: 4, 722–729 (2015).
29. Namiesnik J, Vearasilp K, Leontowicz H, Leontowicz M, Ham K, Kang S, Park Y, Arancibia-Avila P, Toledo F and Gorinstein S, Comparative assessment of two extraction procedures for determination of bioactive compounds in some berries used for daily food consumption. *Int J Food Sc Technol* **49:** 337–346 (2014).
30. Arancibia-Avila P, Namiesnik J, Toledo F, Werner E, Martinez-Ayala AL, Rocha-Guzmán NE, Gallegos-Infante JA and Gorinstein S, The influence of different time durations of thermal processing on berries quality. *Food Control* **26:** 587–593 (2012).
31. Zapata Acosta K, Piedrahita AM, Alzate AF, Cortés FB and Rojano BA, Oxidative stabilization of Sacha Inchi (*Plukenetia Volubilis* Linneo) oil with Mortiño (*Vaccinium Meridionale* SW) suspensions addition. *Revista Ciencia En Desarrollo* **6:** 141–153 (2015).
32. Ganhão R, Morcuende D and Estévez M, Protein oxidation in emulsified cooked burger patties with added fruit extracts: Influence on colour and texture deterioration during chill storage. *Meat Sci* **85:** 402–409 (2010).
33. AMSA, *AMSA Meat Color Measurement*, 2012th ed., no. December. Champaign, Illinois, 2012.

Figure captions

Fig. 1. Relation between TEAC values and the TPC content of the extracts obtained by PLE using (♦) ethanol:water (50:50), ( ) ethanol and ([2]) UAE using ethanol.

Fig. 2. Effect of the addition of mortiño material (MM) or PLE extract (ME) on TBARS values of beef burgers under refrigerated storage at day 0 (▩) and day 7 (□). Bars with different letters upon them mean statistical difference $p<0.05$. Mean value ± standard deviation (n=3)

Table 1. Total extraction yield (Y=mass of extract/mass of mortiño, g/kg), total phenolic compounds (g GAE/kg) and antioxidant activity (mol Trolox equivalent/kg) of the mortiño extracts obtained by PLE and UAE.

Extraction technique	Solvent	Temperature (ºC)	Y* (g/kg)	TPC** (g GAE/kg)	TEAC*** (mol/kg)
PLE	ethanol:water (50:50)	50	585.6 ± 6.4^{bcd}	26.97 ± 2.2^{cd}	0.646 ± 0.02^{bc}
		100	628.4 ± 0.7^{bc}	34.62 ± 1.2^{bc}	0.745 ± 0.04^{b}
		150	673.0 ± 27^{b}	50.02 ± 3.6^{b}	1.033 ± 0.07^{a}
		200	774.0 ± 3.6^{a}	71.70 ± 6.7^{a}	1.034 ± 0.07^{a}
	ethanol	50	382.5 ± 18^{e}	9.26 ± 2.52^{d}	0.421 ± 0.01^{d}
		100	559.6 ± 10.7^{cd}	18.97 ± 1.33^{cd}	0.464 ± 0.02^{cd}
		150	601.4 ± 13.7^{bcd}	21.36 ± 3.27^{cd}	0.553 ± 0.02^{bcd}
		200	635.8 ± 6.3^{bc}	30.47 ± 0.51^{bc}	0.699 ± 0.01^{b}
UAE	ethanol	25	514.2 ± 28.2^{d}	16.41 ± 0.41^{cd}	0.140 ± 0.01^{e}
		75	531.0 ± 26.9^{d}	17.40 ± 6.75^{cd}	0.180 ± 0.04^{e}

* Mean value ± standard deviation (n=2), ** Mean value ± standard deviation (n=3); *** Mean value ± standard deviation (n=3), [a-e] mean values with different letters within columns are significantly different ($P \leq 0.05$).

Table 2. Color instrumental parameters (L*, a*, b* and ΔE_M) of beef burger with *Vacciniun meridionale* Sw addition under refrigerated storage

Time (days)	treatment	L*	a*	b*	ΔE_M
0	Control	43.51 ± 2.89^{a}	10.90 ±1 .80^{a}	8.36 ± 1.69^{a}	-
	ME	42.05 ±1 .88^{a}	7.31 ± 0.92^{b}	7.43 ± 1.19^{b}	5.63 ± 2.55^{a}
	MM	41.34 ±2 .08^{a}	6.53 ± 0.63^{bc}	5.60 ± 0.74^{c}	6.32 ± 2.12^{a}
1	Control	44.64 ± 4.38^{a}	9.29 ± 1.97^{a}	8.02 ± 2.04^{a}	-
	ME	40.32 ± 1.58^{b}	6.61 ± 0.63^{b}	7.63 ± 0.97^{b}	6.55 ± 2.95^{a}
	MM	39.92 ± 2.15^{c}	5.92 ± 0.51^{c}	5.57 ± 1.01^{c}	7.96 ± 3.98^{a}
2	Control	43.32 ± 2.28^{a}	4.84 ± 1.15^{a}	5.99 ± 1.05^{a}	-
	ME	40.43 ± 3.78^{a}	5.29 ± 0.68^{a}	6.89 ± 1.14^{b}	5.06 ± 2.99^{a}
	MM	40.92 ± 2.28^{a}	4.56 ± 0.70^{a}	4.84 ± 0.94^{c}	3.83 ± 1.96^{a}
3	Control	43.64 ± 3.74^{a}	3.90 ± 0.65^{a}	6.53 ± 1.02^{a}	-
	ME	41.94 ± 3.38^{b}	4.80 ± 0.91^{b}	7.66 ± 1.84^{b}	5.69 ± 3.09^{a}
	MM	42.71 ± 3.10^{c}	3.66 ± 0.85^{ac}	5.84 ± 0.94^{c}	4.73 ± 2.75^{a}
6	Control	43.73 ± 2.02^{a}	4.07 ± 0.48^{a}	7.52 ± 1.69^{a}	-
	ME	43.19 ± 3.65^{b}	3.71 ± 0.44^{b}	8.26 ± 1.83^{b}	3.31 ± 1.83^{a}
	MM	38.55 ± 2.06^{c}	2.31 ± 0.44^{c}	5.64 ± 1.35^{c}	6.05 ± 2.42^{b}
7	Control	41.58 ± 2.30^{a}	4.66 ± 0.99^{a}	7.79 ± 1.41^{a}	-
	ME	41.91 ± 1.13^{b}	3.62 ± 0.38^{b}	7.69 ± 1.11^{b}	2.25 ± 0.88^{a}
	MM	39.01 ± 1.35^{c}	2.30 ± 0.28^{c}	5.70 ± 0.80^{c}	4.75 ± 1.34^{b}

ΔE_M: Differences between samples against their control each day.

$^{a-c}$: For the same coordinate, within a column, means with different letters are significantly different ($P \leq 0.05$). n = 9; mean ± standard deviation

Figure 1

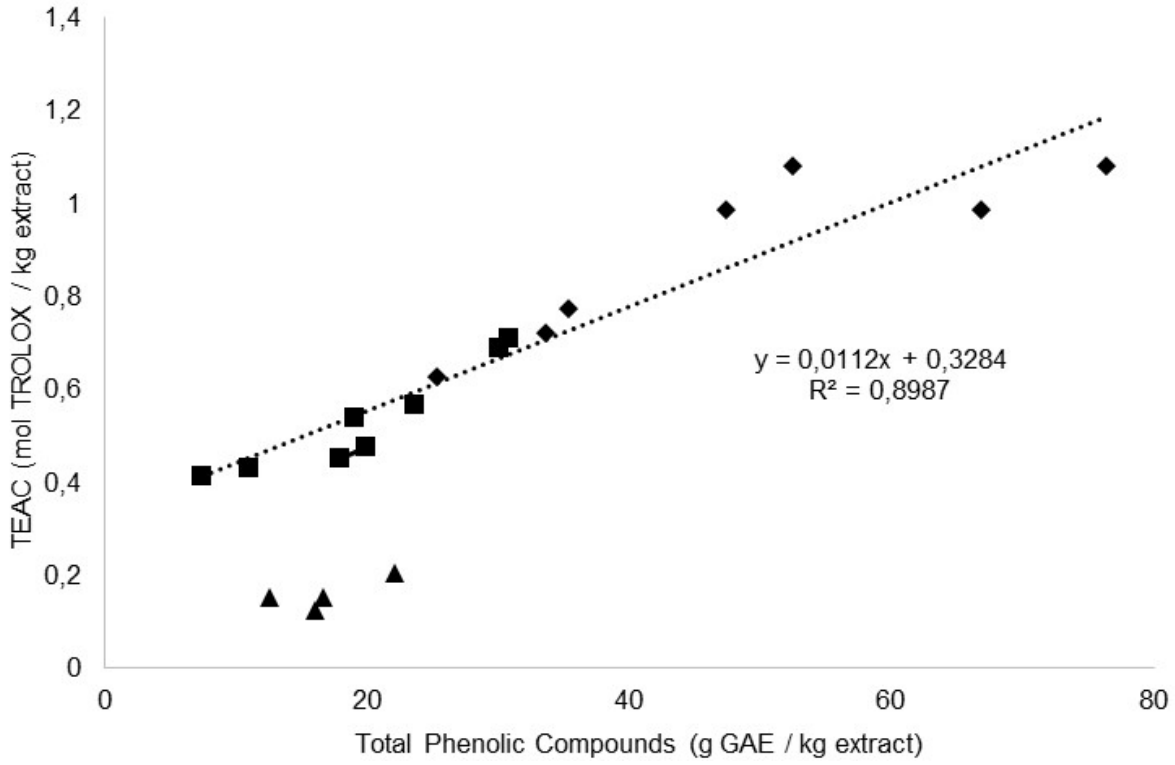

Figure 2

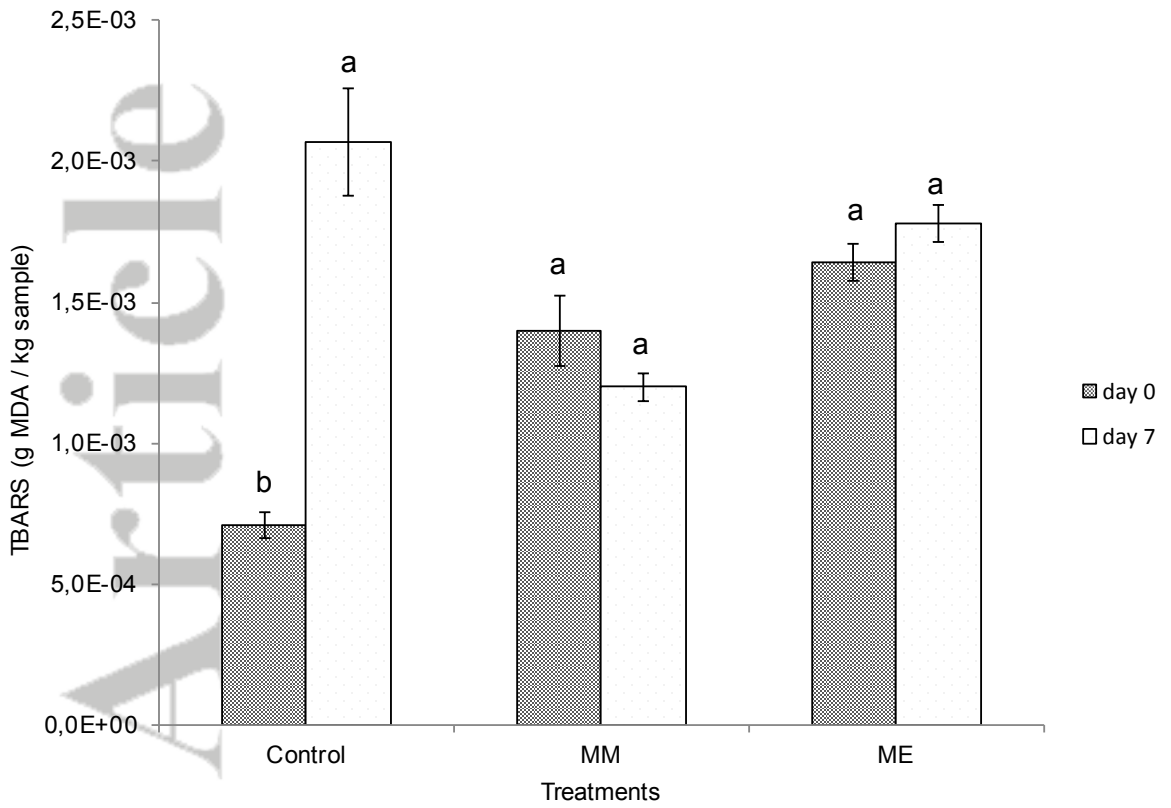

2. Biological activities of Asteraceae (*Achillea millefolium* and *Calendula officinalis*) and Lamiaceae (*Melissa officinalis* and *Origanum majorana*) plant extracts.

Mónica R. García-Risco, Lamia Mouhid, Lilia Salas-Pérez,
Alexis López-Padilla, Susana Santoyo, Laura Jaime,
Ana Ramírez de Molina, Guillermo Reglero & Tiziana Fornari

Plant Foods for Human Nutrition, 72 (2017) 96-102.
DOI: 10.1007/s11130-016-0596-8

Plant Foods Hum Nutr
DOI 10.1007/s11130-016-0596-8

ORIGINAL PAPER

Biological Activities of Asteraceae (*Achillea millefolium* and *Calendula officinalis*) and Lamiaceae (*Melissa officinalis* and *Origanum majorana*) Plant Extracts

Mónica R. García-Risco[1] · Lamia Mouhid[2] · Lilia Salas-Pérez[3] · Alexis López-Padilla[1] · Susana Santoyo[1] · Laura Jaime[1] · Ana Ramírez de Molina[2] · Guillermo Reglero[1,2] · Tiziana Fornari[1]

Abstract Asteraceae (*Achillea millefolium* and *Calendula officinalis*) and Lamiaceae (*Melissa officinalis* and *Origanum majorana*) extracts were obtained by applying two sequential extraction processes: supercritical fluid extraction with carbon dioxide, followed by ultrasonic assisted extraction using green solvents (ethanol and ethanol:water 50:50). The extracts were analyzed in terms of the total content of phenolic compounds and the content of flavonoids; the volatile oil composition of supercritical extracts was analyzed by gas chromatography and the antioxidant capacity and cell toxicity was determined. Lamiaceae plant extracts presented higher content of phenolics (and flavonoids) than Asteraceae extracts. Regardless of the species studied, the supercritical extracts presented the lowest antioxidant activity and the ethanol:water extracts offered the largest, following the order *Origanum majorana* > *Melissa officinalis* ≈ *Achillea millefolium* > *Calendula officinalis*. However, concerning the effect on cell toxicity, Asteraceae (especially *Achillea millefolium*) supercritical extracts were significantly more efficient despite being the less active as an antioxidant agent. These results indicate that the effect on cell viability is not related to the antioxidant activity of the extracts.

Keywords *Origanum majorana* · *Melissa officinalis* · *Achillea millefolium* · *Calendula officinalis* · Antioxidant · Antiproliferative

Abbreviations

ABTS	2 2′-azino-bis (3-ethylbenzothiazoline-6-sulphonic acid)
DMSO	Dimethyl sulfoxide
DPPH	2,2-Diphenyl-1-picrylhydrazyl
GC-MS	Gas chromatography–mass spectrometry
MTT	3-(4, 5-dimethylthiazolyl-2)-2, 5-diphenyltetrazolium bromide
SFE	Supercritical fluid extraction
UAE	Ultrasonic assisted extraction

Introduction

In recent decades, the interest in the use of plants in medicine research has leaned towards finding therapies that replace synthetic drugs by herbal derived products. Plant-type products are used to flavor beverages and food goods, but also as antioxidants with a strong ability to stabilize vegetable fats [1]. Particularly, flavonoids and other phenolic compounds, wildly present in plant extracts [2] possess a chemical structure that has shown a high capacity as free radical scavengers (antioxidants) and therefore, to act against free radical damage [3].

It is well known that oxidative stress and free radicals are involved in triggering cell damage and in carcinogenesis

Mónica R. García-Risco, Lamia Mouhid and Lilia Salas-Pérez contributed equally to this work.

Electronic supplementary material The online version of this article (doi:10.1007/s11130-016-0596-8) contains supplementary material, which is available to authorized users.

✉ Tiziana Fornari
tiziana.fornari@uam.es

[1] Institute of Food Science Research (CIAL), Madrid, Spain

[2] Madrid Institute for Advanced Studies on Food (IMDEA-Food), Madrid, Spain

[3] Polytechnic University of Gomez Palacio (UPGOP), Durango, Mexico

Published online: 18 January 2017

process [4]. In this sense, antioxidants were initially proposed as an alternative to struggle against cancer. However, clinical trials in humans and recent *in vivo* experiments determine a lack of success and even tumorigenic promotion [5], in part because they do not induce oxidative damage reduction *in vivo* [6]. In this regard, it is still a challenge to elucidate if the anticancer potential of plant extracts is related to their effect on free radicals.

Plant extracts are part of the current trend towards functional foods and therapies, and a source of natural biomolecules proposed against tumoral cells. In the present work is reported the study and comparison of the antitumor effect of extracts derived from different family plants: two from Asteraceae (*Achillea millefolium* and *Calendula officinalis)* and two plants from Lamiaceae (*Melissa officinalis* and *Origanum majorana*), obtained by using supercritical fluid extractions (SFE) and ultrasonic assisted extractions (UAE).

SFE uses supercritical carbon dioxide ($SCCO_2$) and extracts the lipophilic fraction of the plant; while UAE with ethanol and/or water results in the extraction of polar compounds such as flavonoids and phenols. Thus, these two techniques may be complemented, by first applying SFE to extract the plant volatile oils, followed by a UAE step to recover the polar compounds from the residual plant matrix. This two-step extraction scheme was applied to produce extracts from *Achillea millefolium* L. (yarrow), *Calendula officinalis* (marigold), *Melissa officinalis* (balm) and *Origanum majorana* (marjoram). The extracts were analyzed in terms of their antioxidant capacity and their antiproliferative effect, in order to determine whether these two biological activities are related, or by contrast, to identify within these herbal species and extracts the most active as an antioxidant or an anticancer agent.

Materials and Methods

A more detailed description of chemicals and sample preparation can be found as supplementary material.

Extractions The SFE (see Table 1) assays were carried out in duplicate using a pilot-plant supercritical fluid extractor (Thar Technology, Pittsburgh, PA, USA, model SF2000) comprising a 2 L cylinder extraction cell. Extraction pressure and temperature were 140 bar and 40 °C, respectively. CO_2 flow was 70 g/min and extraction time 180 min. The oleoresin resulting in the separator was collected using ethanol. Then, ethanol was removed using a rotavapor at low temperature (30 °C). The residual vegetal material obtained after the SFE step was re-extracted using an ultrasound probe (Branson Digital Sonifier, Branson Ultrasonics, model 250; Danbury, USA). The UAE assays were carried out using green polar solvents (ethanol or ethanol:water 50:50). It was demonstrated [7] that UAE with low ethanol:water ratios is more efficient than UAE with ethanol to the recovery of phenolic compounds. In this work, both ethanol and ethanol:water (50:50) solvents were used in the extractions in order to find the best conditions to obtain the maximum polar components.

Chemical Characterization To determine the chemical composition, the supercritical extracts were analyzed by GC-MS (Agilent Technologies 7890A). A more detailed description of the GC-MS method can be found as supplementary material.

Regarding the total phenolic content (TPC), the determination was carried out following Folin-Ciocalteu method, and results were expressed as mg gallic acid equivalents in 1 g of extract (mg GAE/g extract). Meanwhile the total flavonoid content (TFC) was determined as described by Zhishen et al. [8], and results were expressed as mg quercetin equivalents in 1 g of extract (mg QE/g extract).

Antioxidant Activity Scavenging activity was determined by a spectrophotometric method based on the reduction of an ethanol solution of 1,1-diphenyl-2-picrylhydrazyl (DPPH), as described previously [9]. The DPPH concentration in the reaction medium was calculated from a calibration curve determined by linear regression ($y = 0.0303\times - .0349$; $R^2 = 0.9955$). Furthermore, the $ABTS^{\bullet+}$ assay, as described by Re et al. [10], was also used to measure the antioxidant activity and results were expressed as TEAC values (mmol TE / g extract).

Antiproliferative Effect The cytotoxicity was studied on pancreatic human tumor-derived cell line MiaPaca-2 and measured by MTT assay, as described in our previous works [9]. Results were expressed through the IC_{50}, which describes the concentration value that produces 50% cell viability inhibition.

Table 1 Supercritical CO_2 extraction of Asteraceae and Lamiaceae plants

Plant part	Yarrow Inflorescences and leaves	Marigold Flowers	Marjoram Leaves	Balm Leaves
Water content (%)	<5	<5	<5	<5
Particle size (μm)	1000	1000	1000	1000
Mass loaded for SFE (g)	383	500	550	713
CO_2/plant ratio (kg/kg)	33	25	23	18

Statistical Analysis The significant differences between extractions and plant extracts were determined by using the GaphPad Prism 6.0 m Software (San Diego, CA, USA).

Results and Discussion

The extraction approach was designed in order to obtain first a lipophilic fraction by CO_2-SFE, which is expected to contain the plant volatile oil. Then, the residual vegetal material was extracted by UAE using polar solvents (ethanol or ethanol:water 50:50) to obtain a second fraction containing the characteristic polar compounds of the plant according to the species. The SFE and UAE extraction yields of both Asteraceae and Lamiaceae plants are given in Table 2. UAE yields were considerably higher than SFE yields for all plants studied, and the yields obtained with ethanol:water were higher than those obtained with pure ethanol. Significant differences ($p < 0.05$) between SFE and UAE (ethanol:water 50:50) yields for marigold and balm were found after carrying out an ANOVA two-way analysis. In general, despite the method or the solvent used, the higher extractions yields were obtained with marigold, followed by marjoram, balm and yarrow.

GC-MS Analysis SFE extracts were analyzed by GC-MS to identify these components, mainly monoterpenes and sesquiterpenes. The results obtained are discussed below.

Marigold. Several sesquiterpenes (γ-muurolen, δ-cadinen, α-muurolol and α-cadinol) were identified in Marigold in different percentages according to sample preparation and SFE parameters [11]. In this work, the sesquiterpenes identified in Marigold SFE extracts are reported in Table 3 and include α- and β-muurolene, α- and β-cadinene, α- cadinol and T cadinol, in agreement with previous works from the literature [12, 13]. Furthermore, also triterpenes, such as α-amyrin (8.67 mg/g) and lupeol (7.39 mg/g) were identified in the SFE extract of marigold (data not shown in Table 3) in accordance with other works which report high content of triterpenes in marigold supercritical CO_2 extracts [14].

Yarrow. Table 4 present the main compounds identified in yarrow SFE extracts. In accordance with the literature, the results obtained in this work indicate that the most important compounds of *Achillea millefolium* volatile oil include monoterpenes such as terpineol and borneol [15], and sesquiterpenes such us germacrene D caryophyllene, bisabolene, α-bisabolol, δ-cadinen [16], spathuleol and cadinol [15].

Table 3 Volatile oil compounds identified by GC-MS in the SFE extract of Marigold

Retention time	Compound	% Area	Type
9795	β-Muurolene	13.86	S (hydrocarbon)
9984	α-Cadinene	23.36	S (hydrocarbon)
10,051	β-Cadinene	21.26	S (hydrocarbon)
10,236	α-Muurolene	9.79	S (hydrocarbon)
11,497	T-Cadinol	13.76	S (bicyclic alcohol)
11,636	α-Cadinol	17.96	S (bicyclic alcohol)

S sesquiterpene, *T* triterpene

Caryophyllene, caryophyllene oxide, β-eudesmol and α-curcumene were identified and quantified in this work in concentrations of 0.14, 2.21, 5.22 and 8.07 mg/g of extract, respectively. Some authors have reported around 4, 7, 16 and 2 mg/g, respectively, to the same compounds [17], in an extract produced by hydrodistillation. Nevertheless, others studies comprising yarrow supercritical extracts have not reported the presence of α-curcumene [18].

Balm. Previous studies indicated that the volatile oil of balm is rich in monoterpenes such as citral [19], citronellal and α-caryophyllene [20], and sesquiterpenes such as caryophyllene oxide [20]. These compounds were identified in the extracts obtained by steam distillation, infusion and by SFE extractions, and were also identified in the SFE extract obtained in this work. Table 5 present the monoterpenes and sesquiterpenes observed in balm SFE extract.

Marjoram. Table 6 shows the marjoram supercritical extract composition. The presence of monoterpenes such as terpineol, and sesquiterpenes like spathulenol or β-caryophyllene as the most abundant compounds, agree with previous works focused on SFE [21]. In addition, 23 isoprenoids were identified in this work as reported in Table 5.

Total Phenolic Compounds (TPC) The assessment of the content of TPC is of great interest due to the recognized capacity of these substances to act as scavenging agents and thus,

Table 2 Extraction yield (mass of extract /mass of plant material)

	Yarrow	Marigold	Marjoram	Balm
SFE	0.79 ± 0.03	2.78 ± 0.21	1.51 ± 0.16	0.65 ± 0.04
UAE (ethanol)	2.82 ± 0.01	6.83 ± 0.49	6.17 ± 0.90	4.35 ± 0.06
UAE (ethanol:water 50:50)	10.82 ± 0.42	29.13 ± 1.41	12.83 ± 0.15	22.99 ± 0.37

Table 4 Volatile oil compounds identified by GC-MS in the SFE extract of yarrow

Retention time	Compound	% Area	Type
4589	Yomogi alcohol	2.56	M (acyclic alcohol)
5115	Eucalyptol	2.23	M (cyclic ether)
5471	Artemisia ketone	2.12	M (acyclic ketone)
5823	Sabinene	2.80	M (bicyclic hydrocarbon)
6078	Linalool	1.31	M (acyclic alcohol)
6224	Thujone	1.84	M (cyclic ketone)
6853	Citronellal	5.63	M (acyclic aldehyde)
7203	Borneol	16.28	M (bicyclic alcohol)
7482	Terpineol	2.56	M (propan-2-ol)
9287	Carvacrol	3.52	M (phenol)
10,411	Verbenol	1.76	M (bicyclic alcohol)
11,234	Caryophyllene	0.95	S (hydrocarbon)
11,356	Nerolidol acetate	0.90	S (acyclic ester)
12,074	α-Curcumene	3.61	S (cyclic hydrocarbon)
13,077	Elemol	1.37	S (propan-2-ol)
13,469	Cubenol	5.43	S (bicyclic alcohol)
13,541	Spathulenol	5.55	S (tricyclic alcohol)
13,637	Caryophillene oxide	4.90	S (oxide)
13,765	Viridiflorol	5.12	S (tricyclic alcohol)
14,300	α-Cadinol	8.22	S (bicyclic alcohol)
14,555	Eudesmol	11.19	S (propan-2-ol)
14,900	Bisabolol	2.73	S (cyclic alcohol)
16,833	Corymbolone	7.44	S (bicyclic keto-alcohol)

M monoterpene, *S* sesquiterpene

they are closely connected with the antioxidant activity of the plant extracts. Main phenolic compounds reported in yarrow were flavonoids, highlighting rutin, vicenin-2, or apigenin and luteolin and their glycosylic derivatives [22, 23]. In addition, caffeic acid derivatives and ascorbic acids were also found in yarrow [24] ultrasonic extracts. Regarding marigold, the other Asteraceae plant investigated in this work, triterpenoids with several hydroxyl substitutions were described previously [18], such as α- and β-amyrin, lupeol and faradiol. Concerning Lamiaceae plants, both Balm and Marjoram were reported to contain phenolic acids and flavonoids, mainly apigenin, luteolin and quercetin [25, 26].

Table 5 Volatile oil compounds identified by GC-MS in the SFE extract of balm

Retention time	Compound	% Area	Type
6078	Linalool	3.70	M (acyclic alcohol)
6853	Citronellal	23.87	M (acyclic aldehyde)
7203	Borneol	4.37	M (bicyclic alcohol)
7482	Terpineol	4.79	M (propan-2-ol)
9125	Thymol	6.13	M (phenol)
9287	Carvacrol	25.44	M (phenol)
11,234	Caryophyllene	4.79	S (hydrocarbon)
13,077	Elemol	2.90	S (propan-2-ol)
13,637	Caryophyllene oxide	17.73	S (oxide)
13,763	Epiglobulol	2.34	S (bicyclic alcohol)
14,555	Eudesmol	3.94	S (propan-ol alcohol)

M monoterpene, *S* sesquiterpene, *D* diterpene, *T* triterpene

Table 6 Volatile oil compounds identified by GC-MS in the SFE extract of marjoram

Retention time	Compound	% Area	Type
5115	Eucalyptol	11.48	M (cyclic ether)
6078	Linalool	9.84	M (acyclic alcohol)
6865	Camphor	0.55	M (ketone)
7203	Borneol	4.16	M (bicyclic alcohol)
7482	Terpineol	0.38	M (propan-2-ol)
9125	Thymol	2.52	M (phenol)
9287	Carvacrol	50.72	M (phenol)
9927	γ- Elemen	0.94	S (hydrocarbon)
10,077	α- Terpineol acetate	1.71	M (ester)
105,075	Neryl acetate	0.34	M (ester)
11,234	Caryophyllene	2.57	S (hydrocarbon)
12,076	Longiborneol	0.46	S (bicyclic alcohol)
12,373	α-Elemen	0.76	S (hydrocarbon)
12,456	α-Himachalen	0.48	S (hydrocarbon)
126,115	γ- Cadinene	0.34	S (hydrocarbon)
12,701	Epiglobulol	1.30	S (tricyclic alcohol)
127,785	Globulol	0.57	S (tricyclic alcohol)
13,541	Ent-spathulenol	3.13	S (tricyclic alcohol)
13,637	Caryophyllene oxide	1.70	S (oxide)
13,778	Ledol	2.02	S (tricyclic alcohol)
14,276	γ- Eudesmol	0.76	S (propan-2-ol)
143,665	β- Guaiene	0.83	S (hydrocarbon)
14,555	β- Eudesmol	2.44	S (propan-2-ol)

M monoterpene, *S* sesquiterpene, *D* diterpene, *T* triterpene

The TPC of plant extracts investigated in this work is show in Fig. 1a. The SFE extracts presented values of 12.6 to 56.2 mg GAE /g extract, compared with those obtained by UAE extractions, with values of 65.0 to 232.7 mg GAE /g extract. Although all SFE extracts exhibit low content of TPC in comparison with UAE extracts, marjoram extract showed considerably higher amounts than the other supercritical extracts. In the case of UAE extracts, despite the solvent used, marjoram resulted statistically with the highest content of TPC, followed by balm, yarrow and marigold (Fig. 1a, Table S1).

Total Flavonoid Compounds (TFC) Content of TFC is shown in Fig. 1b. As in the case of phenolic compounds,

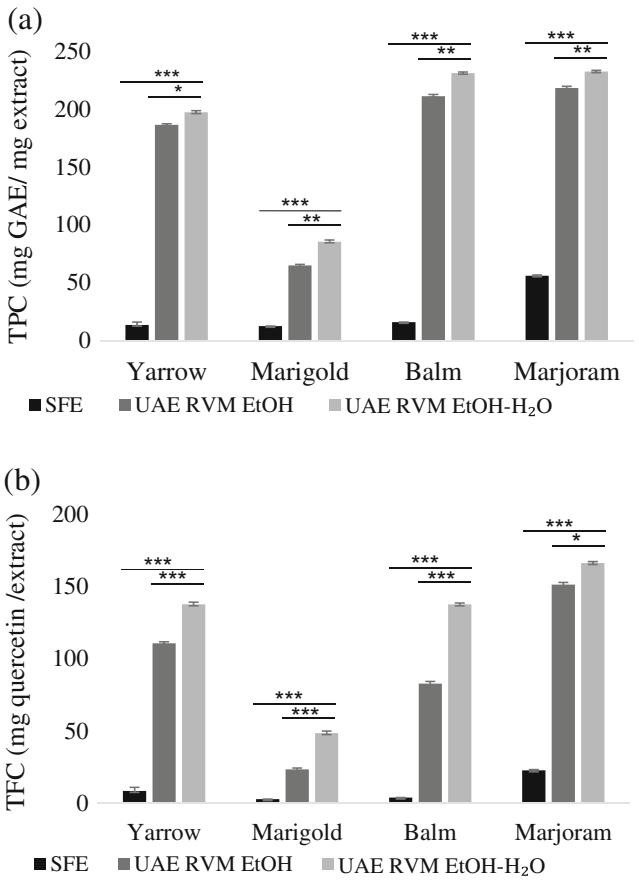

Fig. 1 **a** TPC and **b** TFC of the extracts. Data represent means ± SEM of at least two independent experiments. Asterisks indicate statistical differences between treatments after one-way Anova comparison. *$p < 0.05$, **$p < 0.01$; ***$p < 0.001$

low amounts of flavonoids were determined in the SFE extracts in comparison with UAE extracts. Marjoram extracts were those with the highest significant TFC content, despite the method or the solvent used in the extraction (Fig. 1b, Table S2). In general, TFC follow the same tendency observed in TPC. Furthermore, a lineal connection between TPC and TFC can be established for all the extracts, as illustrated in Fig. S1, although somewhat more scattering relationship is observed in the case of balm extracts.

Antioxidant Activity The antioxidant activity of all extracts produced was determined by to different methods: the DPPH radical method, stating the antioxidant capacity in terms of the EC_{50} value, and the ABTS radical method, by means of the TEAC value. Table 7 shows the results obtained for all plant extracts produced. As can be observed, both methods indicate the same tendency for all plant extracts: UAE ethanol:water extracts presented the highest antioxidant activity (lowest EC_{50} values and highest TEAC values), followed by UAE ethanol extracts. Additionally, for all plants studied, SFE extracts exhibit significantly lower antioxidant activity than UAE extracts. The highest antioxidant activity was found in marjoram extracts, despite the type of extraction or solvent used. Results were rather similar for balm and yarrow, and definitively marigold extracts presented the lowest antioxidant capacity. Particularly, the EC_{50} value resulted for marjoram ethanol:water extract (13.74 μg/ml) is in the same order of magnitude that reported for rosemary extracts, which is a commercial antioxidant for foodstuffs (E392) [9]. As can be observed in Fig. S2(a), high correlation resulted between the EC_{50} values and TPC ($R^2 = 0.985$).

Nevertheless, although the ABTS test show the same tendency regarding the antioxidant capacity of the extracts (marjoram > balm ≈ yarrow > marigold) the TEAC values do not show a linear correlation with TPC Fig. S2(b). The same conclusions can be established regarding the connection between the total content of flavonoid compounds (TFC) and the antioxidant activity of the UAE extracts, although in this case the regression coefficient of the EC_{50} vs. TFC correlation is somewhat lower ($R^2 = 0.858$).

Antiproliferative Activity Cells were treated with different concentrations (from 10 to 100 μg/mL) of each extract during 48 h. Extracts from Lamiaceae family (balm and marjoram) do not demonstrate any effect on the growth of MiaPaca-2 cells: the IC_{50} was higher than 100 μg/mL, showing the absence of a

Table 8 Antiproliferative effect in MiaPaCa-2 cell line: IC_{50} (μg/mL) values after 48 h of exposure (mean ± SEM of three independent experiments)

	SFE	UAE ethanol	UAE ethanol:water
Marjoram	> 100	> 100	> 100
Balm	> 100	> 100	> 100
Yarrow	31.45 ± 8.56	65.04 ± 2.55	> 100
Marigold	39.84 ± 4.57	> 100	> 100

Table 7 Antioxidant activity of extracts: EC_{50} (mg/ml) and TEAC (mmol/g) values

	Yarrow		Marigold		Balm		Marjoram	
	EC_{50}	TEAC	EC_{50}	TEAC	EC_{50}	TEAC	EC_{50}	TEAC
SFE	367.15	0.077	442.40	0.046	318.38	0.033	229.84	0.642
UAE (ethanol)	43.44	0.327	154.77	0.062	38.04	0.238	22.17	0.967
UAE (ethanol:water)	40.27	0.644	123.35	0.331	22.67	0.697	13.74	1550

significant effect on cell proliferation in the range of concentrations tested. By contrast, yarrow and marigold extracts (Asteraceae family) show a clear effect (Table 8). The IC_{50} for yarrow SFE and UAE extracts is in a range between 30 and 65 μg/mL, similar to Rosemary SFE extract tested in other tumor types [27, 28], which can lead to suggest yarrow and marigold extracts as potential antitumorogenic agents.

Conclusions

Lamiaceae plant family seems to be the most appropriate source of antioxidant extracts and the use of polar solvents the best extraction method to produce them. However, Asteraceae family shows the most promising results as source of potential antiproliferative agents and SFE the most efficient method to produce extracts for this purpose. These results support previous studies suggesting a potential anticancer activity of plant extracts independently of their antioxidant activity.

Related to composition, Lamiaceae species are particularly rich in phenolic monoterpenes and sesquiterpenes (around 32% balm and 53% marjoram), with 7–12% of cyclic alcohols. In the contrary, the volatile oil content in Asteraceae plants comprise high amounts of bicyclic and tricyclic alcohols (52% yarrow and 32% marigold) and almost no phenolic alcohols were identified. This result encourage further studies to elucidate a possible effect of bicyclic and tricyclic monoterpene and sesquiterpene alcohols as responsible of the antiproliferative effect of these Asteraceae extracts.

Acknowledgements The authors gratefully acknowledge the financial support from Ministerio de Economía y Competitividad of Spain (project AGL2013-48943-C2) and the Comunidad Autónoma de Madrid (ALIBIRD, project number S2013/ABI-2728).

Compliance with Ethical Standards

Conflict of Interest The authors declare that they have no conflict of interest.

References

1. Ìnanç T, Maskan M (2012) The potential application of plant essential oils/extracts as natural preservatives in oils during processing: a review. J Food Sci Eng 2:1–9. doi:10.1007/s11746-013-2351-8
2. Kähkönen MP, Hopia AI, Vuorela HJ, Rauha J, Pihlaja K, Kujala TS et al (1999) Antioxidant activity of plant extracts containing phenolic compounds. J Agric Food Chem 47(10):3954–3962. doi:10.1021/jf990146l
3. Rice-Evans CA, Miller NJ, Paganga G (1996) Structure-antioxidant activity relationships of flavonoids and phenolic acids. Free Radical Bio Med 20(7):933–956. doi:10.1016/0891-5849(95)02227-9
4. Dreher D, Junod AF (1996) Role of oxygen free radicals in cancer development. Eur J Cancer 32(1):30–38. doi:10.1016/0959-8049(95)00531-5
5. Sayin VI, Ibrahim MX, Larsson E, Nilsson JA, Lindahl P, Bergo MO (2014) Antioxidants accelerate lung cancer progression in mice. Sci Transl Med 6(221):221ra15. doi:10.1126/scitranslmed.3007653
6. Halliwell B (2012) Free radicals and antioxidants: updating a personal view. Nutr Rev 70(5):257–265. doi:10.1111/j.1753-4887.2012.00476.x
7. Paini M, Casazza AA, Aliakbarian B, Perego P, Binello A, Cravotto G (2016) Influence of ethanol/water ratio in ultrasound and high-pressure/high-temperature phenolic compound extraction from agri-food waste. Int J Food Sci Tech 51(2):349–358. doi:10.1111/ijfs.12956
8. Zhishen J, Mengcheng T, Jianming W (1999) The determination of flavonoid contents in mulberry and their scavenging effects on superoxide radicals. Food Chem 64(4):555–559. doi:10.1016/S0308-8146(98)00102-2
9. Vicente G, Molina S, González-Vallinas M, García-Risco MR, Fornari T, Reglero G et al (2013) Supercritical rosemary extracts, their antioxidant activity and effect on hepatic tumor progression. J Supercrit Fluid 79:101–108. doi:10.1016/j.supflu.2012.07.006
10. Re R, Pellegrini N, Proteggente A, Pannala A, Yang M, Rice-Evans C (1999) Antioxidant activity applying an improved ABTS radical cation decolorization assay. Free Radical Bio Med 26(9):1231–1237. doi:10.1016/S0891-5849(98)00315-3
11. Campos LM, Michielin EM, Danielski L, Ferreira SR (2005) Experimental data and modeling the supercritical fluid extraction of marigold (*Calendula officinalis*) oleoresin. Journal Supercrit Fluid 34(2):163–170. doi:10.1016/j.supflu.2004.11.010
12. Wiłkomirski B (1985) Pentacyclic triterpene triols from *Calendula officinalis* flowers. Phytochemistry 24(12):3066–3067. doi:10.1016/0031-9422(85)80062-5
13. Chalchat J, Garry RP, Michet A (1991) Chemical composition of essential oil of *Calendula officinalis* L.(pot marigold). Flavour Frag J 6(3):189–192. doi:10.1002/ffj.2730060306
14. Hamburger M, Adler S, Baumann D, Förg A, Weinreich B (2003) Preparative purification of the major anti-inflammatory triterpenoid esters from marigold (*Calendula officinalis*). Fitoterapia 74(4):328–338. doi:10.1016/S0367-326X(03)00051-0
15. Rahimmalek M, Tabatabaei BES, Etemadi N, Goli SAH, Arzani A, Zeinali H (2009) Essential oil variation among and within six *Achillea* species transferred from different ecological regions in Iran to the field conditions. Ind Crop Prod 29(2):348–355. doi:10.1016/j.indcrop.2008.07.001
16. Rohloff J, Skagen EB, Steen AH, Iversen T (2000) Production of yarrow (*Achillea millefolium* L.) in Norway: essential oil content and quality. J Agric Food Chem 48(12):6205–6209. doi:10.1021/jf000720p
17. Candan F, Unlu M, Tepe B, Daferera D, Polissiou M, Sökmen A et al (2003) Antioxidant and antimicrobial activity of the essential oil and methanol extracts of *Achillea millefolium subsp. millefolium* Afan. (Asteraceae). J Ethnopharmacol 87(2):215–220. doi:10.1016/S0378-8741(03)00149-1
18. Bocevska M, Sovová H (2007) Supercritical CO_2 extraction of essential oil from yarrow. J Supercrit Fluids 40(3):360–367. doi:10.1016/j.supflu.2006.07.014
19. Topal U, Sasaki M, Goto M, Otles S (2008) Chemical compositions and antioxidant properties of essential oils from nine species of Turkish plants obtained by supercritical carbon dioxide extraction and steam distillation. Int J Food Sci Nutr 59(7–8):619–634. doi:10.1080/09637480701553816
20. Schnitzler P, Schuhmacher A, Astani A, Reichling J (2008) *Melissa officinalis* oil affects infectivity of enveloped herpesviruses. Phytomedicine 15(9):734–740. doi:10.1016/j.phymed.2008.04.018

21. Vagi E, Simandi B, Suhajda A, Hethelyi E (2005) Essential oil composition and antimicrobial activity of *Origanum majorana* L. extracts obtained with ethyl alcohol and supercritical carbon dioxide. Food Res Int 38(1):51–57. doi:10.1016/j.foodres.2004.07.006
22. Benedek B, Kopp B (2007) *Achillea millefolium* L. sl revisited: recent findings confirm the traditional use. Wien Med Wochenschr 157(13–14):312–314. doi:10.1007/s10354-007-0431-9
23. Benetis R, Radusiene J, Janulis V (2008) Variability of phenolic compounds in flowers of *Achillea millefolium* wild populations in Lithuania. Medicina (Kaunas) 44(10):775–781
24. Vitalini S, Beretta G, Iriti M, Orsenigo S, Basilico N, Dall'Acqua S et al (2011) Phenolic compounds from *Achillea millefolium* L. and their bioactivity. Acta Biochim Pol 58(2):203–219
25. Dastmalchi K, Dorman HD, Oinonen PP, Darwis Y, Laakso I, Hiltunen R (2008) Chemical composition and *in vitro* antioxidative activity of a lemon balm (*Melissa officinalis* L.) extract. LWT-Food Sci Technol 41(3):391–400. doi:10.1016/j.lwt.2007.03.007
26. Hossain MB, Camphuis G, Aguiló-Aguayo I, Gangopadhyay N, Rai DK (2014) Antioxidant activity guided separation of major polyphenols of marjoram (*Origanum majorana* L.) using flash chromatography and their identification by liquid chromatography coupled with electrospray ionization tandem mass spectrometry. J Sep Sci 37(22):3205–3213. doi:10.1002/jssc.201400597
27. Yesil-Celiktas O, Sevimli C, Bedir E, Vardar-Sukan F (2010) Inhibitory effects of rosemary extracts, carnosic acid and rosmarinic acid on the growth of various human cancer cell lines. Plant Foods Hum Nut 65(2):158–163. doi:10.1007/s11130-010-0166-4
28. González-Vallinas M, Molina S, Vicente G, de la Cueva A, Vargas T, Santoyo S et al (2013) Antitumor effect of 5-fluorouracil is enhanced by rosemary extract in both drug sensitive and resistant colon cancer cells. Pharmacol Res 72:61–68. doi:10.1016/j.phrs.2013.03.010

ANEXO B. Otras Publicaciones

Recovery of betulinic acid from plane tree (*Platanus acerifolia* L.)

José María Pinilla, Alexis López-Padilla, Gonzalo Vicente, Tiziana Fornari, J.C. Quintela & G. Reglero

Journal of Supercritical Fluids, 95 (2014) 541-545.
DOI: 10.1016/j.supflu.2014.09.001

J. of Supercritical Fluids 95 (2014) 541–545

Contents lists available at ScienceDirect

The Journal of Supercritical Fluids

journal homepage: www.elsevier.com/locate/supflu

Recovery of betulinic acid from plane tree (*Platanus acerifolia* L.)

José María Pinilla[a], Alexis López-Padilla[b], Gonzalo Vicente[b], Tiziana Fornari[b,*], J.C. Quintela[a], G. Reglero[b]

[a] Natac Biotech, Parque Científico de Madrid, C/Faraday, 7, 28049 Madrid, Spain
[b] Instituto de Investigación en Ciencias de la Alimentación (CIAL), CEI UAM/CSIC, C/Nicolás Cabrera 9, 28049 Madrid, Spain

ARTICLE INFO

Article history:
Received 1 July 2014
Received in revised form 2 September 2014
Accepted 2 September 2014
Available online 16 September 2014

Keywords:
Supercritical fluid extraction
Pressurized liquid extraction
Ultrasound assisted extraction
Betulinic acid
Plane tree bark
Platanus acerifolia

ABSTRACT

Betulinic acid (3β, hydroxy-lup-20(29)-en-28-oic acid) is a bioactive triterpenic acid which was identified in various botanical sources and in considerable amounts in the bark of plane tree (*Platanus acerifolia* L.). In this work, the recovery of betulinic acid from plane tree bark was studied using different liquid solvent based extraction methods, namely solid–liquid extraction (SLE), ultrasound assisted extraction (UAE) and pressurized liquid extraction (PLE). Furthermore, preliminary studies of the supercritical fluid extraction (SFE) of plane tree bark are also reported.

The liquid solvent based extraction techniques (SLE, UAE and PLE) were carried out using ethanol and ethyl acetate, and produced a recovery of betulinic acid in the range 10–15 mg/g of bark, with concentrations around 25–35% mass. A betulinic acid enrichment in the ethanolic extracts was possible by means of a simple precipitation step adding water. The precipitate contained 42–46% mass of betulinic acid and high recovery (>95%). Increasing the extraction temperature, by means of the PLE assays, has not resulted in an improvement of betulinic acid recovery.

The preliminary SFE assays produced lower recoveries of betulinic acid (0.5–8 mg/g) with respect to liquid extraction. The addition of ethanol as cosolvent produced a significant improvement of both betulinic acid recovery and concentration in the SFE extract.

1. Introduction

Triterpenic acids are secondary plant metabolites that are widespread in plants, mainly located in the peel, leave and stem bark [1]. They are part of the chemical family of isoprenoids, owning polycyclic structures of thirty carbon atoms, and presenting very low solubility in water and hydrophilic solvents. On the other hand, their solubility in organic solvents such us acetone or methanol has been demonstrated to be moderately high [2].

Betulinic acid (3β, hydroxy-lup-20(29)-en-28-oic acid) is a triterpenic acid which can be isolated from various botanical sources, including clove (*Syzygium aromaticum*), Lamiaceae herbs such as rosemary (*Rosmarinus officinalis*) and java tea (*Orthosiphon stamineus*), and the bark of several betula species (birch trees), eucalyptus (*Eucalyptus globulus*) and plane (*Platanus acerifolia*) trees [1,3–8].

Betulinic acid as well as its derivatives, have demonstrated a wide range of biological activities, including anti HIV-1 activity [9], anti-inflammatory activity [10], antimalarial activity [11], anticancer and apoptotic activity [12,13]. Additionally, it has been demonstrated that some changes in betulinic acid structure can lead to significant differences in its anticancer and antiproliferative activity [14,15].

The presence of betulinic acid at concentrations up to 3% (30 mg/g) in the external dried bark of plane tree (*P. acerifolia* L.) was previously reported [1,16,17]. These works focused in the extraction of betulinic acid from the bark of plane tree through conventional solid–liquid extraction with methanol, chloroform and heptane. Nevertheless, to our knowledge, the extraction of phytochemicals present in this botanical source has not been thoroughly studied yet.

Novel liquid solvent based extraction methods include the assistance of solid–liquid extraction using ultrasounds (UAE), and the use of high extraction temperatures by increasing also pressure to maintain the solvent in liquid state (PLE).

The use of UAE to recover triterpenic acids from different plant matrix has been recently studied [18–20] and has proved to present several advantages in comparison with conventional solid–liquid extraction. These advantages include reduction of the amount of solvent required, time and temperature, which represents an important factor when extracting thermolabile compounds [21]. Ultrasonic cavitation enhances mass transfer through its capability

* Corresponding author. Tel.: +0034 910017927; fax: +0034 900017905.
E-mail address: tiziana.fornari@uam.es (T. Fornari).

http://dx.doi.org/10.1016/j.supflu.2014.09.001
0896-8446/

to facilitate hydrating and swelling of vegetal tissues as well as diffusion and osmotic processes [22].

Also PLE to recover triterpenic acids from different botanical sources has been previously reported [19,23]. PLE uses high pressures in order to remain solvents in liquid state beyond their normal boiling point. The combination of high pressures and high temperatures enhances mass transfer, thus facilitating the extraction process. It has demonstrated several advantages in comparison to traditional extraction procedures, mainly the decrease of both time and amount of solvent. However, the lack of industrial scale pressurized liquid extraction equipments, lead to a moderate application of this technique.

Supercritical fluid extraction (SFE) using carbon dioxide (CO_2) was also utilized to recover triterpenoid acids from different plant matrix, as reported by Domingues et al. [6–8], Felföldi-Gáva et al. [24], De Melo et al. [25] and Zhao [26] among others. Due to its low polarity, supercritical CO_2 has shown a moderate capacity to dissolve this type of compounds and thus, the use of ethanol as cosolvent has been employed as a suitable alternative to increase triterpenic acid recovery. An appropriate combination of pressure and ethanol as cosolvent may increase the yield of triterpenic acids profusely [7].

In this paper different advanced extraction techniques (UAE, PLE and SFE) and conventional solid–liquid extraction (SLE) are studied and compared, with the target of recovering betulinic acid from the bark of *P. acerifolia* L. Different GRAS (General recognized as safe) solvents were utilized (ethanol, ethyl acetate and $SCCO_2$) and different process conditions were investigated.

2. Material and methods

2.1. Chemicals

Ethanol absolute (99.5% purity), Ethyl acetate (99%, purity) was purchased from Panreac (Barcelona, Spain). CO_2 was used as the supercritical solvent with a purity of 99.9% produced by Carburos Metalicos, S.A. (Madrid, Spain). Betulinic Acid reference Standar was purchased from Extrashyntesse (Genay, Cedex, France).

2.2. Analysis

Quantification of betulinic acid (BA) in the extracts was performed by HPLC Agilent 1200 series from Agilent Technologies Inc. (Santa Clara, California, USA) according to a method previously described [19] with some modifications. Briefly, separation was carried out using a C-18 reverse phase column (250 × 4.6 mm, 5 μm), with a mobile phase consisting of HPLC grade acetonitrile-Milli-Q water–phosphoric acid (80:20:0.04, v/v/v). Elution was performed isocratically at a flow rate of 1 mL/min, at 25 °C, and with a total analysis time of 30 min. Injection volume was 10 μL and spectral data was recorded at 210 nm. Data analysis was performed by ChemStation version B.04.03. Samples were prepared using methanol at 0.7 mg/mL. Calibration curves of BA were constructed with reference standard.

2.3. Preparation of sample

4 kg of plane tree bark (*P. acerifolia* L.) were collected in the Campus of Universidad Autónoma de Madrid (Madrid, Spain) and were air dried at ambient temperature for 72 h. The final content of water in the dried sample was determined in an oven at 105 °C (48 h) and resulted 9.5% mass. The bark was ground in a grind Premil 250 (Lleal S.A., Barcelona, Spain) to a mean particles size of 500 μm and packed and stored at room temperature until utilization.

2.4. Extraction techniques

2.4.1. Solid–liquid extraction (SLE)

35 g of ground Platanus bark were extracted with 350 mL of solvent (ethanol or ethyl acetate) at 45 °C using a magnetic stirrer. Extraction time was 1.5 h. The infusion was filtrated in a vacuum flask with a Büchner funnel and the sifted material was washed with 50 mL of solvent. The liquid phase was concentrated at low temperature (35 °C) in a rotavapor (VWR from IKA Works GmbH & Co., Staufen, Germany).

In order to produce a triterpenic acid enrichment, 35 g of raw material were extracted with 350 mL of ethanol, as aforementioned, and the ethanol was removed in rotavapor until 1/3 of the initial volume. Then, an equal volume of deionized water was added, and the mixture was stored at room temperature for 30 min until a white precipitated was formed. The precipitated was collected by filtration and was dried in a freeze dryer from Labconco Corporation (Missouri, USA). The liquid mixture (water/ethanol) was concentrated in rotavapor and freeze-dried.

Extractions were carried out by duplicate and all samples were stored under refrigeration until they were analyzed.

2.4.2. Ultrasound assisted extraction (UAE)

35 g of ground Platanus bark with the corresponding solvent (ethanol or ethyl acetate) in a ratio 1:5 (bark:solvent) were submitted to ultrasounds for 15 min using a 1/2″ diameter disruptor horn probe at 70% amplitude (maximum power output of 400 W at 60 Hz) (Branson Digital Sonifier, Branson Ultrasonics, model 250; Danbury, USA) maintaining temperature at 45 °C. Sonication at the desired amplitude level was started once the set temperature was reached. The ultrasound probe was submerged to a depth of 25 mm in the sample. The input range of the selected variables was determined by preliminary experiments and the UAE conditions were selected on the basis of previous studies reported in the literature [27–30].

Extractions were carried out by duplicate. After sonication, the samples were filtrated and dried in rotavapor. In the case of ethanol experiments, the same procedure described in the case of SLE was applied after UAE in order to attain a triterpenic acid enrichment. All samples were stored under refrigeration until they were analyzed.

2.4.3. Supercritical fluid extraction (SFE)

Extractions were carried out using a pilot plant supercritical fluid extractor from Thar Technology (model SF2000; Pittsburgh, Pensilvania, USA) comprising a 2 L cylindrical extraction vessel (internal diameter = 0.07 m; height = 0.388 m) and two different separators, with 0.5 L capacity each one, independent temperature control (±2 K) and pressure (±0.1 MPa). The extraction device also includes a recirculation system where CO_2 is condensed and pumped up to the desired extraction pressure. A detail explanation of the experimental SFE device employed can be found elsewhere [31].

For each experiment, the extraction vessel was packed with 0.57 kg of ground plane tree bark (apparent density = 381.7 kg/m^3). The extraction conditions are given in Table 4, and were performed at 313 K, pressure range of 25–50 MPa and with an upwards CO_2 flow rate of 50 g/min. The overall extraction time was set to 4 h. Extractions 1 and 2 (see Table 4) were carried out in two different steps: the first step (1.5 h) at 25 MPa and without cosolvent and the second step (2.5 h) at 30 MPa and using, respectively, 10% and 20% of ethanol cosolvent. Extraction conditions were selected on the basis of previous studies reported in the literature [6].

2.4.4. Pressurized liquid extraction (PLE)

Extractions were carried out in an accelerated solvent extraction system ASE 350 from Dionex Corporation (Sunnyvale, CA,

Table 1
Solid–liquid extraction (SLE) of plane tree bark at 45 °C. BA: betulinic acid.

Solvent		Yield (%)	BA concentration (% mass in the extract)	BA recovery (mg/g dry matter)
Ethanol		3.69	29.51	10.89
Ethanol	Precipitate	2.22	41.48	9.21
	Supernatant	0.93	3.10	0.29
Ethyl acetate		3.19	32.63	10.41

Table 2
Pressurized liquid extraction (PLE) of plane tree bark at 100, 150 and 200 °C. BA: betulinic acid.

Solvent	T (°C)	Yield (%)	BA concentration (% mass in the extract)	BA recovery (mg/g dry matter)
Ethanol	100	4.88	25.03	12.21
	150	6.88	18.52	12.74
	200	11.92	10.89	12.98
Ethyl acetate	100	4.39	26.69	11.72
	150	4.70	21.79	10.24
	200	6.21	18.87	11.72

USA) equipped with a solvent controller unit. Extractions were performed with two different liquid solvents (ethanol and ethyl acetate) at three different extraction temperatures (100, 150 and 200 °C) using 1 g of solid sample and 1 g of sea sand as a sandwich. The consumption of solvent during extraction (amount of solvent required to fill the extraction cell) was around 10 mL. Extraction conditions were selected on the basis of previous studies reported in the literature [32]. All extractions were made by duplicate. Extracts were dried using a rotavapor and were stored under refrigeration until analysis.

3. Results and discussion

Tables 1–3 present, respectively, the results obtained in the SLE, UAE and PLE experiments. The results reported in the tables include the extraction yield (mass of extract/mass of dried bark), the concentration of betulinic acid (BA) in the extract (% mass) and its recovery (mg BA/g of dried bark).

The extracts obtained by SLE using ethanol or ethyl acetate present similar yield and BA concentration and thus, similar BA recovery. Fractionation of the ethanolic extract by adding water resulted in a precipitate with 41.48% mass of BA, and around 96% of BA recovery in the solid phase.

The assistance of solid–liquid extraction with ultrasounds (UAE temperature was maintained equal to the SLE temperature) produced a slight increase of BA recovery when ethanol is employed (≈10%), while significant higher recovery was obtained with ethyl acetate (14.74 vs. 10.41 mg/g, i.e. an increase close to 40%). Nevertheless, the concentration of BA in the ethyl acetate UAE extract is lower than that obtained in the SLE extract (27.76 vs. 32.63% mass). Moreover, it has to be taken into account that UAE consumed half the amount of solvent (solvent/bark ratio = 5) and lower extraction time (15 min) in comparison with SLE.

Table 3
Ultrasound assisted extraction (UAE) of plane tree bark at 45 °C. BA: betulinic acid.

Solvent		Yield (%)	BA concentration (% mass in the extract)	BA recovery (mg/g dry matter)
Ethanol		3.52	33.82	11.90
Ethanol	Precipitate	2.70	46.21	12.48
	Supernatant	0.98	1.52	0.15
Ethyl Acetate		5.31	27.76	14.74

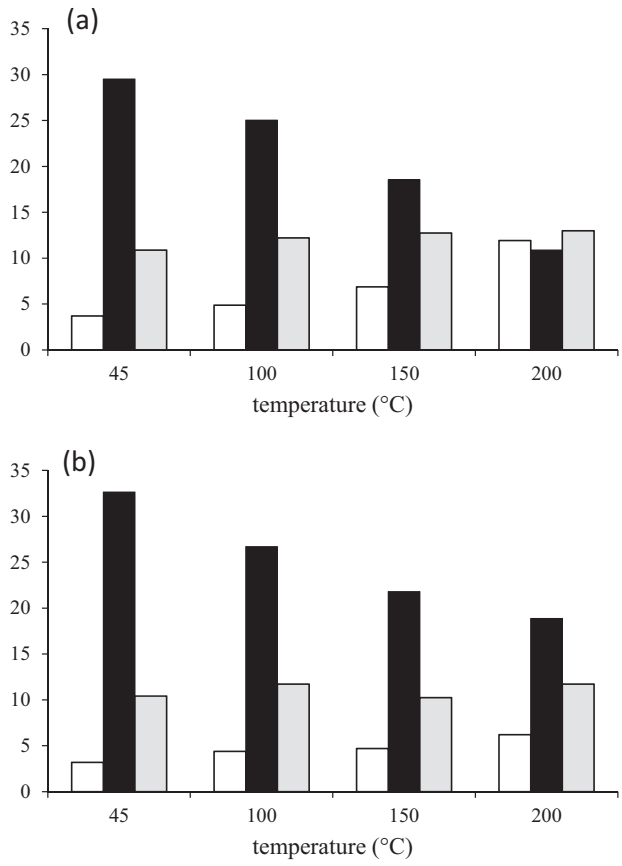

Fig. 1. Effect of temperature on the extraction of betulinic acid from *Platanus acerifolia* bark: % mass betulinic acid in the extract (black columns), extraction yield (white columns) and betulinic acid recovery (gray columns). SLE: 45 °C; PLE: 100, 150 and 200 °C. (a) Ethanol; (b) ethyl acetate solvent.

The fractionation procedure applied to the ethanolic UAE extract produced similar result than in the case of the ethanolic SLE extract: a BA enriched precipitate was obtained (46.21% mass) with 98% recovery (slight loss of BA in the supernatant aqueous phase).

The results obtained in the PLE of plane tree bark are given in Table 3. The effect of increasing temperature in PLE (100, 150 and 200 °C) is producing higher yields but lower BA concentrations in the extract. That is, higher extraction temperatures favor the extraction of compounds other than BA, which was almost exhausted from the raw material, as can be deduced from the similar recoveries obtained despite the extraction temperature applied. Accordingly, in SLE (extraction temperature of 45 °C) the lowest yields and the highest BA concentrations were obtained, maintaining almost the same (slightly lower) BA recovery. These conclusions hold for both ethanol and ethyl acetate solvents, as illustrated in Fig. 1. Although the optimization of solvent consumption was not a target of this work, it is evident that the UAE extracts were obtained using half the amount of the solvent employed in the SLE and PLE, and higher BA concentrations and similar BA recovery were attained. Thus, no advantage can be established in favor of using PLE instead of SLE or UAE, particularly if extracts with high betulinic acid content are target.

Table 4 present the results obtained from the SFE of plane tree bark. Extractions 1 and 2 were carried out in two steps: the first step was carried out at 25 MPa and 40 °C, without using cosolvent, while the second step was performed at 30 MPa, 40 °C and using 10% ethanol (Ext. 1) or 20% ethanol (Ext. 2) as cosolvent.

Table 4
SC–CO_2 extraction of plane tree bark at 40 °C. BA: betulinic acid.

	Ext 1		Ext 2		Ext 3
	Step 1	Step 2	Step1	Step 2	
Pressure (MPa)	25	30	25	30	50
Time (h)	1.5	2.5	1.5	2.5	4
Ethanol cosolvent (% mass)	0	10	0	20	0
Extraction yield (%)	0.66	4.94	0.69	4.34	0.35 (S1) 0.74 (S2)
BA concentration (% mass in the extract)	0.23	14.99	2.36	18.30	10.85 (S1) 2.18 (S2)
BA recovery (mg/g dry matter)	0.02	7.41	0.16	7.94	0.38 (S1) 0.16 (S2)

The two-step approach was accomplished expecting that low amounts of BA were extracted in the first step, and high concentration of the acid may possibly be achieved in the extract produced in the second step due to the addition of ethanol as CO_2 cosolvent. Ext. 3 in Table 4 was carried out at higher pressure (50 MPa) and without cosolvent. Additionally, fractionation of the extract using the cascade decompression system was employed with the objective of producing a sample with high concentration of BA in the first separator.

The low yield obtained in the first step of Extractions 1 and 2 resulted in just a slight increase of BA concentration in the second fraction of the two-step procedure. On the other side, the on-line fractionation applied when pure CO_2 was utilized (Ext. 3 in Table 4) produced a significant concentration of BA in the extract precipitated in the first separator. Although this fractionation alternative can produce a sample with 10.85% mass of BA, the use of ethanol as cosolvent is an important variable to be investigated in order to maximize SFE of betulinic acid from plane tree bark (BA % mass was 15 and 18% when, respectively, 10 and 20% ethanol cosolvent was utilized). The CO_2/feed ratio employed in this work was 21 kg/kg, similar to the value utilized by Domingues et al. [6] (27 kg/kg) in the SFE of triterpenic acids from eucalyptus bark. Despite the % cosolvent was proven to be a very important variable in the SFE of plane bark, the CO_2/feed ratio is also a variable that should be investigated and optimized.

In the range of SFE experimental conditions investigated all liquid solvent based extraction techniques (SLE, UEA and PLE) produced higher recovery of BA (10–15 mg/g) than those obtained with SFE (ca. 8 mg/g when using ethanol as CO_2 cosolvent). With respect to the concentration of BA in the extract, ethanol and ethyl lactate produced extracts with values up to 25–35% mass, higher than the maximum obtained in SFE (18% mass).

Fig. 2 shows a comparison between the extraction methods using liquid ethanol (SLE, UAE and PLE) and the SFE using ethanol as CO_2 cosolvent. Fig. 2(a) indicate that all liquid solvent based methods produce high BA recovery (≈12 mg BA/g bark) while very low BA recovery is obtained by SFE with pure CO_2 despite the high extraction pressure applied (50 MPa). The addition of 10–20% ethanol significantly increases BA recovery up to values close to those obtained by liquid ethanol extraction.

Fig. 2(b) depicts the concentration of BA (% mass) obtained in the different extracts. It can be observed in the figure how the addition of ethanol cosolvent in the SFE results in an increase of BA % mass in the extract. Yet, UAE extract present around a two-fold increase of BA concentration in comparison with the SFE extracts. Finally, Fig. 2(c) compares the ethanol consumed by each technological approach. Although the consumption of ethanol was not optimized in this work, it can be concluded from the figure that lower amount of ethanol is required in SFE technology per unit of mass of target BA recovery.

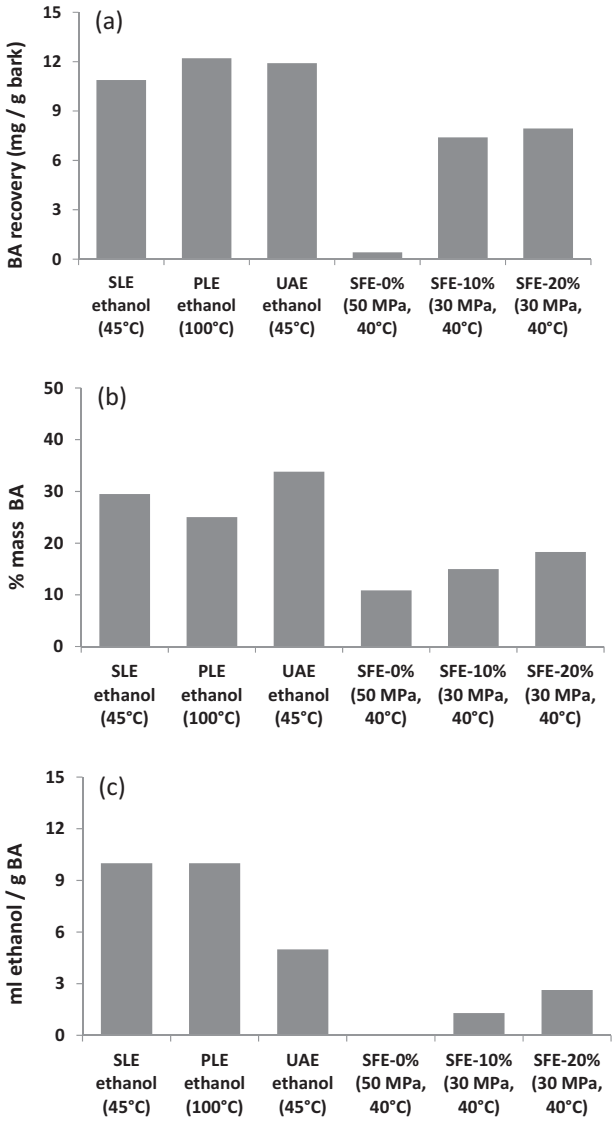

Fig. 2. Comparison between the extraction methods using liquid ethanol (SLE, UAE and PLE) and SFE with 0, 10 and 20% ethanol cosolvent. (a) BA recovery; (b) BA concentration; (c) ethanol consumption.

4. Conclusions

Considering the results obtained in this work, it can be concluded that the plane tree bark extract with higher concentration of betulinic acid was obtained by ethanol extraction assisted with

ultrasounds and followed by a simple pre-fractionation step using water. This approach produced an extract with 46.21% mass of betulinic acid and 2.7% yield. Furthermore, ethyl acetate UAE can produce almost a two fold increase of extraction yield (5.31%) with ca. 28% mass of betulinic acid in the extract.

The preliminary SFE accomplished in this work, permit to presume that the use of ethanol as CO_2 cosolvent has the most significant effect on the extraction of betulinic acid from plane tree bark. In comparison with SLE, UAE and PLE, 20% ethanol cosolvent resulted in high yield (4.34%), good concentration of betulinic acid in the extract (18.30% mass) and almost one third of ethanol consumption. Further investigation to optimize SFE conditions and attain higher betulinic acid recovery is necessary.

Acknowledgements

This work has been supported by project ALIBIRD-S2009/AGR-1469 from Comunidad Autónoma de Madrid. López-Padilla A. thanks to COLCIENCIAS (568–2012) and Medellin Mayor's Office (Sapiencia/Enlaza Mundos Program, 2013) for the Ph.D. fellowship.

References

[1] S. Jäger, H. Trojanet, T. Kopp, M.N. Laszczyk, A. Cheffler, Pentacyclic triterpene distribution in various plants—rich sources for a new group of multi-potent plant extracts, Molecules 14 (2009) 2016–2031.
[2] L. Liu, X. Wang, Solubility of oleanolic acid in various solvents from (288.3 to 328.3) K, J. Chemical and Engineering 52 (2007) 2527–2528.
[3] J. Freysdottir, M.B. Sigurpalsson, S. Omarsdottir, E.S. Olafsdottir, A. Vikingsson, I. Hardardottir, Ethanol extract from birch bark (*Betula pubescens*) suppresses human dendritic cell mediated Th1 responses and directs it towards a Th17 regulatory response in vitro, Immunology Letters 30 (2011) 90–96.
[4] A. Aisha, K.M. Abu-Salah, S.A. Alrokayan, M.J. Siddiqui, Z. Ismail, A.M.S.A. Majid, *Syzygium aromaticum* extracts as good source of betulinic acid and potential anti-breast cancer, Brazilian J. Pharmacognosy 22 (2012) 335–343.
[5] Y. Tezuka, P. Stampoulis, A.H. Banskota, S. Awale, K.Q. Tran, I. Saiki, S. Kadota, Constituents of the Vietnamese medicinal plant *Orthosiphon stamineus*, Chemical & Pharmaceutical Bulletin 48 (2000) 1711–1719.
[6] R.M.A. Domingues, M.M.R. De Melo, E.L.G. Oliveira, C.P. Neto, A.J.D. Silvestre, C.M. Silva, Optimization of the supercritical fluid extraction of triterpenic acids from *Eucalyptus globulus* bark using experimental design, J. Supercritical Fluids 74 (2013) 105–114.
[7] R.M.A. Domingues, M.M.R. Melo, C.P. Neto, A.J.D. Silvestre, C.M. Silva, Measurement and modeling of supercritical fluid extraction curves of *Eucalyptus globulus* bark: influence of the operating conditions upon yields and extract composition, J. Supercritical Fluids 72 (2012) 176–185.
[8] R.M.A. Domingues, E.L.G. Oliveira, C.S.R. Freire, R.M. Couto, P.C. Simões, C.P. Neto, A.J.D. Silvestre, C.M. Silva, Supercritical fluid extraction of *Eucalyptus globulus* bark—a promising approach for triterpenoid production, International J. Molecular Science 13 (2012) 7648–7662.
[9] P. Yogeeswari, D. Sriram, Betulinic acid and its derivatives a review on their biological properties, Current Medicinal Chemistry 12 (2005) 657–666.
[10] W. Lee, E.J. Yang, S.K. Ku, K.S. Song, J.S. Bae, Anti-inflammatory effects of oleanolic acid on lps-induced inflammation in vitro and in vivo, Inflammation 36 (2013) 1–9.
[11] J.C. Steele, D.C. Warhurst, G.C. Kirby, M.S. Simmonds, In vitro and in vivo evaluation of betulinic acid as an antimalarial, Phytotherapy Research 13 (1999) 115–119.
[12] S. Fulda, Betulinic acid for cancer treatment and prevention, International J. Molecular Science 9 (2008) 1096–1107.
[13] S. Fulda, G. Kroemer, Targeting mitochondrial apoptosis by betulinic acid in human cancers, Drug Discovery Today: Therapeutic Strategies 14 (2009) 885–890.
[14] H. Kommera, G.N. Kaluderović, J. Kalbitz, B. Dräger, R. Paschke, Small structural changes of pentacyclic lupane type triterpenoid derivatives lead to significant differences in their anticancer properties, European J. Medicinal Chemistry 45 (2010) 3346–3353.
[15] R.C. Santos, J.A. Salvador, R. Cortés, G. Pachón, S. Marín, M. Cascante, New betulinic acid derivatives induce potent and selective antiproliferative activity through cell cycle arrest at the S phase and caspase dependent apoptosis in human cancer cells, Biochimie 93 (2011) 1065–1075.
[16] V. Bruckner, J. Kovács, I. Koczka, Occurrence of betulinic acid in the bark of the plane tree, J. Chemical Society 8 (1948) 948–951.
[17] T. Galgon, D. Höke, B. Dräger, Identification and quantification of betulinic acid, Phytochemical Analysis 10 (1999) 187–190.
[18] S.R. Pai, M.S. Nimbalkarb, N.V. Pawarc, G.B. Dixita, Optimization of extraction techniques and quantification of betulinic acid (BA) by RP-HPLC method from *Ancistrocladus heyneanus* Wall, Ex Grah, Industrial Crops and Products 34 (2011) 1458–1464.
[19] M. Wojciak-Kosior, I. Sowa, R. Kocjan, R. Nowak, Effect of different extraction techniques on quantification of oleanolic and ursolic acid in Lamii albi flos, Industrial Crops and Products 44 (2013) 373–377.
[20] E.Q. Xia, Y.Y. Yu, X.R. Xu, G.F. Deng, Y.J. Guo, H.B. Li, Ultrasound-assisted extraction of oleanolic acid and ursolic acid from *Ligustrum lucidum* Ait, Ultrasonics Sonochemistry J. 19 (2012) 772–776.
[21] Q. Chen, M. Fu, J. Liu, H. Zhang, G. He, H. Ruan, Optimization of ultrasonic-assisted extraction (UAE) of betulin from white birch bark using response surface methodology, Ultrasonics Sonochemistry J. 16 (2009) 599–604.
[22] M. Vinatoru, An overview of the ultrasonically assisted extraction of bioactive principles from herbs, Ultrasonics Sonochemistry J. 8 (2011) 303–313.
[23] B. Rhourri-Frih, I. Renimel, P. Chaimbault, P. André, G. Herbette, M. Lafosse, Pentacyclic triterpenes from *Manilkara bidentata* resin. isolation, identification and biological properties, Fitoterapia 9 (2013) 101–108.
[24] A. Felföldi-Gáva, B. Simándi, S. Plánder, S. Szarka, É. Szőke, Á. Kéry, Betulaceae and platanaceae plants as alternative sources of selected lupane-type triterpenes. Their composition profile and betulin content, Acta Chromatographica 21 (2009) 671–681.
[25] M.M.R. De Melo, E.L.G. Oliveira, A.J.D. Silvestre, C.M. Silva, Supercritical fluid extraction of triterpenic acids from *Eucalyptus globulus* bark, J.Supercritical Fluids 70 (2012) 137–145.
[26] J. Zhao, The Extraction of High Value Chemicals from Heather (*Calluna vulgaris*) and Bracken (*Pteridium aquilinum*), The University of York, York, UK, 2011.
[27] M.B. Hossain, N.P. Brunton, A. Patraset, B. Tiwari, C.P. O'Donnell, A.B. Martin-Diana, C. Barry-Ryan, Optimization of ultrasound assisted extraction of antioxidant compounds from marjoram (*Origanum majorana* L.) using response surface methodology, Ultrasonics Sonochemistry 19 (2012) 582–590.
[28] M. Plaza, S. Santoyo, L. Jaime, B. Avalo, A. Cifuentes, G. Reglero, G. García-Blairs, F.J. Señoráns, E. Ibáñez, Comprehensive characterization of the functional activities of pressurized liquid and ultrasound-assisted extracts from *Chlorella vulgaris*, LWT—Food Science and Technology 46 (2012) 245–253.
[29] S.R. Shirsath, S.H. Sonawane, P.R. Gogate, Intensification of extraction of natural products using ultrasonic irradiations—a review of current status, Chemical Engineering and Processing: Process Intensification 53 (2012) 10–23.
[30] K. Vilkhu, R. Mawson, L. Simons, D. Bates, Applications and opportunities for ultrasound assisted extraction in the food industry—a review, Innovative Food Science & Emerging Technologies 9 (2008) 161–169.
[31] M.R. García-Risco, G. Vicente, G. Reglero, T. Fornari, Fractionation of thyme (*Thymus vulgaris* L.) by supercritical fluid extraction and chromatography, J. Supercritical Fluids 55 (2011) 949–954.
[32] D.V. Bermejo, P. Luna, M.S. Manic, V. Najdanovi-Visak, G. Reglero, T. Fornari, Extraction of caffeine from natural matter using a bio-renewable agrochemical solvent, Food and Bioproducts Processing 91 (2013) 303–309.